BIOLOGICAL CONSEQUENCES OF CURRENT-TOPOGRAPHY INTERACTIONS AT COBB SEAMOUNT

by
John F. Dower
B.Sc. Memorial University of Newfoundland, 1989

A Dissertation Submitted in Partial Fulfilment of the Requirements for the Degree of

DOCTOR OF PHILOSOPHY

in the Department of Biology

We accept this thesis as conforming to the required standard

Dr. V.J. Tunnicliffe, Supervisor (Department of Biology)

Dr. L.A. Hobson, Departmental Member (Department of Biology)

Dr. D.L. Mackas, Departmental Member
(Institute of Ocean Sciences)

Dr. C.R. Barnes, Outside Member
(School of Earth and Ocean Sciences)

Dr. H.J. Freeland, Additional Member
(Institute of Ocean Sciences)

Dr. K.L. Denman, External Examiner
(Institute of Ocean Sciences)

Name JOHN F. DOWER

Dissertation Abstracts International is arranged by broad, general subject categories. Please select the one subject which most nearly describes the content of your dissertation. Enter the corresponding four-digit code in the spaces provided.

Oceanography
SUBJECT TERM

0416
SUBJECT CODE

U·M·I

Subject Categories

THE HUMANITIES AND SOCIAL SCIENCES

COMMUNICATIONS AND THE ARTS

Architecture 0729
Art History 0377
Cinema 0900
Dance 0378
Fine Arts 0357
Information Science 0723
Journalism 0391
Library Science 0399
Mass Communications 0708
Music 0413
Speech Communication 0459
Theater 0465

EDUCATION

General 0515
Administration 0514
Adult and Continuing 0516
Agricultural 0517
Art 0273
Bilingual and Multicultural 0282
Business 0688
Community College 0275
Curriculum and Instruction 0727
Early Childhood 0518
Elementary 0524
Finance 0277
Guidance and Counseling 0519
Health 0680
Higher 0745
History of 0520
Home Economics 0278
Industrial 0521
Language and Literature 0279
Mathematics 0280
Music 0522
Philosophy of 0998
Physical 0523

Psychology 0525
Reading 0535
Religious 0527
Sciences 0714
Secondary 0533
Social Sciences 0534
Sociology of 0340
Special 0529
Teacher Training 0530
Technology 0710
Tests and Measurements 0288
Vocational 0747

LANGUAGE, LITERATURE AND LINGUISTICS

Language
- General 0679
- Ancient 0289
- Linguistics 0290
- Modern 0291

Literature
- General 0401
- Classical 0294
- Comparative 0295
- Medieval 0297
- Modern 0298
- African 0316
- American 0591
- Asian 0305
- Canadian (English) 0352
- Canadian (French) 0355
- English 0593
- Germanic 0311
- Latin American 0312
- Middle Eastern 0315
- Romance 0313
- Slavic and East European 0314

PHILOSOPHY, RELIGION AND THEOLOGY

Philosophy 0422
Religion
- General 0318
- Biblical Studies 0321
- Clergy 0319
- History of 0320
- Philosophy of 0322

Theology 0469

SOCIAL SCIENCES

American Studies 0323
Anthropology
- Archaeology 0324
- Cultural 0326
- Physical 0327

Business Administration
- General 0310
- Accounting 0272
- Banking 0770
- Management 0454
- Marketing 0338

Canadian Studies 0385
Economics
- General 0501
- Agricultural 0503
- Commerce-Business 0505
- Finance 0508
- History 0509
- Labor 0510
- Theory 0511

Folklore 0358
Geography 0366
Gerontology 0351
History
- General 0578
- Ancient 0579
- Medieval 0581
- Modern 0582
- Black 0328
- African 0331
- Asia, Australia and Oceania 0332
- Canadian 0334
- European 0335
- Latin American 0336
- Middle Eastern 0333
- United States 0337

History of Science 0585
Law 0398
Political Science
- General 0615
- International Law and Relations 0616
- Public Administration 0617

Recreation 0814
Social Work 0452
Sociology
- General 0626
- Criminology and Penology 0627
- Demography 0938
- Ethnic and Racial Studies 0631
- Individual and Family Studies 0628
- Industrial and Labor Relations 0629
- Public and Social Welfare 0630
- Social Structure and Development 0700
- Theory and Methods 0344

Transportation 0709
Urban and Regional Planning 0999
Women's Studies 0453

THE SCIENCES AND ENGINEERING

BIOLOGICAL SCIENCES

Agriculture
- General 0473
- Agronomy 0285
- Animal Culture and Nutrition 0475
- Animal Pathology 0476
- Food Science and Technology 0359
- Forestry and Wildlife 0478
- Plant Culture 0479
- Plant Pathology 0480
- Plant Physiology 0817
- Range Management 0777
- Wood Technology 0746

Biology
- General 0306
- Anatomy 0287
- Biostatistics 0308
- Botany 0309
- Cell 0379
- Ecology 0329
- Entomology 0353
- Genetics 0369
- Limnology 0793
- Microbiology 0410
- Molecular 0307
- Neuroscience 0317
- Oceanography 0416
- Physiology 0433
- Radiation 0821
- Veterinary Science 0778
- Zoology 0472

Biophysics
- General 0786
- Medical 0760

EARTH SCIENCES

Biogeochemistry 0425
Geochemistry 0996
Geodesy 0370
Geology 0372
Geophysics 0373
Hydrology 0388
Mineralogy 0411
Paleobotany 0345
Paleoecology 0426
Paleontology 0418
Paleozoology 0985
Palynology 0427
Physical Geography 0368
Physical Oceanography 0415

HEALTH AND ENVIRONMENTAL SCIENCES

Environmental Sciences 0768
Health Sciences
- General 0566
- Audiology 0300
- Chemotherapy 0992
- Dentistry 0567
- Education 0350
- Hospital Management 0769
- Human Development 0758
- Immunology 0982
- Medicine and Surgery 0564
- Mental Health 0347
- Nursing 0569
- Nutrition 0570
- Obstetrics and Gynecology 0380
- Occupational Health and Therapy 0354
- Ophthalmology 0381
- Pathology 0571
- Pharmacology 0419
- Pharmacy 0572
- Physical Therapy 0382
- Public Health 0573
- Radiology 0574
- Recreation 0575
- Speech Pathology 0460
- Toxicology 0383

Home Economics 0386

PHYSICAL SCIENCES

Pure Sciences

Chemistry
- General 0485
- Agricultural 0749
- Analytical 0486
- Biochemistry 0487
- Inorganic 0488
- Nuclear 0738
- Organic 0490
- Pharmaceutical 0491
- Physical 0494
- Polymer 0495
- Radiation 0754

Mathematics 0405
Physics
- General 0605
- Acoustics 0986
- Astronomy and Astrophysics 0606
- Atmospheric Science 0608
- Atomic 0748
- Electronics and Electricity 0607
- Elementary Particles and High Energy 0798
- Fluid and Plasma 0759
- Molecular 0609
- Nuclear 0610
- Optics 0752
- Radiation 0756
- Solid State 0611

Statistics 0463

Applied Sciences

Applied Mechanics 0346
Computer Science 0984
Engineering
- General 0537
- Aerospace 0538
- Agricultural 0539
- Automotive 0540
- Biomedical 0541
- Chemical 0542
- Civil 0543
- Electronics and Electrical 0544
- Heat and Thermodynamics 0348
- Hydraulic 0545
- Industrial 0546
- Marine 0547
- Materials Science 0794
- Mechanical 0548
- Metallurgy 0743
- Mining 0551
- Nuclear 0552
- Packaging 0549
- Petroleum 0765
- Sanitary and Municipal 0554
- System Science 0790

Geotechnology 0428
Operations Research 0796
Plastics Technology 0795
Textile Technology 0994

PSYCHOLOGY

General 0621
Behavioral 0384
Clinical 0622
Developmental 0620
Experimental 0623
Industrial 0624
Personality 0625
Physiological 0989
Psychobiology 0349
Psychometrics 0632
Social 0451

Supervisor: Dr. V.J. Tunnicliffe

ABSTRACT

Shallow oceanic seamounts have long been known to support rich nektonic stocks. However, the mechanism by which this occurs has never been satisfactorily explained. This thesis examines the role of current-topography interactions in the planktonic community at Cobb Seamount, a shallow seamount 500km west of Vancouver Island.

Current-topography interactions at seamounts give rise to a variety of flow phenomena, the two most important being (i) the formation of closed clockwise vortices, known as Taylor cones, and (ii) isopycnal doming of the density field near the topography. Since the 1950's the classical explanation for the high biological productivity of shallow seamounts has been based on the notion that (i) nutrient-rich water upwells over seamounts, promoting enhanced primary production and that (ii) a Taylor cone then traps and concentrates this primary production over the seamount. This classical explanation further suggests that energy is transmitted from the phytoplankton to zooplankton stocks, and leads to an accumulation of zooplankton near the seamount, which acts as the food source to support seamount fish. This thesis challenges the validity of this mechanism, based on extensive physical and biological sampling carried out during three cruises to Cobb Seamount in the summers of 1990, '91 and '92: isopycnal doming and

Taylor cone recirculations both occur at Cobb, but the Taylor cone does not penetrate close enough to the surface to trap plankton.

Nevertheless, phytoplankton stocks are consistently high near Cobb, with local chlorophyll concentrations at least twice as high as background levels. These regions of high chlorophyll concentration map closely with areas where isopycnal surfaces dome upward by as much as 30m. These data provide the first evidence that high phytoplankton stocks may be *permanent* features near shallow seamounts.

Spatial patterns in the mesozooplankton community composition are examined using the Percent Similarity Index. Based on simple straight-line separation between samples, community composition around Cobb changes only slightly over distances of up to 150km. When samples are compared on the basis of relative distance to the seamount, however, it is seen that proximity to the seamount is a better predictor of community variability. Between-sample resemblance is found to be *lower* among samples within 30km of Cobb. This pattern may be caused by (i) predation by seamount fish or (ii) behavioural responses causing the zooplankton to avoid the seamount.

A simple four-compartment ecosystem model is used to address the questions of (i) how a persistent high phytoplankton stock can be maintained over a seamount in the absence of a trapping mechanism, and (ii) whether seamount

fish stocks rely on autochthonous energy sources. The model shows that persistent high phytoplankton stocks are caused primarily by the improved light conditions experienced by the phytoplankton as they dome over the seamount. Depending on the degree of nutrient limitation, the addition of nutrients to the near-surface waters via doming may also be important. The model demonstrates that phytoplankton stocks show almost no response to predation on zooplankton by seamount fish.

Together, the field data and the ecosystem model show that while current-topography interactions *do* contribute to the maintenance of high-biomass communities at shallow seamounts, the classical bottom-up enrichment/retention mechanism does not apply to Cobb. Additionally, this work suggests that seamount fish stocks rely on allochthonous energy sources. Rather than a long chain that begins with phytoplankton and ends with rich nektonic stocks, the "seamount effect" near Cobb is the result of a wide assortment of physical-biological interactions. Different organisms operating at several levels of the food web "feel" the influence of the seamount in different ways that are only loosely and occasionally coupled.

Examiners:

Dr. V.J. Tunnicliffe, Supervisor (Department of Biology)

Dr. L.A. Hobson, Departmental Member (Department of Biology)

Dr. D.L. Mackas, Departmental Member
(Institute of Ocean Sciences)

Dr. C.R. Barnes, Outside Member
(School of Earth and Ocean Sciences)

Dr. H.J. Freeland, Additional Member
(Institute of Ocean Sciences)

Dr. K.L. Denman, External Examiner
(Institute of Ocean Sciences)

CONTENTS

Contents (continued)

TABLES

FIGURES

Figures (continued)

Figures (continued)

Page

ACKNOWLEDGEMENTS

Many thanks to Verena Tunnicliffe for her support, for believing in what I was trying to do and for encouraging (and allowing!) me to go beyond the bounds of ecology in order to address ecological problems. I am indebted to Howard Freeland for taking the time to explain the mysteries of ocean physics (over and over) to a biologist. Thanks to Dave Mackas for discussions on plankton ecology and for the loan of equipment. Ken Denman encouraged me to persevere in my early attempts at mathematical modelling. Thanks, as well, to the many people who helped me in the collection of data: Doug Yelland, Reg Bigham, Kerry Wilson, Ken Morgan, Pascale Martineau, Todd Mudge, Rolf Lueck, Graham Quinn and Marie Robert. Special thanks to Pat Finnigan both for help at sea and in plankton identifications. Kim Juniper, Télésphore Sime-Ngando, Luc Comeau, Myriam Bourgeois and Alain Vézina were kind enough to share their data with me. Charlie Eriksen and Dan Codiga invited me on their TOPO cruise and allowed me to use their Hydrosweep data. The captains and crews of the CSS Parizeau and the John P. Tully performed admirably at sea under what, at times, were less than ideal conditions. Finally, I offer my thanks to my parents for their continued encouragement and for giving me the love of learning that guided me along the road to this point. To Lia, I can only say thank you for sticking by me throughout this work under what, at times, can also only be described as less than ideal conditions.

FRONTISPIECE

High resolution map of Cobb Seamount (46° 46'N, 130° 48'W). The seamount rises from a depth of 2800m to a shallowest depth of only 24m. The main summit is visible as a 10km wide terrace extending from 100-300m depth. The map was produced using a Hydrosweep mapping system during a University of Washington cruise to Cobb Seamount in October of 1991. Thanks to Dr. Charlie Eriksen (UW Oceanography) for permission to use these data, and to Dan Codiga who actually processed the data.

Cobb Seamount

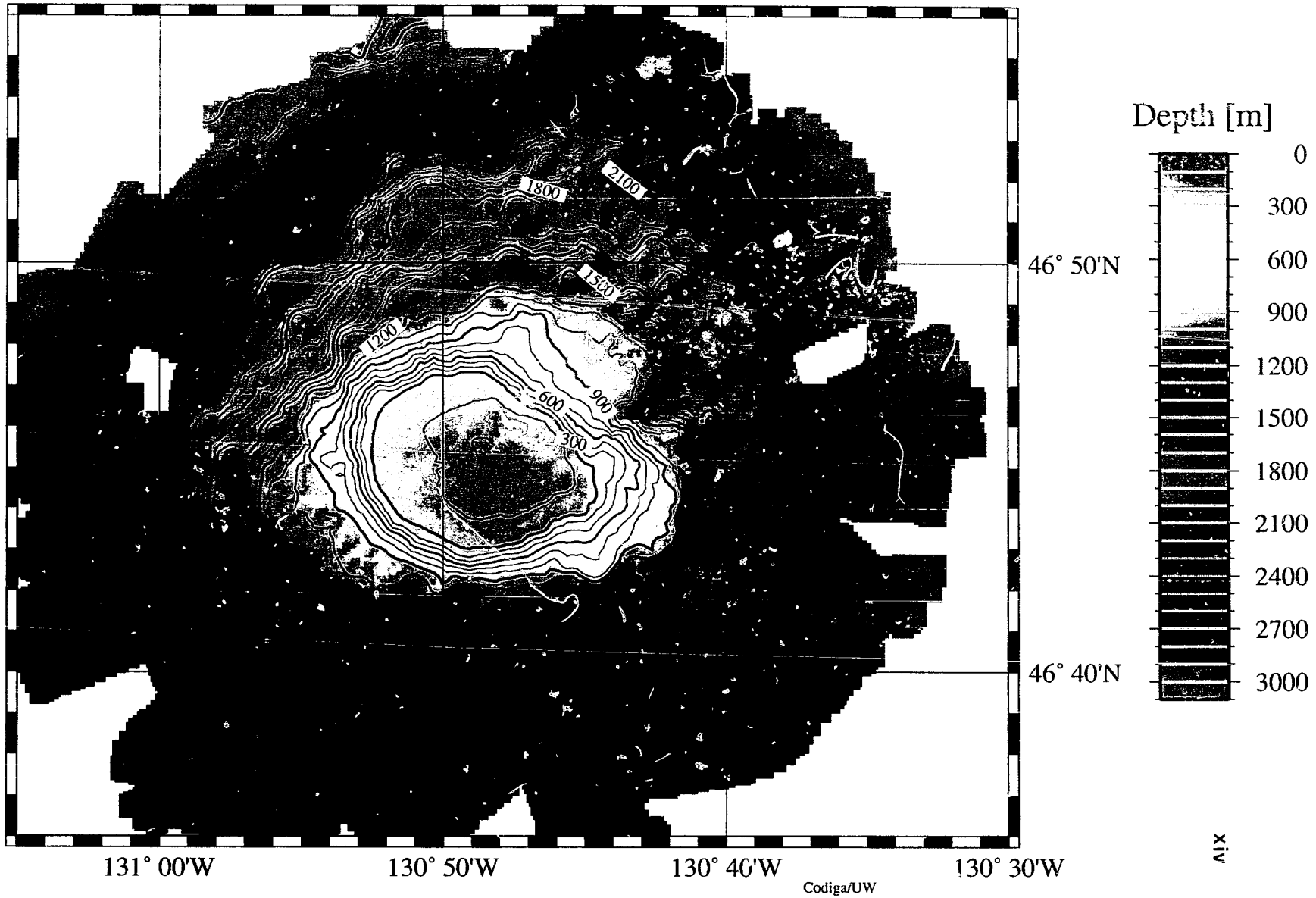

Introduction

Oceanic currents interact with topographic features over a wide range of temporal and spatial scales. For instance, the long term behaviour of basin-scale current systems such as the Gulf Stream and the Kuroshio results, in part, from interactions with boundaries formed by the continental shelves in the western Atlantic and Pacific Oceans. Meandering of these currents gives rise to both warm- and cold-core mesoscale eddies, with lifetimes of up to a couple of years. Seasonally, the interplay among equatorward winds, alongshore currents and coastal topography produces regions of strong coastal upwelling in eastern boundary current systems. On smaller scales, the daily interaction of tidal flow with local bottom topography produces regions of intense mixing and contributes to the formation of tidal fronts in some continental shelf waters. Locally, persistent eddies and small-scale upwellings result from current flow past headlands, peninsulas and around reefs and islands.

This thesis deals with one particular class of current-topography interactions: those resulting from oceanic flow past isolated seamounts, and the importance of these interactions to oceanic planktonic communities. Seamounts are submarine mountains, greater than 1000m in height (Uchida and Tagami, 1986), produced by undersea volcanic

activity. Smith and Jordan (1988) estimate that there are more than 30,000 such seamounts in the Pacific Ocean alone, making them among the most ubiquitous topographic features in the deep ocean.

Beginning in the late 1950's a number of shallow seamounts in the North Pacific were found to support commercially valuable fish stocks (Hubbs, 1958; Uchida and Tagami, 1986). By the late 1960's Japanese and Russian vessels had begun harvesting some of these stocks in the southern Emperor and northern Hawaiian seamount chains. In 1970 alone, Russian trawlers reported catches of 133,400 tonnes of pelagic armorhead from Kinmei and the Hancock Seamounts (Uchida and Tagami, 1986). More recently, significant stocks of rockfish, sablefish and king crab have been discovered on seamounts in the Northeast Pacific (Hughes, 1981). Since these initial discoveries, there has been much speculation as to how such rich biological communities are created and maintained on seamounts. The most common explanation has been that oceanic flow past shallow seamounts produces both upwelling conditions and a horizontal recirculation that combine to foster high local primary productivity which is then trapped over the seamount long enough for energy to be transferred to higher trophic levels (Boehlert and Genin, 1987). Implicit in this hypothesis is the assumption of strong coupling among the various compartments in the planktonic food web, such that a

pulse of primary production eventually propagates throughout the entire seamount food web.

Recently, this explanation has been challenged. Some workers have suggested that the metabolic requirements of seamount fish populations cannot be met by *in situ* production, and that nektonic stocks must therefore rely on allochthonous energy inputs (Tseitlen, 1985; Pudyakov and Tseitlen, 1986). Additionally, despite a growing number of field studies on seamounts, there have been few observations of recirculating flows persisting long enough to accommodate energy transfer from phytoplankton to zooplankton to fish.

In this thesis, I investigate the response of an oceanic planktonic food web to flow past Cobb Seamount, a shallow seamount in the Northeast Pacific (Fig. 1). Previous studies have shown that Cobb supports rich benthic and pelagic populations (Powell *et al.* 1952; Parker and Tunnicliffe, *submitted*). Data were collected on three cruises during the summers of 1990-1992 as part of the Cobb Seamount Experiment (CSEX), a multidisciplinary program designed to study physical-biological coupling at shallow seamounts. The main goal of the thesis is to test the hypothesis that the high productivity of shallow seamounts results from a long causal chain of events,

Figure 1: Schematic map of the North Pacific Ocean, showing major oceanographic features and the location of Cobb Seamount (After Favorite *et al.*, 1976).

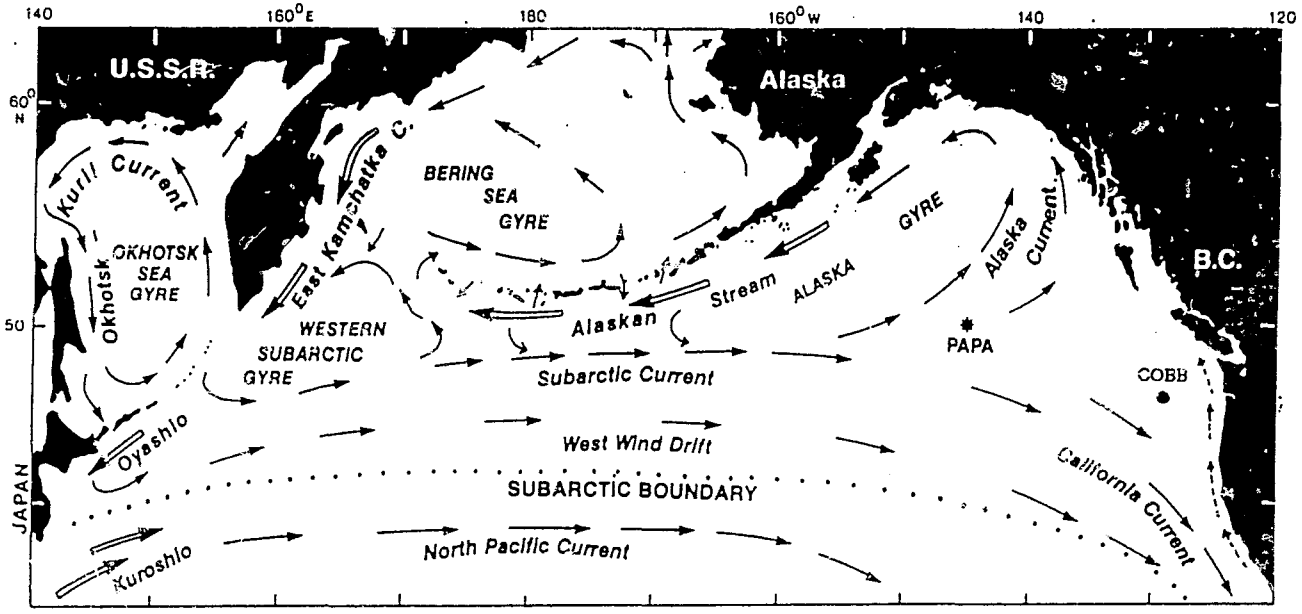
140
160°E
180
160°W
140
120
60°N
50
U.S.S.R.
Alaska
B.C.
Kuril Current
Okhotsk
OKHOTSK SEA GYRE
East Kamchatka C.
BERING SEA GYRE
ALASKA GYRE
Alaska Current
Stream
Alaskan
WESTERN SUBARCTIC GYRE
Subarctic Current
PAPA
COBB
Oyashio
West Wind Drift
SUBARCTIC BOUNDARY
California Current
JAPAN
Kuroshio
North Pacific Current

beginning with the enhancement and isolation of primary production by a recirculating current and leading to the production of high nektonic biomass.

Chapter 1 provides a brief review of the physical oceanographic literature on flow past seamounts. This review provides a framework within which subsequent chapters dealing with various biological questions are set. Chapter 1 also looks in detail at the mesoscale hydrographic structure near Cobb Seamount during the CSEX cruises. Chapters 2-4 explore the response of the planktonic community to flow over Cobb. Specifically, Chapter 2 (published in *Deep-Sea Research* in 1992) deals with the formation of regions of persistently high chlorophyll water over Cobb Seamount. Chapter 3 examines how spatial patterns and composition of the mesozooplankton community are affected by passage over the seamount.

In Chapter 4, I combine the results from the previous chapters with other data collected during the CSEX program to formulate a mathematical ecosystem model simulating the passage of a parcel of water over Cobb Seamount. I use the model in a series of mathematical experiments to explore further the planktonic food web structure and the persistence of high chlorophyll conditions near Cobb. Results from the modelling exercise are also used to address the broader issue of how nektonic stocks are maintained at shallow seamounts.

I should point out that the ordering of Chapters 2-4 reflects the fact that this thesis evolved over three field seasons and, in large part, through the exchange of ideas between biologists and physicists. It was the finding of the strong phytoplankton response during the 1990 CSEX cruise (Chapter 2) that led me to look more closely at patterns in the zooplankton community during the 1991 and 1992 cruises (Chapter 3). Finally, the model presented in Chapter 4 was developed after the final CSEX cruise, in 1992, as a means of integrating what had been learned about the biological community at Cobb with what the physicists had learned about the flow regime near the seamount.

Chapter 1

CURRENT-TOPOGRAPHY INTERACTIONS: THEORETICAL BACKGROUND AND HYDROGRAPHIC OBSERVATIONS FROM COBB SEAMOUNT

Seamount flow phenomena fall into two broad groups: those associated with the formation of recirculating currents (*i.e.* Taylor cones), and those associated with internal wave features. Roden (1987) provides an extensive review of both theoretical and observational studies of these phenomena. More recently, Smith (1991), Chapman and Haidvogel (1992) and Haidvogel *et al.* (1993) have used numerical models to simulate Taylor cone formation and flow patterns around very tall seamounts (*i.e.* fractional height >0.9) in stratified flows. Here, I summarize the findings of these and a few other key studies, focusing specifically on those phenomena most likely to be of importance to biological communities over shallow seamounts.

1.1 Physical Considerations

1.1.1 Taylor Cone Formation

Taylor cones are closed anticyclonic vortices that form as a consequence of flow past abrupt topography. Numerous laboratory and field studies have noted such anticyclonic motions over seamounts. In some cases, only an anticyclonic deflection of the current occurs (Vastano and Warren, 1976; Roden 1984; Roden and Taft, 1985). In other cases, fully

closed anticyclonic vortices (*i.e.* Taylor cones) are observed over the topography (Meincke, 1971; Owens and Hogg, 1980; Davies et al., 1990; Freeland, *submitted*).

Seamounts can be considered as abrupt topographies embedded in an otherwise relatively flat surface and overlain by a stratified rotating flow. Most seamounts have diameters on the order of 10-200km. Therefore, a particle travelling in a 10cm/s current requires ~2-20 days to transit such a feature (Roden, 1987). Taking a mid-latitude seamount at 45°N, the approximate latitude of Cobb Seamount, the Coriolis parameter, f, is $2\Omega\sin\phi = \sim 10^{-4}$ rad•sec^{-1}, giving an inertial period of $2\pi/f$ = 17 hours. Since typical transit times are >17 hours, oceanic flow past seamounts is therefore dominated by rotational (*i.e.* Coriolis) forces (Roden, 1987). At the same time, however, the horizontal scale of most seamounts is small enough that the latitudinal variation in f can be ignored. Consequently, theoretical considerations of flow past seamounts generally use an f-plane approximation in which f is held constant.

Consider a steady oceanic current as it approaches a seamount. By virtue of being on a rotating planet this current has a spin, f, known as the Coriolis parameter or *planetary* vorticity. However, the current also has rotational motion relative to that of the earth, a *relative* vorticity, denoted ζ (Roden, 1987). The sum of f and ζ scaled against the water depth, D, yields a quantity, Q,

known as the potential vorticity, defined as $Q = (f+\zeta)/D$. Hogg (1973) shows that for flow in a frictionless fluid, Q is conserved.

Away from the seamount, the water depth remains large and fairly constant. As the current approaches the leading edge of the seamount, however, D begins to decrease. Recall that f can be considered constant over the horizontal scales of most seamounts. From the above equation it can be seen that if Q is to be conserved, then the relative vorticity, ζ, must decrease (Roden, 1987). To decrease ζ, the fluid must generate *negative* relative vorticity. As the earth's rotation is counterclockwise (*i.e.* cyclonic), the generation of negative relative vorticity implies rotation in a clockwise (*i.e.* anticyclonic) direction.

Most laboratory studies have dealt with situations in which there is no vertical stratification of the water column (Johnson, 1982; Verron and LeProvost, 1985). Under these conditions, the vertical motion and anticyclonic vorticity produced as the fluid impinges on the seamount penetrate all the way to the surface. In such cases, the closed anticyclonic flow is termed a Taylor *column* (Roden, 1987). As ocean waters are usually vertically stratified, however, Taylor *columns* are unlikely in the real ocean.

For the more realistic situation in which the water column is vertically stratified, Hogg (1973) shows that Taylor columns are of only limited height, as the

stratification damps out much of the vertical and clockwise motion. Therefore, the recirculating flows reported from field studies near seamounts take the form of a bottom-intensified cone, which Hogg (1973) calls a Taylor cone. Along with the degree of stratification, Taylor cone formation is controlled by two other parameters: (i) the upstream velocity, U, and (ii) the fractional height of the seamount, $\delta = h/H$, where h is the seamount height and H is the depth of the water column (Chapman and Haidvogel, 1992).

The effect of increasing U is to increase Ro, the Rossby number, where $Ro = U/fL$, f is the Coriolis parameter and L is the horizontal length scale of the seamount. Ro is a measure of the relative importance of advective versus rotational forces (Chapman and Haidvogel, 1992). As Ro increases, advective forces become more important. Boyer and Zhang (1990) show that for a seamount with $\delta = 0.7$, a Taylor cone remains centred over the seamount when the upstream flow is very weak (*i.e.* $Ro \leq 0.01$) . For moderate flows, with $0.01 \leq Ro \leq 0.1$, the Taylor cone is displaced into the lee of the seamount until, for strong flows with $Ro \geq 0.1$, the Taylor cone actually separates from the seamount and is advected downstream. Under such conditions a "vortex street" of alternating cyclonic and anticyclonic eddies extends downstream of the seamount (Davies et al., 1990; Boyer and Zhang, 1990). Schematic representations of these three regimes are shown in Figure 2.

Figure 2: Interpretive sketches of the three seamount flow regimes observed experimentally by Boyer and Zhang. (A) Fully attached flow in which a Taylor cone is centred over the seamount, and Ro = 0.01, (B) Attached leeside eddies, with Ro = 0.07, and (C) Eddy shedding regime, with Ro = 0.18, in which alternating cyclonic and anticyclonic eddies are advected away from the seamount. The columns show the development of each flow regime over time, in an oscillating flow (From Boyer and Zhang, 1990).

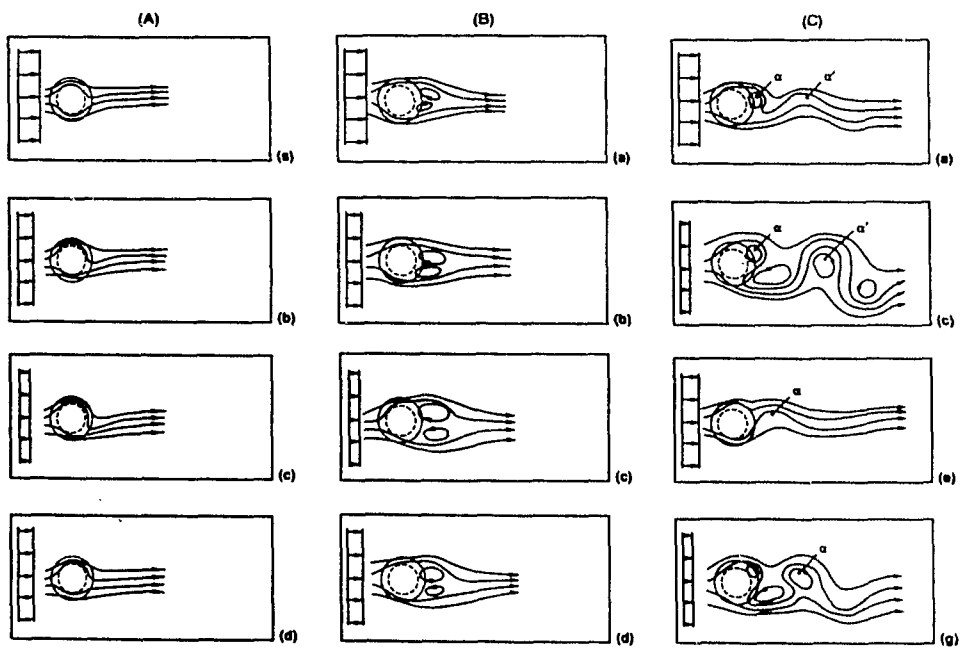
(A)
(B)
(C)
α
α'
(a)
(b)
(c)
(d)
(e)
(g)

Chapman and Haidvogel (1992) find that the critical *Ro* number at which Taylor cones can exist varies with δ. Specifically, as seamount amplitude increases, the critical *Ro*, beyond which the Taylor cone detaches from the seamount, also increases. For low amplitude seamounts (*i.e.* $\delta \leq 0.4$), this critical *Ro* number is ~0.8. With very high amplitude seamounts like Cobb ($\delta \geq 0.9$) they find that Taylor cones occur in flows with $Ro \leq 0.15$. For a mid-latitude seamount of diameter 30km (approximate size of Cobb), $Ro \leq 0.15$ for flows less than ~45cm/s.

1.1.2 Isopycnal/Isothermal Doming

Another consequence of flow over an abrupt topography such as a seamount is a distortion of the local density field, that results from vortex compression over the obstacle (Hogg, 1973; Owens and Hogg, 1980). Depending on whether density or temperature is being measured, this phenomenon is referred to either as isopycnal or isothermal doming. The result is that as a current impinges on a seamount slope, some of the water is uplifted as it passes over the obstacle. Consequently, water at a given depth over a seamount is often colder than the surrounding waters, as a result of having been uplifted along the seamount flank. As with Taylor cone generation, however, the vertical penetration of the "cold dome" is limited by the degree of stratification of the water column.

One of the earliest reports of doming is from Great Meteor Seamount, where Meincke (1971) notes isothermal doming of ~100m. Since then, other studies have detected similar cold domes over seamounts, with typical penetration heights of 100-300m (Vastano and Warren, 1976; Roden and Taft, 1985; Genin and Boehlert, 1985, Agapitov and Gritsenko, 1988). Surveys from smaller topographies, <1000m in height, show doming of >500m (Owens and Hogg, 1980; Gould *et al.*, 1981), presumably because the stratification at abyssal depths is weaker than in near-surface waters.

In none of these cases, including those from very shallow seamounts, has a cold dome been shown to penetrate to the sea surface. In fact, Genin (1990) suggests that doming events over seamounts may not be as common as is currently believed. From a collection of eighteen hydrographic surveys from ten North Pacific seamounts, Genin notes that only about half show clear evidence of a cold dome over the seamount. As with Taylor cone formation, the degree of doming depends on the strength of the upstream flow and the degree of stratification. Consequently, Taylor cones and associated doming are more likely to occur over seamounts situated in steady currents than over seamounts in very weak, variable flows. As Genin's (1990) brief note does not specify the hydrographic settings of the seamounts in question, it is therefore difficult to weigh the importance of his conclusion.

1.1.3 Internal Wave Phenomena

Enhanced internal wave activity has been observed over a number of seamounts (Roden, 1987). As with other types of waves, when an internal wave meets a solid barrier, the wave energy is reflected away from the barrier such that the angle of reflection equals the incident angle (relative to the horizonatal). However, as the slope of the internal wave ray approaches the slope defined by the barrier (in this case the seamount flank), rather than being reflected away from the seamount, the internal wave energy is reflected parallel tc the bottom (Eriksen, 1982; Gilbert and Garrett, 1989).

Internal waves generally have steeper slopes than most gently sloping topographies, such as continental slopes. Huthnance (1981) shows that this leads to an essentially free exchange of most internal waves across continental slopes. Over an abrupt topography such as a seamount, however, the bottom slope is not only quite steep but, due to features such as terraces and outcrops, can be locally quite variable. This steep topography and small-scale irregularity increases the likelihood that the slope of a given internal wave will be near the critical slope at which wave energy is reflected parallel to the bottom rather than away from it (Eriksen, 1982, 1985; Boehlert and Genin, 1987, Gilbert and Garrett, 1989).

Apart from a general increase in internal wave energy,

other internal wave phenomena have also been detected near seamounts. Noble *et al.* (1988) and Noble and Mullineaux (1989) report strong semidiurnal internal tides over Horizon Guyot and Cross Seamount in the Hawaiian Islands. Similarly strong tidal currents are noted by Genin *et al.* (1990) from Fieberling Guyot, 800km west of San Diego. In each case, the currents produced by these internal tides (up to ~7cm/s) are 2-4 times higher than those predicted for the surrounding oceans. It appears that these internal tides are generated over the seamounts, probably near regions of very abrupt slope break. This mechanism may explain an earlier report of unusually high diurnal tides at Cobb Seamount (Larsen and Irish, 1975).

Brink (1989, 1990) suggests that these internal tides can excite a new class of topographically trapped waves, which he calls seamount trapped waves. These subinertial bottom-trapped waves, which propagate *around* seamounts, are similar to the coastally trapped Kelvin waves discussed by Huthnance (1981) and documented by Hogg (1980) around Bermuda. Recently, seamount trapped waves have been identified from an intensive 72 hour ADCP survey carried out over Cobb in the fall of 1991 (Codiga, *pers. comm.*).

1.2 Mesoscale Hydrography Near Cobb Seamount

1.2.1 Physiographic Setting

Cobb Seamount (46°46'N, 130°48'W), located 500km southwest of Vancouver Island (Fig.1), forms the southern end of the Cobb-Eickelberg seamount chain, one of the two main seamount chains in the Northeast Pacific (Davis and Karsten, 1986). From a 30km diameter base at 2800m, Cobb rises with an average slope of 12° to a shallowest depth of only 24m (See Frontispiece for detailed view). The main summit of the seamount, however, is a relatively flat terrace that extends from 100-250m depth, since the pinnacle that approaches the surface is only about 200m x 400m. The main summit has a diameter of about 10km.

Potassium-Argon dating and the composition of summit basalts suggest that Cobb formed ~1.5 million years ago and originally stood at least 300m above sea level (Dymond *et al.* 1968, Merrill and Burns, 1972). Rounded basaltic pebbles and a steep wave-cut terrace at a present depth of 310m also support the contention that the summit formed subaerially (Farrow and Durant, 1985). Wave-cut terraces at shallower depths were probably produced as the seamount subsided (~260m) and sea level fluctuated during subsequent Quaternary glacial/interglacial episodes (Farrow and Durant, 1985).

1.2.2 Regional Oceanographic Setting

Cobb is situated near the boundary between the North Pacific Transition Zone (NPTZ hereafter) and the subarctic Pacific (Fig. 1). The NPTZ is formed by the Subarctic Current (*aka* West Wind Drift) which flows eastward across the North Pacific at an average velocity of ~10cm/s (McNally *et al.*, 1983). As it nears the west coast of North America, the Subarctic Current splits into the northward flowing Alaska Current and the southward flowing California Current (Uda, 1963; Dodimead *et al.* 1963). Recent satellite-tracked drifter buoy data suggest that Cobb is positioned near the point where this bifurcation takes place (Freeland, *submitted*). However, interannual variation in the latitudinal position of the NPTZ (Uda, 1963) makes it difficult to determine whether the waters around Cobb are best characterized as subarctic or transitional. While this distinction may seem trivial, it may nonetheless have important biological consequences.

Dissolved nutrient concentrations differ between the subarctic Pacific and the NPTZ. The subarctic Pacific has been identified as one of three oceanic regions characterized by persistent excess nutrients and low phytoplankton stocks. These areas have come to be termed high-nutrient-low-chlorophyll (HNLC) regions (Cullen, 1991). The debate over whether phytoplankton growth in HNLC regions is limited by the availability of a micronutrient such as

iron (*sensu* Martin *et al.*, 1991) or by grazing pressure (Miller *et al.*, 1991; Frost, 1991) remains unresolved. By comparison, NPTZ waters are more similar to the oligotrophic conditions of the subtropical North Pacific, where nutrient levels in the surface waters drop below detection limits during the summer (Levitus *et al.*, 1993).

A common element of most hypotheses explaining the high productivity of shallow seamounts is that phytoplankton growth is enhanced by nutrient injection via doming/upwelling (Boehlert and Genin, 1987). Since added nutrients are more likely to affect primary production in oligotrophic NPTZ waters than in the subarctic Pacific, knowledge of where the northern boundary of the NPTZ is located can provide clues as to the expected biological response to flow past Cobb Seamount. This information is also central to the choice of parameters used to formulate the model presented in Chapter 4.

Freeland *et al.* (1984) state that the Subarctic Current lies between 45°-50°N as it approaches the North American coast. However, other studies put the northern edge of the NPTZ further south, at about 42°-45°N (Uda, 1963; McNally *et al.*, 1983; Talley *et al.* 1991). The only work to specifically study the NPTZ was carried out by Roden in the early 1970's. Based on temperature-salinity characteristics, Roden (1970, 1972) shows that in the western and central North Pacific, the boundary between NPTZ

and subarctic waters occurs near 42°N. Near the North American coast this boundary turns southeastward so that near 130°W, the approximate longitude of Cobb Seamount, it lies near 40°N (Roden, 1971).

Since Cobb is located at ~47°N, hydrographic conditions near the seamount should be more subarctic than transitional. Salinity profiles collected during the CSEX cruises support this idea. Subarctic waters are identifiable by (i) a near-isohaline layer between 0-100m depth, with salinities <33o/oo, and (ii) a strong permanent halocline extending from 100-250m (Uda, 1963). Crossing from subarctic into NPTZ waters, the halocline begins to erode until, at the southern NPTZ boundary, the water column is isohaline ~200m (Uda, 1963; Roden 1971, 1972).

Figure 3 shows that both the near-surface isohaline layer and the permanent halocline are well developed near Cobb. Additionally, surface salinities near the seamount, ~32.5 o/oo, are lower than the 33.6-33.7 o/oo usually encountered in NPTZ waters during the summer. Low surface salinities are found throughout the southeast corner of the subarctic Pacific, in a region termed Dilute Domain (Favorite *et al.*, 1976), due to freshwater inputs from the Columbia River, the Strait of Juan de Fuca, Queen Charlotte Sound and Dixon Entrance (Fig.4). From this evidence, it is concluded that the waters around Cobb should be considered subarctic, rather than transitional.

Figure 3: Typical temperature, salinity and T-S plots from the three CSEX cruises. Note the near-surface isohaline layer at 0-25m and the main halocline between 100-250m. The QED cast is a reference cast collected 900km northwest of Cobb during CSEX91. With the exception that temperatures at the QED site were about 2°C colder, note the similarity in structure between the CSEX casts and this cast from deep within the subarctic Pacific.

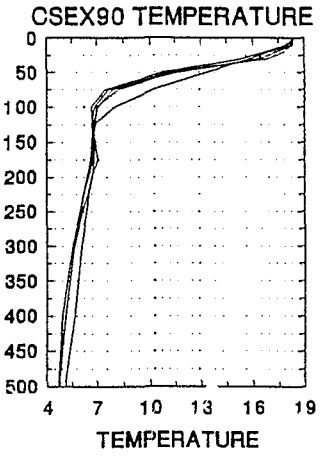
CSEX90 TEMPERATURE
0
50
100
150
200
250
300
350
400
450
500
4 7 10 13 16 19
TEMPERATURE

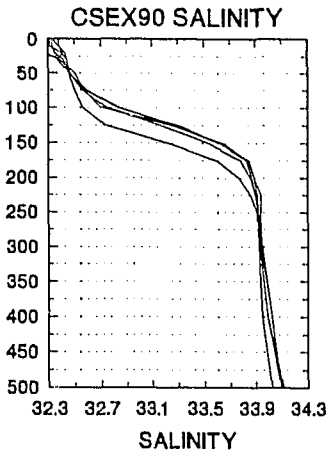
CSEX90 SALINITY
0
50
100
150
200
250
300
350
400
450
500
32.3 32.7 33.1 33.5 33.9 34.3
SALINITY

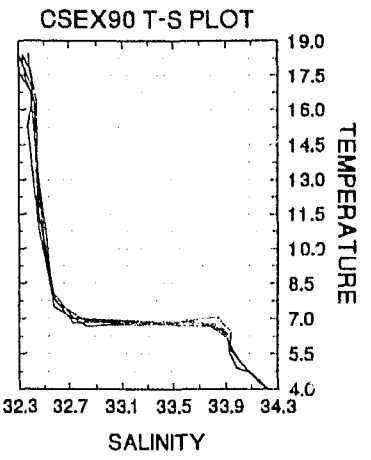
CSEX90 T-S PLOT
19.0
17.5
16.0
14.5
13.0
11.5
10.0
8.5
7.0
5.5
4.0
TEMPERATURE
32.3 32.7 33.1 33.5 33.9 34.3
SALINITY

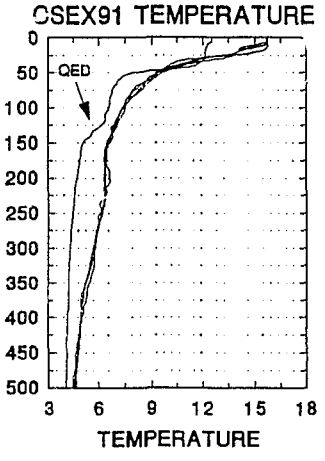
CSEX91 TEMPERATURE
QED
0
50
100
150
200
250
300
350
400
450
500
3 6 9 12 15 18
TEMPERATURE

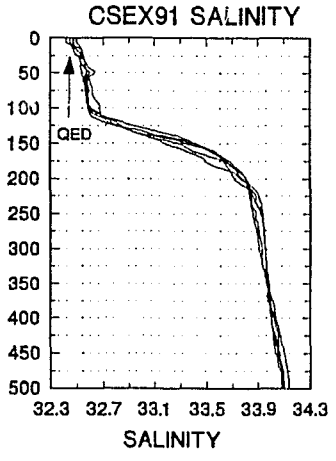
CSEX91 SALINITY
QED
0
50
100
150
200
250
300
350
400
450
500
32.3 32.7 33.1 33.5 33.9 34.3
SALINITY

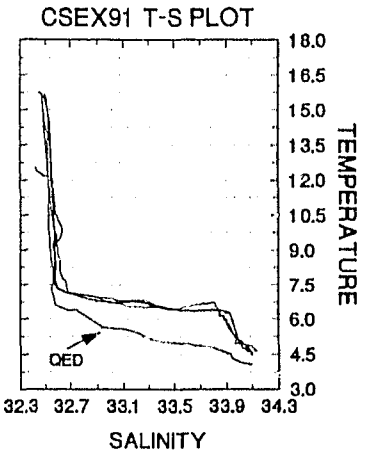
CSEX91 T-S PLOT
QED
18.0
16.5
15.0
13.5
12.0
10.5
9.0
7.5
6.0
4.5
3.0
TEMPERATURE
32.3 32.7 33.1 33.5 33.9 34.3
SALINITY

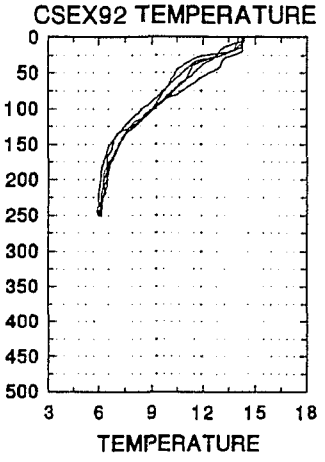
CSEX92 TEMPERATURE
0
50
100
150
200
250
300
350
400
450
500
3 6 9 12 15 18
TEMPERATURE

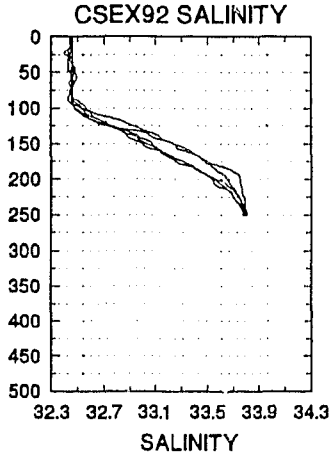
CSEX92 SALINITY
0
50
100
150
200
250
300
350
400
450
500
32.3 32.7 33.1 33.5 33.9 34.3
SALINITY

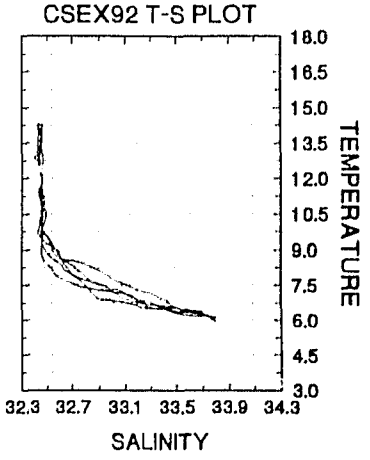
CSEX92 T-S PLOT
18.0
16.5
15.0
13.5
12.0
10.5
9.0
7.5
6.0
4.5
3.0
TEMPERATURE
32.3 32.7 33.1 33.5 33.9 34.3
SALINITY

Figure 4: Location and extent of the Dilute Domain as indicated by the salinity distribution at 100m (from Favorite et al., 1976)

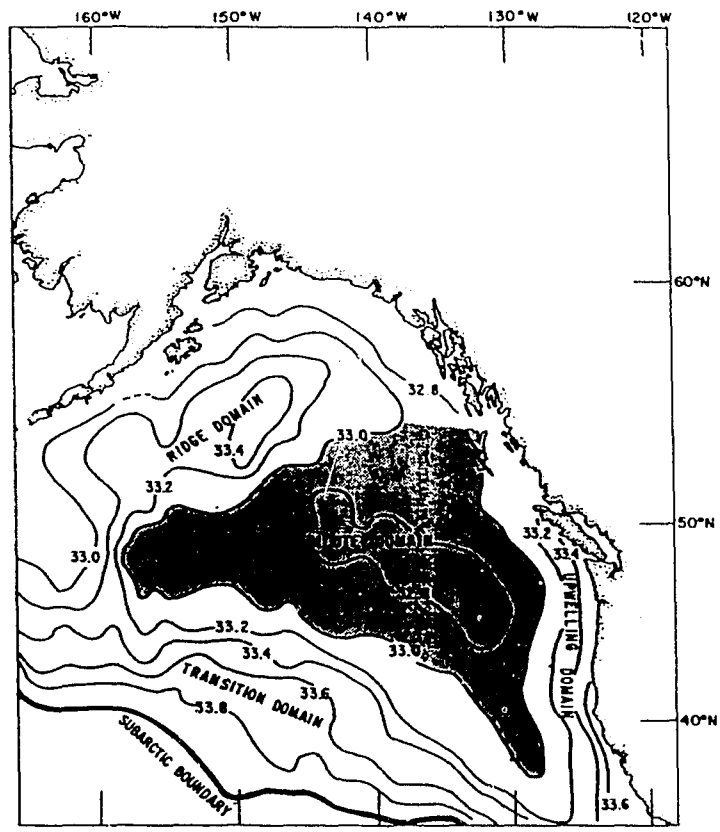

FIGURE 37. Location and extent of the Dilute Domain as indicated by the salinity distribution at 100 m.

1.2.3 CSEX Hydrographic Sampling

CSEX included three cruises to Cobb Seamount in the summers of 1990-1992. In addition to biological sampling programs (detailed in subsequent chapters), each cruise included an intensive hydrographic survey. These surveys provide (i) regional oceanographic data and (ii) detailed information on mesoscale perturbations to the hydrographic field, associated with flow past Cobb. Sampling details for the three cruises are detailed in the Appendix.

Hydrographic data were collected using a Conductivity-Temperature-Depth (CTD) sensor. During CSEX90, vertical casts to 1000m were carried out using a Guildline digital CTD fitted with a 25cm-path Seatech transmissometer. Water samples for dissolved nutrient analyses were collected using Niskin bottles. For the CSEX91 and CSEX92 cruises, a rosette water sampling system and an *in situ* fluorometer were added to the basic CTD/transmissometer package. Vertical profiles were to 500m depth in 1991 and to 250m depth in 1992 (a light sensor on the CTD in 1992 was only rated to 300m).

Current meters were also deployed on Cobb during each CSEX cruise. Freeland (*submitted*) describes the near-field flow regime around Cobb using data from the current meters, satellite-tracked drifter buoys, plus two Acoustic Doppler Current Profiler (ADCP) surveys. As this work is central to our understanding of current-topography interactions at

Cobb, I will briefly summarize Freeland's findings before moving on to a discussion of the mesoscale hydrographic structure near the seamount.

1.2.4 Circulation Around Cobb Seamount

Freeland (*submitted*) demonstrates that a bottom-intensified Taylor cone does exist over Cobb Seamount. Current meters deployed 3m, 10m and 50m above bottom show currents flowing around the seamount in a clockwise direction with maximum speeds of 12cm/s. At the same time, satellite-tracked drifter buoys drogued to follow near-surface flow were released over the seamount. These drifters moved rapidly off the seamount at speeds of about 10-15cm/s, showing no evidence of a recirculating flow in the surface layer (Dower *et al.* 1992). ADCP surveys in 1990 and 1991 show that anticyclonic motion first appears over the seamount at a depth of about 80m and is fully developed into a closed anticyclonic streamline by 120m depth. Together, these observations indicate a Taylor-cone that penetrates about 80-100m above the summit of Cobb Seamount and to within ~100m of the surface (Freeland, *submitted*). These data also suggest that the Taylor cone may be a *permanent* feature at Cobb.

The flow regime is complicated, however, by the fact that the currents recorded by the deepest current meters (*i.e.* 3m above bottom) are rotated off-seamount relative to

currents higher in the water column. Freeland (*submitted*) explains that this results from the anticlockwise rotation induced by a bottom Ekman layer. This presents a problem in that an off-seamount flow in the near-bottom layer implies a compensatory inflow somewhere else in the water column. Similar near-bottom outflows have been observed on Fieberling Guyot (Codiga, *pers. comm.*) but the problem of return flow has yet to be treated in the seamount literature.

Freeland suggests that an inflowing current could result from either (i) a convergent flow of about 0.3cm/s over the entire height of the Taylor cone or (ii) an upslope flow within the bottom Ekman layer itself. Results from a turbulence study conducted during CSEX92 show anomalously low temperatures within 1-2m of the bottom (R. Lueck and T. Mudge, *pers. comm.*). Freeland cites this as evidence that upslope flow *is* occurring in the bottom layer, but below the depth monitored by the deepest current meters. The existence of such inflows and outflows raises an interesting point as it implies that, rather than being trapped, the water in a Taylor cone is flushed out over some period of time. A flushing time of about 17 days is calculated for the dimensions of the Taylor cone at Cobb (Freeland, *submitted*). The biological implications of such a flushing mechanism are considered in Section 1.3.1.

1.2.5 Thermohaline Structure Around Cobb Seamount

a) Vertical Structure: Figures 5-7 show the near-surface distributions of temperature, salinity and density along west-east sections over Cobb Seamount during CSEX90, 91 and 92, respectively. I begin with the CSEX92 data (Fig.7), as this hydrographic survey was larger than the others and therefore provides the best regional picture.

West of Cobb Seamount, conditions during 1992 were typical of those described for the southern subarctic during the summer months (Uda, 1963; Favorite *et al.*, 1976). Figure 7a shows surface temperatures of 14°C. Below this, temperatures in the main thermocline decrease steadily, from ~13°C at 25m to ~8°C at 125m. The top of the permanent halocline is encountered at 90m, and extends past the bottom of the section at 200m.

A region of isopycnal/isothermal doming is evident, beginning about 30km west of the Cobb summit. Isotherms/isopycnals are also more widely spaced in this region, perhaps indicating an increase in turbulent mixing in this region as well. Doming amplitude increases eastward and, rather than being centred over the seamount, is strongest about 30km east of the summit. Similar offsets have been noted over some of the Emperor Seamounts (Roden and Taft, 1985) where cold domes can be displaced by as much as 50-100km downstream of seamount summits. Such downstream displacements are reminiscent of Boyer and Zhang's (1990)

Figure 5: Vertical sections of temperature, salinity and density (as sigma-t) along a 55km west-east transect over Cobb Seamount during CSEX90.

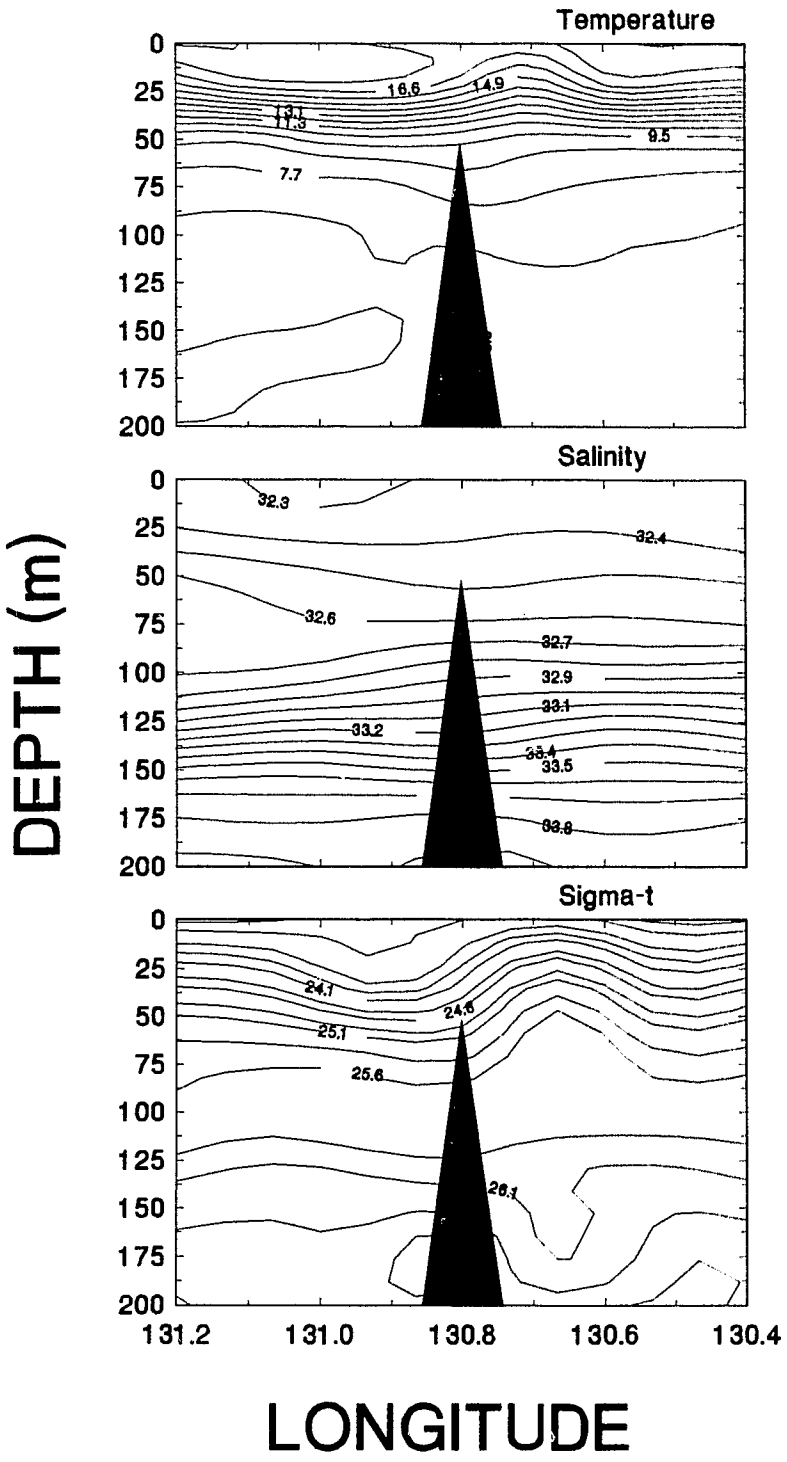
Temperature
16.6
14.9
13.1
11.3
9.5
7.7
Salinity
32.3
32.4
32.6
32.7
32.9
33.1
33.2
33.4
33.5
33.6
Sigma-t
24.1
24.6
25.1
25.6
26.1
0
25
50
75
100
125
150
175
200
DEPTH (m)
131.2
131.0
130.8
130.6
130.4
LONGITUDE

"moderate flow regime", in which Taylor cones move off the summit and into the lee of the seamount (Fig.2b). Heywood *et al.* (1990) note comparable leeward movement of doming regions near atolls in the Indian Ocean.

Figure 7 also shows the doming to be bottom-intensified (*i.e.* vertical displacement of isopycnals decays with height above the seamount). Whereas the 25.05 σ_t contour rises from 100m to ~65m (Fig.7c), shallower isopycnals are uplifted by only 10-20m. Below the top of the halocline at ~90m (Fig.7b), however, vertical perturbations are quite small. For instance, isopycnals between 25.32-26.11 o/oo are uplifted by ≤15m (Fig.7c). It may be that doming in the halocline is damped out by the strong stratification. The cold dome does not penetrate to the surface, and disappears at a depth of about 15m.

Comparing Figures 5 and 6 with Figure 7 shows that hydrographic conditions near Cobb were similar during the three CSEX cruises. The higher surface temperatures recorded during CSEX90 and '91 (17°C and 15.5-16°C) reflect the fact that these cruises took place in July-August, whereas CSEX92 took place in June. As expected in the Dilute Domain (Favorite *et al.*, 1976), surface salinities were <32.5 o/oo during all three CSEX cruises. Values <32.3 o/oo in 1990 may have been caused by increased riverine inputs during 1990 or by coastal waters penetrating further offshore than usual. The top of the permanent halocline is

Figure 6: Vertical sections of temperature, salinity and density (as sigma-t) along a 60km west-east transect over Cobb Seamount during CSEX91.

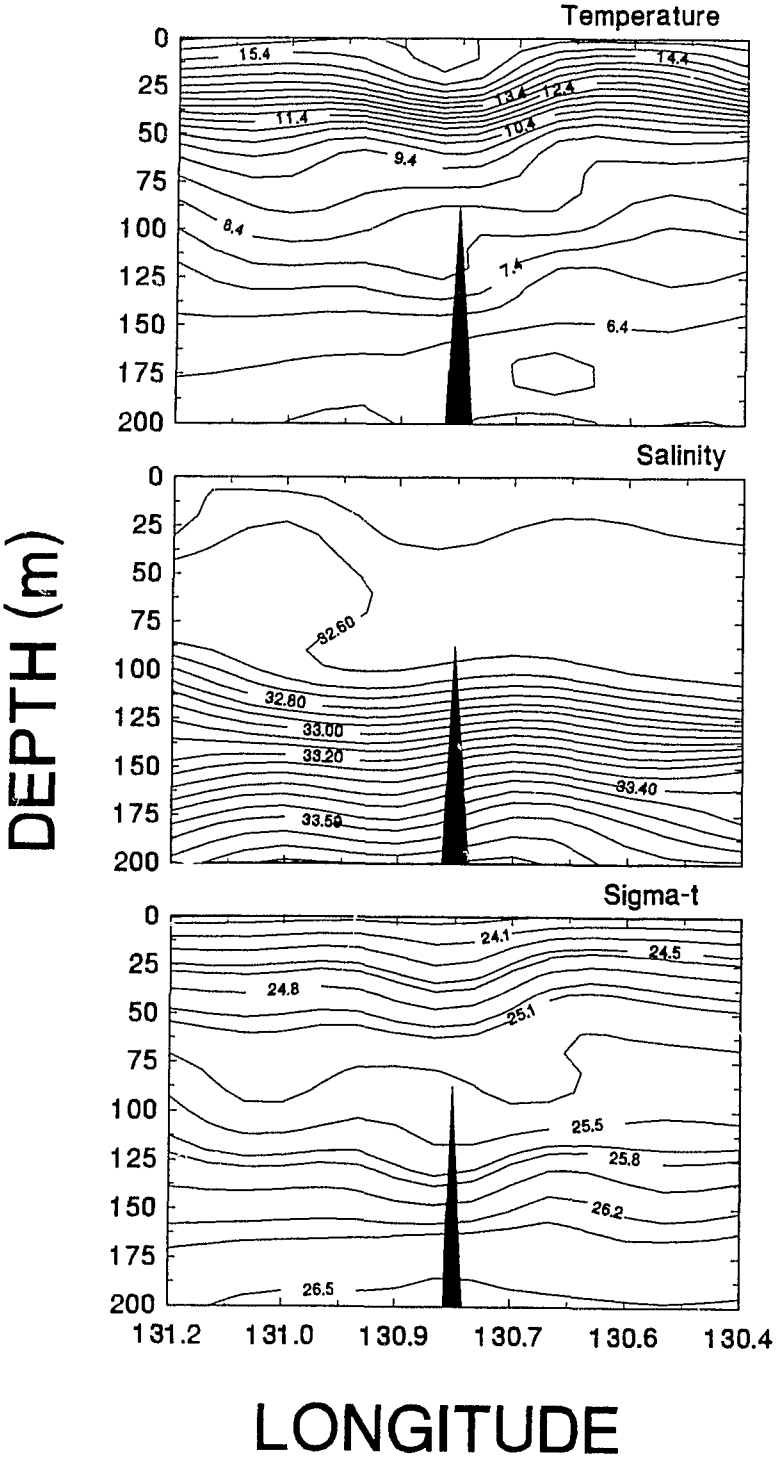
Temperature
15.4
14.4
13.4
12.4
11.4
10.4
9.4
8.4
7.4
6.4
Salinity
32.60
32.80
33.00
33.20
33.40
33.59
Sigma-t
24.1
24.5
24.8
25.1
25.5
25.8
26.2
26.5
0
25
50
75
100
125
150
175
200
131.2
131.0
130.9
130.7
130.6
130.4
DEPTH (m)
LONGITUDE

Figure 7: Vertical sections of temperature, salinity and density (as sigma-t) along a 200km west-east transect over Cobb Seamount during CSEX92.

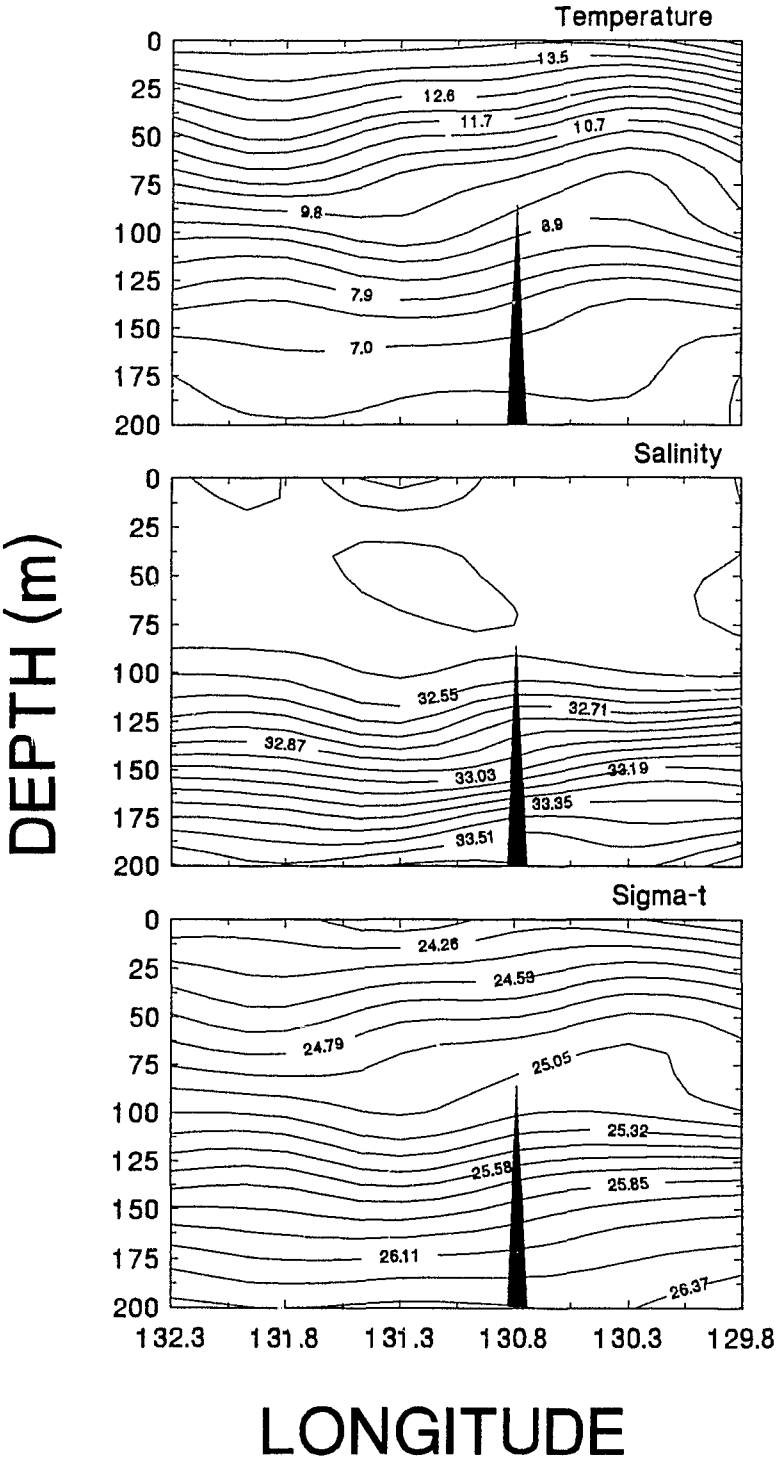
Temperature
13.5
12.6
11.7
10.7
9.8
8.9
7.9
7.0
Salinity
32.55
32.71
32.87
33.03
33.19
33.35
33.51
Sigma-t
24.26
24.59
24.79
25.05
25.32
25.58
25.85
26.11
26.37
0
25
50
75
100
125
150
175
200
DEPTH (m)
132.3
131.8
131.3
130.8
130.3
129.8
LONGITUDE

consistently located at ~100m. Salinity profiles near Cobb show that the base of the halocline occurs between 200 and 225m (Fig.3).

Isopycnal doming is also evident in the 1990 and '91 profiles and, as in 1992, is centred 10-30km east of the seamount summit. Since surface currents in the region are a relatively invariable 10-12cm/s east-southeastward (Freeland, *submitted*), it seems reasonable to expect that doming should occur in roughly the same area each year. The vertical extent of the cold dome in the 1991 profile (Fig.6) is comparable to that observed in 1992: doming decays with height above bottom, and disappears at about 10-15m depth. As in 1992, maximum vertical displacements were 20-30m. Deeper isolines again show reduced doming.

The 1990 profiles differ from the other two years in that doming extends to the sea surface. Figure 5c shows that the $23.45\sigma_t$ contour, that lies at about 10m depth upstream of Cobb, outcrops at the surface over a 20km region east of the pinnacle. A similar effect is visible in the temperature section (Fig.5a). This outcropping of cold water at the surface was not associated with the persistent recirculating flow. During the 1990 cruise, two satellite-tracked drifter buoys that were released within 2km of the pinnacle moved almost directly eastward, showing no evidence of current deflection over the seamount. Likewise, ADCP data collected during CSEX90 indicate that anticyclonic

motion was confined to depths below 80m (Freeland, *submitted*).

One possibility is that the hydrographic section shown in Figure 5 was fortuitously conducted during a brief episode in which the Taylor cone had penetrated to the surface. This idea is supported by an anecdotal report from one of the ship's officers, who claimed that while attempting to hold position over the Cobb pinnacle, the ship began to slowly rotate in a clockwise direction. However brief the episode, this would represent the first report of a Taylor cone penetrating to the surface over a seamount. Whether such episodes are common over Cobb remains unknown. However, several years of remotely sensed sea-surface chlorophyll data (collected with the Coastal Zone Color Scanner) show no evidence of phytoplankton blooms over Cobb (M. Abbott, *pers. comm.*). This suggests that the surface outcropping observed during CSEX90 was probably a rare event, at least during the summer.

b) Horizontal Structure: Figures 8-10 present plan views of temperature, salinity and density at various depths around Cobb Seamount. Overlays are provided to show the approximate location of the 2000m isobath on the seamount. These figures provide a three dimensional picture of the hydrographic regime during the CSEX cruises. In nearly every case, the most prominent feature is a region of cold, salty, dense water situated near Cobb.

Figure 8: Plan views of Temperature at 50m, 100m and 250m (a, b, c respectively), Salinity at 50m, 100m and 250m (d, e, f respectively), and Density (as sigma-t) at 50m, 100m and 250m (g, h, i respectively) during CSEX90. Overlay #1 shows the location of the 2000m isobath on Cobb Seamount.

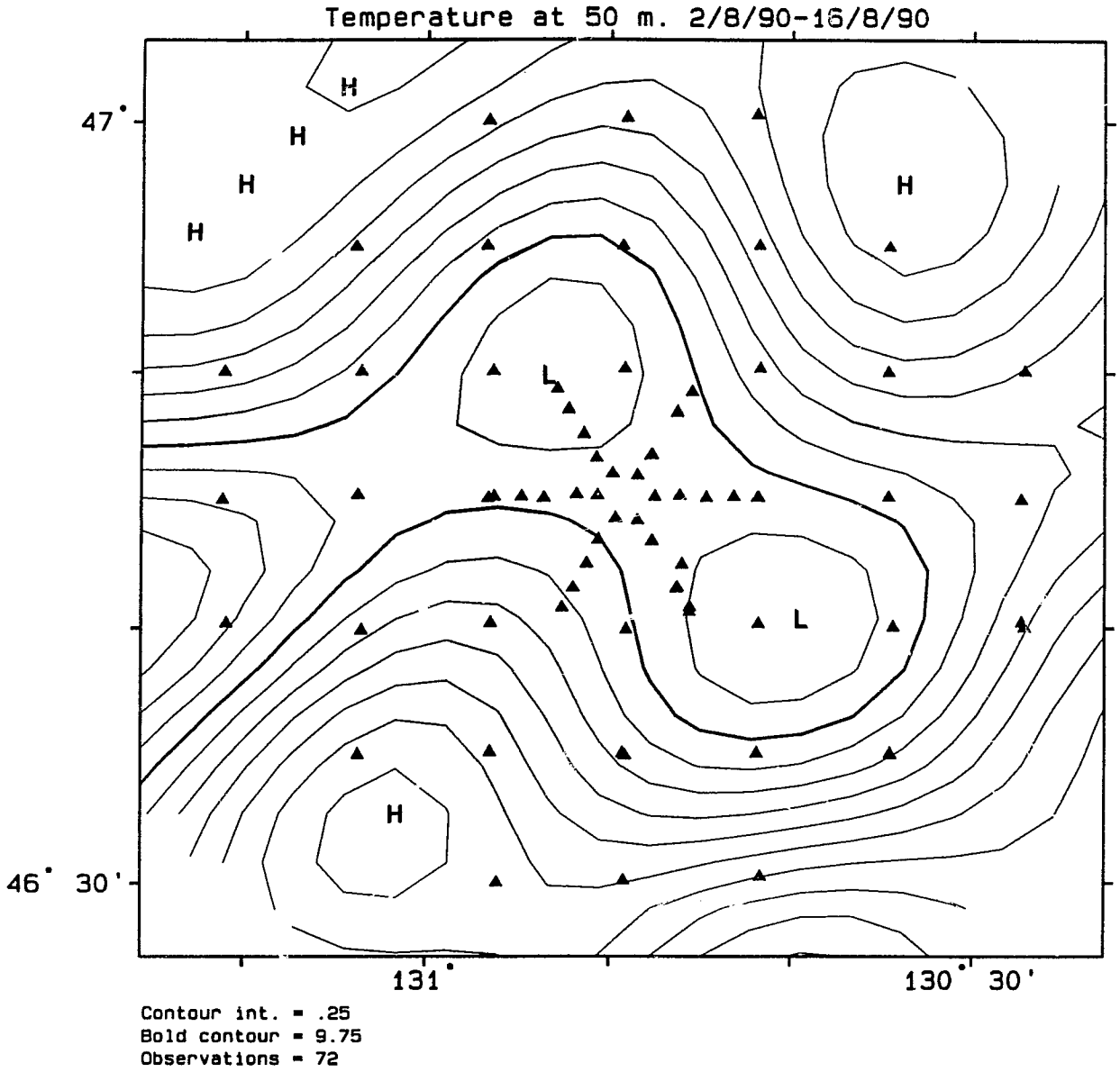
Temperature at 50 m. 2/8/90-16/8/90
8a
47°
46° 30'
131°
130° 30'
H
H
H
H
H
H
L
L
Contour int. = .25
Bold contour = 9.75
Observations = 72

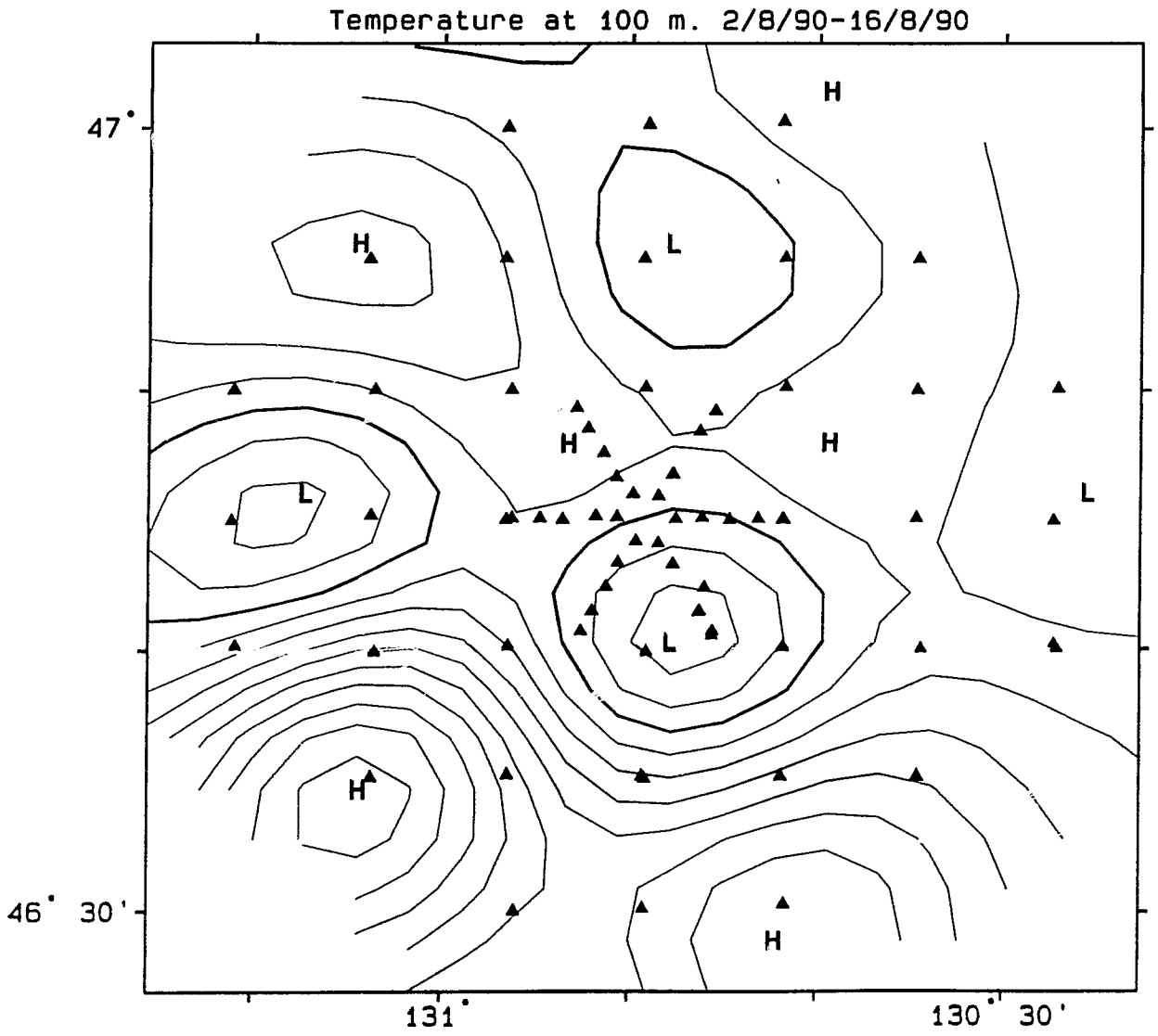
Temperature at 100 m. 2/8/90-16/8/90
8b
47°
46° 30'
131°
130° 30'
H
L
Contour int. = .1
Bold contour = 6.8
Observations = 72

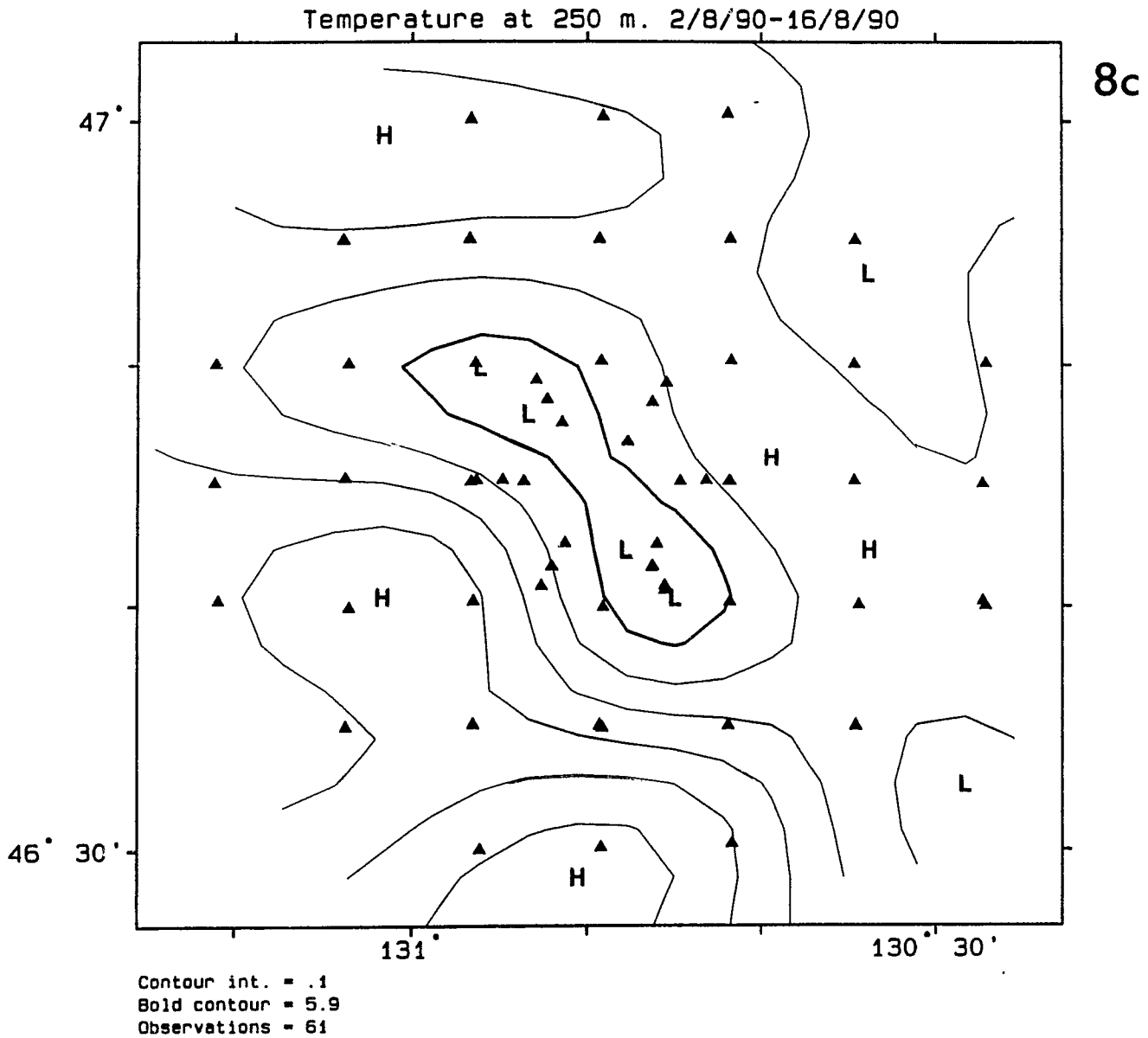
Temperature at 250 m. 2/8/90-16/8/90
8c
47°
46° 30'
131°
130° 30'
H
L
Contour int. = .1
Bold contour = 5.9
Observations = 61

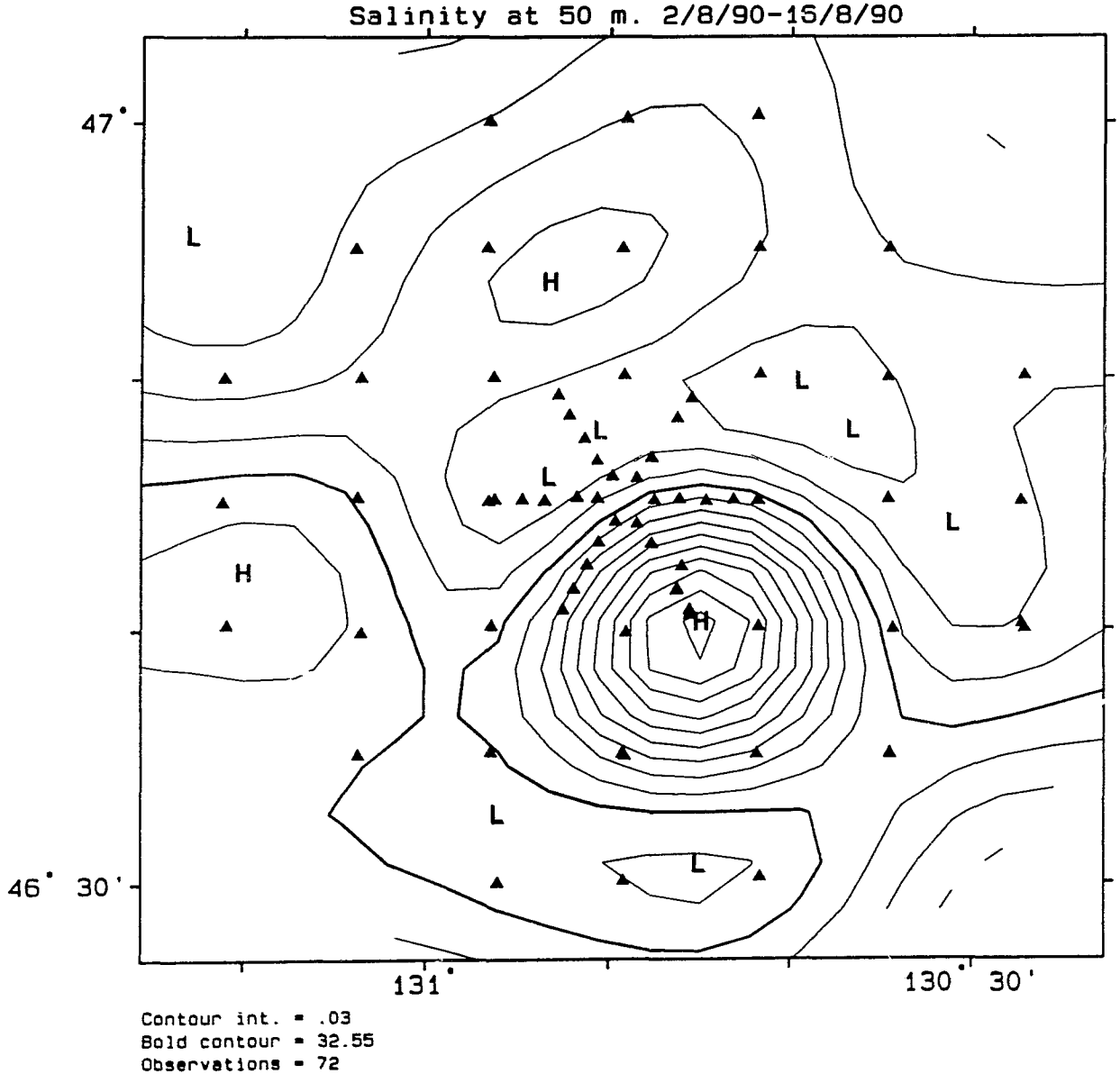
Salinity at 50 m. 2/8/90-15/8/90
8d
47°
46° 30'
131°
130° 30'
L
H
L
L
L
L
L
H
H
L
L
Contour int. = .03
Bold contour = 32.55
Observations = 72

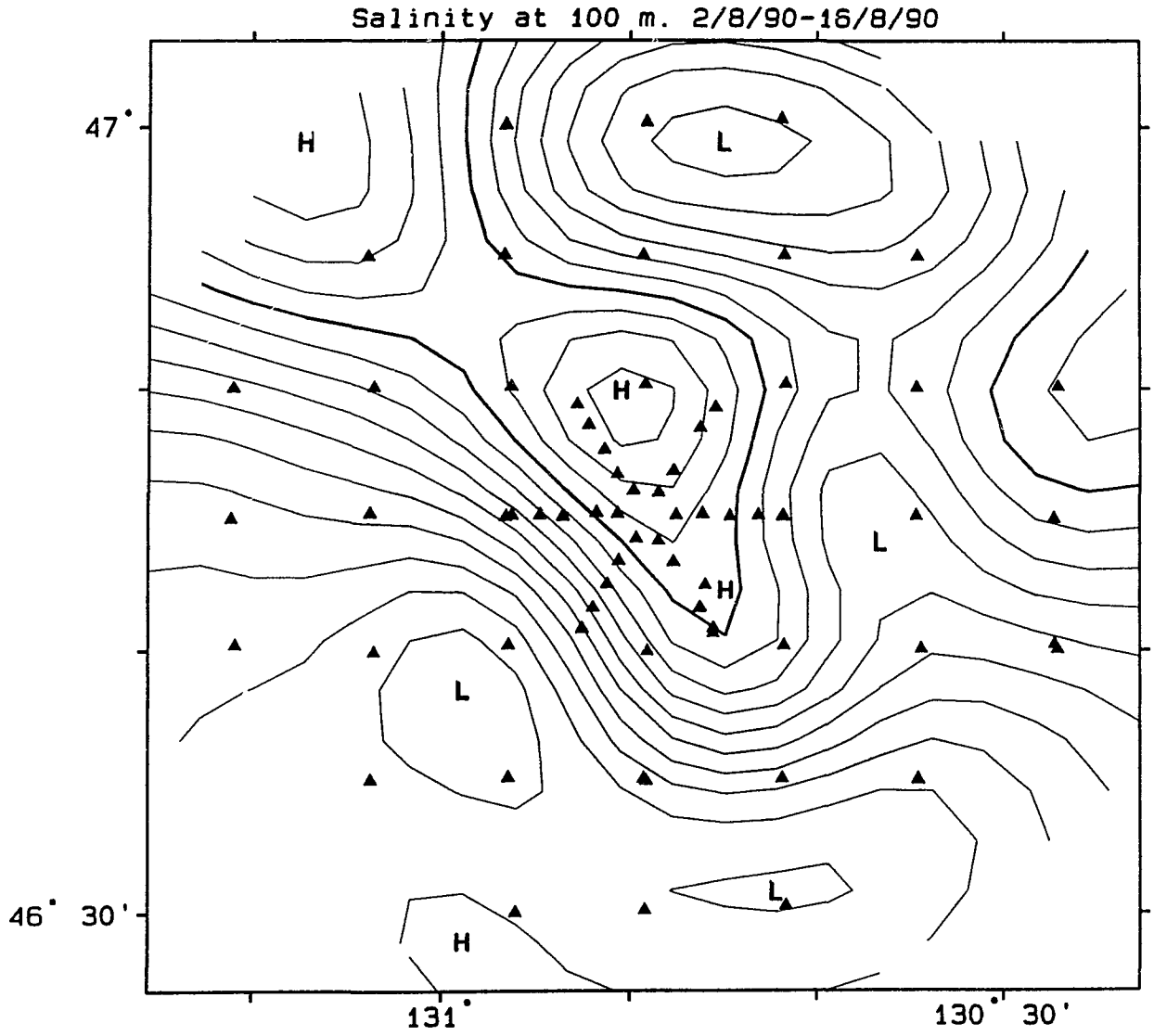
Salinity at 100 m. 2/8/90-16/8/90
47°
46° 30'
131°
130° 30'
H
L
H
H
L
L
L
H
Contour int. = .03
Bold contour = 32.91
Observations = 72

8e

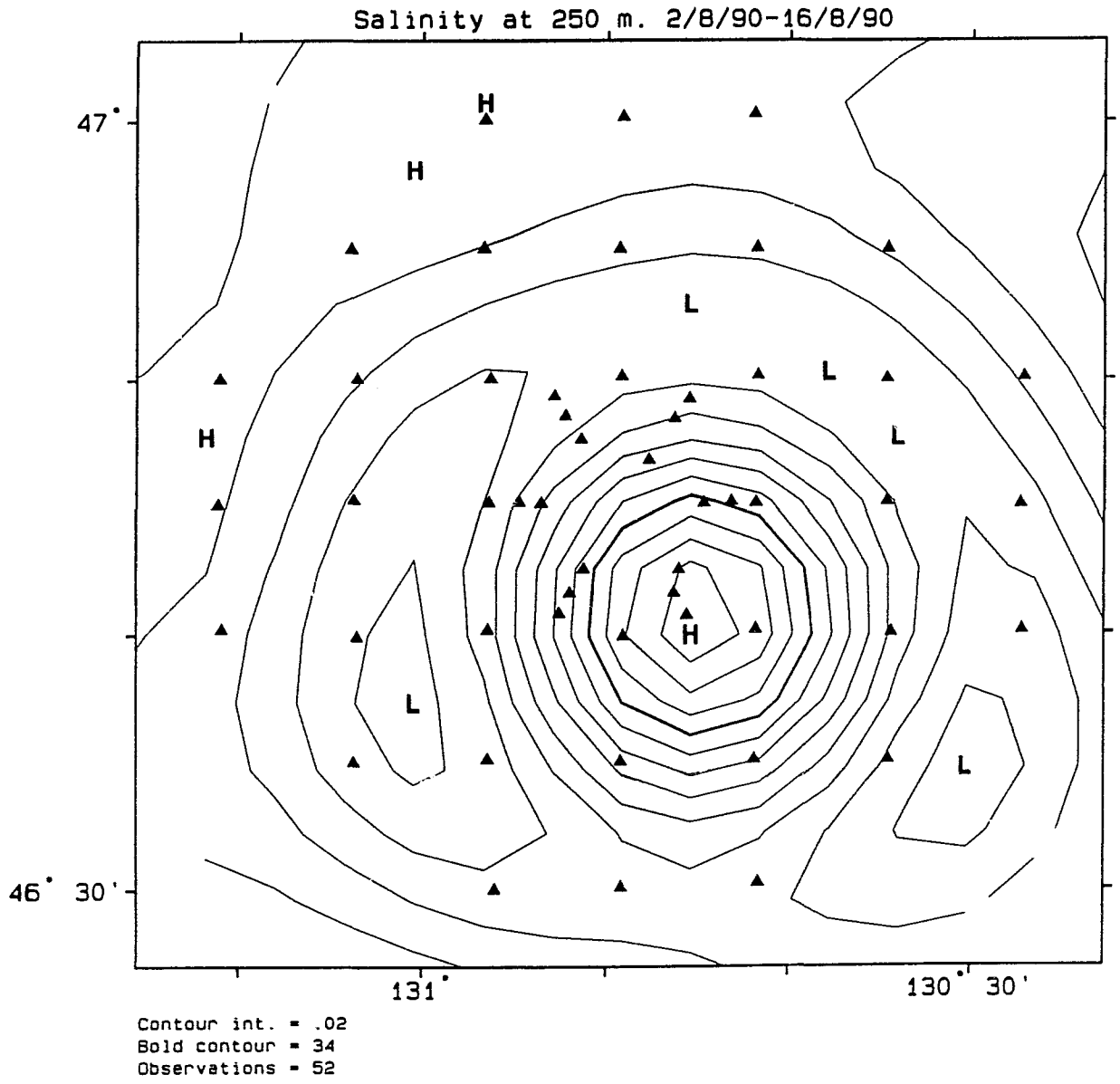
Salinity at 250 m. 2/8/90-16/8/90
8f
47°
46° 30'
131°
130° 30'
H
H
H
H
L
L
L
L
L
Contour int. = .02
Bold contour = 34
Observations = 52

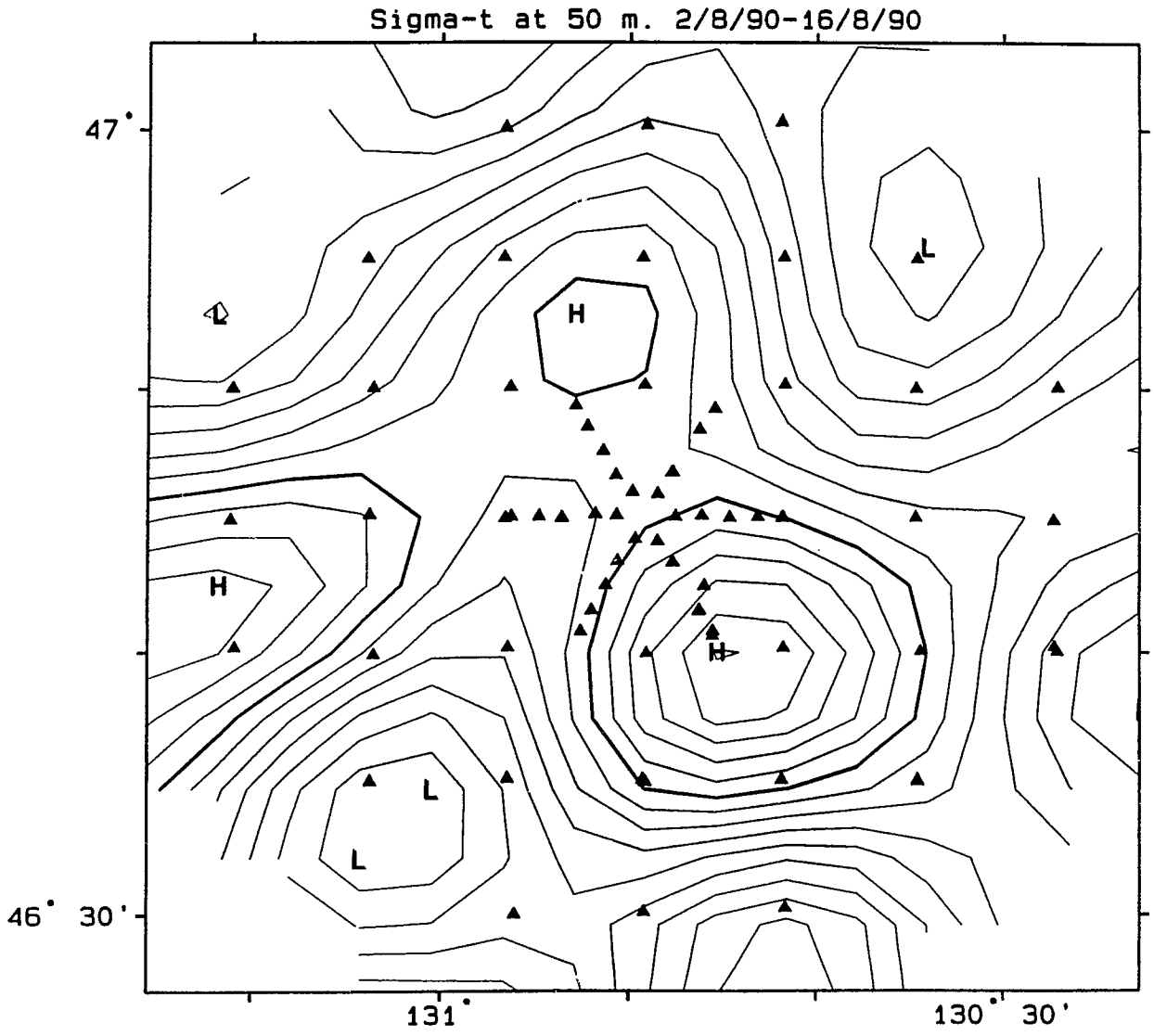
Sigma-t at 50 m. 2/8/90-16/8/90
47°
46° 30'
131°
130° 30'
L
H
L
H
H
L
L
Contour int. = .05
Bold contour = 25.1
Observations = 72

8g

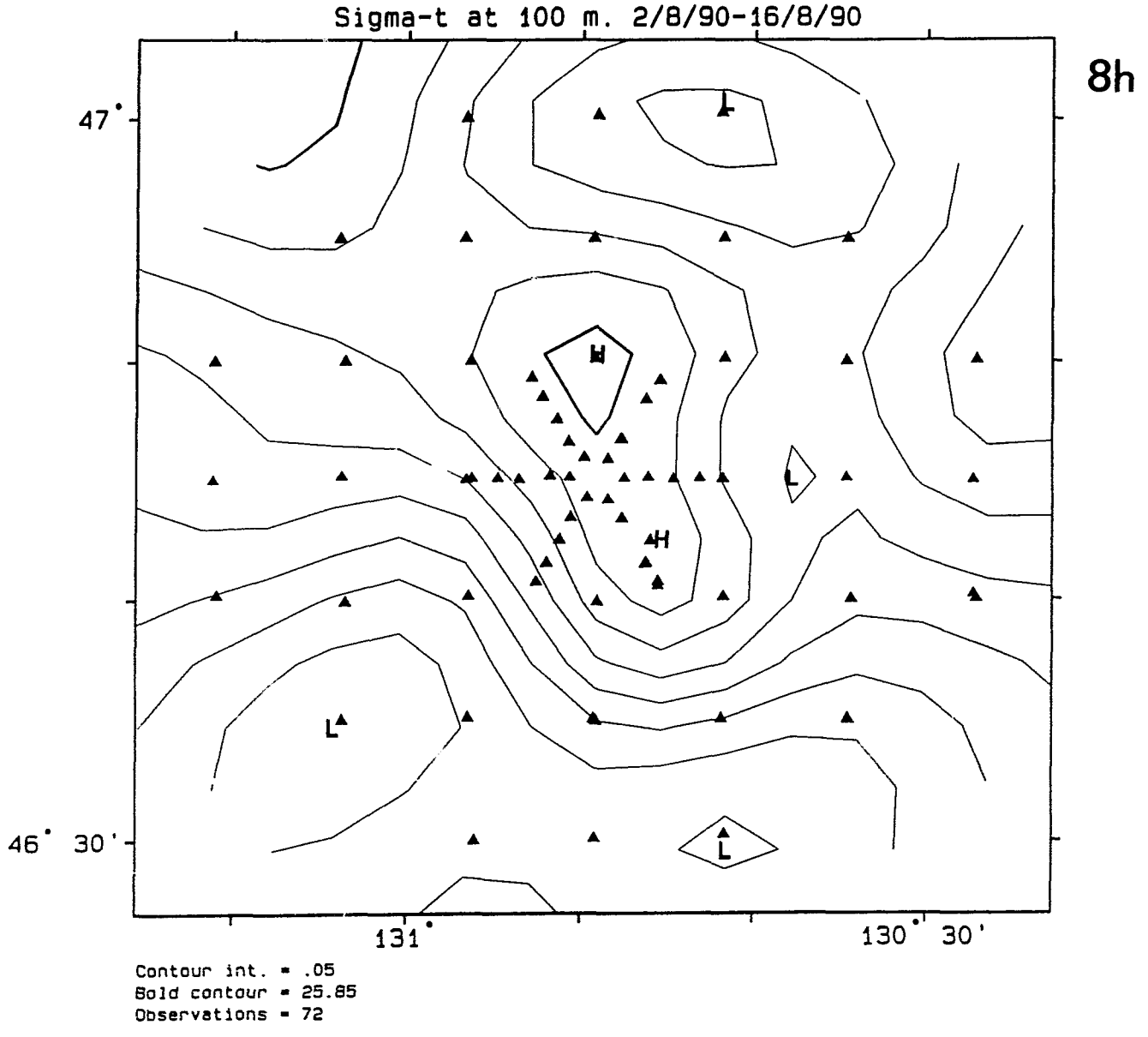
Sigma-t at 100 m. 2/8/90-16/8/90
8h
47°
46° 30'
131°
130° 30'
H
H
L
L
L
L
Contour int. = .05
Bold contour = 25.85
Observations = 72

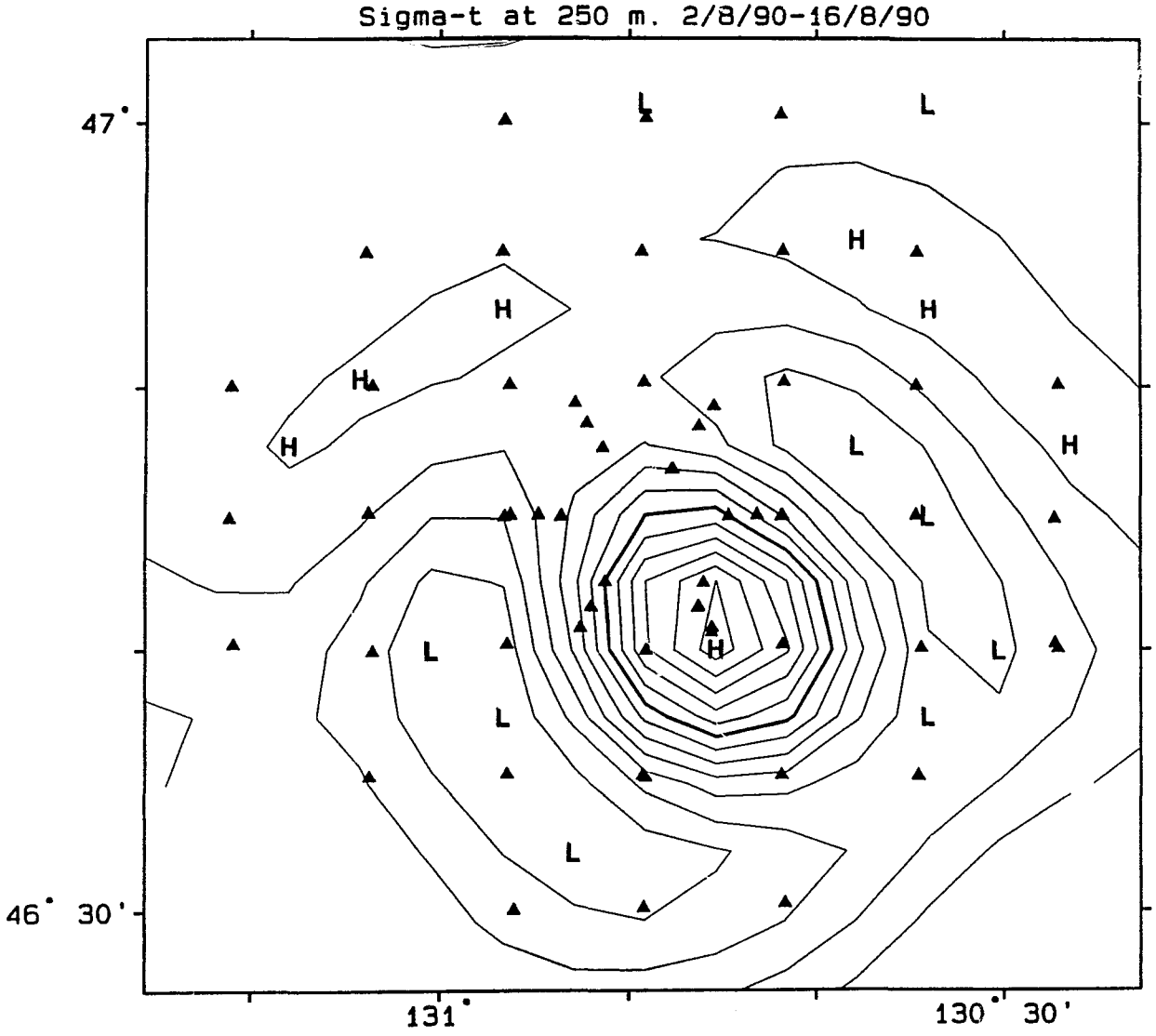
Sigma-t at 250 m. 2/8/90-16/8/90
8i
47°
46° 30'
131°
130° 30'
Contour int. = .025
Bold contour = 26.775
Observations = 61

In 1990, this cold dome was roughly circular in shape and was situated over the southeast flank of the seamount (Fig.8). At 50m, temperatures in the centre of this dome were about 1.5°C colder than the surrounding waters. Based on the temperature profiles in Figure 3, a differential of 1.5°C implies that water in the cold dome at 50m has been uplifted by 15-20m. This is in agreement with the doming shown in Figure 5. The position of the cold region shows only minor changes over the depth range considered.

There is some indication that the dome is elongated over the summit along a northwest-southeast axis, particularly in the temperature fields (Fig.8a). This corresponds with the direction of the mean background flow past the seamount (Freeland, *submitted*). The Taylor cone circulation is most evident in the distribution of density at 250m (Fig.8c). The high density core surrounded by a ring of low density water denotes anticyclonic flow. The weaker signal in temperature at 250m (Fig.8a) results from its near-isothermal distribution between ~100-300m.

Although a cold dome is evident near the seamount in the 1991 data, its location and intensity appear more variable (Fig.9). A strong signal is present in both temperature and density at 30m. The cold region is again oriented northwest-southeast. Temperatures in the centre of the dome were also about 1.5°C colder than the surrounding waters.

Figure 9: Plan views of (a) temperature, (b) salinity and (c) density (as sigma-t) at 30m, 100m, 250m and 500m during CSEX91. Overlay #2 shows the location of the 2000m isobath on Cobb Seamount.

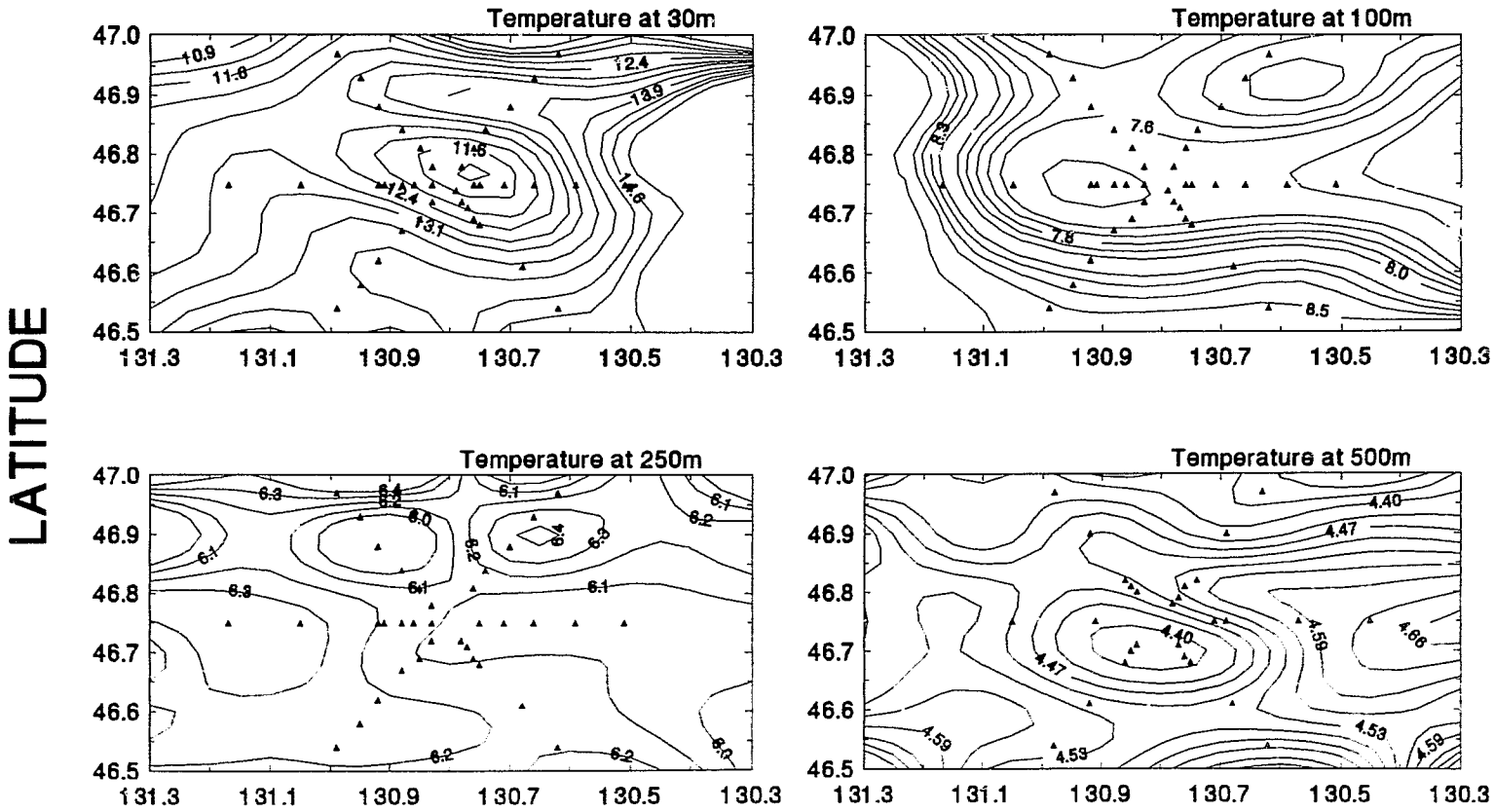
Temperature at 30m
Temperature at 100m
Temperature at 250m
Temperature at 500m
47.0
46.9
46.8
46.7
46.6
46.5
131.3
131.1
130.9
130.7
130.5
130.3
LATITUDE
LONGITUDE

9a

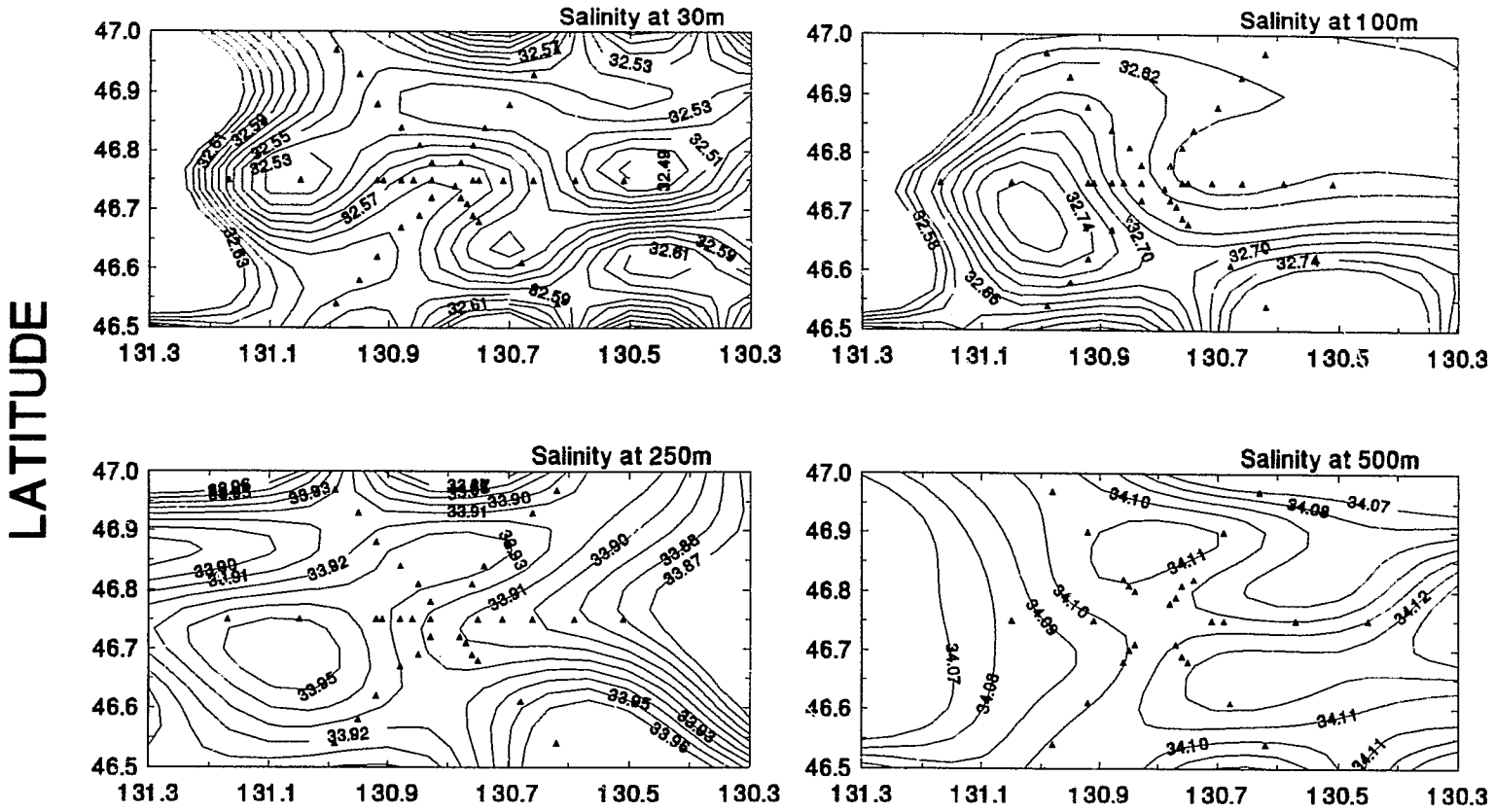
Salinity at 30m
Salinity at 100m
Salinity at 250m
Salinity at 500m
47.0
46.9
46.8
46.7
46.6
46.5
131.3
131.1
130.9
130.7
130.5
130.3
LATITUDE
LONGITUDE

9b

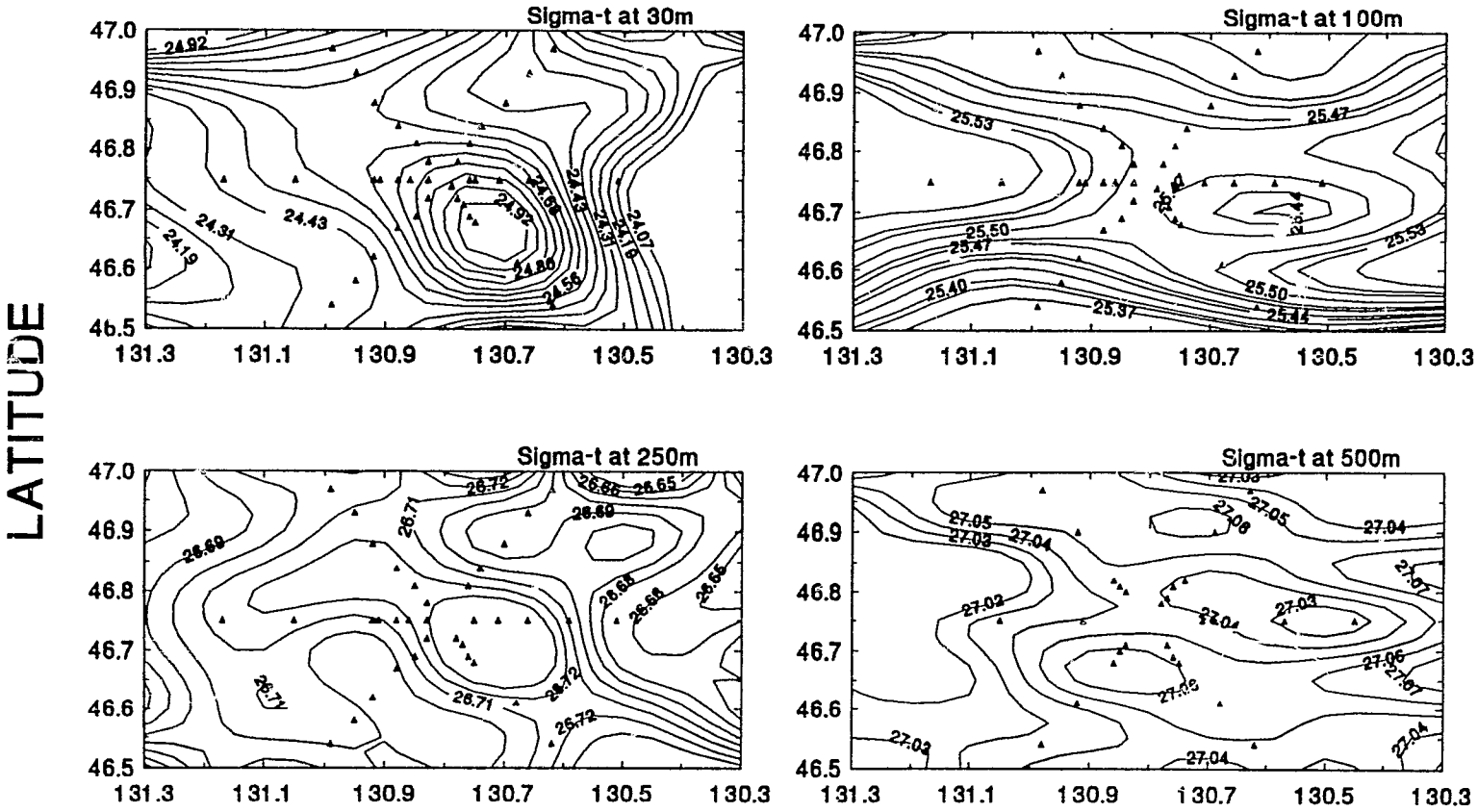
Sigma-t at 30m
Sigma-t at 100m
Sigma-t at 250m
Sigma-t at 500m
47.0
46.9
46.8
46.7
46.6
46.5
131.3
131.1
130.9
130.7
130.5
130.3
LATITUDE
LONGITUDE

9c

Figure 10: Plan views of (a) temperature, (b) salinity and (c) density (as sigma-t) at 10m, 50m, 100m and 250m during CSEX92. Overlay #3 shows the location of the 2000m isobath on Cobb Seamount.

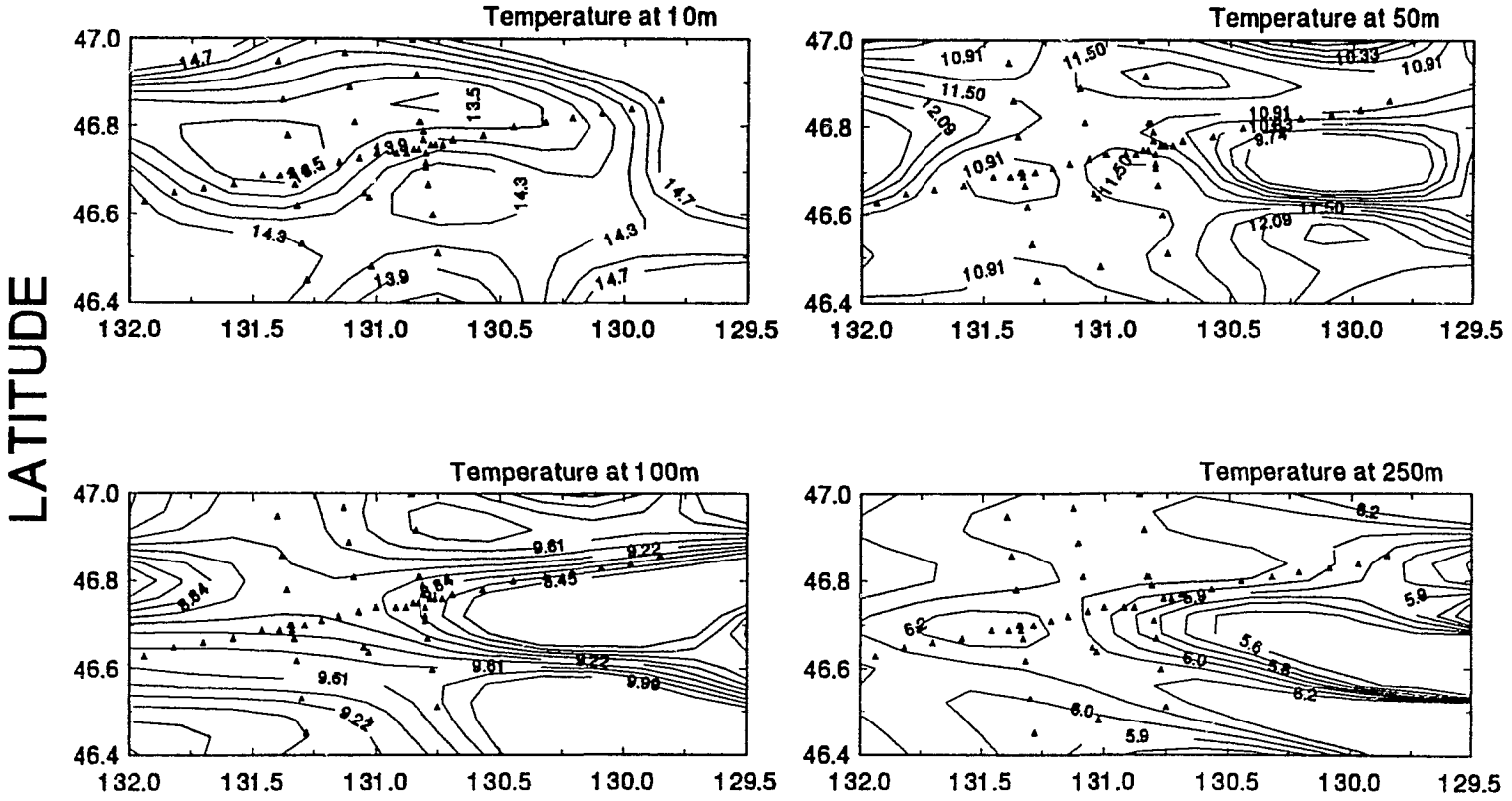
Temperature at 10m
Temperature at 50m
Temperature at 100m
Temperature at 250m
LATITUDE
47.0
46.8
46.6
46.4
132.0
131.5
131.0
130.5
130.0
129.5
LONGITUDE

10a

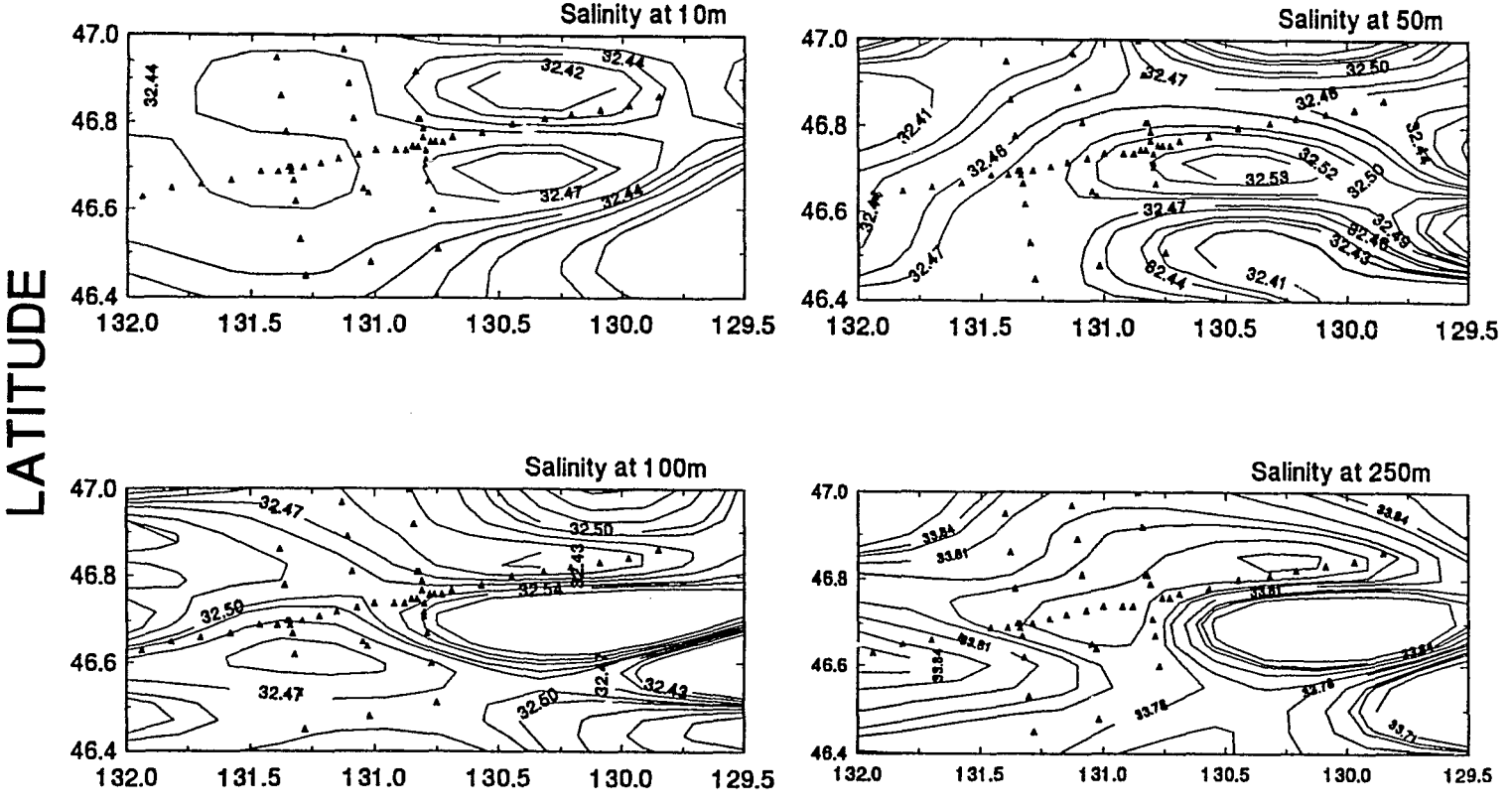
Salinity at 10m
Salinity at 50m
Salinity at 100m
Salinity at 250m
47.0
46.8
46.6
46.4
132.0
131.5
131.0
130.5
130.0
129.5
LATITUDE
LONGITUDE

10b

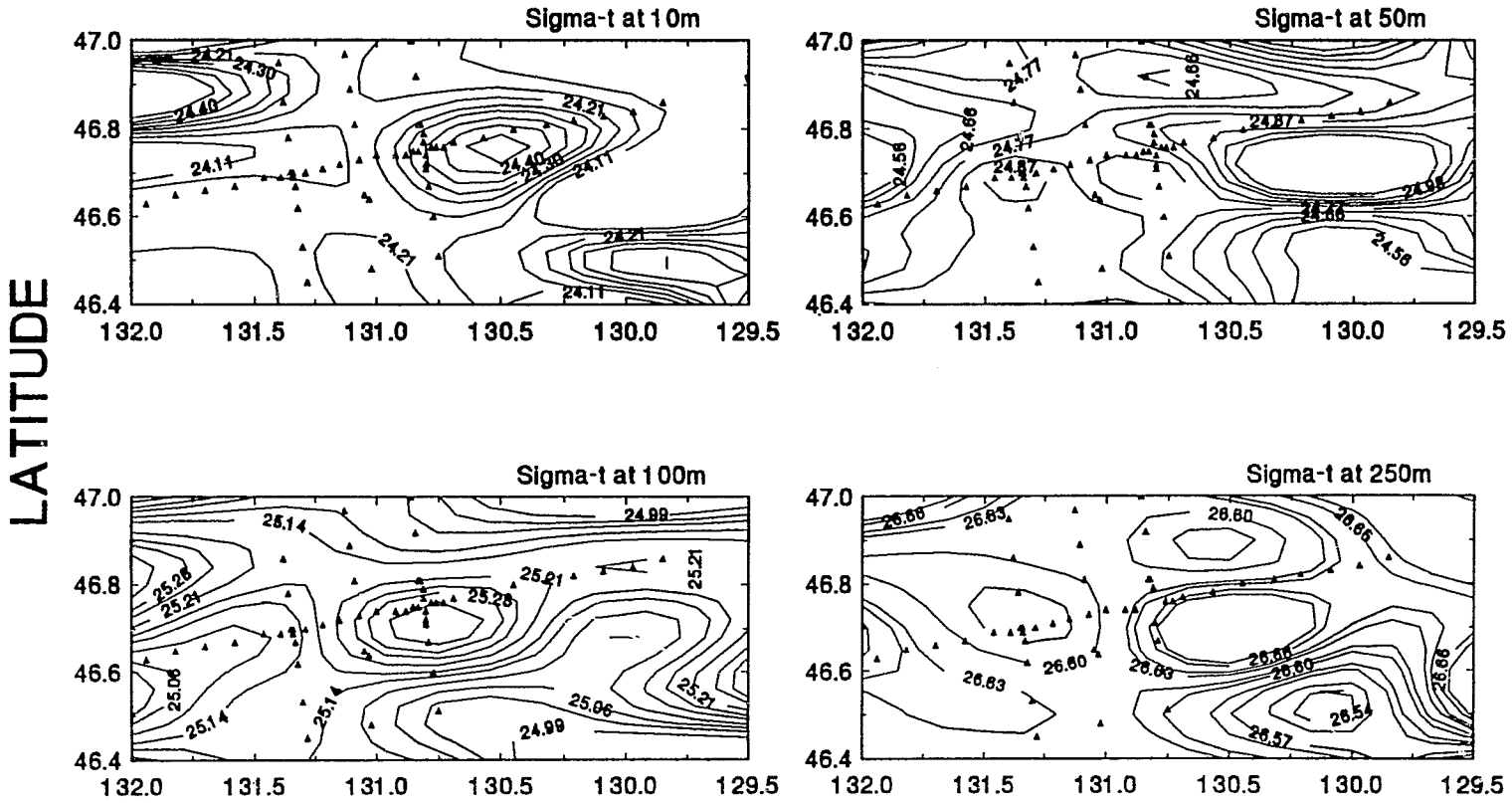
Sigma-t at 10m
Sigma-t at 50m
Sigma-t at 100m
Sigma-t at 250m
47.0
46.8
46.6
46.4
132.0
131.5
131.0
130.5
130.0
129.5
LATITUDE
LONGITUDE

10c

Views at 100m and 250m are more complex. Temperature and salinity distributions show a region of cold salty water on the western flank of the seamount, and a region of less saline water to the east at 100m (Figs.9a,b). At 250m, salinities remain high to the west of Cobb, with some evidence of an interleaving of high-salinity and low-salinity waters over the seamount (Fig.9b). As in the 1990 data, temperature signals at 250m are weak. At 500m, a cold region is again detectable on the southern side of the seamount. The depth-variable nature of the 1991 data may result from greater vertical shearing of the flow past the seamount than in 1990.

In 1992, a region of uplifted water appears to extend eastward from Cobb (Fig.10). As in 1990, temperatures in the cold dome at 50m were ~9.5°C (Fig.10a), which in this case indicates an uplift of about 30m (see CSEX92 temperature profiles in Fig.3). This feature is seen in each of temperature, salinity and density between 10m and 250m depth but lies in a region for which only a few hydrographic observations were collected, making the plots shown in Figure 10 prone to error. However, comparison of the plots shown in Figure 10 with comparable plots produced using the method of objective analysis (See Section 2.2) confirms the existence of a cold region east of Cobb (Freeland, *pers. comm.*). If, as Figure 10 suggests, the cold region *is* displaced further downstream than in either

1990 or'91, it could be indicative of a stronger background flow past the seamount: fluid dynamics studies by Boyer and Zhang (1990) and Davies *et al.* (1990) note similar downstream displacements with increasing background flow.

c) Internal Wave Activity: One of the goals of the CSEX current meter program was to investigate the internal wave field near Cobb. As yet, this study remains incomplete. However, preliminary work indicates that significant amplification of internal wave energy does occur over the seamount, particularly above the region of steep slope break near 300m (Freeland, *pers. comm.*). During CSEX91 and '92 several short CTD time series were conducted to observe internal wave activity over Cobb.

Figure 11 depicts density profiles from two such time series collected during CSEX91. The first series was carried out on the eastern side of the Cobb summit in 300m of water. The CTD was yoyo-ed up and down to a maximum depth of 100m. A total of 26 casts were made in 4½ hours. The second series was conducted 25km north west of Cobb in ~3000m of water. Eighteen 200m CTD casts were collected, also in 4½ hours.

The off-seamount profile is dominated by a single downward displacement of isopycnals in the upper water column by about 10m. This is indicative of an internal wave with a period about twice the length of the time series (*i.e.* 9 hours). Between 60 and 100m, there is no indication

Figure 11: 4½ hour time series of density collected during CSEX91 at (a) an on-seamount site 5km east of the Cobb pinnacle in ~300m of water and (b) an off-seamount site 25km NW of Cobb Seamount. Casts were made every 10 minutes at the on-seamount site, and every 15 minutes at the off-seamount site.

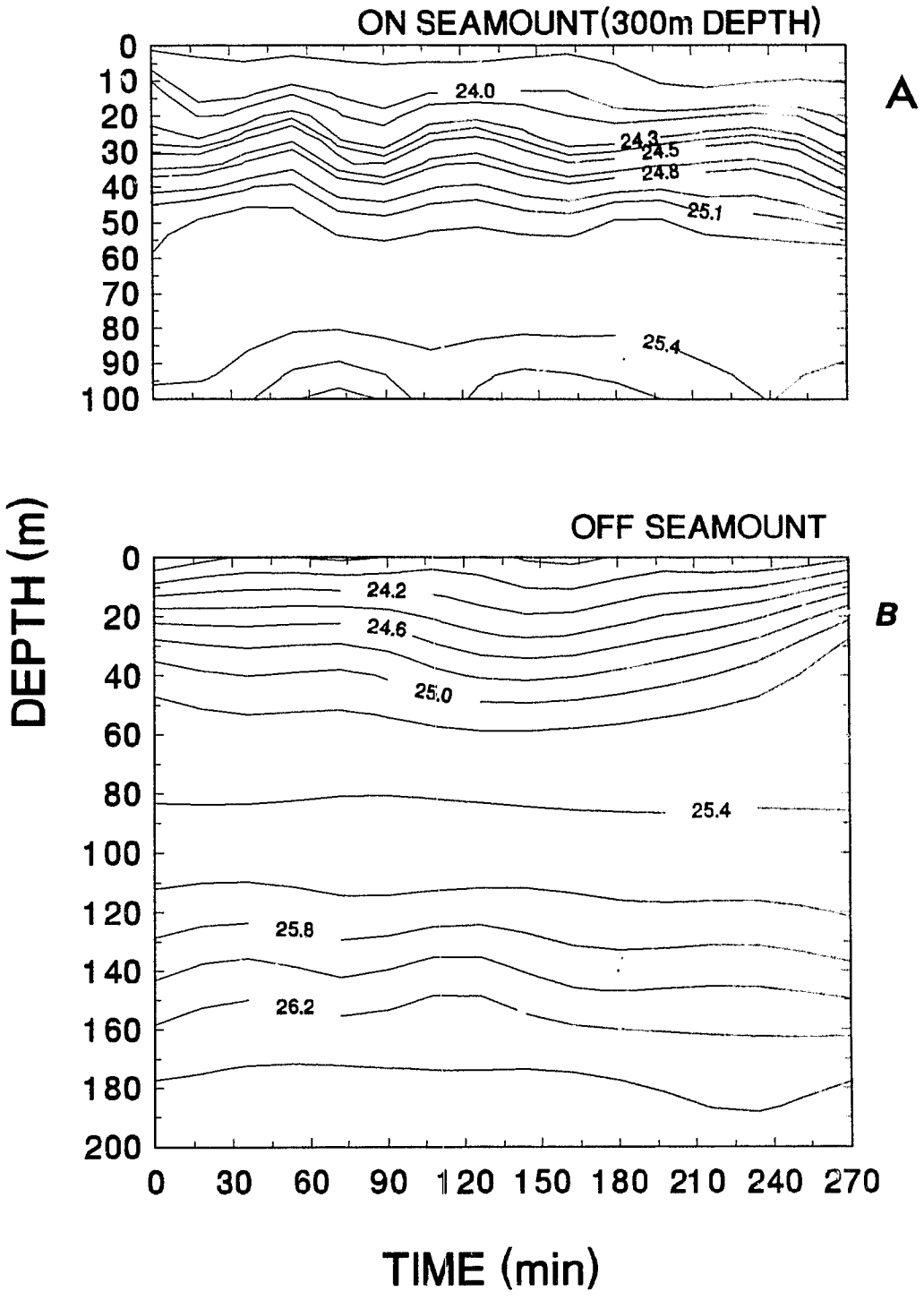
ON SEAMOUNT(300m DEPTH)
A
24.0
24.3
24.5
24.8
25.1
25.4
OFF SEAMOUNT
B
24.2
24.6
25.0
25.4
25.8
26.2
DEPTH (m)
0
10
20
30
40
50
60
70
80
90
100
120
140
160
180
200
0
30
60
90
120
150
180
210
240
270
TIME (min)

of any internal wave activity. Near the bottom of the off-seamount section, internal waves with periods of ~2hrs propagate along the upper surface of the halocline between 110m-160m.

The on-seamount profile shows a different situation. Whereas the near-surface isopycnals off-seamount showed only gentle sloping, a much shorter period internal wave dominates the near-surface density field over Cobb. Between 10m-50m, the isopycnals undergo 2½ cycles during the time series, indicating the presence of internal waves with a period of about 100 minutes, and an amplitude of 10m. Internal wave activity is greatly reduced in a pycnostad between 50m-90m, as in the off-seamount series. The more energetic internal waves over the seamount may act to increase the mixing of nutrients into near surface waters.

d) Nutrient Profiles: As discussed previously, the subarctic Pacific is one of three oceanic HNLC regions. 30 years of observations from Station P (50°N, 145°W) show that NO_3 concentrations rarely fall below ~6uM (Miller *et al.*, 1991). Upwelling in the Alaska Gyre brings nutrient-rich water to the surface in the subarctic Pacific and leads to an export of near-surface water to the southeast (Dodimead *et al.*, 1963; Favorite *et al.*, 1976). As this water moves southward, nutrient concentrations decline steadily toward the NPTZ, south of which the near-surface nutrient concentrations fall to near zero during the summer months

Figure 12: Typical nitrate profiles from hydrographic surveys conducted during CSEX90, '91 and '92. Data from 1990 represent all casts from which nutrient samples were collected during CSEX90, while those from 1991 and '92 represent subsets which were chosen at random from the larger CSEX91 and CSEX92 datasets. Note that near-surface nitrate is generally between 1-3μM. The nitracline usually occurs between 40-50m.

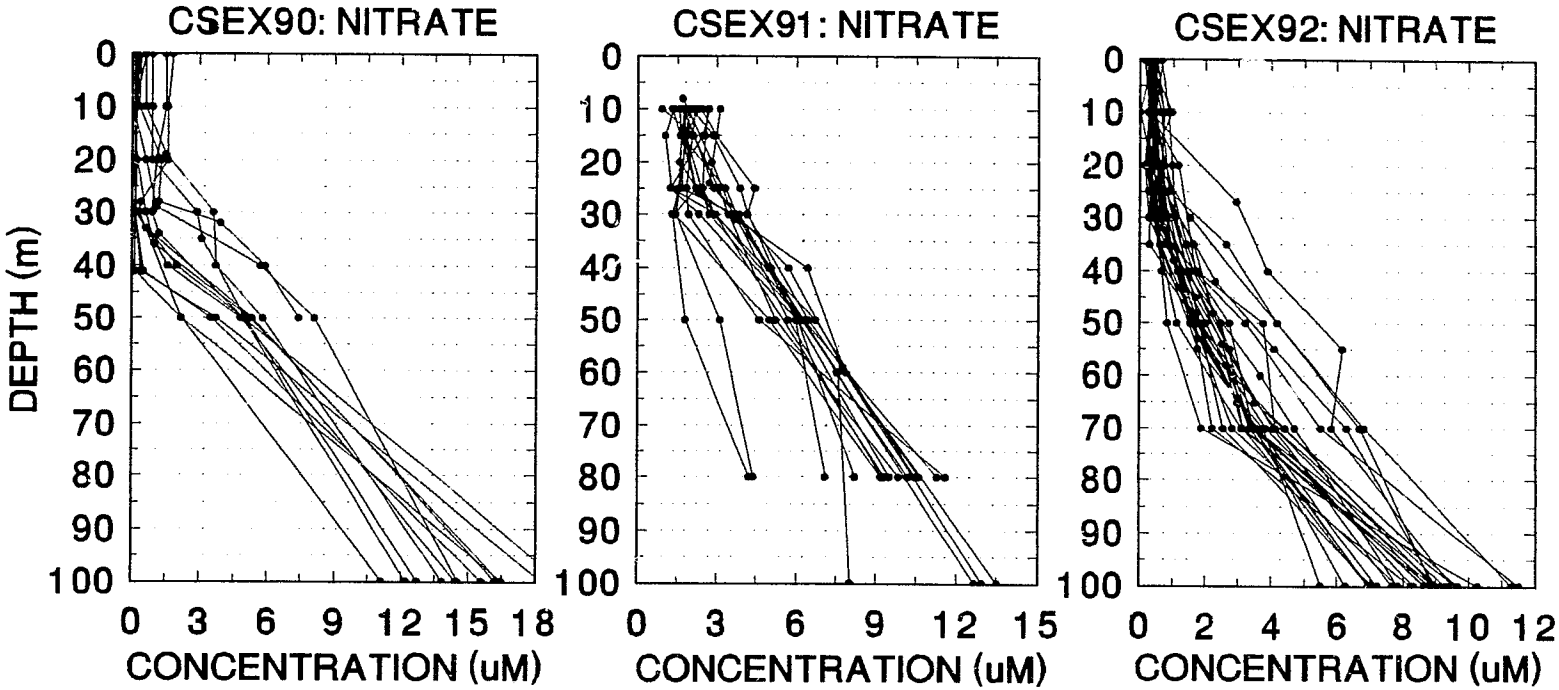
CSEX90: NITRATE
CSEX91: NITRATE
CSEX92: NITRATE
DEPTH (m)
0
10
20
30
40
50
60
70
80
90
100
0 3 6 9 12 15 18
0 3 6 9 12 15
0 2 4 6 8 10 12
CONCENTRATION (uM)
CONCENTRATION (uM)
CONCENTRATION (uM)

(Levitus *et al.*, 1993).

During the CSEX cruises, water samples for analyses of dissolved nutrients were collected using Niskin bottles on the CTD rosette. Samples were analyzed for nitrates, phosphates and silicates using an autoanalyser. Figure 12 shows nitrate profiles from the three CSEX cruises. Nitrate concentration in the upper 50m ranged from <1uM to >6uM, with the highest values occurring during CSEX91. The mean concentration across all three years was about 2.5uM. The position of the main nitracline showed little variation within and between years, and was usually located at ~40-50m. Nitrate concentrations in the nitracline rose rapidly from 5uM at 50m to 12uM at 80-100m.

Relative to conditions at Station P (50°N, 145°W), these nitrate concentrations are rather low. However, in comparison to the truly oligotrophic conditions in the subtropical North Pacific where near-surface nitrate goes to zero in the summer, nutrient levels near Cobb are moderately high. Chlorophyll profiles from Cobb are characterized by a subsurface chlorophyll maximum (SCM) (Dower *et al.*, 1992), which is usually taken as evidence for some degree of nutrient limitation of the phytoplankton. It remains to be seen how important nutrient limitation is near Cobb, as measurements of the phytoplankton half-saturation constant for nitrate have yet to be carried out in the region.

1.3 Biological Implications of Seamount Flow Phenomena

Seamount flow phenomena can affect biological communities in two main ways: (i) by retaining plankton over seamounts, and (ii) by enhancing the stocks of benthic and pelagic populations. As this thesis is concerned with the latter issue, I include only a brief consideration of the former.

1.3.1 Larval Retention

Isolated seamounts commonly support rich benthic communities, usually dominated by species that colonize the seamount from neighbouring continental shelves (Birkeland, 1971; Raymore, 1982; Wishner *et al.* 1990; Levin *et al.*, 1991; Parker and Tunnicliffe, *submitted*). In most cases, these species have pelagic larvae, capable of spending days to months in the plankton. For such a species to establish a viable population on a seamount requires that three conditions be met. First, pelagic larvae must remain viable sufficiently long to be carried to the seamount by ocean currents. Second, unless the organisms are capable of self-fertilization, a successful recruitment event requires that multiple larvae be transported to the seamount in either the same or successive recruitment events. Finally, unless colonization events are fairly regular, there must be some mechanism to ensure the long-term maintenance of the new population.

It is this last point that relates to current-topography interactions. Consider a new population established on an isolated seamount via long distance dispersal of pelagic larvae. The long-lived larvae that enabled colonization become a liability once the population is established. This is because the currents that carried the original larvae *to* the seamount will carry the larvae of future generations *away* from the seamount. It has been suggested, however, that the recirculating flow of a Taylor cone could act to retain dispersive larvae over seamounts long enough to ensure the long-term stability of such isolated populations (Boehlert and Genin, 1987; Parker and Tunnicliffe, *submitted*).

The effectiveness of such a mechanism will depend on the persistence and flushing times of the Taylor cone, the mean background flow velocity and the amount of time that larvae spend in the plankton. As pointed out by Freeland (*submitted*), the near-bottom outflow of water in the Taylor cone at Cobb Seamount implies an inflow elsewhere in the water column. Thus, water in the Taylor cone is flushed over some period of time: Freeland calculates a flushing time of ~17 days for the Taylor cone at Cobb. A recent survey of the benthic invertebrate fauna of Cobb Seamount shows that species with larvae that remain in the plankton for less than a few weeks are well represented (Parker and Tunnicliffe, *submitted*). Conversely, species with larvae

that spend greater than a few weeks in the plankton are under-represented on Cobb. Parker and Tunnicliffe attribute this to the fact that larvae spending less than ~17 days in the plankton are more likely to settle on the seamount before being flushed out of the system.

While this argument is quite reasonable, situations could also arise in which similar current-topography interactions could be detrimental to population maintenance. As explained previously, Taylor cones remain stable over only a certain range of upstream velocities (Chapman and Haidvogel, 1992). Above these velocities, anticyclonic eddies are shed from the seamount. Under such conditions, any larvae produced on the seamount would likely be carried away.

1.3.2 Enhanced Production

Both benthic and pelagic stocks can be enhanced by current-topography interactions at seamounts. Genin *et al.* (1986) and Parker and Tunnicliffe (*submitted*) show that the distributional patterns in benthic communities on seamounts reflect the near-bottom current regime. For instance, densities of suspension feeders (*eg.* corals, sponges and crinoids) are usually highest near local topographic highs and abrupt slope breaks. These are the same regions where enhanced internal wave reflection and current acceleration are expected on the seamount (Boehlert and Genin, 1987).

Genin *et al.* (1986) propose that locally accelerated flow over microscale topographic highs increases the flux of food to the suspension feeders, resulting in higher growth and survival rates. Similar patterns of high suspension feeder biomass are found on other topographies that experience high velocity currents (*eg.* reefs, submarine cliffs, shallow shoals).

As mentioned previously, it has been proposed that primary production over seamounts can be enhanced through the combination of (i) the trapping action of a Taylor cone and (ii) injection of nutrients into near-surface waters by isopycnal doming (Boehlert and Genin, 1987). Nutrients may also be added by the increased diapycnal mixing that can result from enhanced internal wave activity (Gilbert and Garrett, 1989).

This mechanism has been proposed to explain observations of high chlorophyll water over Minami-Kasuga Seamount, in the Mariana Archipelago (Genin and Boehlert, 1985). During one hydrographic survey a cold dome penetrated into the euphotic zone over the seamount, to about 80m depth. It was suggested that the 50% increase in chlorophyll concentration observed over the seamount resulted from the injection of nutrients into the euphotic zone via doming associated with Taylor cone formation. The generation time of the high chlorophyll patch was estimated to be on the order of a few days (Genin and Boehlert, 1985).

Increased zooplankton biomass was also recorded over the seamount. Hydrographic surveys two and seventeen days later found neither evidence of a cold dome, nor enhanced chlorophyll or zooplankton biomass over the seamount. Therefore, if Taylor cone effects *did* foster enhanced chlorophyll concentrations, the effect was quite ephemeral.

Doming can also enhance primary production by lifting phytoplankton nearer to the surface, where cells are exposed to higher average illumination. Although this aspect of doming has received surprisingly little attention in the seamount literature, it may be particularly important over shallow seamounts at mid to high latitudes, where primary production is often limited by light rather than by nutrients.

In each of the above cases, seamount flow phenomena must penetrate the euphotic zone in order to affect primary production. Given that stratification damps out such vertical motions (Roden, 1987), it might be expected that Taylor cones and isopycnal doming will only affect primary production over shallow seamounts. This idea is supported by the finding that enhanced phytoplankton biomass has only been reported from seamounts that are less than a few hundred metres below the surface.

Finally, the temporal scale of current-topography interactions must be considered. For instance, the cold dome observed over Minami-Kasuga Seamount lasted only a few

days, yet still produced a pulse of phytoplankton (Genin and Boehlert, 1985). This merely reflects the fact that the doubling time of phytoplankton is also on the order of days. It is unlikely, however, that this same event affected higher trophic levels near the seamount. In a study of biomass transfer in coastal waters, Denman *et al.* (1989) calculate timescales on the order of weeks and months for a pulse of phytoplankton to be incorporated into higher biomass of zooplankton and larval fish, respectively. Consequently, since different organisms interact with, and integrate changes in their environments over different timescales, the biological importance of a given current-topography interaction likely differs among species. In the following chapters I will examine how the various components of an oceanic planktonic community respond to current-topography interactions associated with flow over Cobb Seamount.

Chapter 2

A STRONG BIOLOGICAL RESPONSE TO OCEANIC FLOW PAST COBB SEAMOUNT

This chapter is based on a paper published in *Deep-Sea Research* in 1992 (*i.e.* Dower *et al.*, 1992). It represents the first contribution from the Cobb Seamount Experiment, and summarizes the findings from the CSEX90 cruise. Although a collaborative effort among me and Drs. Freeland and Juniper, the task of writing the original manuscript was primarily mine.

The figures used in the paper (Figs.13-16 here) were produced by Dr. Freeland using an objective analysis plotting package of his own design. The sections explaining (i) the choice of correlation function and (ii) the predicted height of the Taylor cone were written by Dr. Freeland. The original hydrographic data were collected jointly by me and Drs. Freeland and Juniper. Dr. Juniper's other contributions were largely editorial.

I present the paper largely unchanged from the Deep-Sea Research version, but have added a section at the end that includes additional observations from the CSEX91 and '92 cruises. This section shows the similarity in the "strong biological response" during all three cruises and addresses a few points about which our understanding has grown since the initial CSEX90 cruise.

2.1 Introduction

Cobb Seamount, located 500km off the west coast of Canada, rises from a 2800m abyssal plain to 24m depth (Fig. 1). As part of our current effort to understand the interactions between the physics and biology of seamounts we examined the hydrographic structure around Cobb in August 1990. Vertical profiles were taken with a Guildline digital CTD and a Seatech transmissometer in a 55 x 55km grid centred over the seamount and in three fine-scale survey transects (Fig.13 and Appendix). CTD profiles were to 1000m off-seamount and to within 10m of the bottom on-seamount.

Water samples for chlorophyll analyses were collected with Niskin bottles from 14 stations at depths of 0m, 10m, 20m, 40m, 50m and 100m. Bottle cast stations were positioned to provide detailed sections of property variation close to the seamount summit, and a description of the property variations and flow in the far field away from the immediate influence of the seamount, (Fig.13.

The large scale background flow past Cobb was investigated by following four near-surface satellite tracked drifters (tracked by Système Argos) drogued to track water between 5m and 13m depth. The flow close to the seamount was examined by three moorings deployed in a line extending roughly northeast from the pinnacle (Fig.14). Each mooring was instrumented identically and carried

Figure 13: Contour plot of the % light transmission at the depth of the transmission minimum (which varied by no more than 5-10m between adjacent stations). Circles mark CTD and transmissivity sampling stations, triangles indicate where those variables plus chlorophyll were sampled. The three intersecting lines of circles represent the three fine-scale sampling transects, and their point of intersection marks the summit of Cobb Seamount. The letters L and H indicate local areas of Low and High % light transmission.

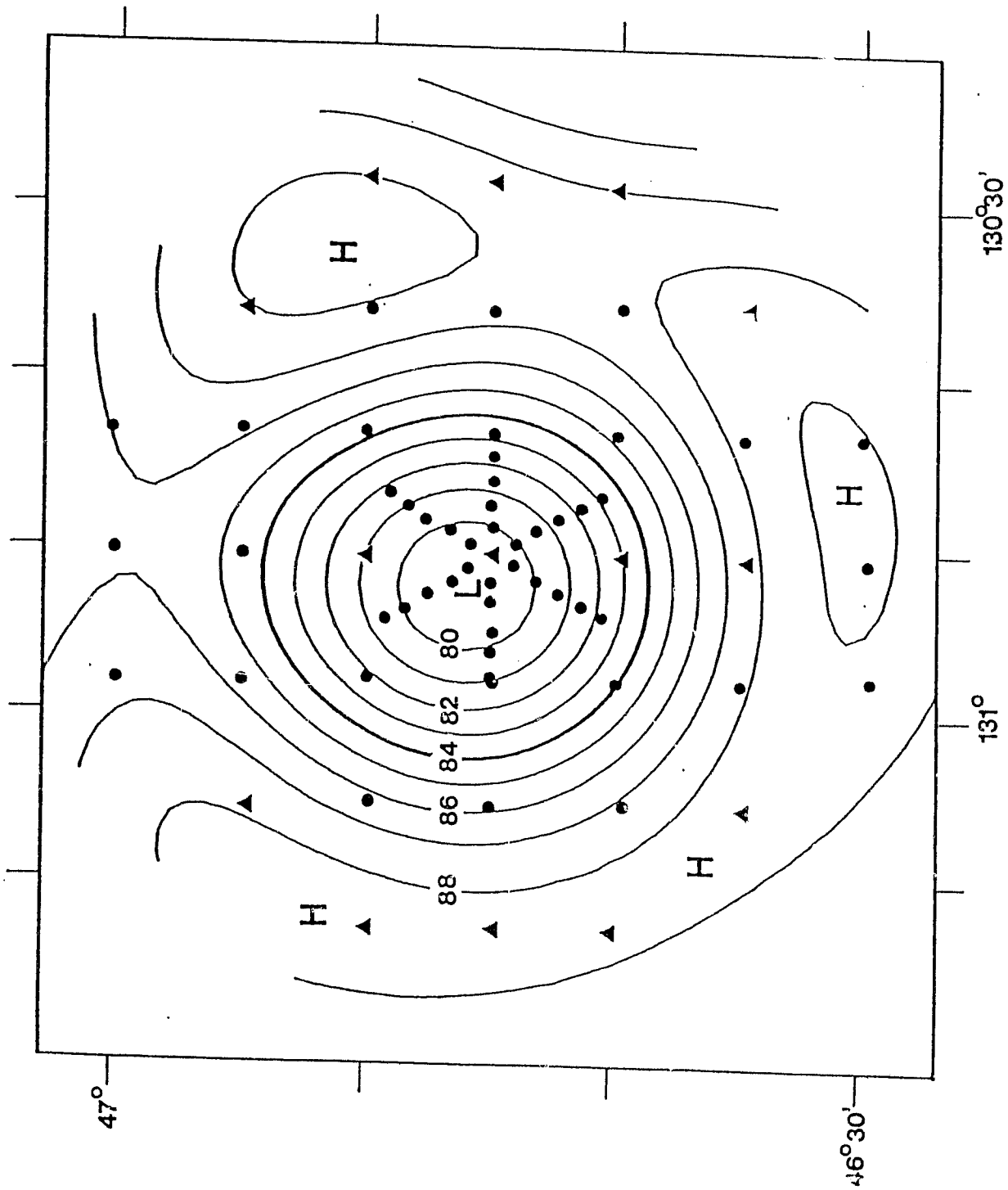
H
H
H
H
L
80
82
84
86
88
47°
46°30'
131°
130°30'

Figure 14: 16 x 16km around the summit of Cobb Seamount showing the detailed bathymetry and near bottom velocity vectors at each of the three mooring locations. Locations of moorings correspond with the beginning points of the arrows. For scale, arrow length is proportional to current speed and the largest arrow represents a speed of 5 cm/sec. Contours are in fathoms (1 fathom = 1.83 metres), for depths less than 100 fathoms the contour interval is 10 f.

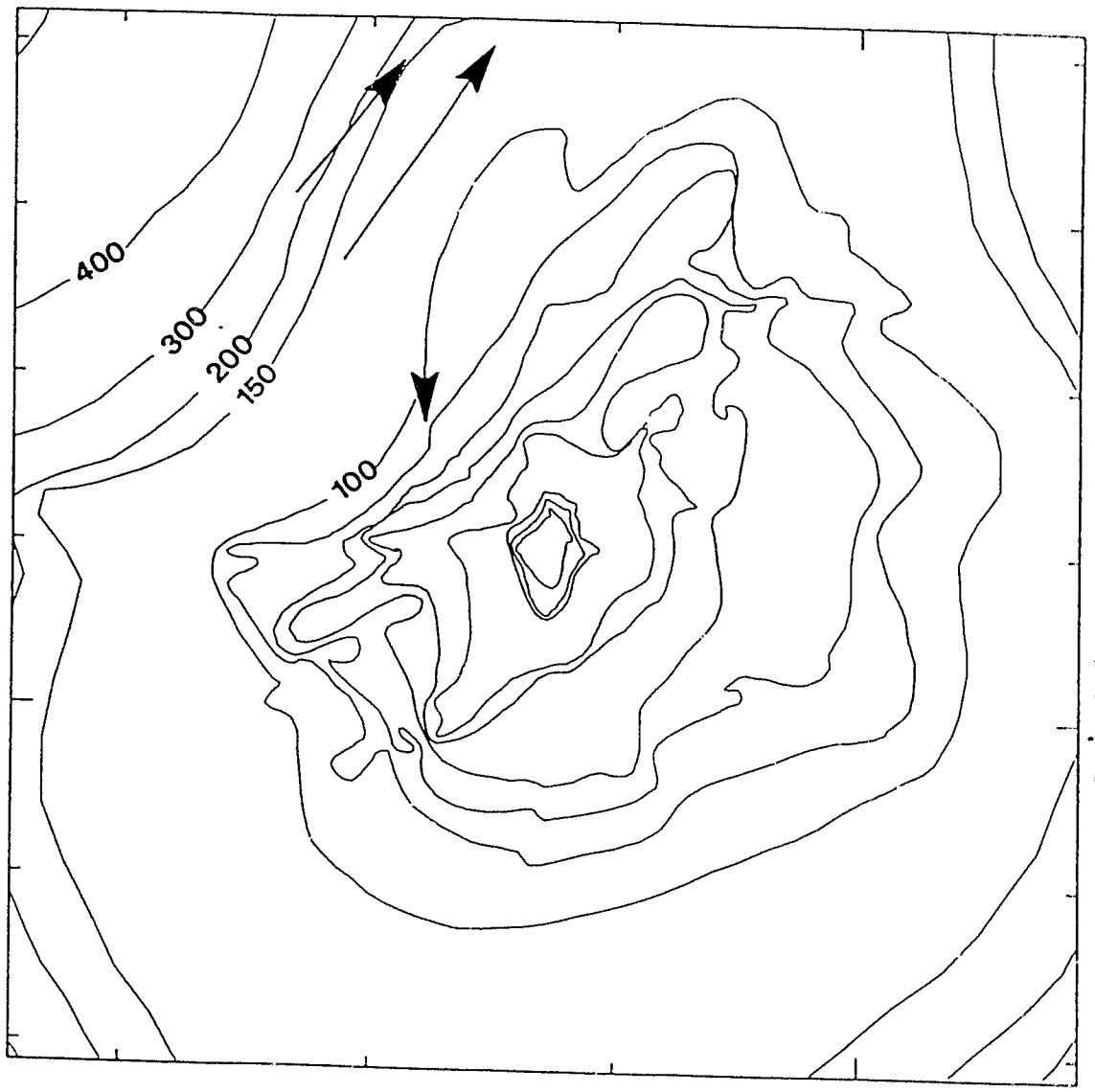
400
300
200
150
100
130° 50'

InterOcean S4 (electromagnetic) current meters located 3m, 10m and 50m off the bottom. Thus the bottom two instruments at each mooring monitored flow well within and near the upper boundary of the bottom boundary layer and the upper instrument examined the geostrophic interior of the ocean.

The three moorings were placed half-way between the pinnacle and seamount rim (140m water depth), on the rim (210m depth) and on the flank of the seamount (400 m depth). Mooring deployment and recovery were the first and last operations, respectively, on the cruise to give maximum time for the instruments actually in the water, a total duration of about 3 weeks.

2.2 Observations

Transmissivity profiles near Cobb Seamount contain a sharp minimum usually localized to a layer between 35 and 45m depth (Fig.15). CTD profiles also show a sharp density discontinuity at this depth, marking the boundary between the surface mixed water and deeper stratified waters (Fig.15). Figure 16 shows the vertical distribution of % light transmission along 55km east-west transect across the seamount. The section clearly indicates that this minimum layer represents a feature that (i) is isolated both horizontally and vertically from any other similar feature and (ii) is located over the seamount.

Figure 15: Profile of density anomaly (thin line) and the percent light transmission (bold line) against depth in the water column. This station was occupied near the seamount rim to the west of the pinnacle.

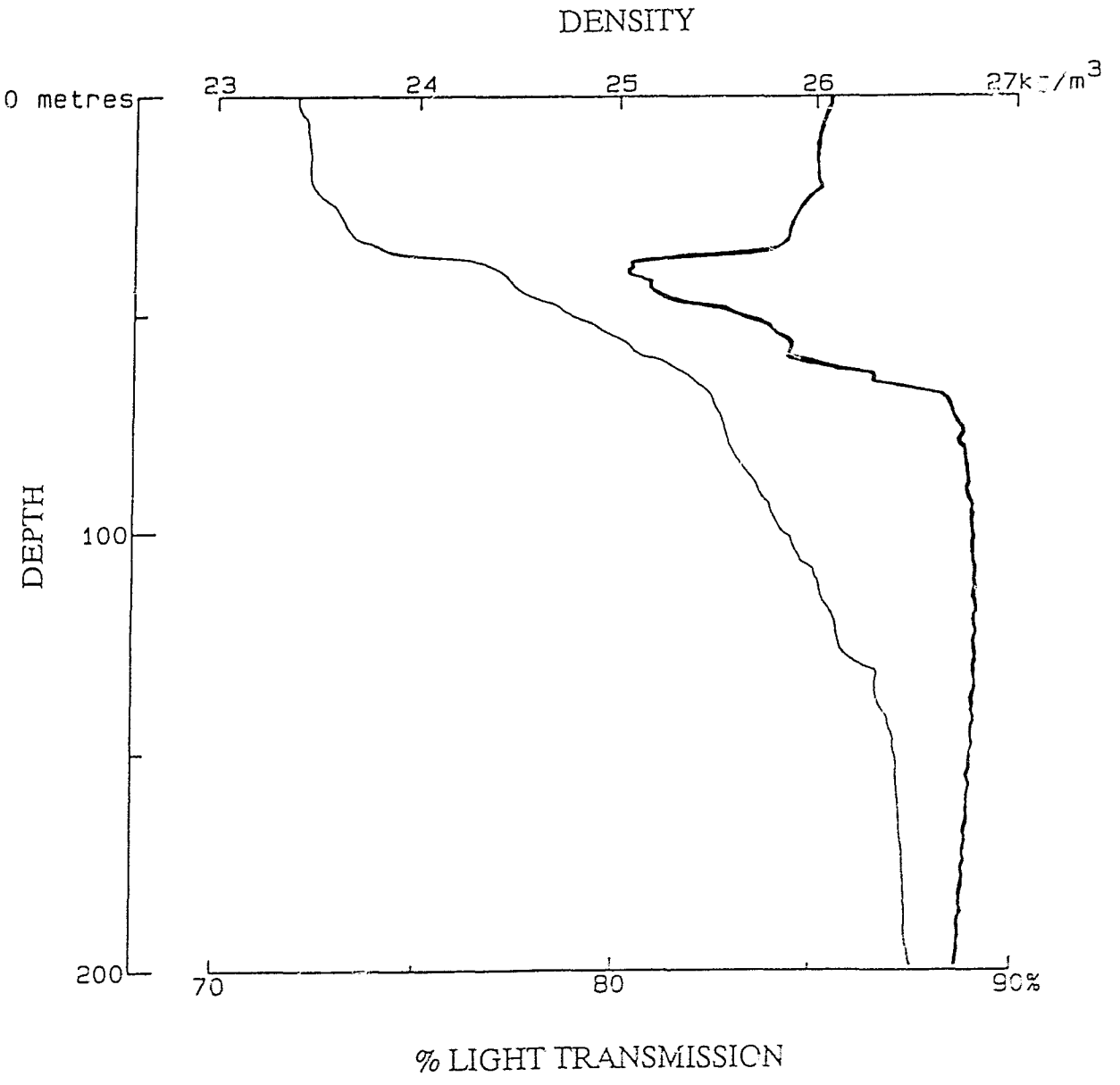
DENSITY
0 metres
23
24
25
26
27kg/m3
DEPTH
100
200
70
80
90%
% LIGHT TRANSMISSION

Figure 16: % light transmission along a 55km east-west transect across the pinnacle of Cobb Seamount. The contour interval is 1% light transmission. The bold line is a rather coarse representation of the bottom profile across the seamount; specifically it represents the lower limit of each CTD cast.

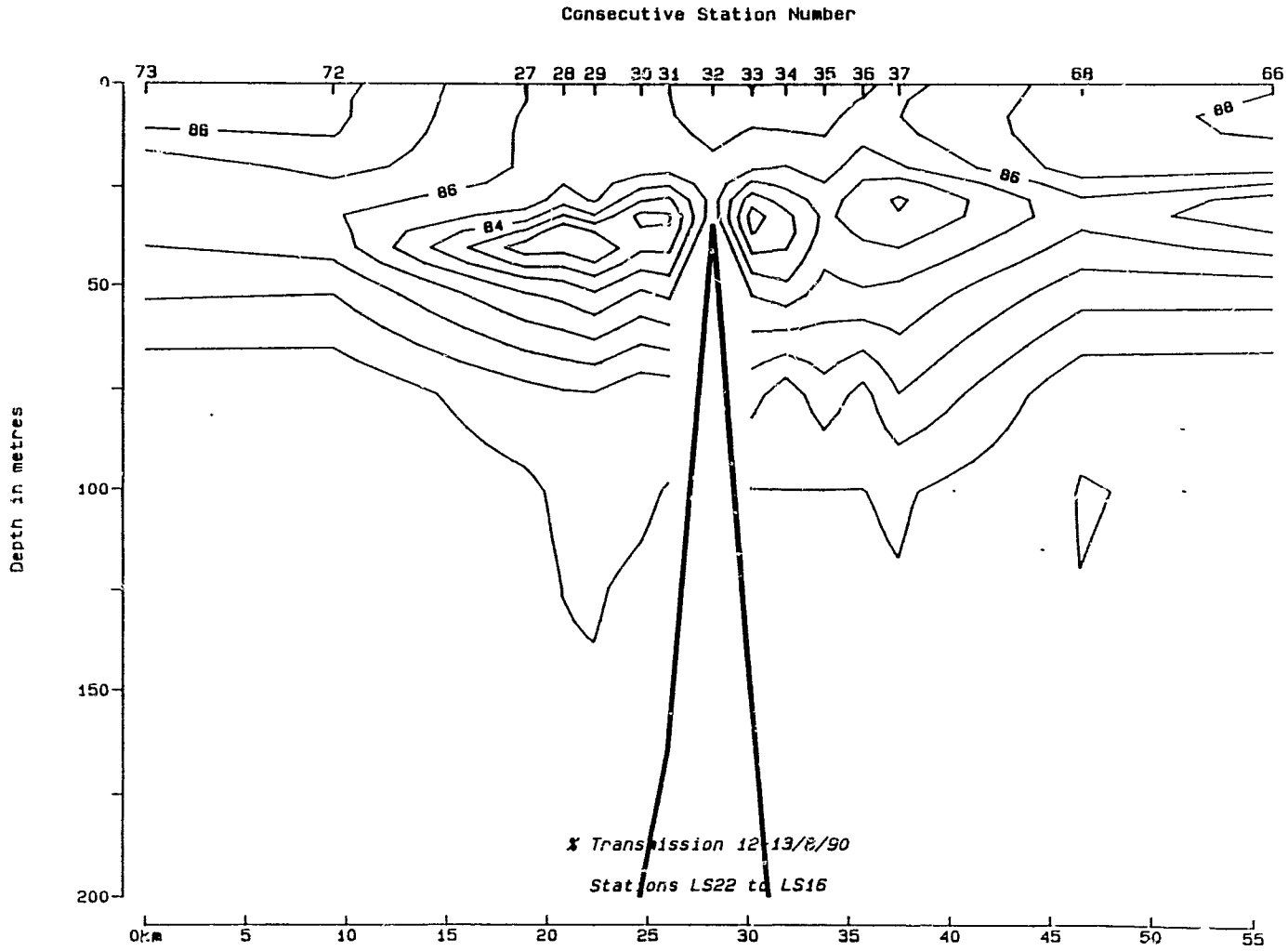
Consecutive Station Number
73
72
27
28
29
30
31
32
33
34
35
36
37
68
66
86
86
84
86
88
Depth in metres
0
50
100
150
200
0km
5
10
15
20
25
30
35
40
45
50
55
* Transmission 12-13/8/90
Stations LS22 to LS16

Figure 13 provides a plan view of the distribution of % light transmission at the light transmission minimum for each station. The map was computed using the method of objective analysis (see Freeland and Gould, 1976) and used a Gaussian correlation function viz:

$$C(r) = (1-\varepsilon)\exp(-r^2/a^2)$$

where the fractional noise level $\varepsilon = 0.2$ and the length scale $a = 10$ km. These parameters were chosen in an entirely *ad hoc* manner. We have no reason for expecting a Gaussian correlation function, let alone those specific parameters. However, we did compute the same map using a variety of different correlation functions and found that the main characteristics (i.e. the location and depth of the minimum and the bullseye pattern) to be invariant. In particular, we observed that the greatest attenuation of light transmission occurs over the southwest flank of the seamount.

Chlorophyll extraction was carried out using ice cold 95% acetone (in the dark) over 12 hrs. Chlorophyll fluorescence was measured using a laboratory fluorometer. Extracted chlorophyll values showed a strong negative correlation with corresponding transmissivity measurements (correlation coefficient $r = -0.81$). For n=14 independent observations the 95% confidence level occurs at $r = \pm 0.5$. However, these observations are not entirely independent, rather they represent a single survey of a deterministic

field. Thus we interpret the transmissivity minima to represent subsurface chlorophyll maxima (SCM). The patterns in Figures 13 and 16 therefore indicate a chlorophyll distribution where the isolines form a strong bullseye pattern, with the highest values centred above the seamount from 30-45m depth. Interestingly, while there is usually an SCM between ~40-60m in the Northeast Pacific (Anderson, 1969; Longhurst and Harrison, 1989; Booth, 1988) the layer is generally more diffuse than that seen in transmissivity profiles from Cobb.

Enhanced chlorophyll concentrations have also been noted over other seamounts (Genin and Boehlert, 1985; Wishner *et al.*, 1990), and observations in the Northwest Atlantic (Longhurst and Harrison, 1989) show the SCM above the Corner Rise Seamounts to be shallower than in the surrounding waters. However, in none of these cases is the difference between on- and off-seamount conditions as marked as at Cobb.

Laboratory and theoretical studies of rotating flow past seamount-like structures show that such topographies support closed-streamline anticyclonic flows called Taylor columns under certain conditions of upstream flow, degree of stratification and relative seamount height (Hogg, 1973; Boyer and Zhang, 1990; Chapman and Haidvogel, 1992). In the presence of significant stratification, such as occurs in the Northeast Pacific around Cobb, Taylor columns decay

upward and form a "Taylor *cone*" (Hogg, 1973; Roden, 1987).

Let us assume that a Taylor Cone forms over the top of Cobb Seamount and that the sides of the cone have a slope of about $f/N = 0.05$, where f is the Coriolis parameter and N is a local Brunt-Väisäla frequency. Taking a length scale as the radius of the seamount, L = 2.6km from the pinnacle to the second mooring on the seamount rim (Fig.14), we estimate a scale height for the Taylor cone of about $H = Lf/N = 120m$, which is less than the bottom depth of 210m at the seamount rim. Thus, we conclude that a closed recirculation should exist over Cobb but that it probably will not penetrate to the surface.

Figure 14 shows the location of the current meter moorings relative to the seamount topography. Current velocities are averaged over the entire deployment (~3 weeks) and averaged over the bottom two current meters at each site. These current vectors show an obvious tendency for the averaged flows near bottom to follow the isobaths. However, the satellite-tracked drifter buoys that followed the near surface currents during the cruise moved in a straight line from west to east, showing no evidence of an anticyclonic flow. Similarly, the current meters set 50 metres above the bottom showed marked differences in direction from those deeper down, and did not appear to be following bottom contours. Thus it appears that the strength of the Taylor column does diminish with height

above the bottom, presumably due to the damping of vertical momentum transfer by stratification (Hogg, 1973).

2.3 Discussion

We suggest that currents interact with the topography to produce an anticyclonic bottom-intensified Taylor cone above Cobb Seamount. Similar flow phenomena have been reported from other seamounts (Owens and Hogg, 1980; Gould *et al.*, 1981; Boehiert and Genin, 1987). It has been suggested that such flows penetrating the euphotic zone may act to stimulate primary productivity above seamounts, perhaps via the upwelling of deeper nutrient-rich water. In this case some form of trapping would appear to be necessary for the maintenance of the region of high chlorophyll concentration near the seamount.

During our cruise, the satellite-tracked drifters moved, as previously mentioned, from west to east. However, the speed of the surface current was quite high, about 15 km/day. If the layer of low light transmission shown in Figures 13 and 16 was influenced by this same flow field, then the residence time of this feature over Cobb Seamount would be, at most, one day. However, we spent almost three weeks in the vicinity of Cobb Seamount in July- August of 1990 and can verify that this bullseye of low transmission was a persistent feature.

While Taylor cone formation does imply some amount of isopycnal doming we saw little evidence for it over Cobb, perhaps a result of the choice of scale for our sampling regime. While enhanced chlorophyll levels have been reported from a Taylor cone penetrating the lower euphotic zone above Minami-Kasuga Seamount (Genin and Boehlert 1985), this effect was not manifested above 80 m depth. Additionally, the high chlorophyll levels over Minami-Kasuga lasted for only about two days, suggesting that the feature may not have been caused by a Taylor cone. Cobb differs from this and virtually all other seamounts studied to date, (Wilson & Kaufmann, 1987) in that its summit penetrates well into the euphotic zone, making any associated recirculating flow more likely to be of biological importance.

In a review of primary productivity levels from the North Pacific, Hobson (1980) reports that summertime chlorophyll concentrations typically remain below 0.3 μg/l in that part of the North Pacific where Cobb is situated. While the resolution of our chlorophyll sampling is quite coarse, it still indicates that chlorophyll concentrations in the SCM around the seamount (ranging from 0.4-1.3 μg/l) are well above normal background levels. At the station nearest the centre of the transmissivity bullseye, depth integrated chlorophyll in the top 100m of the water column was 122.4 mg/m^2 compared to values generally less than 35 mg/m^2 at more distant stations.

Whether the energy represented by this additional phytoplankton biomass can be transferred to higher trophic levels near Cobb depends largely on the persistence time of the feature. Persistence on the order of weeks to months would be necessary to increase zooplankton or micronekton biomass (Boehlert & Genin 1987; Denman *et al.*, 1989). Field observations elsewhere indicate that Taylor columns have some temporal stability (Owens & Hogg, 1980; Gould *et al.*, 1981), and the present study indicates stability for at least ~3 weeks. Submersible surveys on Cobb show that the seamount supports both a rich benthic community and dense nektonic stocks (Tunnicliffe, *pers. comm.*). It appears then, that this increased standing crop of phytoplankton may persist long enough to have a substantial effect in the local food chain.

2.4 Observations from CSEX91 and CSEX92

Section 1.2.5 reviewed the thermohaline structure around Cobb Seamount during the three CSEX cruises. In general, conditions showed only minor changes between years with respect to the structure of the water column and the location of the doming region (see Figs.5-10). Figure 17 shows plan views of the chlorophyll distribution near Cobb during CSEX91 and '92 using the objective analysis method described in Section 2.2. Although more variable than the physical properties examined in Section 1.2.5, chlorophyll

distributions do show evidence of a seamount effect in both 1991 and 92'.

In 1991 a strong chlorophyll front, visible as a southward loop in the chlorophyll isolines (Fig.17a), was situated over Cobb. Chlorophyll concentrations on both the west and east flanks of the seamount represented local maxima, while a region of lower chlorophyll water was found over the northern flank (Fig.17a). At 30m, a band of high chlorophyll water runs northwest-southeastward over the seamount (Fig.17b). Maximum chlorophyll concentrations at 30m were in excess of 2 μg/l.

In 1992 a bullseye of high chlorophyll water was centred ~30km east of Cobb at a depth of 10m (Fig.17c). Chlorophyll concentrations in the centre of this bullseye, >0.3 μg/l, were about twice the background concentration away from the seamount. The picture at 30m is harder to interpret, as a band of high chlorophyll water runs north-south throughout the region covered by the hydrographic survey (Fig.17d). The highest chlorophyll concentrations in the band occur to the north and south of Cobb, while a "saddle point" between these two local maxima is situated over the seamount summit (Fig.17d). Comparison of Figure 17 with Figures 6,7,9 and 10 suggests that regions of high chlorophyll water are generally located in the same regions where isopycnal doming occurs, downstream of the seamount.

Figure 17: Plan views of chlorophyll at (a) 10m and (b) 30m during CSEX91, and (c) 10m and (d) 30m during CSEX92. Overlays #4 and # 5 show the location of the 2000m isobath on Cobb Seamount for the 1991 and '92 plots respectively.

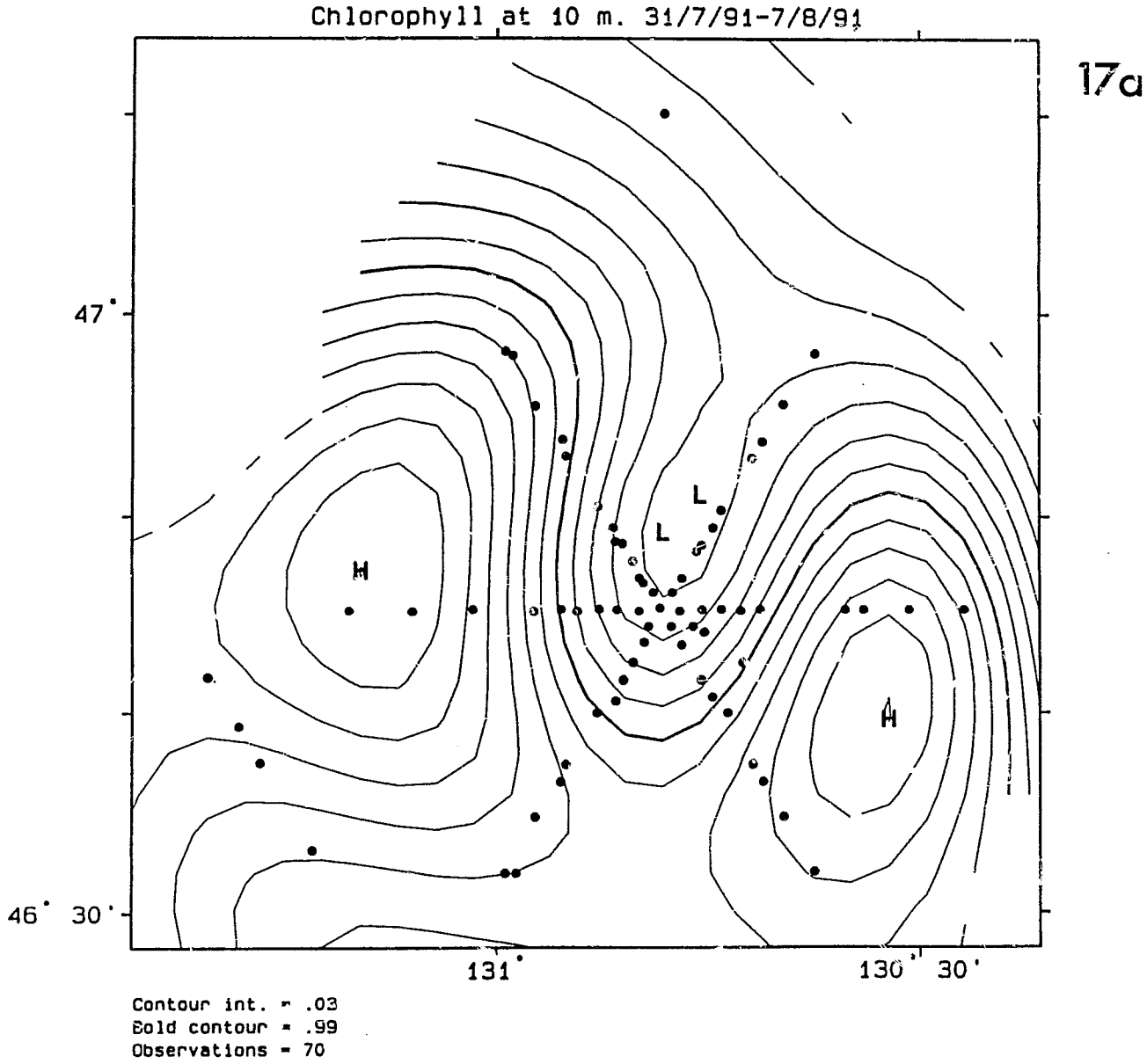
Chlorophyll at 10 m. 31/7/91-7/8/91
17a
47°
46° 30'
131°
130° 30'
H
L
L
H
Contour int. = .03
Bold contour = .99
Observations = 70

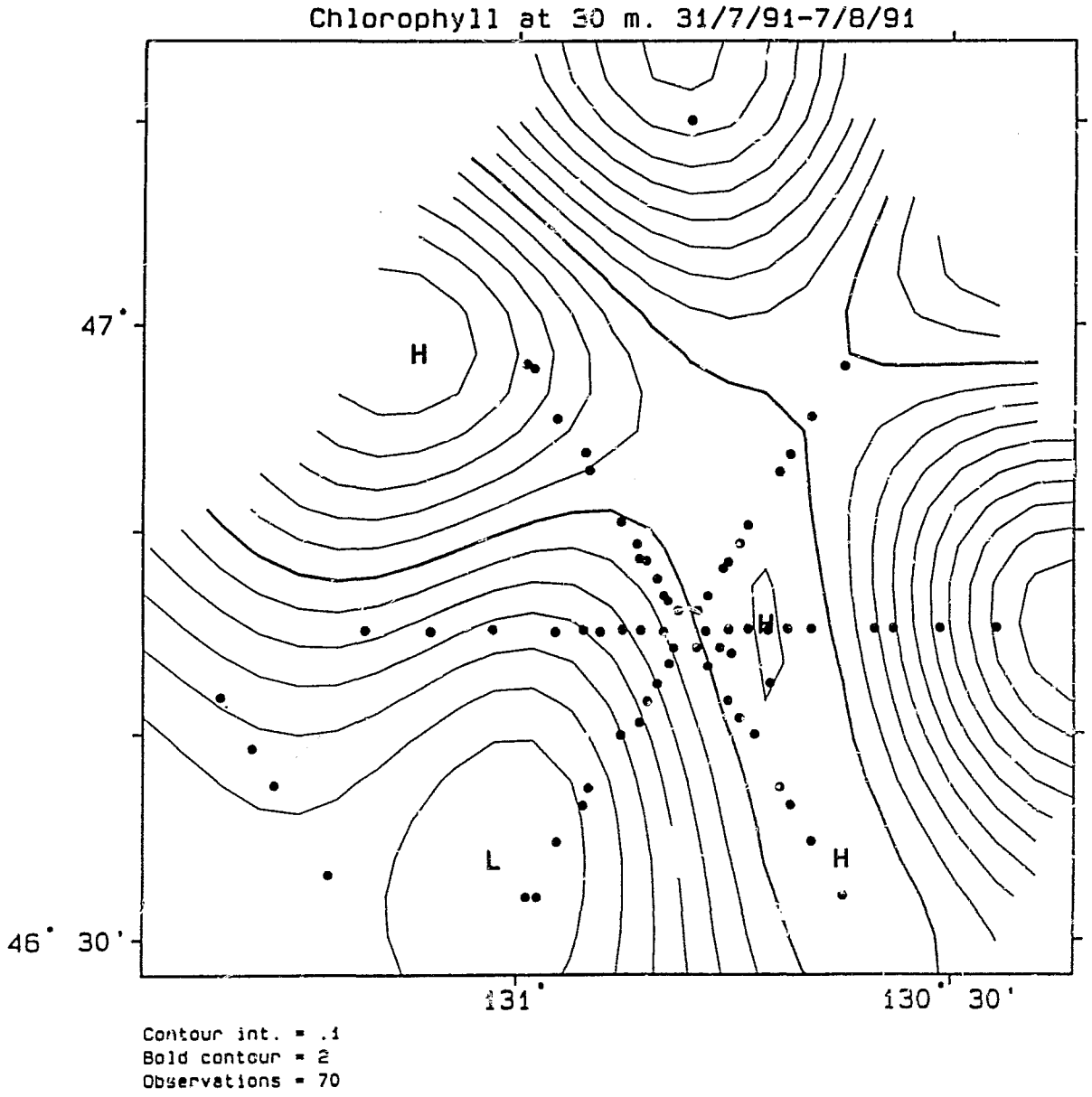
Chlorophyll at 30 m. 31/7/91-7/8/91
17b
47°
46° 30'
131°
130° 30'
H
H
L
H
Contour int. = .1
Bold contour = 2
Observations = 70

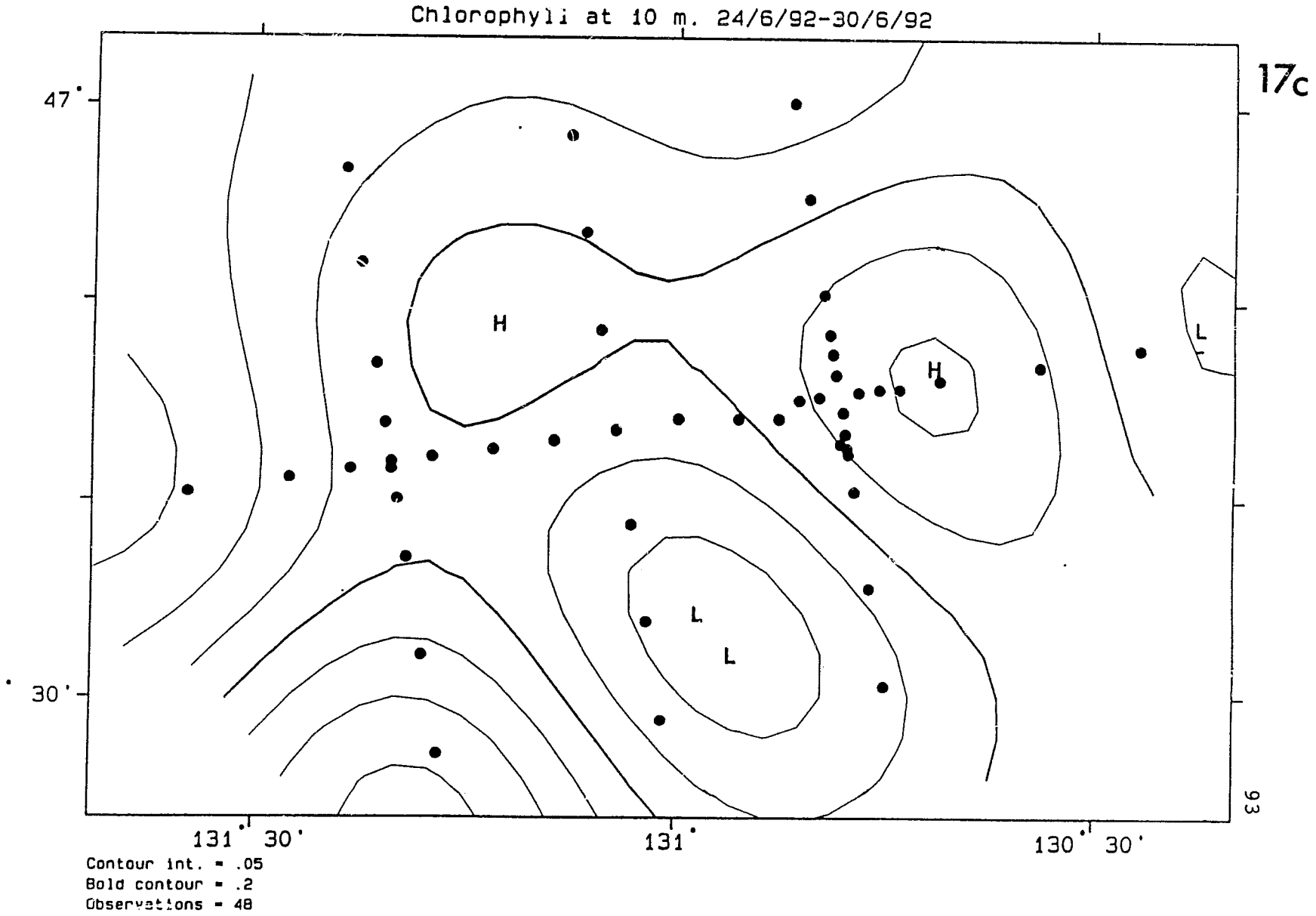
Chlorophyll at 10 m. 24/6/92-30/6/92
17c
47°
30°
H
H
L
L
L
131° 30'
131°
130° 30'
93
Contour int. = .05
Bold contour = .2
Observations = 48

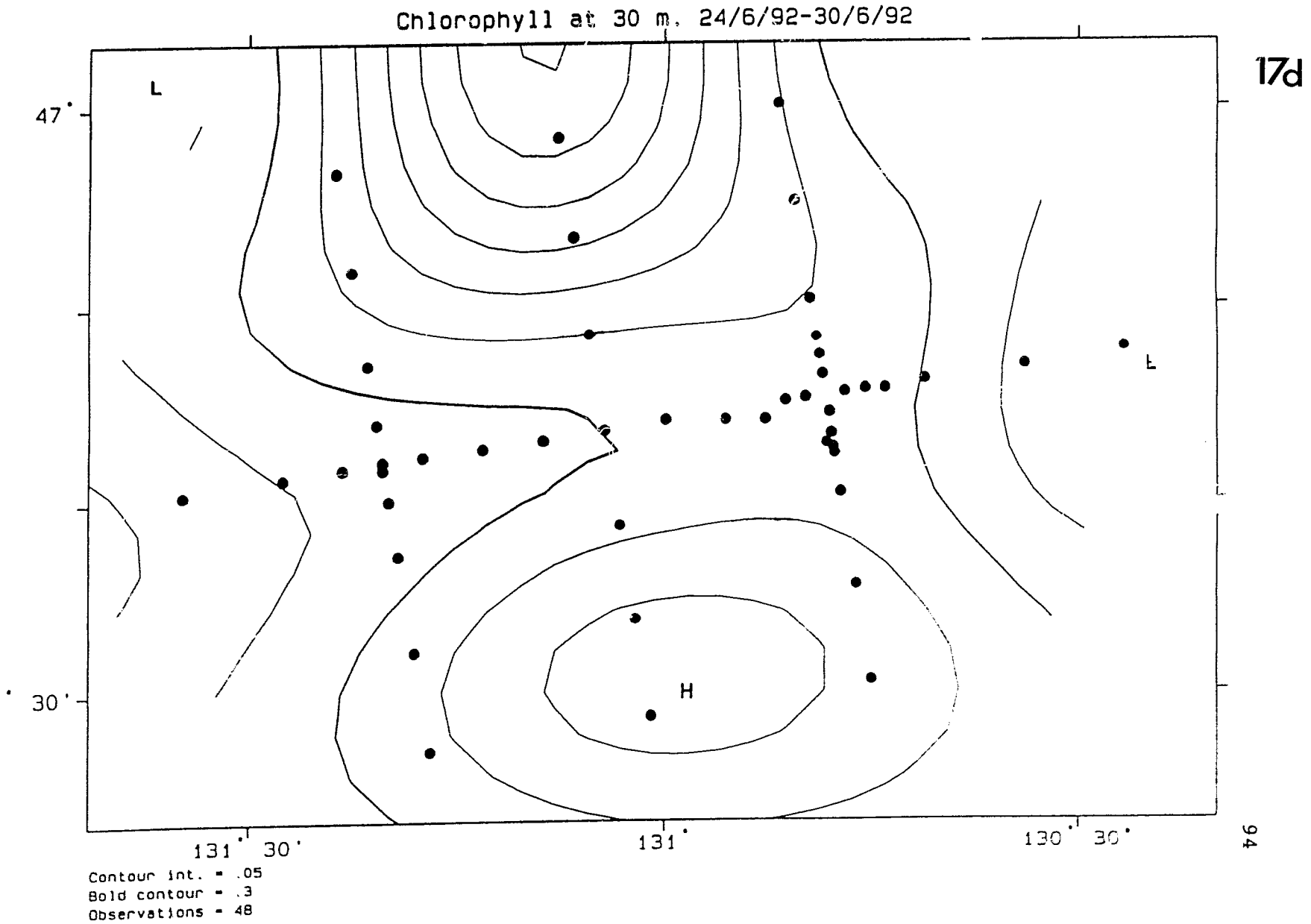
Chlorophyll at 30 m, 24/6/92-30/6/92
17d
L
L
H
47°
30°
131° 30'
131°
130° 30'
94
Contour int. = .05
Bold contour = .3
Observations = 48

Recent re-examination of the data on which the original *Deep-Sea Research* paper is based supports the idea put forth in Section 1.2.5 that during the 1990 cruise isopycnal doming penetrated to the surface over Cobb Seamount. Figure 18 shows plan views of density (as Sigma-t) and % light transmission at 10m during CSEX90. The dome of uplifted cold dense water and the bullseye in % light transmission shown in Figures 8a and 13 are quite evident in the near surface views of Figure 18.

Reports of enhanced standing stocks of phytoplankton near shallow seamounts have generally been based on single observations from individual cruises. This has made it difficult to generalize about the frequency of occurrence and the persistence times of such conditions. These observations from Cobb Seamount represent the first repeated reports of consistently high chlorophyll concentrations near a single seamount. The CSEX data also indicate that such conditions have persistence times on the order of at least several weeks at Cobb (*i.e.* length of the longest CSEX cruise).

Clearly, high standing stocks of phytoplankton appear to be the rule rather than the exception at Cobb. Based on our CSEX observations and given the relatively invariable background flow near Cobb, it seems likely that similar conditions persist throughout the entire summer. This satisfies one of the main requirements of the classical

Figure 18: Plan views of (a) density, as Sigma-t, and (b) the % light transmission at 10m during CSEX90.

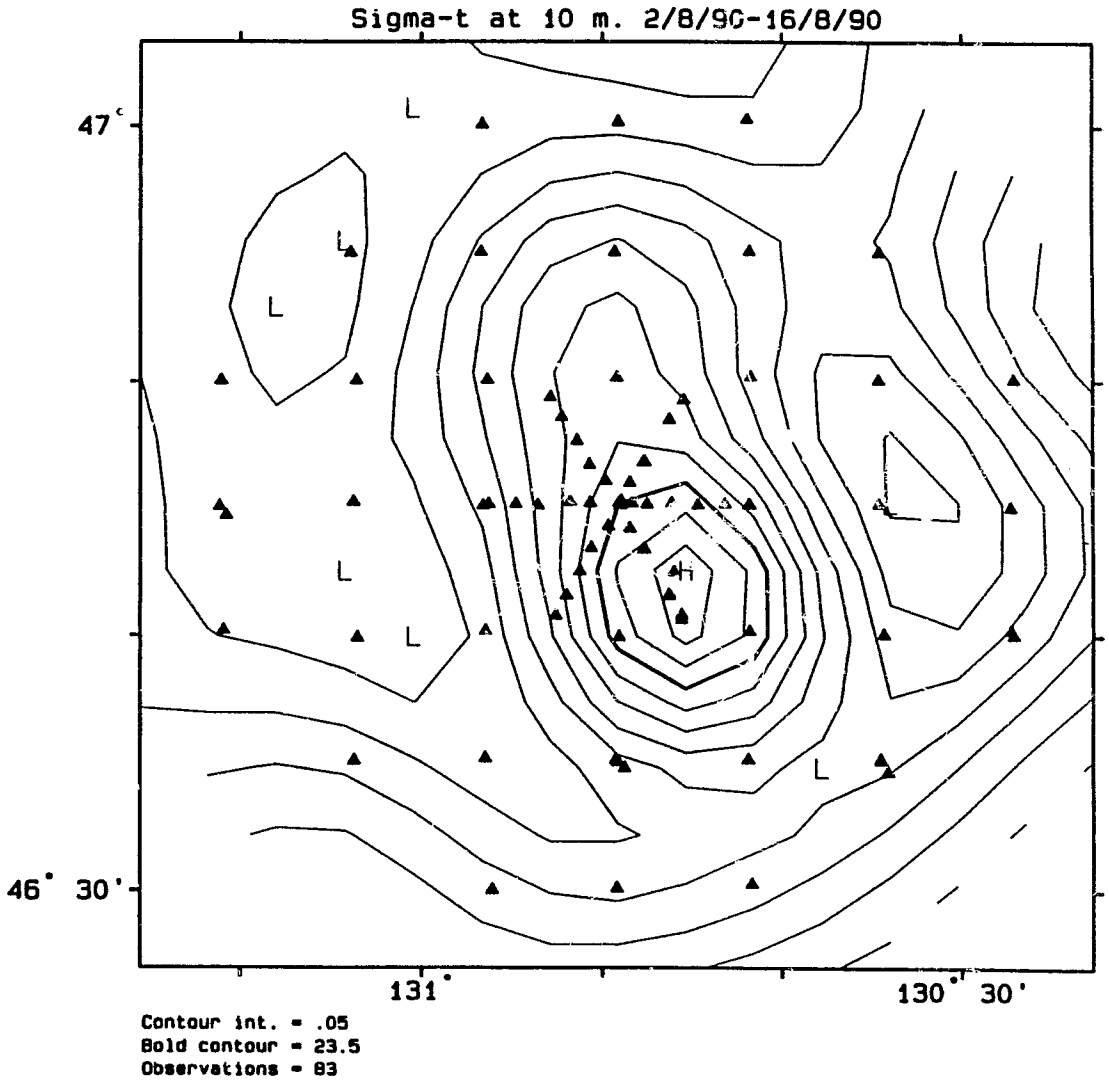
Sigma-t at 10 m. 2/8/90-16/8/90
47°
46° 30'
131°
130° 30'
L
L
L
L
L
H
Contour int. = .05
Bold contour = 23.5
Observations = 83

18a

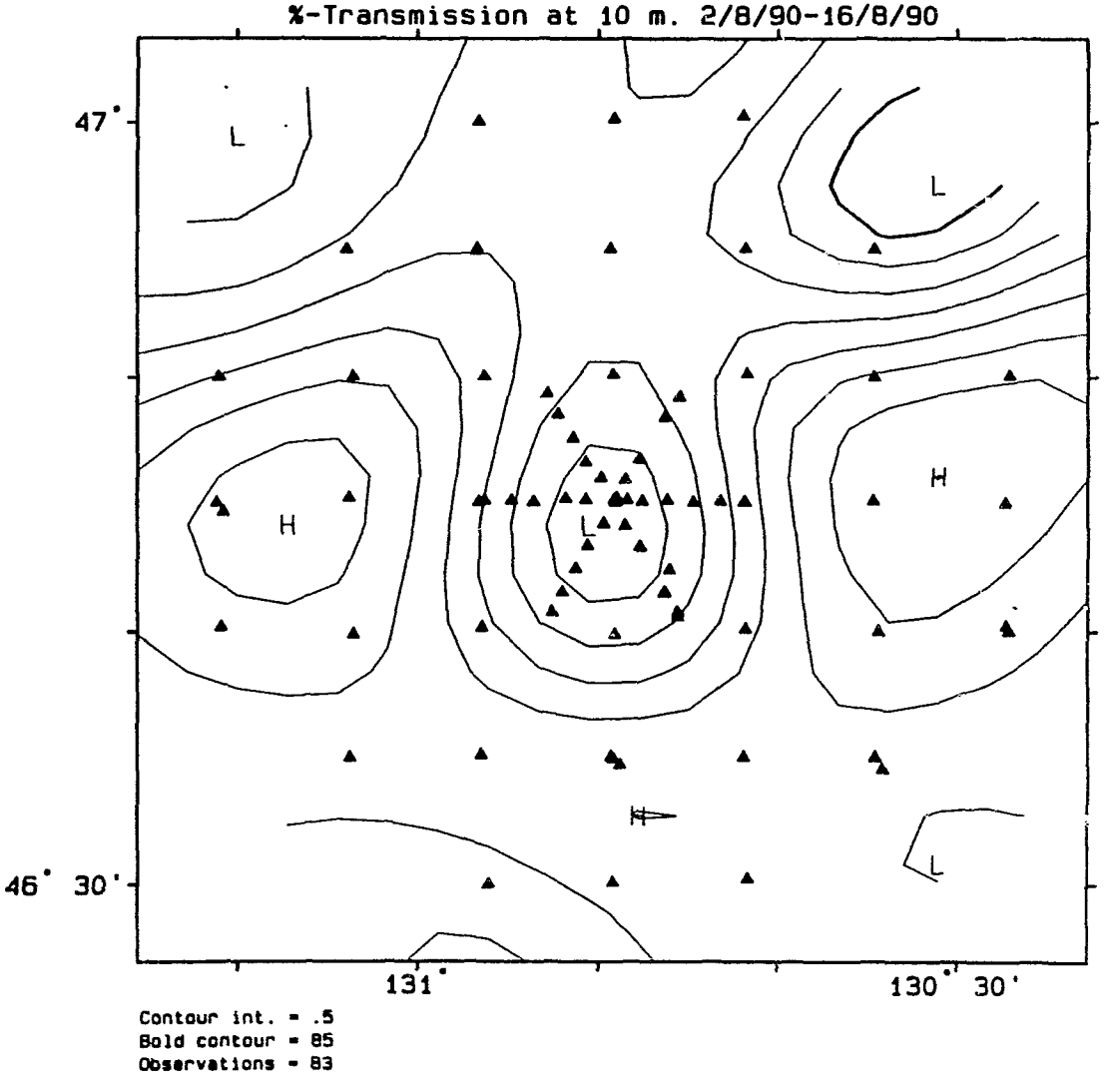
%-Transmission at 10 m. 2/8/90-16/8/90
47°
46° 30'
131°
130° 30'
L
L
H
H
L
L
Contour int. = .5
Bold contour = 85
Observations = 83

18b

hypothesis explaining the high productivity of shallow seamounts; namely, that the current-topography interactions that lead to increased phytoplankton stocks persist long enough to allow energy transfer to higher trophic levels. In Chapter 4 I investigate the other assumptions of this classical hypothesis. In particular, I examine the contentions that enhanced phytoplankton growth over shallow seamounts requires the existence of some form of trapping mechanism, and that the high nektonic biomass near seamounts ultimately derives from enhanced primary production.

Chapter 3:

SHIFTS IN MESOZOOPLANKTON COMMUNITY COMPOSITION NEAR AN ISOLATED SEAMOUNT IN THE SUBARCTIC PACIFIC OCEAN

3.1 Introduction

Seamounts are among the most common topographic features in the deep ocean: some estimates put the number of seamounts of height greater than 1000m at over 30,000 in the Pacific Ocean alone (Smith and Jordan, 1988). However, only a small fraction penetrate to within 1000m of the sea surface. Studies have shown that shallow seamounts often support rich stocks of pelagic and demersal fishes (Uda and Ishino, 1958; Herlinveaux, 1971; Uchida and Tagami, 1986). About a dozen such shallow seamounts in the subarctic Pacific are regularly visited by Canadian and American fishing vessels.

Over the last decade there has been a growing interest in shallow seamounts among both physical and biological oceanographers. In particular, two seamounts have been the focus of multi-year multidisciplinary research efforts: between 1990 and 1992 a series of cruises were made to Fieberling Guyot (1000km west of San Diego, shallowest depth ~500m) as part of the TOPO Project. The other study, the Cobb Seamount Experiment (CSEX), focused on Cobb Seamount, a very shallow seamount (minimum depth only 24m) located 500km southwest of Vancouver Island (Fig. 1 and Frontispiece). A

series of three cruises were made to Cobb in the summers of 1990-1992. Previous work at Cobb included exploratory cruises by the U.S. Department of Fish and Wildlife and the University of Washington Department of Oceanography in the 1950's, which described the basic geology, hydrography and biology of Cobb (Powell *et al.* 1952, Budinger and Enbysk, 1960). Detailed submersible surveys were also carried out at Cobb in the early 1980's (Farrow and Durant, 1985; Parker and Tunnicliffe, *submitted*).

Physical oceanographic research has focused mainly on flow phenomena that arise through the interaction of ocean currents with abrupt isolated topographies. Theoretical and laboratory studies show that under certain conditions seamount-like topographies are capable of supporting closed recirculations known as Taylor cones (Hogg, 1973; Roden, 1987). Theory also predicts some interesting internal wave phenomena: Eriksen (1982, 1985) shows how internal wave energy can be locally amplified through interaction with abrupt seamount topographies. Noble *et al.* (1988) note that seamounts can generate strong internal tides. Brink (1989, 1990) demonstrates that these internal tides can lead to the formation of seamount-trapped waves, similar to coastal Kelvin waves.

Biological oceanographers have focused on shallow seamounts as productive ecosystems. The occurrence of rich fish stocks around many seamounts suggests a shared

mechanism for generating such conditions. Unusually high chlorophyll concentrations have also been reported from a number of seamounts (Genin and Boehlert, 1985; Dower *et al.*, 1992). One hypothesis is that recirculating currents and upwelling over shallow seamounts foster enhanced primary production which is then transmitted to higher trophic levels (Boehlert and Genin, 1987).

Enhancement of secondary standing stocks by seamount flow fields requires that at least two conditions be met. First, as typical generation times for most zooplankton are on the order of weeks to months (Boehlert and Genin,1987; Denman *et al.*, 1989) regions of high phytoplankton production over a seamount would have to persist for comparable periods to produce higher zooplankton stocks. Second, to accumulate biomass via energy transfer from primary to secondary stocks zooplankton must also remain in the immediate vicinity of the seamount for weeks to months. There is evidence to support the first condition: regions of high chlorophyll water have been found over Cobb Seamount on several occasions. In at least one case, the high chlorophyll patch lasted for three weeks (Dower *et al.*, 1992).

To date, few data are available to support either the idea of the retention of zooplankton or of enhanced zooplankton biomass at isolated seamounts. Although Genin and Boehlert (1985) found zooplankton biomass and

chlorophyll concentrations over Minami-Kasuga Seamount to be higher than at off-seamount sites, they were unable to detect any such differences during another survey only two days later. In fact, there is growing evidence that zooplankton biomass may be *reduced* over shallow seamounts. For instance, mesozooplankton biomass over Cobb Seamount in July 1991 was generally about 30% lower than background levels (Dower, *unpublished data*). In a study on a shallow bank, Haury *et al.* (*in press*) document regions of reduced zooplankton abundance, termed "zooplankton holes", over the shallow topography. They suggest that this reduction in zooplankton abundance may result from increased levels of predation by fish resident on the shoal.

The goal of this chapter is to explore the effect that proximity to a shallow seamount has on mesozooplankton community composition. I examine spatial patterns of between-site similarity of community composition around Cobb Seamount during the June 1992 CSEX cruise. If taxon-specific differences in growth or mortality occur at Cobb Seamount then a shift in mesozooplankton community structure should be observed at sites nearest the seamount. Additionally, I address the issue of the spatial extent of such a "seamount effect": if there is a detectable seamount effect on mesozooplankton community composition, is it confined to the area directly over the seamount, or does it extend into the surrounding waters?

A number of workers have used Percent Similarity (Whittaker, 1975) or similar community resemblance indices to study zooplankton communities. Unlike techniques that examine the spatial patterns of individual species (reviewed in Legendre and Fortin, 1989), community resemblance indices share the ability to summarize shifts in the relative abundances of a number of species as a single number. Haury (1976) and Star and Mullin (1981) used Percent Similarity in comparative studies of small-scale spatial patterns in zooplankton communities off the Baja Peninsula and in the North Pacific Central Gyre. A "squared chord length" metric was used to estimate characteristic correlation scales of community composition and biomass for zooplankton and phytoplankton on the western North American continental shelf (Mackas and Sefton, 1982; Mackas, 1984; Mackas *et al.*, 1991).

As these resemblance indices measure shifts in the relative rather than absolute abundances of species they are particularly useful in situations where community composition is more smoothly varying than biomass, as is often the case for zooplankton. For instance, zooplankton community composition west of Vancouver Island shows little variation at scales <100km, while biomass is patchy at scales <25km (Mackas, 1984). Spatio-temporal patchiness in biomass unaccompanied by changes in community composition suggests different forcing mechanisms for biomass and

community patterns. Mackas *et al.* (1985) propose that the large-scale patterns in zooplankton community composition result from physical forcing (*eg.* currents, mesoscale eddies, etc.) while the small-scale biomass patchiness reflects zooplankton behavioral response. LeBrasseur (1965) and McGowan and Walker (1979) note similar patterns in the subarctic Pacific and the North Pacific Central Gyre.

3.2 Methods

3.2.1 Data Collection/Reduction

Samples were collected from June 24-27, 1992, from 28 stations on and around Cobb Seamount, 46°46'N, 130°48'W (Fig.19 and Frontispiece). Samples consisted of integrated vertical tows collected using a bongo-net with a 0.50m² mouth and a 236μm mesh. Nets were towed from 250m to the surface at ~1m/s. Exact locations of sampling sites are listed in the Appendix. No distinction was made between day and night sampling since, with the exception of most of the mesozooplankton species in the subarctic Pacific do not undergo extensive diel vertical migrations (Frost, 1987; Mackas *pers. comm.*). Samples were preserved in Borax-buffered 5% formalin.

Zooplankton were identified and enumerated using a dissecting microscope at 25x magnification. Identification followed Gardner and Szabo (1984), Morris (1970) and Park (1968). To facilitate counting, samples were typically

Figure 19: Map showing location of CSEX92 zooplankton sampling stations. Open circle denotes the 2000m isobath on Cobb Seamount. Exact locations for stations are listed in Appendix.

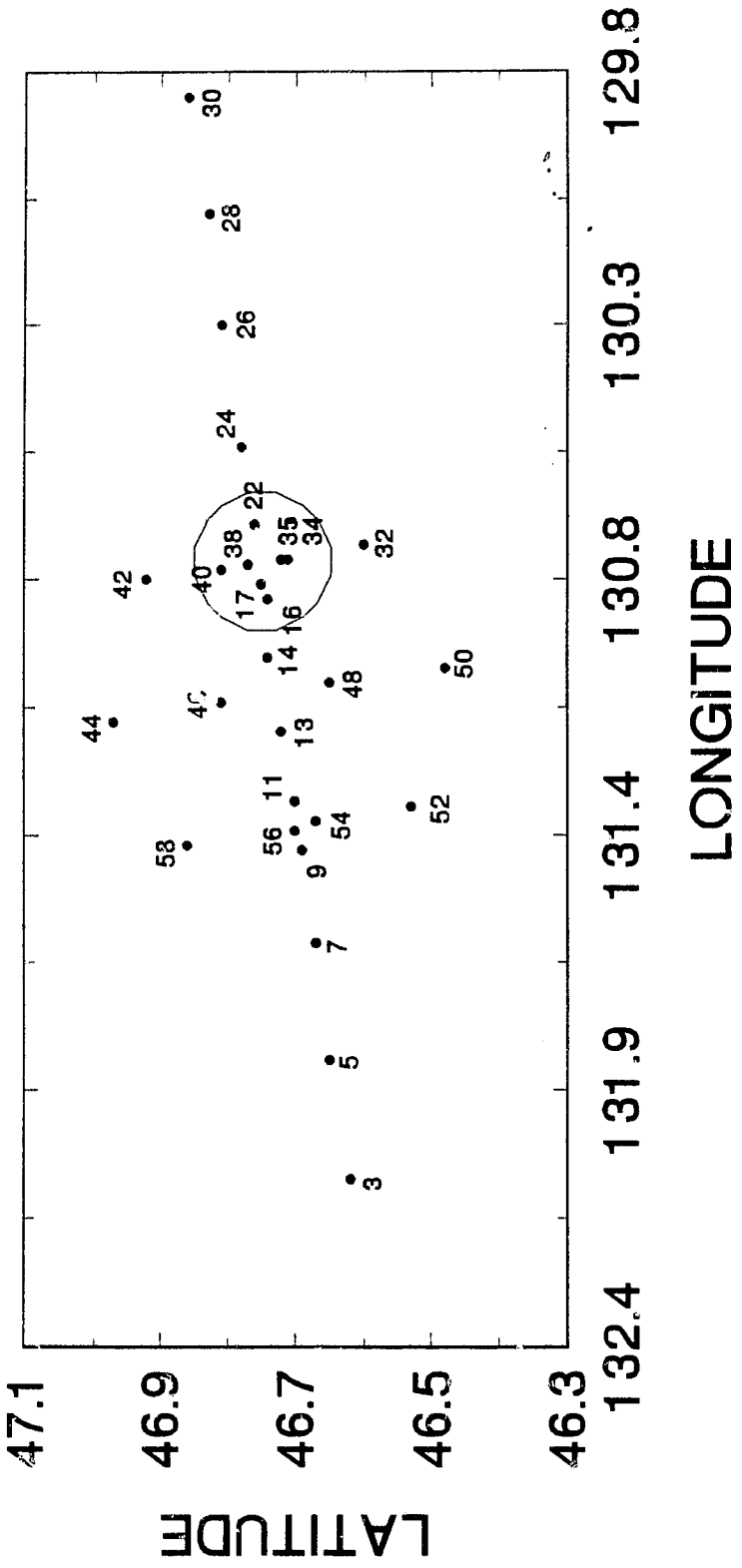
LATITUDE
47.1
46.9
46.7
46.5
46.3
132.4
131.9
131.4
130.8
130.3
129.8
LONGITUDE
30
28
26
24
22
35
34
38
40
42
32
17
16
14
48
50
44
13
11
52
56
54
58
9
7
5
3

split into eighths in a Folsom splitter and the mesozooplankton from one eighth were then identified and enumerated. Resultant counts were scaled up to give estimates of total numbers. All abundances are expressed as numbers per m^2 rather than as numbers per m^3, since time constraints did not permit depth-stratified tows. Larval fish were also enumerated but were not included in further analyses. The decision not to include larval fish was based on the assumption that, as most had probably originated at the seamount (particularly the rockfish larvae), their inclusion would tend to artificially decrease the similarity between on- and off-seamount stations.

Presence/absence differences in the mesozooplankton among the 28 stations were confined to a few very rare species. Given the rarity of such species I chose not to include them in further analyses. In addition, as I was uncertain of my identification of some of the smaller copepods (*i.e.* <1mm), I chose to concentrate primarily on the better censused mesozooplankton species. Among these, only *Metridia pacifica* showed significant differences in day/night abundance and was excluded from the analysis for this reason. Thirteen taxa remained. Abundance data were left untransformed since Percent Similarity standardizes against within station total abundances (Whittaker, 1975).

3.2.2 Statistical Methods

A Percent Similarity matrix was generated for the 28 samples, resulting in $(n^2-n)/2 = 378$ pairwise comparisons. The Percent Similarity Index (PSI hereafter) is defined as:

$$P.S.I. = 1-(0.5\sum_{1}^{i}|A_i-B_i|)$$

where A_i and B_i are the percent contributions of species *i* from samples A and B (Whittaker,1975). PSI then, is an inverse measure of ecological distance between samples in that it estimates the degree of similarity of the various percent contributions made by species 1,2...i in the samples. Typically, PSI decreases as the spatial distance between a pair of samples increases. PSI values for oceanic zooplankton usually range from ~90%, for samples less than 1km apart, to ~70% for samples separated by 10's of kilometres Haury (1976).

Normally, PSI is plotted as function of straight line geographical separation between samples. This is also the basis of most other spatial autocorrelation techniques (Odland, 1988). Rather than straight line separation, my main interest was in whether proximity to Cobb Seamount disrupted PSI patterns in the mesozooplankton community. I therefore needed to distinguish between changes in PSI due to (1) straight line distance between sample sites and (2) the relative proximity of the various sampling sites to the seamount. Hereafter, straight line separation between

samples is denoted SEP, and I define a second measure, delta radial (DELRAD), as the absolute value of the difference in radial distance to the seamount pinnacle for the elements of a given sample pair (see Fig.20). If it is assumed that localized seamount effects on mesozooplankton community composition are particularly strong and symmetrical about the seamount, then PSI should vary more strongly with DELRAD than with SEP.

As a first step, the dependence of PSI on SEP and DELRAD was examined using Cleveland's locally weighted scatterplot smoothing (LOWESS) method (Cleveland 1979). LOWESS is used to explore the nature of the dependence of an independent variable *Y* on a dependent variable *X* when there is no *a priori* reason to suspect that one functional form of the relationship provides a better fit to the data than another (Cleveland 1985, Trexler and Travis 1993). LOWESS fits a line through a scatterplot by estimating each value of *Y* from a weighted average of neighbouring points. The fraction of the total number of points in the scatterplot used to fit each estimate of *Y* is controlled by the choice of a "tension" parameter, *f*, which varies between 0 and 1.

As another means of visualizing any "seamount effect" on mesozooplankton community structure, I subjected the covariance matrix of the abundance data to a Principal Components Analysis (PCA). PCA is an ordination technique that summarizes variation in a multidimensional dataset and

Figure 20: Schematic diagram of distance measures used in LOWESS plots and ANOVA. All distances are in kilometres. The open circle denotes the position of a hypothetical seamount. The seamount pinnacle is at C. Points A, B and D are hypothetical sample sites at 40, 20 and 10km from the pinnacle. **SEP** is merely the straight line separation between two samples. **DELRAD** measures the relative difference in distance to the seamount for a given sample pair. **MINRAD** is the distance from the seamount to the nearest element of a given sample pair.

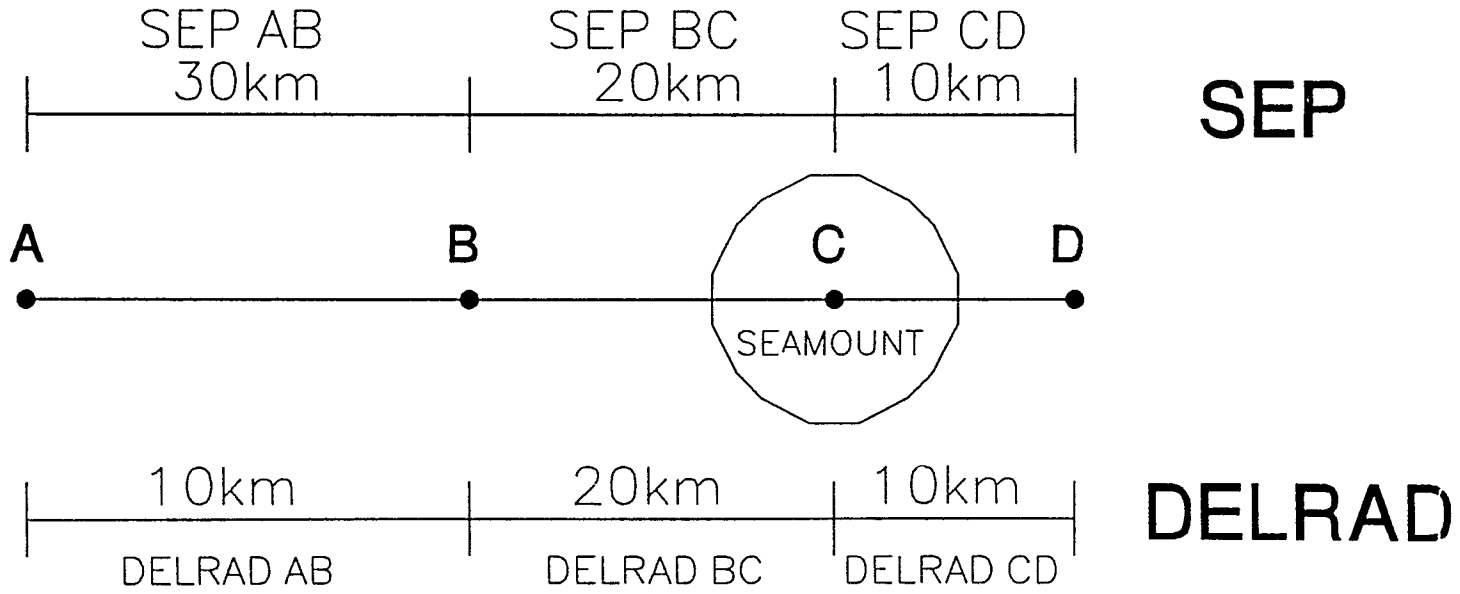

NOTE:

MINRAD AB is 20km, as 20km is the distance from the seamount to the nearest element of the pair.
Likewise, MINRAD BC is 0km, and MINRAD AD is 10km

allows that variation to be plotted along a few key axes (Wilkinson, 1990). In this case, for instance, 13 taxa were enumerated in each sample. Obviously, there is no simple method to map samples in 13-dimensional space. Instead, PCA constructs the composite axis, a "principal component", that accounts for the greatest amount of covariation in the 13 variables (Sneath and Sokal, 1973). Additional axes are added orthogonally until all of the variation is accounted for. Component axes are linear combinations of the original variables and usually 2-4 such components are sufficient to account for most of the total variation. The contribution that an individual variable makes to a component axis is its "component loading" for that axis, and reflects the correlation between the original variable and the principal component (Wilkinson, 1990).

When plotted in this reduced dimensional space, samples with similar compositions cluster together. If a seamount effect in the form of taxon-specific growth or mortality occurs near Cobb Seamount, it could result in a higher degree of between-sample resemblance among samples collected near the seamount. Consequently, we might expect these samples to cluster together in PCA space.

In order to quantify the effect of proximity to Cobb Seamount on PSI, I also grouped the 378 sample pairs into classes based on DELRAD and a third distance measure, MINRAD, which I define as radial distance (in kilometres)

from the Cobb pinnacle to the nearest element of a pair of sample sites (Fig.20). Let us assume that any seamount effect on zooplankton community composition only extends some limited distance into the surrounding waters. If we suppose that the effect extends ~50km from Cobb, then a DELRAD of 25km will likely have a greater effect on PSI for a pair of samples 0 and 25km from the seamount than for samples at 100 and 125km. The addition of this third distance measure, MINRAD, allows such effects to be distinguished.

I analyzed the grouped PSI data using a two-way ANOVA with MINRAD and DELRAD grouped into discrete distance classes denoted MINCLASS and DELCLASS. Class limits are defined in Table 1.

Table 1: Distance classes used for ANOVA. MINCLASS is based on MINRAD, DELCLASS is based on DELRAD.

DISTANCE CLASS DESIGNATION	CLASS LIMITS (km)
MINCLASS 1	0 - 10
MINCLASS 2	10 - 25
MINCLASS 3	25 - 50
MINCLASS 4	>50
DELCLASS 1	0 - 20
DELCLASS 2	20 - 40
DELCLASS 3	40 - 80
DELCLASS 4	>80

MINCLASS divisions reflect distances imposed by the choice of sampling scheme. For instance, there is a cluster of seven samples within ~10km of Cobb, a further ring of three more stations between 10-25km, etc. (Fig.19). DELCLASS limits are multiples of the seamount diameter (about 40km). In the absence of other information, a distance of one seamount diameter seemed a reasonable estimate for the horizontal extent of a potential seamount effect. Further subdividing of MINRAD and DELRAD results in numerous classes with very few observations.

3.3 Results

Raw abundances of the 13 taxa used in the analyses are presented in Table 2. Actual counts can be retrieved by dividing values in Table 2 by eight. The mesozooplankton fauna near Cobb Seamount is typical of that presented by LeBrasseur (1965) for the subarctic Pacific in summer. The dominant large copepods in the collections were *Neocalanus plumchrus*, *Eucalanus bungii* and *Calanus pacificus*. Interestingly, *Lucicutia flavicornis*, not usually numerous in the subarctic Pacific, was slightly more abundant than *C. pacificus*. Numerically, small cyclopoids of the genus *Oithona* were the most abundant copepods. Large numbers of chaetognaths (primarily *Sagitta elegans*), larvaceans (*Oikopleura sp.*) and the medusa *Aglantha digitale* were recorded. High densities of doliolids, often

TABLE 2: Abundances of 13 taxa used in all subsequent analyses. Taxa designations are as follows:

COPEPODA

NPLUM . . . . *Neocalanus plumchrus*

NCRIS . . . . *Neocalanus cristatus*

CPAC . . . . *Calanus pacificus*

OITH . . . . *Oithona spp.*

EBUN . . . . *Eucalanus bungii*

LFLAV . . . . *Lucicutia flavicornis*

ONCAEA . . . *Oncaea spp.*

AMPHIPODA

AMPHIS . . . *Parathemisto spp.*

CHAETOGNATHA

CHAETO . . . *Sagitta spp., Eukrohnia hamata*

POLYCHAETA

TOMOP . . . . *Tomopteris spp.*

MEDUSAE

AGLAN . . . . *Aglantha sp.*

DOLIOLIDS

DOLIOS . . . *Doliolum sp.*

LARVACEAN

LARVS . . . . *Oikopleura spp.*

Also listed are the mean abundance, the average number of individuals counted and mean:variance ratios.

TAXA

STATION	NPLUM	NCRIS	CPAC	OITH	EBUN	CHAETO	LFLAV	ONCAEA	DOLIOS	TOMOP	LARVS	AMPHIS	AGLAN
3	52	172	192	4880	88	912	36	228	2876	220	572	60	12
5	80	460	276	2452	180	488	112	132	3088	260	3312	88	524
7	152	3112	384	4296	600	1240	328	72	1872	40	2760	296	680
9	16	176	24	128	128	408	256	40	808	88	2520	288	264
11	4	48	4	1660	40	160	40	20	484	24	1004	48	88
13	16	936	136	4216	248	884	200	88	960	64	2912	144	824
14	1	584	136	3304	384	816	208	96	3504	216	3976	96	664
16	40	216	48	2560	248	548	208	80	1448	56	1952	48	240
17	1	72	152	4312	376	712	240	40	1480	64	4928	207	440
22	144	248	152	3808	520	1272	368	88	7368	104	4368	112	632
24	72	448	64	4872	88	352	40	56	2448	168	904	216	344
26	176	448	112	3376	160	496	176	224	1360	32	1440	192	288
28	96	592	176	5832	272	528	48	128	784	96	528	288	240
30	16	680	224	5872	272	920	184	160	368	32	2088	160	400
32	48	440	104	3752	264	704	296	104	1984	112	2408	328	456
34	40	736	264	2240	432	696	352	168	2880	80	3896	432	760
35	1	144	408	4280	256	1064	432	120	1592	168	7584	120	336
38	16	1456	304	6800	640	960	416	160	7232	144	4888	172	320
40	16	1552	304	11264	1312	736	336	112	5200	240	3328	288	864
42	1	296	128	1064	64	328	72	80	688	128	1520	232	568
44	40	408	192	2640	192	976	224	224	1904	80	4096	248	384
46	104	328	120	2784	288	1048	224	120	1232	80	3752	216	640
48	40	1576	320	3976	616	1560	296	176	1824	88	2976	248	1880
50	64	1920	320	6272	736	1616	416	112	1776	272	4112	736	816
52	64	696	368	4888	488	1408	360	200	2248	96	4888	608	808
54	176	592	320	3736	392	968	536	128	456	72	4480	348	408
56	48	1880	296	5424	408	1440	432	312	1344	48	4528	184	936
58	40	284	265	2932	404	1004	76	36	2380	176	2844	348	384
MEAN	55.86	731.86	206.89	4043.57	360.57	875.14	246.86	125.14	2199.57	116.00	3155.86	241.11	542.14
AVE NUMBER COUNTED	6.98	91.48	25.86	505.45	45.07	109.39	30.86	15.64	274.95	14.50	394.48	30.14	67.77
VARIANCE:MEAN RATIO	49.63	693.45	61.90	1084.47	191.13	163.66	79.54	37.64	1448.66	45.19	814.86	102.65	234.28

indicative of Transitional waters, were also noted. Table 2 also gives mean abundances, the average number of individuals counted and the variance:mean ratios for the 13 taxa. Recall that samples were split into eighths, and then scaled up to give estimates of total abundance.

The error associated with estimating abundance in thismanner varies inversely with the square root of the numberof individuals counted. For abundant taxa, this error is small. For instance, the average number of larvaceans counted was about ~400 (Table 2), giving an associated error of ±20. When scaled up by a factor of eight this translates into a mean of 3200 and an error of only ±160, or ±5% of the mean. For rare taxa, however, this error can become quite large. The numbers of individuals counted for most of the taxa in Table 3 was large enough that the associated error was usually <15% of the estimated mean. The highest errors are associated with *Neocalanus plumchrus*, *Tomopteris spp.* and *Oncaea*.

Larval fish were more abundant over Cobb than in the surrounding waters. Figure 21 shows the mean abundances of larval fish collected in night tows (from 250m to surface) and off Cobb. For samples collected within 10km of Cobb, mean abundance was about four times higher than in samples collected greater than 10km from the seamount. Larvae were not identified to species but the bulk of the samples were larval rockfish, the dominant group of fish at Cobb.

Figure 21: Mean abundances of larval fish collected in night tows (from 250m to the surface) near Cobb Seamount during CSEX92. On-seamount samples (n=5) were those night tows within 10km of Cobb, while off-seamount samples (n=9) were collected >10km from Cobb. Mean on-seamount abundance is about 4 times higher than mean off-seamount abundance. Error bars show standard deviations within groups.

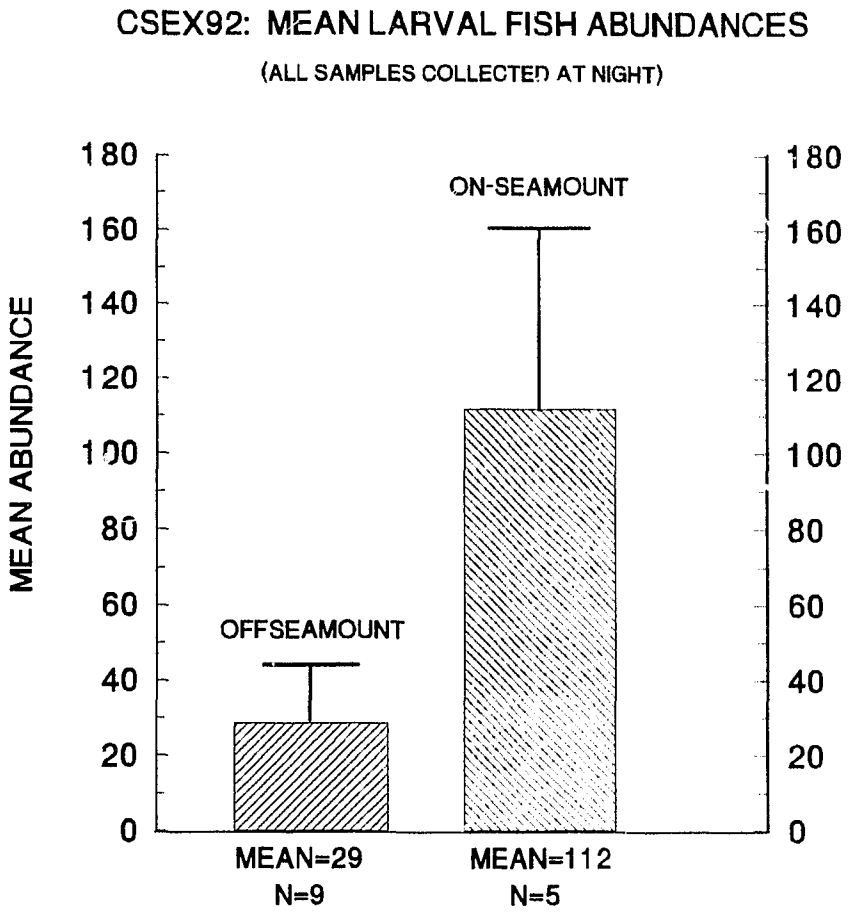
CSEX92: MEAN LARVAL FISH ABUNDANCES
(ALL SAMPLES COLLECTED AT NIGHT)
MEAN ABUNDANCE
180
160
140
120
100
80
60
40
20
0
ON-SEAMOUNT
OFFSEAMOUNT
MEAN=29
N=9
MEAN=112
N=5

Figure 22 shows LOWESS plots of PSI against SEP and DELRAD. PSI values range from 45-90%, with a median value of 78%. These values are comparable to those reported from other studies in the North Pacific (Haury, 1976; Star and Mullin, 1981). Figure 22 also shows PSI to have a different functional relationship with SEP than with DELRAD. Although PSI declines as both SEP and DELRAD increase, the decline with increasing DELRAD is steeper. There is also evidence of a slight "knee" in PSI near DELRAD values of 50km, beyond which PSI declines more rapidly.

The results of the Principal Components Analysis are shown in Figure 23. Samples are plotted against the first three principal components, which together account for 60% of the variation in the raw abundance data. Component loadings for the 13 taxa are provided in Table 3. Component 1 is positively correlated with abundances of most of the larger mesozooplankton: *Neocalanus plumchrus*, *Aglantha sp.*, *Eucalanus bungii*, chaetognaths, *Parathemisto spp.*, and *Calanus pacificus*. Component 2 shows strong correlations with abundances of doliolids, *Tomopteris spp.* and *Oithona spp.* Component 3 correlates with larvaceans and *Lucicutia flavicornis*.

Figures 23(a-c) each contain a single cloud of samples, suggestive of high overall similarity among the samples. The 10 samples collected within 30km of Cobb do not form an obvious cluster separate from the off-seamount stations.

Figure 22: LOWESS Plots of Percent Similarity against (a) SEP and (b) DELRAD. Both SEP and DELRAD are measured in kilometres. Note the steeper slope in the PSI vs. DELRAD plot, and the "knee" at DELRAD = 50km. N = 378 and tension, *f*, is 0.6 for both plots.

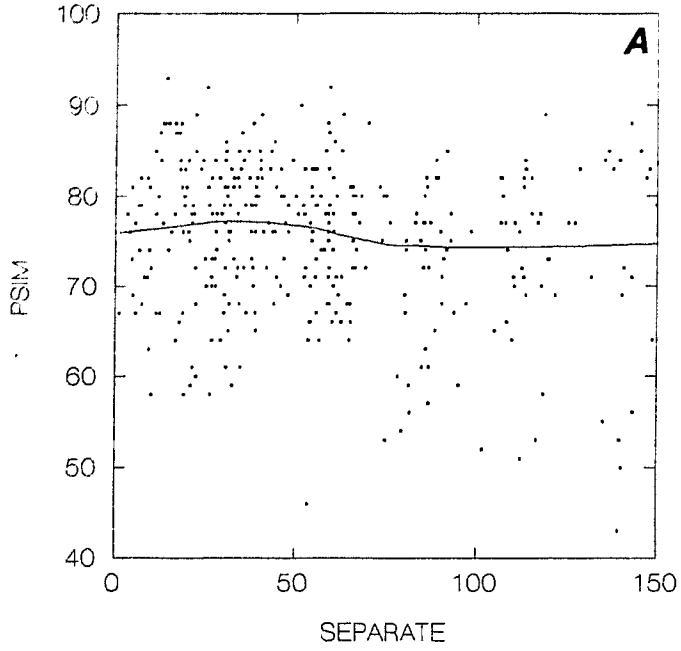
A
100
90
80
70
60
50
40
PSIM
0
50
100
150
SEPARATE

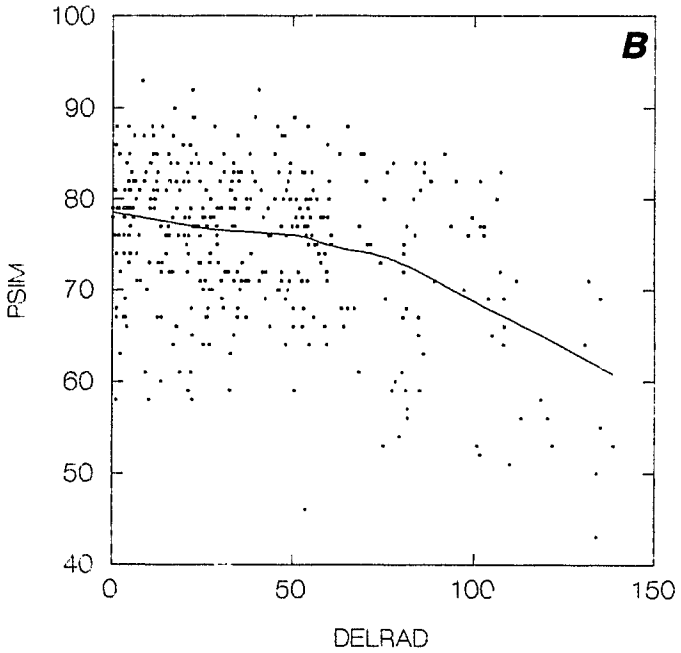
B
100
90
80
70
60
50
40
PSIM
0
50
100
150
DELRAD

Figure 23(a-c): Ordination of the 28 mesozooplankton samples using the first three components from the Principal Components Analysis. Triangles represent the 10 samples collected within 30km of Cobb Seamount, squares represent samples collected 30-200km from the seamount. Bracketed numbers represent percent of total variation explained by each principal component.

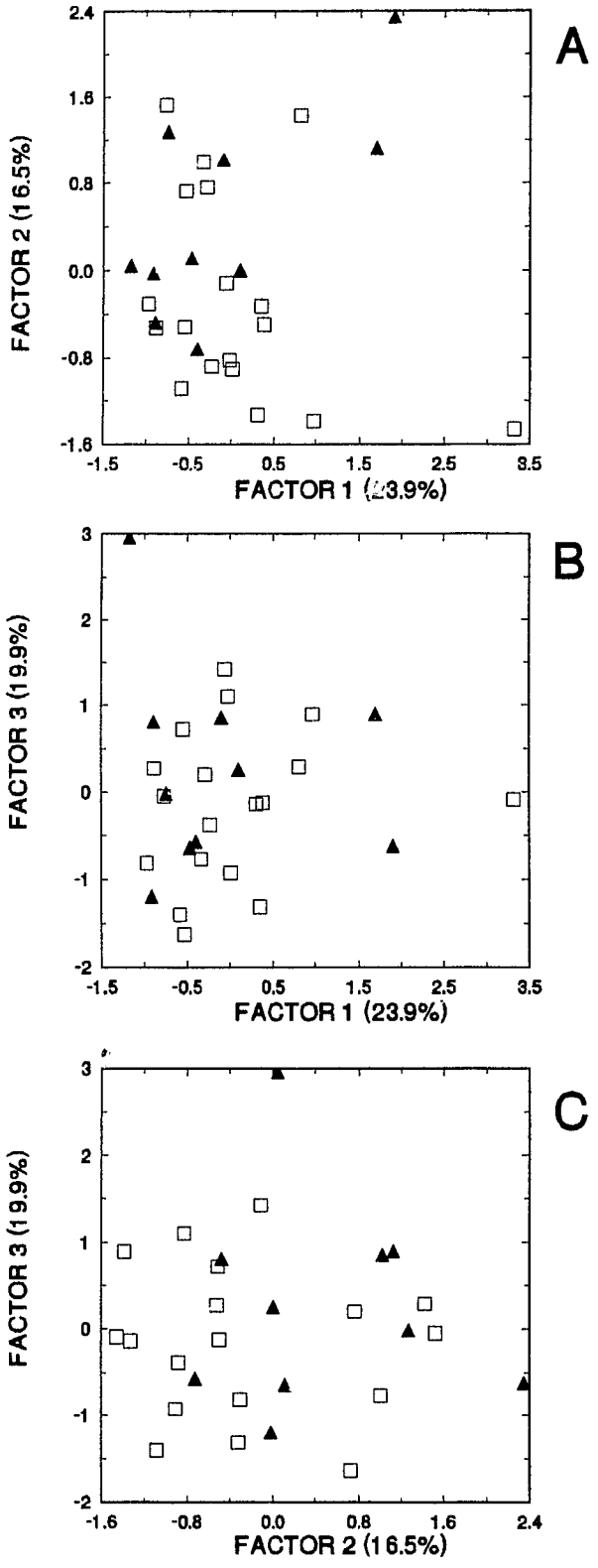
A
FACTOR 2 (16.5%)
FACTOR 1 (23.9%)
B
FACTOR 3 (19.9%)
FACTOR 1 (23.9%)
C
FACTOR 3 (19.9%)
FACTOR 2 (16.5%)

TABLE 3: Component loadings for Principal Components Analysis, and the variance explained by each component.

TAXA	AXIS 1	AXIS 2	AXIS 3
Neocalanus plumchrus	.828	.159	.083
Aglantha sp.	.752	-.062	.251
Eucalanus bungii	.644	.595	.282
Chaetognaths	.591	.046	.588
Parathemisto spp.	.570	-.067	.277
Calanus pacificus	.553	.251	.570
Oithona spp.	.517	.675	.003
Doliolids	-.084	.833	.221
Tomopteris spp.	.045	.702	.012
Larvaceans	.040	.135	.952
Lucicutia flavicornis	.325	.096	.732
Neocalanus cristatus	.051	-.061	.035
Oncaea spp.	.277	-.040	.200
VARIANCE EXPLAINED BY EACH COMPONENT	**23.9%**	**16.5%**	**19.9%**

The only possible means of distinguishing the two groups of samples would appear to be along principal component axis 2. A *t*-test of the two groups of sample scores for Component 2 shows that the mean value among samples collected within 30km of Cobb is significantly higher (p = 0.03) than the mean score among those samples collected further from the seamount. Even this result must be viewed with some degree of caution, however, given the small sample sizes used in the *t*-test (*i.e.* n = 11 and n = 17 for samples collected less than 30km from Cobb and those collected further than

30km from Cobb, respectively).

Table 4 summarizes the ANOVA results. The effects of DELCLASS and MINCLASS are both highly significant. Taken together, the two distance measures account for about 21% of the total variation in PSI. The degrees of freedom for the error term is an approximation and was arrived at as follows. The *df* in the PSI matrix is determined multiplicatively by the number of independent stations and the number of independent taxa. From Figure 19 it can be seen that the clustered nature of the sampling grid makes it unlikely that all 28 samples are spatially independent: I conservatively chose to assume only 10 independent locations from the 28 samples.

TABLE 4: Summary of ANOVA results

ANALYSIS OF VARIANCE					
SOURCE	**SS**	**DF**	**MS**	**F-RATIO**	**P**
DELCLASS	3378.743	3	1126.248	18.373	≤0.005
MINCLASS	1184.042	3	394.681	6.439	≤0.005
*DELCLASS*MINCLASS*	1414.012	9	157.112	2.563	≤0.05
ERROR	22189.874	40#	61.298		

R^2=.206 #See text for explanation.

A variety of interactions can cause planktonic organisms to covary spatially. These include ecological interactions such as predator-prey or commensal

relationships, plus physically forced spatial covariation via advection by currents, etc. Consequently, the 13 taxa used here also cannot be assumed to be independent of each other. The number of significant principal components produced by the PCA of the abundance data provides a reasonable estimate of the number of independent dimensions (Sneath and Sokal, 1973). The first four components from the PCA each described over 10% of the variation in mesozooplankton abundance and so my final estimate of the error degrees of freedom was 10 x 4 = 40.

Figure 24 represents the ANOVA results graphically. Each grid point represents one combination of MINCLASS and DELCLASS. The reduced Percent Similarity among samples near Cobb is quite evident (*i.e.* MINCLASS and DELCLASS=1). The abrupt decline in PSI where MINCLASS and DELCLASS = 4 may be exaggerated, as this category contained only 4 pairs. The general trend is visible in the three surrounding cells, however. All other categories contained 10-50 sample pairs.

To estimate the spatial extent of the seamount effect on PSI, I performed a series of *post hoc* pairwise multiple comparisons on the mean PSI of the four MINCLASSes when DELCLASS = 1. I used a Bonferroni-adjustment procedure (Wilkinson, 1990) in which the critical *p*-value is calculated by dividing the usual critical *p*-value of 0.05 by the number of comparisons being made. In this case then, for means to be significantly different *p*-values had to be

Figure 24: Three dimensional representation of ANOVA results. Vertical scale is PSI, grid points correspond to combinations of MINCLASS and DELCLASS. The upper right corner of the figure, MINCLASS 1 and DELCLASS 1 are those pairs of stations within 30km of Cobb Seamount.

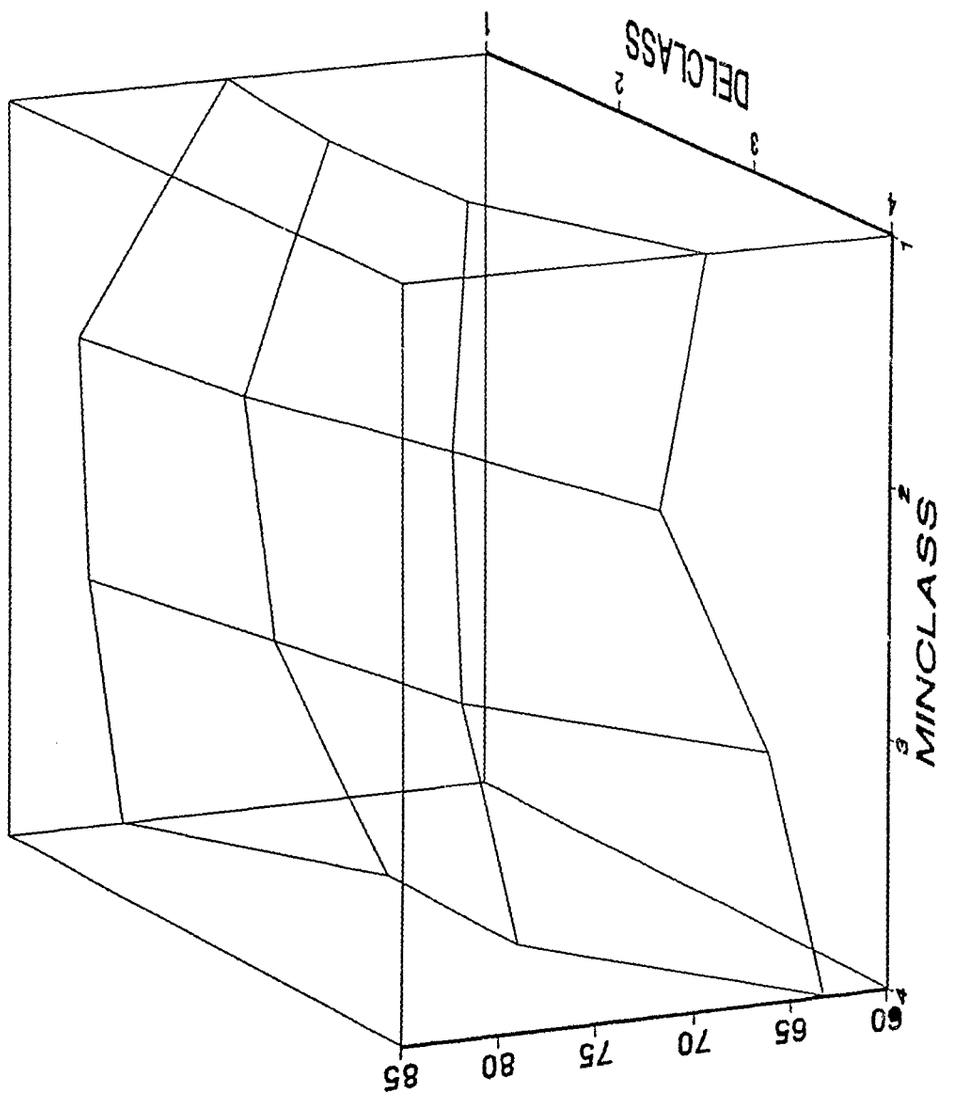
DELCLASS
1
2
3
4
MINCLASS
1
2
3
4
60
65
70
75
80
85

less than 0.05/4 = 0.0125. The means of the four groups are given in Table 5. The test showed that when both DELCLASS and MINCLASS = 1, mean PSI (73.7%) is significantly *lower* than the mean PSI when MINCLASS = 2-4 (81.4%, 80.8% and 79.0% respectively). The other three MINCLASS means did not differ significantly from each other.

TABLE 5: Multiple comparison of PSI among MINCLASSes 1-4 when DELCLASS=1.

DISTANCE CLASS	MEAN PSI	STD ERR MEAN	N
MINCLASS[1]DELCLASS[1]	73.7	1.19	43
MINCLASS[2]DELCLASS[1]	81.8	1.90	17
MINCLASS[3]DELCLASS[1]	80.8	1.57	25
MINCLASS[4]DELCLASS[1]	79.0	1.60	24

3.4 Discussion

Compositional changes in oceanic zooplankton communities usually occur quite gradually. McGowan and Walker (1979) found that zooplankton community composition shows only minor shifts over distances of up to 100km. A similar characteristic autocorrelation scale has been found for zooplankton communities west of Vancouver Island (Mackas, 1984), and in offshore directed filaments in the Coastal Transition Zone of the California Current (Mackas *et al.*, 1991).

Cobb is situated in the subarctic Pacific, a region in

which, like the North Pacific Central Gyre, zooplankton community structure is known to be spatially homogeneous over large distances (LeBrasseur 1965). In addition, recent drifter data show that surface currents near Cobb move east/southeastward at a consistent 10cm/s (McNally *et al.* 1983; Freeland, *submitted*), making it likely that patterns of community composition will remain constant over large distances along the current axis (Mackas *et al.*, 1991). Indeed, on the basis of straight line separation between samples, mesozooplankton community composition near Cobb Seamount shows little change over distances of up to at least 150km (Fig.22).

When these samples are compared on the basis of their relative distances from Cobb Seamount, however, PSI values decrease rapidly over short distances (Fig.22). This more rapid decline indicates PSI to be more sensitive to changes in the relative distance to Cobb Seamount than to simple geographic separation between samples, and suggests the existence of a seamount effect on community composition.

The ANOVA and multiple comparisons tests show that (i) both DELRAD and MINRAD are good predictors of percent similarity among samples (accounting for ~20% of the total variation), and that (ii) the mean PSI is among stations within 30km of Cobb Seamount is significantly lower than among stations further away from the seamount (Tables 4,5).

The principal components analysis also provides some

evidence in support of a "seamount effect" on the mesozooplankton, as mean on- and off-seamount scores differed significantly principal component 2 (with those for on-seamount stations being higher). However, attaching any biologically meaningful interpretation to this difference is difficult. Table 3 shows that high scores for component 2 correlate with high abundances of doliolids, *Tomopteris spp.*, and *Oithona spp.*; why these particular taxa should be more abundant near the seamount remains unclear.

Spatial patterns in other components of the planktonic food web at Cobb are quite patchy. Comeau *et al.* (*submitted*) find that while there is a general increase in primary production near the seamount, the distribution is very patchy. They suggest that small-scale patchiness in primary production near Cobb results from the local shoaling of the pycnocline, which reduces vertical mixing and provides the phytoplankton with improved light conditions. It may be that when integrated over longer temporal and larger spatial scales this process produces the persistent and areally more extensive regions of high chlorophyll water regularly observed near Cobb.

Sime-Ngando *et al.* (1992) show that both abundance and small-scale heterogeneity increase in the ciliate community near Cobb, and calculate characteristic patch sizes on the order of 6km. They propose that rapid growth in response to

very localized bursts of phytoplankton production is involved in generating these ciliate patches.

Although rapid *in situ* growth in response to favourable environmental conditions may account for small-scale patchiness in primary production and ciliate stocks near Cobb, it cannot explain the "seamount effect" in the mesozooplankton community structure. Whereas standing stocks of phytoplankton and ciliates can double in a day, differential growth leading to shifts in the mesozooplankton community composition would require weeks to months (Boehlert, 1988; Denman *et al.*, 1989). Freeland (*submitted*) demonstrates that while a persistent recirculating current does exist over Cobb, it does not penetrate much shallower than ~100m. As nearly all of the common mesozooplankton taxa at Cobb reside in the upper 100m of the water column elsewhere in the subarctic Pacific (LeBrasseur, 1965; Mackas, *pers. comm*) retention over the seamount by a Taylor cone is a remote possibility.

A more likely possibility is that the shift in mesozooplankton community composition near Cobb Seamount results not from taxon-specific growth, but from taxon-specific mortality or behavioural responses. Haury (*in press*) and Genin *et al.* (1988) attributed "zooplankton holes" and enhanced spatial patchiness over 60 Mile Bank to increased predation pressure from fish. For taxa that display diel vertical migratory behaviour, they also found

evidence suggesting that such taxa actively avoid the shallow topography.

Submersible surveys to Cobb in 1982 and 1984 found large schools of rockfish, mainly *Sebastes spp.*, resident on the seamount (Tunnicliffe *pers. comm.*). Both juveniles and adults were abundant in the waters on and around the seamount and, as this study shows, larval fish are also quite abundant over Cobb. As well, fishing vessels were encountered on Cobb during each of the three CSEX cruises; indirect evidence of the appreciable fish stocks at Cobb. Calanoid copepods and other larger zooplankton (*eg.* euphausiids, fish larvae) are known to make up a large proportion of the diet of many *Sebastes spp.*, particularly among the pelagic juveniles (Reilly *et al.*, 1992; Brodeur and Pearcy, 1984). It is possible that mortality associated with predation by seamount fish affects patterns in the mesozooplankton community composition near Cobb Seamount. Furthermore, if such predation was neither size-selective nor evenly distributed around the seamount its effect might be to decrease between-sample similarity among samples near the seamount. Information on both the diets and stock size of the Cobb rockfish population are required to properly test this hypothesis. To date, little information is available on either subject.

With respect to avoidance mechanisms, although the mesozooplankton taxa near Cobb are generally not known to be

strong vertical migrators, it is nevertheless possible that the shallow summit penetrates close enough to the surface to induce some sort of avoidance behaviour. Recently, Mackas *et al.* (1993) have shown that vertical zonation in mesozooplankton communities may involve taxa actively seeking out specific turbulent regimes within the water column. If this is true, then it may be that "seamount effect" detected in the mesozooplankton community near Cobb involves taxa responding to the increased levels of turbulent mixing and internal wave activity in the waters around the seamount. This idea also warrants further work.

Finally, these results again raise the issue of whether the abundant nektonic stocks found at many seamounts can be supported by autochthonously derived energy sources (Boehlert and Genin, 1987; Tseitlen, 1985). Certainly, this study provides at least indirect evidence that seamount fish *do* consume zooplankton advected over the topography by ocean currents. While it remains to be seen just how important advected energy sources are to nektonic stocks, the lack of an effective means to retain zooplankton over Cobb Seamount makes the idea of energy transfer from phytoplankton to zooplankton to fish seem highly unlikely. In the next section, I combine these results with those from previous chapters in a model that explores the nature of the trophic linkages between the components of the planktonic food webs of shallow seamounts.

Chapter 4

PLANKTONIC FOOD WEB STRUCTURE AND THE PERSISTENCE OF HIGH CHLOROPHYLL CONDITIONS NEAR A SHALLOW NORTH PACIFIC SEAMOUNT

4.1 Introduction

Shallow seamounts often support abundant pelagic communities. Rich stocks of squid and tuna are found in the northern Hawaiian and Emperor seamount chains in the western North Pacific (Inoue, 1983; Uchida and Tagami, 1986). Eastern North Pacific seamounts also support substantial populations of commercially valuable species (Hubbs, 1959; Isaacs and Schwartzlose, 1965; Hughes, 1981; Raymore, 1982). These and other shallow seamounts are regularly visited by commercial fishing vessels.

"Seamount effects" are evident in other trophic levels, too. Numerous seamounts are known to support rich benthic communities (Herlinveaux, 1971; Birkeland, 1971; Genin *et al.*, 1986; Levin *et al.*, 1986), including species of crab and precious coral (Raymore, 1982; Grigg, 1984) that are also of economic value. High standing stocks of phytoplankton and an enhanced patchiness of primary production persist over some shallow seamounts (Genin and Boehlert, 1985; Dower *et al.* 1992, Comeau *et al.*, *submitted*).

The response of zooplankton, ichthyoplankton and micronekton stocks to shallow seamounts is more complex. In

some cases, zooplankton and ichthyoplankton are more abundant over shallow seamounts (Fedosova, 1974; Boehlert and Seki, 1984; Genin and Boehlert, 1985; Parin and Prutko, 1985; Boehlert *et al.*, 1990)). In other cases, seamount stocks have been found to be equal to (Voronina and Timonin, 1986) or lower than background levels (Boehlert, 1985; Genin *et al.*, 1988). Protozoan and bacterioplankton stocks show similarly complex patterns: Sime-Ngando et al. (1992) report increased protozoan biomass over Cobb Seamount, while Moiseyev (1986) and Sorokin and Sorokina (1985) detect no differences between on and off seamount abundances.

Theoretical and laboratory studies show that the interaction of seamount-like topographies with oceanic currents gives rise to a variety of flow phenomena (reviewed in Roden, 1987). These include upwellings and/or isotherm doming, amplified currents, eddy shedding, closed recirculating currents (*i.e.* Taylor cones), seamount-trapped waves and regions of enhanced internal wave activity. These same phenomena have also been documented in numerous field studies (Meincke, 1971; Vastano and Warren, 1976; Fukasawa and Nagata, 1987; Owens and Hogg, 1980; Gould *et al.*, 1981; Roden 1984; Genin and Boehlert, 1985; Agapitov and Gritsenko, 1988; Roden, 1991).

Although biologists have long been interested in seamount communities, the mechanisms that produce high biomass conditions in such systems remain poorly understood.

It is widely held that current-topography interactions of the type described above play an important role in such communities (Hubbs, 1958; Boehlert and Genin, 1987; Boehlert, 1988; Mullin, 1993). To be of any real importance to pelagic food webs, however, the effects of these flow phenomena must extend into the euphotic zone (Boehlert and Genin, 1987), where most of the biological activity takes place. It is likely then, that current-topography interactions are of greatest biological importance at shallow seamounts, where the summit approaches or penetrates the euphotic zone.

The most common explanation of how seamount flow phenomena could act to enhance biological production near seamounts involves two processes. First, the upwelling of nutrient rich water associated with Taylor cone formation fosters local phytoplankton growth over the seamount (Genin and Boehlert, 1985). Second, a closed recirculation (*i.e.* Taylor cone) retains water over the seamount long enough for the energy represented by the enhanced phytoplankton stocks to be converted into secondary biomass (Boehlert and Genin, 1987; Flint and Yakushev, 1988; Dower et al.,1992). Other workers suggest that nektonic stocks over shallow seamounts rely not on local production but on plankton advected over the seamount from the surrounding waters (Tseitlen, 1985; Genin *et al.*, 1988; Genin et al., *in press*).

In this paper I present a simple ecosystem model

simulating the food web dynamics in a parcel of water as it passes over a shallow seamount. The model is based largely on data collected during the Cobb Seamount Experiment (CSEX), a program designed to study the coupling of physical and biological processes near seamounts (*Dower et al.*, 1992). Specifically, I use the model to address the question of how enhanced phytoplankton stocks can be produced and maintained near shallow seamounts in the absence of any retention mechanism, since Taylor cone recirculations do not generally penetrate the mixed layer over shallow seamounts. It is also hoped that a better understanding of the interactions between open ocean planktonic food webs and shallow topographies will shed light on the question of how rich nektonic stocks are maintained in such systems.

4.2 Model Formulation

The model presented here is developed from the one-dimensional ecosystem model used by Frost (1987) to study food web dynamics at Station P (50°N, 145°W) in the subarctic Pacific. I elaborate on Frost's Experiment 4 which explores the role of mesozooplankton in controlling phytoplankton stocks, using a three compartment system (Fig. 25). The model reproduces annual cycles of phytoplankton, herbivorous microzooplankton and dissolved nitrogenous nutrients in a homogeneous 50m mixed layer. As available

Figure 25: Three compartment food web used by Frost (1987) in his Experiment 4. Arrows point in the direction of energy transfer. Open arrows indicate that changes to the mesozooplankton stock are not modelled explicitly; mesozooplankton are included merely to provide closure to the system. Microzooplankton feed exclusively on phytoplankton. Mesozooplankton feed on both microzooplankton and phytoplankton. Redrawn from Frost (1987).

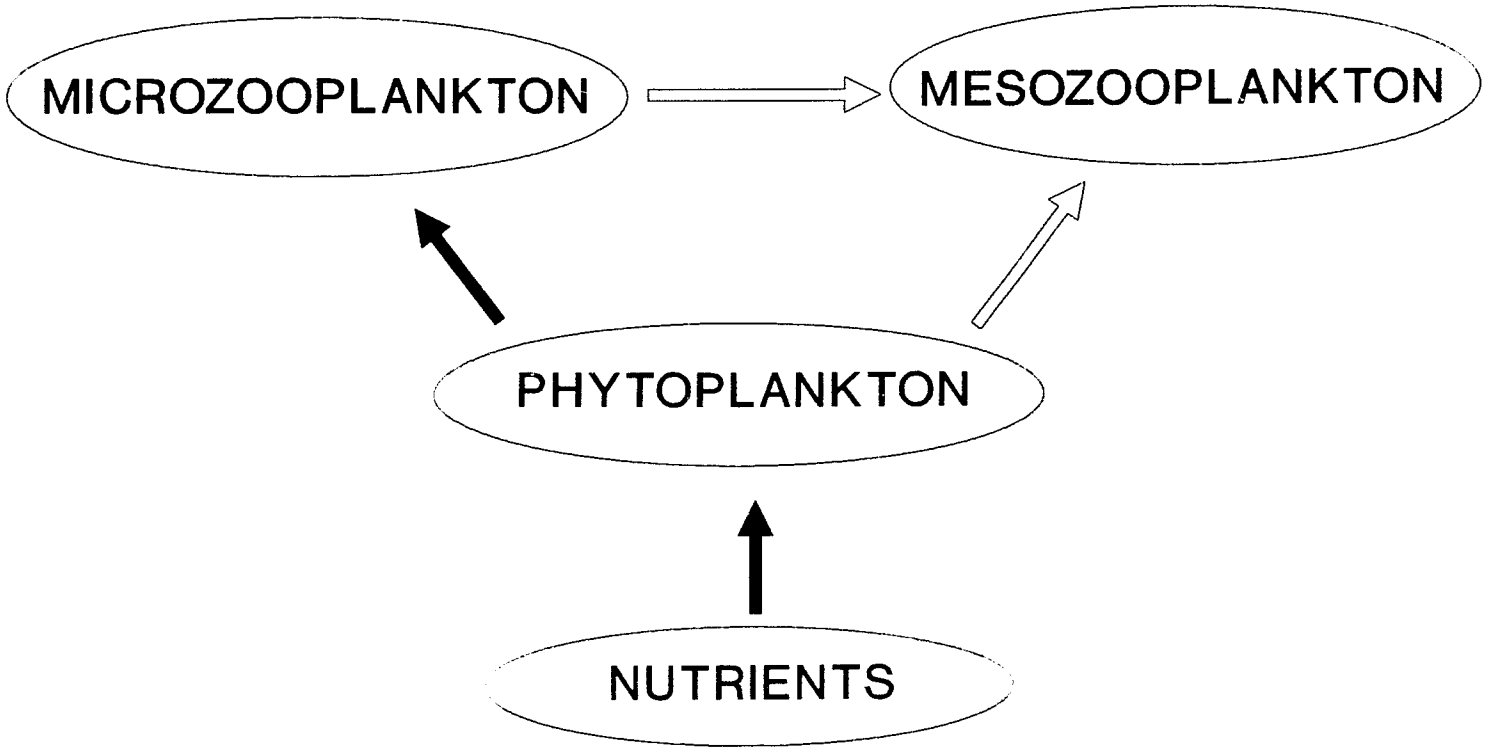
MICROZOOPLANKTON
MESOZOOPLANKTON
PHYTOPLANKTON
NUTRIENTS

light decreases exponentially with depth, the model calculates phytoplankton growth in 1m depth strata and then sums over the entire 50m mixed layer. Frost's model equations are:

Change in Phytoplankton Stock = Phytoplankton Growth - Sinking - Grazing (by Micro- and Mesozooplankton)

$$\frac{\Delta P}{\Delta t}=\frac{1}{Z_m}\left\{\sum_0^{Z_m} P^{*}PMAX^{*}\tanh\left(\frac{\alpha PAR_Z}{PMAX^{*}}\right)\frac{N}{d+N}-r(PMAX)P\right\}-mP-\frac{e_H(P-P_0)H}{f_H+(P-P_0)}-\frac{e_Z P Z}{f_Z+P+H} \quad (1)$$

Change in Microzooplankton Stock = Microzooplankton Growth - Predation by Mesozooplankton

$$\frac{\Delta H}{\Delta t}=H\left\{\frac{0.5\,e_H(P-P_0)}{f_H+(P-P_0)}-\frac{e_Z Z}{f_z+P+H}-m\right\} \quad (2)$$

Change in Dissolved Nutrient = -Uptake by Phytoplankton + Mixing + Regeneration (excretion by Micro- and Mesozooplankton)

$$\frac{\Delta N}{\Delta t}=-\frac{1}{Z_m}\left\{\sum_0^{Z_m} P^{*}PMAX^{*}\tanh\left(\frac{\alpha PAR_Z}{PMAX^{*}}\right)\frac{N}{d+N}\right\}+m(N_0-N)+\frac{0.3e_H(P-P_0)H}{f_H+(P-P_0)}+\frac{0.3\,e_Z(P+H)Z}{f_Z+P+H} \quad (3)$$

with symbols and parameters as defined in Table 6. In this formulation phytoplankton growth depends on the availability of both light and nutrients. Microzooplankton feed exclusively on phytoplankton, and are themselves preyed upon by mesozooplankton. The omnivorous mesozooplankton (i.e. *Neocalanus spp.*) provide closure for the system: changes in mesozooplankton stock are not modelled explicitly. Nutrients are removed from the mixed layer by phytoplankton

growth, and are returned to the mixed layer via: (1) excretion by grazers and mesozooplankton, and (2) mixing from below the mixed layer.

Table 6: Parameters for Equations 1-3, after Frost (1987)

TERM	DESCRIPTION	UNITS/VALUE
α	Photosynthetic efficiency	$\mu gC \cdot \mu gChl^{-1} \cdot ly^{-1}$
c	Carbon: Chlorophyll Ratio	$\mu gC \cdot \mu gChl^{-1}$
d	Half-saturation of Nitrate	1 μM
e_H	Max. Ingestion Rate Microzoop.	$\mu gC \cdot \mu gC^{-1} \cdot day^{-1}$
e_Z	Max. Ingestion Rate Mesozoop.	$\mu gC \cdot \mu gC^{-1} \cdot day^{-1}$
f_H	Half-sat. of Microzoop Ingest.	$\mu gC/l$
f_Z	Half-sat. of Mesozoop Ingest.	$\mu gC/l$
r	Phyto. Resp. (fraction of prod)	0.1 day^{-1}
H	Microzooplankton Standing Stock	$\mu gC/l$
N	Mixed Layer Nitrate Conc.	μM
N_0	Nitrate Conc. Below Mixed Layer	μM
P	Phytoplankton Standing Stock	$\mu gC/l$
P_0	Threshold P conc. for H Grazing	$\mu gC/l$
P^*	Chlorophyll Concentration	$\mu gChl/l$
Z	Mesozooplankton Standing Stock	$\mu gC/l$
PAR_Z	PAR Available at Depth Z	ly
PMAX	Phyto Max Daily Growth Rate	$\mu gC \cdot day^{-1}$
PMAX*	Max. Chl. Specific Growth Rate	$\mu gC \cdot \mu gChl^{-1} \cdot day^{-1}$
m	Daily Mixing Rate	day^{-1}
Z_m	Mixed Layer Depth	m

Based on this model, Frost (1987) concludes that microzooplankton are responsible for the bulk of the phytoplankton grazing in the subarctic Pacific. The role of the mesozooplankton seems to be primarily to regulate the microzooplankton stocks and, to a lesser extent, to regulate growth of the larger diatoms. This idea has since been confirmed by other workers (Miller *et al.*, 1991; Landry and Lehner-Fournier, 1992). Frost also reports that the model is

most sensitive to changes in the ingestion rate and feeding efficiency of the microzooplankton grazers. Changing the μ μ photosynthetic efficiency of the phytoplankton in the model merely alters the standing stocks of phytoplankton and grazers, it does not affect the ability of the microzooplankton to keep the phytoplankton stock under control (Frost 1987).

In a more recent paper Frost (1991) claims that a four compartment model provides a more realistic representation of the planktonic food web in the open subarctic Pacific. He points out that since phytoplankton blooms are never observed at Station P, the herbivorous microzooplankton must also be "insulated from potentially destabilizing predation". Frost (1991) suggests a food web comprised of (1) phytoplankton, (2) herbivorous microzooplankton (mainly protozoans), (3) predators of the herbivorous microzooplankton, and (4) predators of the microzooplankton predators. In this scenario groups 1 and 3 would be limited mainly by predation, while groups 2 and 4 would be limited by food availability. As in the three compartment model, the top predators in the system are taken to be large copepods of the genus *Neocalanus*, which dominate the subarctic Pacific during the spring and early summer (Miller *et al.*, 1984).

4.3 Physical/Biological Background for the Cobb Seamount Model

The Cobb Seamount Experiment involved three cruises to Cobb Seamount (46°46'N, 130°48'W), 500km southwest of Vancouver Island (Fig. 1), during the summers of 1990-1992. Cobb differs from most other seamounts in that its summit penetrates the euphotic zone. The physical and biological sampling programs carried out during the CSEX cruises are detailed in Dower *et al.* (1992), Sime-Ngando *et al.* (1992), Freeland (*submitted*), Comeau et al. (*submitted*) and in Chapters 1-3. Here I summarize these results as background for the current model.

4.3.1 Biological Observations

Localized increases in phytoplankton stock are regularly observed at Cobb Seamount. Summer chlorophyll concentrations in the southern subarctic Pacific are typically about 0.2-0.4 mg/m^{-3} (Takahashi *et al.*, 1972; Hobson, 1980). In August of 1990 a single large bullseye of high chlorophyll water situated directly over Cobb Seamount had maximum chlorophyll concentrations in excess of $1mg/m^{-3}$ (Dower *et al.*, 1992). Multiple patches of high chlorophyll water were also observed around Cobb Seamount during the 1991 and 1992 CSEX cruises. Integrated euphotic zone chlorophyll concentrations in the region are usually about 15-30 $mg \cdot m^{-2}$ during the summer, but are occasionally >100

$mg \cdot m^{-2}$ over the seamount (Dower *et al.*, 1992).

Primary production near Cobb is very patchy. Comeau *et al.* (*submitted*) give integrated primary production values ranging from 130-1300 mgC•m-*2*•d-*1*, with an average value of ~570 mgC•m-*2*•d-*1*. These values are almost identical to data from 6 cruises from the Subarctic Pacific Ecosystem Research (SUPER) program presented by Miller *et al.* (1991): range 240-1300, grand mean 586 mgc•m-*2*•d-*1*. Hobson (1980) also reports maximum primary production values of 600-700 mgC•m-*2*•d-*1* from the Transition Zone. At Cobb, patches of high primary productivity are generally located in areas where the pycnocline shoals by as much as 10-30m (Comeau *et al.*, *submitted*). Sime-Ngando *et al.* (1992) show that for the ciliate fauna, abundance near Cobb is generally higher, but spatial distribution is also more patchy, than at off-seamount sites.

During the 1991 CSEX cruise mesozooplankton biomass over Cobb was about 40% lower than in samples collected off-seamount (Dower, unpublished data). A "seamount effect", evident as a localized decrease in between-sample resemblance in mesozooplankton community composition, is detectable up to 30km from the seamount pinnacle (Figures 22-24). One possible explanation for this pattern is that predation by seamount fish alters the mesozooplankton community composition near the seamount. Submersible surveys in 1982 and 1984 revealed abundant stocks of pelagic

juvenile and adult rockfish (*Sebastes spp.*) in the waters overlying Cobb (Tunnicliffe, *pers. comm.*); these species are known to be omnivorous planktivores (Reilly *et al.*, 1992; Brodeur and Pearcy 1984).

The decreased between-sample resemblance in the mesozooplankton community near Cobb could also result from physical or behavioural interactions. Most of the mesozooplankton common at Cobb are usually found in the upper 100m of the water column elsewhere in the subarctic Pacific (LeBrasseur, 1965; D. Mackas, *pers. comm.*). It may be that the increased internal wave activity (Fig.11) and/or turbulent mixing in the waters over Cobb (R. Lueck and T. Mudge, *pers. comm.*) causes shifts in the mesozooplankton community near Cobb. This could occur directly, through the mixing action of these and other seamount flow phenomena, or indirectly if the zooplankton actively respond to the enhanced kinetic energy. The latter idea is supported by Mackas *et al.* (1993) who suggest that in the subarctic Pacific "the vertical distribution pattern of the copepods could be set by responses to the local intensity of turbulent mixing". If this is the case, the enhanced kinetic energy over Cobb might induce behavioural responses in the zooplankton (eg. vertical migrations, swarming, etc.) that effect local patterns in community composition.

4.3.2 Physical Setting

Cobb Seamount is located in the southeast corner of the subarctic Pacific (Fig.1), near the point where the West Wind Drift splits to form the California Current and Alaskan Gyre (Dodimead *et al.*, 1963, Favorite *et al.*, 1976). Freeland (*submitted*) describes the circulation pattern near Cobb. Satellite-tracked drifter buoys show that surface currents near the seamount move east-southeastward at about 10 cm/s.

A shipboard Acoustic Doppler Current Profiler and moored current meter arrays show a clockwise recirculating flow over the Cobb summit. The recirculation extends from just above the bottom to a shallowest depth of ~100m, and has peak velocities of 12cm/s (Freeland, *submitted*). CTD surveys during the CSEX cruises show isopycnal doming of about 10-30m over Cobb (Figs.5-7). Freeland interprets this recirculating current and isopycnal doming as evidence of a bottom-intensified Taylor cone. The limited penetration height of the Taylor cap results from the damping effects of the very strong stratification characteristic of the subarctic Pacific. A similar recirculating current was observed on each of the three CSEX cruises and also during an October 1991 cruise to Cobb organized by the University of Washington (Codiga, *pers. comm*). In one case, the recirculating current was observed to persist for at least one month (Dower *et al.*, 1992).

Mixed layer depth near Cobb during June/July ranges between ~10m to ~25m. Average mixed layer temperature during June/July is about 12°C. Mixed layer nutrient concentrations remain moderately high throughout the summer: during the CSEX cruises, mean nitrate was about 2.5μM and only rarely did concentrations fall below 1μM (Fig.12).

4.4 Parameterization of the Cobb Model

The model presented here is a one-dimensional, four compartment description of the planktonic food web recently proposed for the subarctic Pacific (Frost, 1991). The basic food web organization is illustrated in Figure 26. Lacking detailed information on the composition of the phytoplankton community near Cobb during the summer, I chose to lump all phytoplankton into a single compartment. It *is* known that the subarctic Pacific phytoplankton community is dominated by cells <5 μm in size (Booth, 1988). Protozoans represent the ciliate fauna documented by Sime-Ngando *et al.* (1992), which appear to be the major grazers of microalgae at Cobb. Microzooplankton are defined here as metazoans less than 500μm in longest dimension, and are comprised mainly of smaller developmental stages of crustacean mesozooplankton. Mesozooplankton are defined as metazoans >500μm and, during the first half of the summer, are dominated by the large copepods *Neocalanus plumchrus*, *N. cristatus* and *Calanus pacificus*.

Figure 26: Four compartment food web used in the current model. Arrows indicate the direction of energy transfer. Open arrows indicate that changes to the mesozooplankton stock are not modelled explicitly: mesozooplankton are included merely to provide closure to the system. Protozoans feed exclusively on phytoplankton. Microzooplankton feed on both protozoans and phytoplankton. Mesozooplankton prey on both microzooplankton and protozoans.

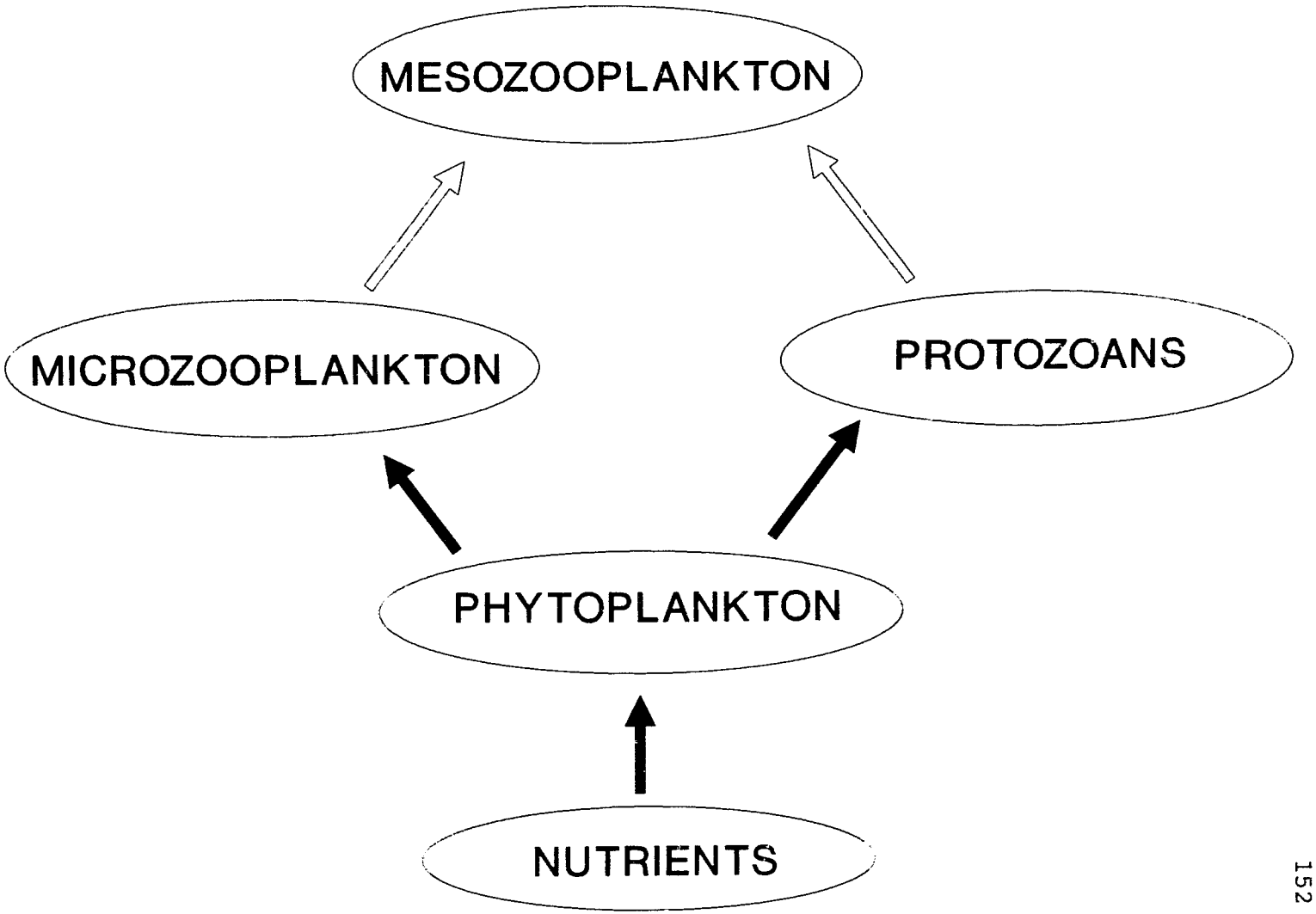
MESOZOOPLANKTON
MICROZOOPLANKTON
PROTOZOANS
PHYTOPLANKTON
NUTRIENTS

Phytoplankton are grazed by both protozoans and microzooplankton. The microzooplankton are modelled as omnivores, and feed indiscriminately on phytoplankton and protozoans. Model closure is provided by the mesozooplankton that prey indiscriminately on microzooplankton and protozoans. Following Frost (1987, 1991), mesozooplankton are included only as predation pressures on these groups. Changes in the mesozooplankton stock are not modelled explicitly since mesozooplankton generation times are typically ≥30 days.

As is often the case in food web studies, information on the state variables in the Cobb Seamount system (*i.e.* biomass) is more complete than the information on flows between various compartments (*e.g.* ingestion rates). To estimate the ingestion rates of grazers and predators I apply a technique similar to the "inverse method" detailed by Vézina and Platt (1988), and recently used in a number of other food web studies (Jackson and Eldridge, 1992). I make the assumption that, over timescales relevant to the passage of a water parcel over a seamount (i.e 1-10 days), the food web can be assumed to approach steady state conditions. Using literature values, I place limits on the range of possible values for the ingestion rates of protozoans, microzooplankton and mesozooplankton (Heinbokel, 1978; Dagg and Wyman, 1983; Frost *et al.*, 1983; Dagg and Walser, 1987; Verity, 1991; Verity *et al.*, 1993; Burkill *et al.*, 1993). I

then search iteratively through parameter space for the combination of values that best satisfies the steady state assumption. Values of the state variables used in this process are estimated from data collected during the CSEX cruises. The solution set obtained by this process is then used to establish the starting conditions for the model.

The present model includes modified forms of equations 1-3, plus a fourth equation to describe changes in the stock of metazoan microzooplankton. The equations can be summarized as:

Change in Phytoplankton Stock = Phytoplankton Growth - Sinking - Grazing (by Protozoans and Microzooplankton)

$$\frac{\Delta P}{\Delta t} = \frac{1}{Z_m}\left\{\sum_{0}^{Z_m} P^{*}PMAX^{*}\tanh\left(\frac{\alpha PAR_Z}{PMAX^{*}}\right)\frac{N}{d+N} - r(PMAX)\,P\right\} - mP - \frac{e_H(P-P_0)H}{f_H+(P-P_0)} - \frac{e_{C1}PC1}{f_{C1}+P+H} \qquad (4)$$

Change in Herbivorous Protozoan Stock = Protozoan Growth - Sinking - Predation (by Micro- and Mesozooplankton)

$$\frac{\Delta H}{\Delta t} = H\left\{0.5\,\frac{e_H(P-P_0)}{f_H+(P-P_0)} - \frac{e_{C1}C1}{f_{C1}+P+H} - \frac{e_{C2}C2}{f_{C2}+H+C1} - m\right\} \qquad (5)$$

Change in Microzooplankton Stock = Microzooplankton Growth - Predation (by Mesozooplankton)

$$\frac{\Delta C1}{\Delta t} = C1\left\{0.3\,\frac{e_{C1}(F_{C1}-F_0)}{f_{C1}+(F_{C1}-F_0)} - \frac{e_{C2}C2}{f_{C2}+H+C1}\right\} \qquad (6)$$

Change in Dissolved Nutrient = -Uptake by Phytoplankton + Mixing + Regeneration (excreted by Protozoans, Micro- and Mesozooplankton)

$$\frac{\Delta N}{\Delta t} = -\frac{1}{Z_m}\left\{\sum_0^{Z_m} P^* PMAX^* \tanh\left(\frac{\alpha PAR_z}{PMAX^*}\right)\frac{N}{d+N}\right\} + m(N_0 - N) + 0.3\,\frac{e_H(P-P_0)H}{f_H + (P-P_0)}$$

$$+ 0.3\,\frac{e_{C1}(P+H)\,C1}{f_{C1}+P+H} + 0.3\,\frac{e_{C2}(H+C1)\,C2}{f_{C1}+H+C1} \qquad \textbf{(7)}$$

Variables and parameters are defined in Table 7. In all cases Δt is a one day time step. Stocks are reported in units of μg C/l. Phytoplankton stocks are also reported in terms of chlorophyll concentration (μg *Chl*/l). Dissolved nitrogenous nutrients are converted to carbon equivalents in the ratio 1μmol N = 75.6μg C (Frost, 1987). For presentation purposes, I report nutrients as μM.

Although mixed layer depth at Cobb during the summer is about 15-30m and chlorophyll profiles display prominent subsurface chlorophyll maxima (SCM) between 30-50m (Dower *et al.*, 1992), I chose instead to use a 50m mixed layer (Z_m = 50) in which plankton stocks are distributed homogeneously for the off-seamount situation in the model . I structured the model this way for two reasons.

First, the primary goal of the modelling exercise was *not* to mimic Cobb Seamount specifically, but to address the general question of how persistent high phytoplankton stocks

Table 7: Definitions and starting values for Equations 4-7 in the current model. Starting values are those used in basic trials.

TERM	DESCRIPTION	UNITS/VALUE
α	Photosynthetic efficiency	.75 $\mu gC \cdot \mu gChl^{-1} \cdot ly^{-1}$
c	Carbon: Chlorophyll Ratio	45 $\mu gC \cdot \mu gChl^{-1}$
d	Half-sat. of Nitrate for Phyto.	1 μM
e_H	Max. Ingestion Rate Protozoans	1 $\mu gC \cdot \mu gC^{-1} \cdot day^{-1}$
e_{c1}	Max. Ingestion Rate Microzoop.	.4 $\mu gC \cdot \mu gC^{-1} \cdot day^{-1}$
e_{c2}	Max. Ingestion Rate Mesozoop.	.25$\mu gC \cdot \mu gC^{-1} \cdot day^{-1}$
f_H	Half-sat. of Protozoan Ingest.	25 $\mu gC/l$
f_{c1}	Half-sat. of Microzoop Ingest.	25 $\mu gC/l$
f_{c2}	Half-sat. of Mesozoop Ingest.	50 $\mu gC/l$
F_{c1}	Microzoop Prey (*i.e.* P+H)	18.5 $\mu gC/l$
F_0	Feeding Threshold for Microzoop	10 $\mu gC/l$
r	Phyto. Resp. (fraction of prod)	0.1 day^{-1}
H	Protozoan Standing Stock	5.0 $\mu gC/l$
N	Mixed Layer Nitrate Conc.	2.5 μM
N_0	Nitrate Conc. Below Mixed Layer	5.0 μM
P	Phytoplankton Standing Stock	13.5$\mu gC/l$
P_0	Feeding Threshold for Protoz.	10 $\mu gC/l$
P^*	Chlorophyll Concentration	0.3 $\mu gChl/l$
C1	Microzooplankton Standing Stock	5.0 $\mu gC/l$
C2	Mesozooplankton Standing Stock	7.0 $\mu gC/l$
PAR_z	PAR Available at Depth Z	$ly \cdot day^{-1}$
PMAX	Phyto Max Daily Growth Rate	1.5 $\mu gC \cdot day^{-1}$
$PMAX^*$	Max. Chl-Specific Growth Rate	.45$\mu gC \cdot \mu gChl \cdot day^{-1}$
m	Daily Mixing Rate	0.02 day^{-1}
Z_m	Mixed Layer Depth	50m

can be created and maintained at shallow seamounts in the absence of a retention mechanism. Therefore, it was not essential that the vertical profile of chlorophyll used in the model reflect that which is observed at Cobb. One of the first principles of mathematical modelling is to begin with the simplest formulation possible, and so a mixed layer in which plankton are distributed homogeneously provides a logical starting point.

Second, the main basis for comparison with the results

from the present model are those of Frost (1987) for Station P, in which a homogeneous 50m mixed layer is used. One of the other goals of this modelling exercise was to evaluate the four compartment food web used here against the three compartment food web used by Frost (1987). I therefore decided to keep the physical structure of the present model similar to Frost's formulation to facilitate comparisons.

Mixing, m, is that fraction of the mixed layer replaced each day via vertical mixing and diffusion between the surface mixed layer and the deeper layer below. In the model, mixing *adds* nutrients from below the surface layer and *removes* a fraction of the phytoplankton and protozoan stocks. Estimates of vertical mixing are unavailable for the waters around Cobb, but it is assumed that m does not differ greatly from values estimated for Station P (50°N, 145°W) (Freeland, *pers. comm.*). I therefore use $m = 0.02$ day^{-1} for the basic trials, a value which lies within the range of mixing rates used by Frost (1987) for Station P.

Estimates of total solar radiation and phytoplankton photosynthetic efficiency, α (*i.e.* the initial slope of the Photosynthesis *vs.* Irradiance curve), are also unavailable from the CSEX data. As above, I estimate these parameters from data collected elsewhere in the subarctic Pacific. Hobson and Ketcham (1974) cite a value of 300 langley$\cdot day^{-1}$ (ly$\cdot day^{-1}$ hereafter) for total daily solar radiation near Cobb in August while Takahashi *et al.* (1972) estimate 400

$ly \cdot day^{-1}$. I use the average value of 350 $ly \cdot day^{-1}$, of which 50% is taken to be photosynthetically available radiation, PAR (Strickland, 1958). For the basic trials, I use a photosynthetic efficiency value of α = 0.75 $\mu gC \cdot (\mu gChl)^{-1} \cdot ly^{-1}$ (Takahashi *et al.*, 1972).

The phytoplankton Carbon:Chlorophyll ratio is set at 45 $\mu gC \cdot \mu gChl^{-1}$, the maximum summer value used by Frost (1987) for Station P. Phytoplankton respiration, r, is taken to be 10% of daily photosynthetic production (Parsons *et al.*, 1984). Again, lacking any data from Cobb, I follow Frost (1987) and use a value of 1μM for the phytoplankton half-saturation constant for nitrate. Protozoans are assumed to assimilate 50% of ingested food (Heinbokel, 1978), micro- and mesozooplankton assimilate 30%. Protozoans, micro- and mesozooplankton excrete 30% of their daily ingestion as nitrogenous compounds (Frost, 1987; Vézina and Platt, 1988). The model does not consider the effect of discrimination between nitrate and ammonia by phytoplankton.

4.4.1 Procedure

Equations 4-7 are solved using 1 day time steps in 30-day trials. If it is assumed that the effect of the seamount extends about one radius into the surrounding water (~15km for Cobb), then for a background flow of 10 cm/s (the average current measured near Cobb) a water parcel requires only ~3.5 days to pass over the seamount (*i.e.* 2x15km radius

= 30km diameter). Given this short timescale and the lack of year-round data from Cobb it seems reasonable to limit model trials to only 30 days. Longer model runs would entail factoring in changes to the physical environment (such as increasing temperature, deepening of the mixed layer, changes in the insolation) that occur as the summer progresses. Shorter timescales do not allow enough time to follow the fate of the planktonic community as it moves downstream of the seamount.

In "seamount trials" the water parcel approaches the seamount over days 1-5, and first encounters seamount conditions on day 6. Seamount conditions are represented as a 15m doming of the seasonal pycnocline, from 50m to 35m, during the time the water parcel is over the seamount. In the basic trial, this amounts to 4 days. The shoaling is imposed as a simple step-function. I do not include any retention or trapping mechanisms over the seamount since Freeland (*submitted*) shows that the recirculation over Cobb does not usually penetrate shallower than ~100m. The model is used in a series of numerical experiments to explore the response of the plankton community to changes in: (i) the time taken for a water parcel to pass over Cobb, (*transit time*, hereafter) , (ii) the amplitude of isopycnal doming over Cobb, (iii) predation by seamount fish, (iv) the supply of dissolved nutrients to the phytoplankton and (v) the photosynthetic efficiency of the phytoplankton.

4.5 Model Results

4.5.1 Experiment 1: Basic Trials

Figure 27 compares basic trials for the "seamount" and "no-seamount" conditions. Starting values are given in Table 7. In the absence of the seamount, stocks of phytoplankton, protozoans and microzooplankton show only minor changes from starting values over the 30-day trial. Protozoans and microzooplankton increase from 5 μgC/l to ~6 μgC/l (Fig.27b-c). Chlorophyll concentration (Chl, hereafter) shows a small increase at the beginning of the trial, rising from 0.3 μg/l to 0.33 μg/l but, thereafter, remains steady throughout the trial (Fig.27a). Nitrate concentration shows only a slight decline from the initial value of 2.5 μM (Fig.27d). Longer trials (not shown) confirm that this "steady state" formulation remains stable for periods of up to 50 days in the absence of the seamount.

In the "seamount" trials, all three stocks show obvious departures from starting values. During days 6-9, while the parcel is over the seamount and Z_m = 35m, a brief phytoplankton bloom occurs, in which the Chl concentration increases by 67% to a peak value of 0.55 μg/l (Fig.27a). This represents an average phytoplankton growth rate during the bloom of 0.12 day^{-1}, or 0.18 doublings day^{-1}. Grazing by protozoans and microzooplankton removes all evidence of this bloom by day 14. Thereafter, the phytoplankton stock increases very slowly until the end of the trial. Mixed

Figure 27: Predicted stocks of (a) phytoplankton, (b) protozoans, (c) microzooplankton and (d) nutrients for the "basic" seamount (open squares) and no-seamount (solid squares) trials. Z_m = 50m off-seamount, and 35m on-seamount.

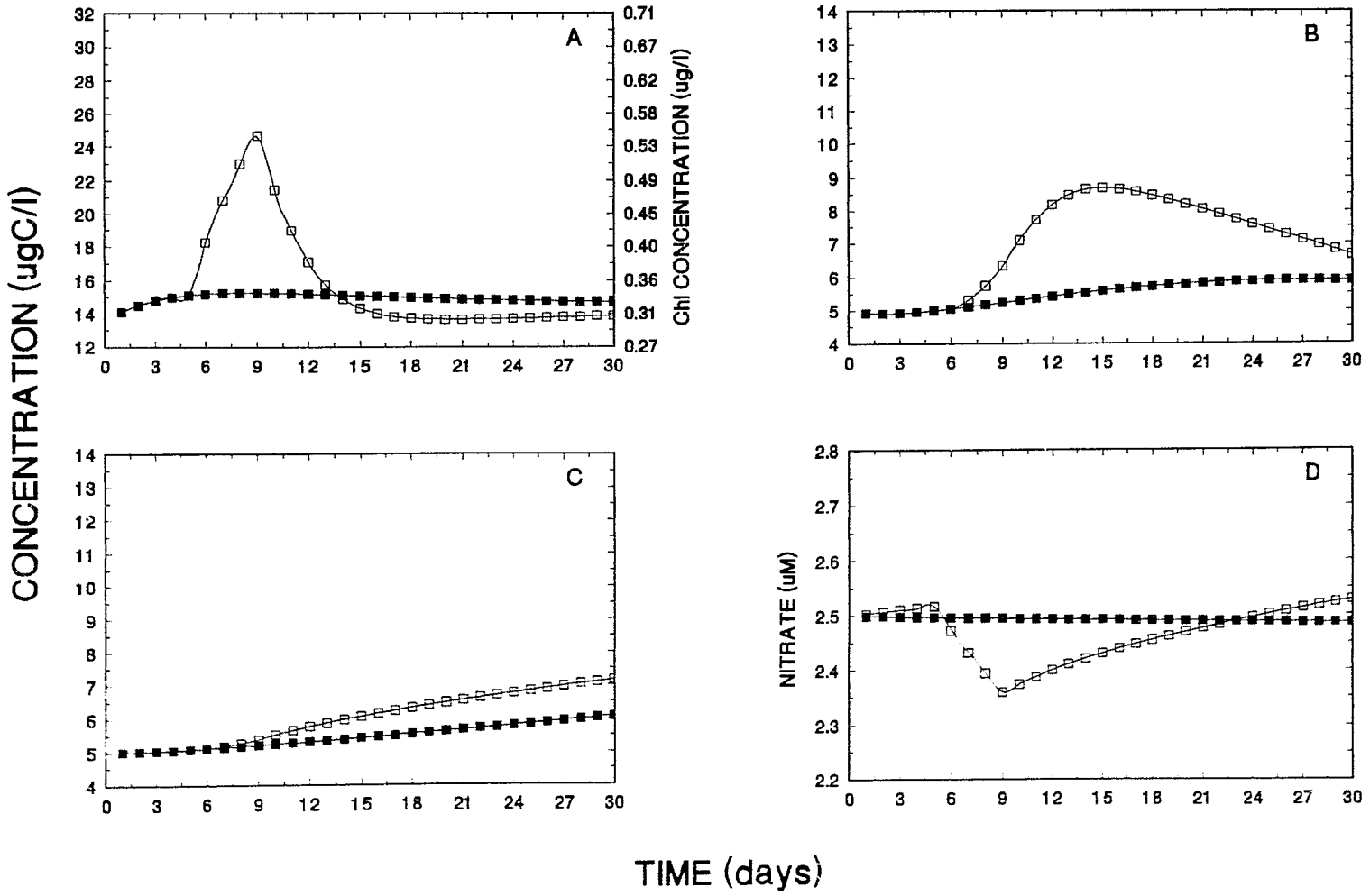
A
B
C
D
CONCENTRATION (ugC/l)
Chl CONCENTRATION (ug/l)
NITRATE (uM)
TIME (days)

layer nitrate decreases only slightly over the seamount and returns to ~2.5 μM by the end of the trial (Fig.27d).

The increase in protozoan stock lags one day behind the beginning of the phytoplankton bloom. Although protozoan stocks may actually respond more quickly than the model suggests, the one day time steps used here are not capable of resolving such a response. The peak concentration of 8.6 μgC/l reached on day 15 represents a 72% increase over the starting value (Fig.27b). By day 30, micro- and mesozooplankton predation brings this number back down to 6 μgC/l, a value comparable to the final concentration in the no-seamount trial. Like the protozoans, the microzooplankton stock begins its increase on day 7. Unlike protozoans, the microzooplankton stock continues to increase, despite mesozooplankton grazing, and by the end of the trial reaches 7 μgC/l (Fig.27c).

4.5.2 Experiment 2: Effect of Transit Time

In the absence of a retention mechanism over the seamount, the time required for a water parcel to transit the seamount, T_{tr}, is inversely proportional to the velocity of the background flow. The basic T_{tr} = 4 days is based on the 10cm/s background current observed near Cobb. Here, I consider cases where the background flow is ~20 cm/s and ~5 cm/s, giving transit times of ~2 days and ~8 days respectively. For comparative purposes, a trial with T_{tr} =

16 days is used to simulate conditions that might result from a water parcel being trapped over a shallow seamount by a recirculating flow that *does* penetrate the surface mixed layer. The results of the experiment are presented in Figure 28.

Increasing T_{tr} has two major effects on the system. First, as T_{tr} increases, stocks of phytoplankton, protozoans and microzooplankton also increase. For T_{tr} = 2, the Chl concentration shows a ~39% increase to a maximum value of 0.46 μg/l over the seamount. For T_{tr} = 8, seamount Chl rises to 0.60 μg/l, an 82% increase over the pre-seamount Chl concentration. Put another way, relative to the basic T_{tr} of 4 days, doubling T_{tr} results in a 12% increase in Chl concentration over the seamount, while halving T_{tr} reduces seamount chlorophyll by 28% (Fig.28a). Unlike the other cases, when T_{tr} = 16 the Chl concentration does not continue increasing throughout the time the water parcel is over the seamount. For T_{tr} = 16, the maximum Chl concentration of 0.59 μg/l is the same as that for T_{tr} = 8 days: after day 13, Chl undergoes a slow decline for the remaining time over the seamount as a result of grazing.

Doubling T_{tr} from 4 to 8 days increases the maximum protozoan concentration by 66% from 8.6 μgC/l to 13.1 μgC/l, while halving T_{tr} from 4 to 2 days reduces the maximum concentration by 20%, to 6.9 μgC/l (Fig.28b). For T_{tr} = 2-8 days, protozoan stocks peak ~6 days after the phytoplankton

Figure 28: Predicted stocks of (a) phytoplankton, (b) protozoans, (c) microzooplankton and (d) nutrients when T_{tr} is: 2 days (solid squares), 4 days (open squares), 8 days (solid triangles) and 16 days (open triangles). Isopycnal doming is 15m in each case.

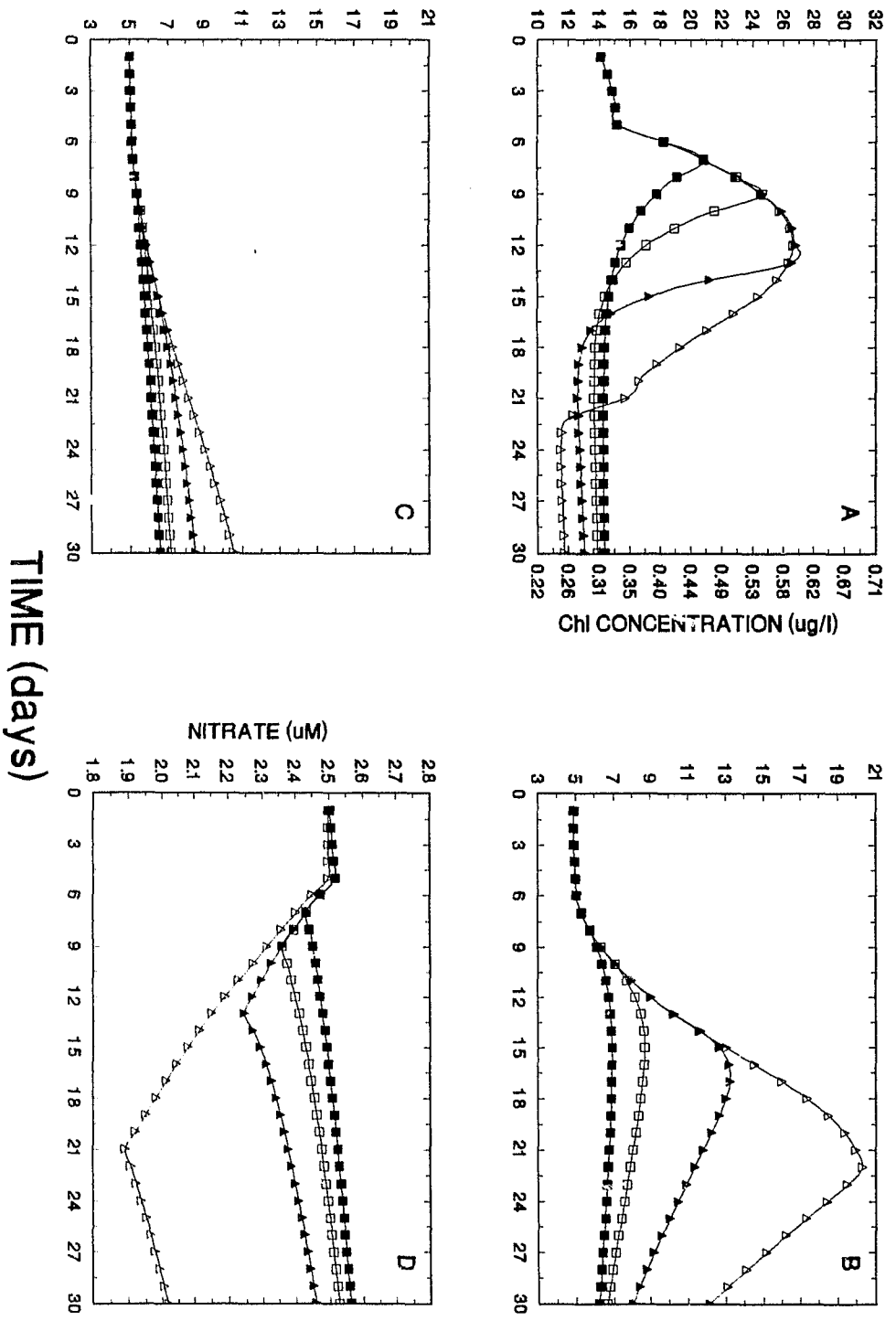
CONCENTRATION (ugC/l)
A
Chl CONCENTRATION (ug/l)
B
C
NITRATE (uM)
D
TIME (days)

stock reaches its maximum value. With a 16 day transit time the protozoan stock actually surpasses the phytoplankton stock on day 19, peaks at a concentration of 20.3 μgC/l on day 22, and thereafter declines rapidly to the end of the trial.

Microzooplankton stocks increase throughout all four trials (Fig.28c). Relative to the basic T_{tr} = 4 days, increasing the transit time to 8 and 16 days increases the final stocks (by 15% and 33%, respectively) to 8.4 μgC/l and 10.6 μgC/l. For T_{tr} = 2 days, although there is still a net increase in microzooplankton over the 30-day trial, the final concentration is 8% lower than the basic T_{tr} = 4 day case. When T_{tr} = 2-8 days, microzooplankton overtake the protozoans by the end of the trial. When T_{tr} = 16 days, however, the final microzooplankton concentration is lower than that of the protozoans.

Increasing T_{tr} results in reduced mixed layer nitrate concentrations while the water parcel is over the seamount (Fig.28d). Still, only for the case where T_{tr} = 16 days does nitrate fall below 2 μM. Except for this last case, by the end of the trials nitrate concentrations again approach 2.5 μM.

The second effect of increasing T_{tr} is seen in the response of the phytoplankton stock to grazing. In each case, after transiting the seamount, the phytoplankton stock declines rapidly in response to protozoan and

microzooplankton grazing pressure (Fig.28a). However, as T_{tr} increases from 2 to 8 days the decline in phytoplankton stock becomes more pronounced. In each case the pre-seamount Chl concentration is 0.33 μg/l. For T_{tr} = 2 days, post-seamount Chl is comparable to pre-seamount values. For T_{tr} = 4, 8 and 16 days, however, grazing reduces post-seamount Chl concentrations (0.30, 0.28 and 0.26 μg/l, respectively) to values *lower* than the pre-seamount values.

4.5.3 Experiment 3: Effect of Doming Amplitude

The amplitude of isopycnal doming over shallow topographies depends on both the intensity of the background flow and the degree of stratification in the water column (Roden, 1987). Near Cobb, strong stratification during the summer usually limits isopycnal doming to between 10-20m (Freeland, *in press*). In this experiment I explore how variation in doming amplitude affects plankton stocks over the seamount.

Figure 29 compares three trials in which isopycnal doming is varied between 10 and 20m, bracketing the values observed at Cobb Seamount. T_{tr} = 4 days, and doming is imposed as a simple step function in each case. In general, the patterns are similar to those shown in Figure 28 for varying T_{tr}. Stocks of phytoplankton, protozoans and microzooplankton all increase proportionally with the amplitude of isopycnal doming.

Figure 29: Predicted stocks of (a) phytoplankton, (b) protozoans, (c) microzooplankton and (d) nutrients when isopycnal doming over the seamount is: 10m (solid squares), 15m (open squares) and 20m (solid triangles). T_{tr} = 4 days in each case.

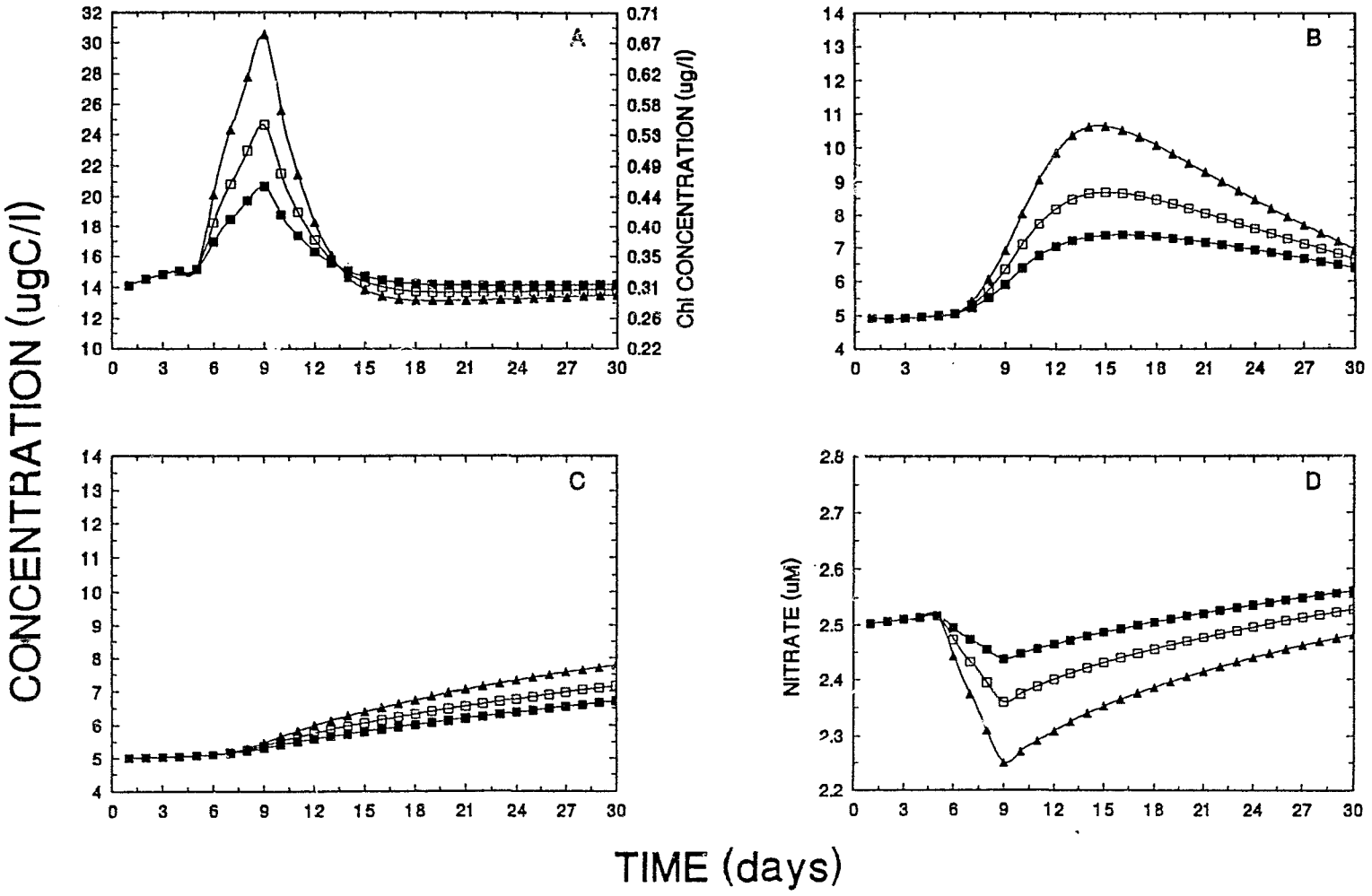
CONCENTRATION (ugC/l)
Chl CONCENTRATION (ug/l)
NITRATE (uM)
TIME (days)
A
B
C
D

For phytoplankton, the maximum Chl concentration over the seamount increases from 0.46 μg/l, to 0.55 μg/l, to 0.68 μg/l for 10m, 15m and 20m doming, respectively (Fig.29a). These values represent 40%, 67% and 106% increases over pre-seamount Chl concentrations. Mean bloom growth rates during the three trials are 0.08, 0.12, and 0.17 day^{-1}, or 0.12, 0.17 and 0.25 doublings day^{-1}. As with increasing T_{tr}, increased doming amplitude results in lower post-seamount Chl concentrations.

With 10m of isopycnal doming, the maximum protozoan concentration of 7.3 μgC/l is 18% lower than in the basic trial (with 15m of doming) where protozoan concentration reaches 8.6 μgc/l (Fig.29b). Increasing the doming amplitude to 20m results in a 22% increase in maximum protozoan concentration, to 10.6 μgC/l. As in Experiment 2, protozoan stocks peak several days after the phytoplankton, and subsequently decline to the end of the trial.

Stocks of microzooplankton increase throughout all three trials (Fig.29c). The final concentrations in the 10m, 15m and 20m cases are 6.6, 7.1 and 7.7 μgC/l, respectively. These represent 32%, 42% and 54% increases over the starting concentration. In each case, the microzooplankton are overtaking the declining protozoan stocks by day 30.

Mixed layer nitrate responds to increased doming amplitude much as for increased T_{tr} (Fig.29d). With

increased doming, the phytoplankton are exposed to a better light regime which results in higher growth rates and, consequently, a more rapid utilization of nutrients. For 15m doming nitrate concentration fall to a low of ~2.2 μM.

4.5.4 Experiment 4: Predation by Seamount Fish

This experiment explores the effect of size-selective predation by seamount-associated fish (mainly adults and pelagic juvenile *Sebastes spp.* at Cobb; V. Tunnicliffe, *pers. comm.*) on the micro- and mesozooplankton. The basic seamount trial, which does not include fish predation, is compared to two trials in which seamount fish prey on (i) mesozooplankton alone and (ii) both micro- and mesozooplankton.

In the first case it is assumed that fish predation reduces mesozooplankton biomass by 50%. The mesozooplankton stock is fixed at 50% of its pre-seamount value on the first day that the water parcel encounters the seamount. Given the slow turnover time of most mesozooplankton (*i.e.* weeks), the stock is then held at the 50% level for the rest of the 30-day trial. In the second case, I also impose a 20% daily mortality on the microzooplankton stock. Given the faster turnover time of most microzooplankton, however, the mortality is imposed only for those days during which the water parcel is over the seamount.

Phytoplankton stocks and mixed layer nitrate remain

Figure 30: Predicted stocks of (a) phytoplankton, (b) protozoans, (c) microzooplankton and (d) nutrients with: no predation from seamount fish (solid squares), fish predation resulting in a 50% reduction of mesozooplankton stock (open squares) and fish predation resulting in a 50% reduction in mesozooplankton stock plus a daily 20% mortality on microzooplankton stocks while over the seamount (solid triangles). T_{tr} = 4 days and isopycnal doming is 15m in each case.

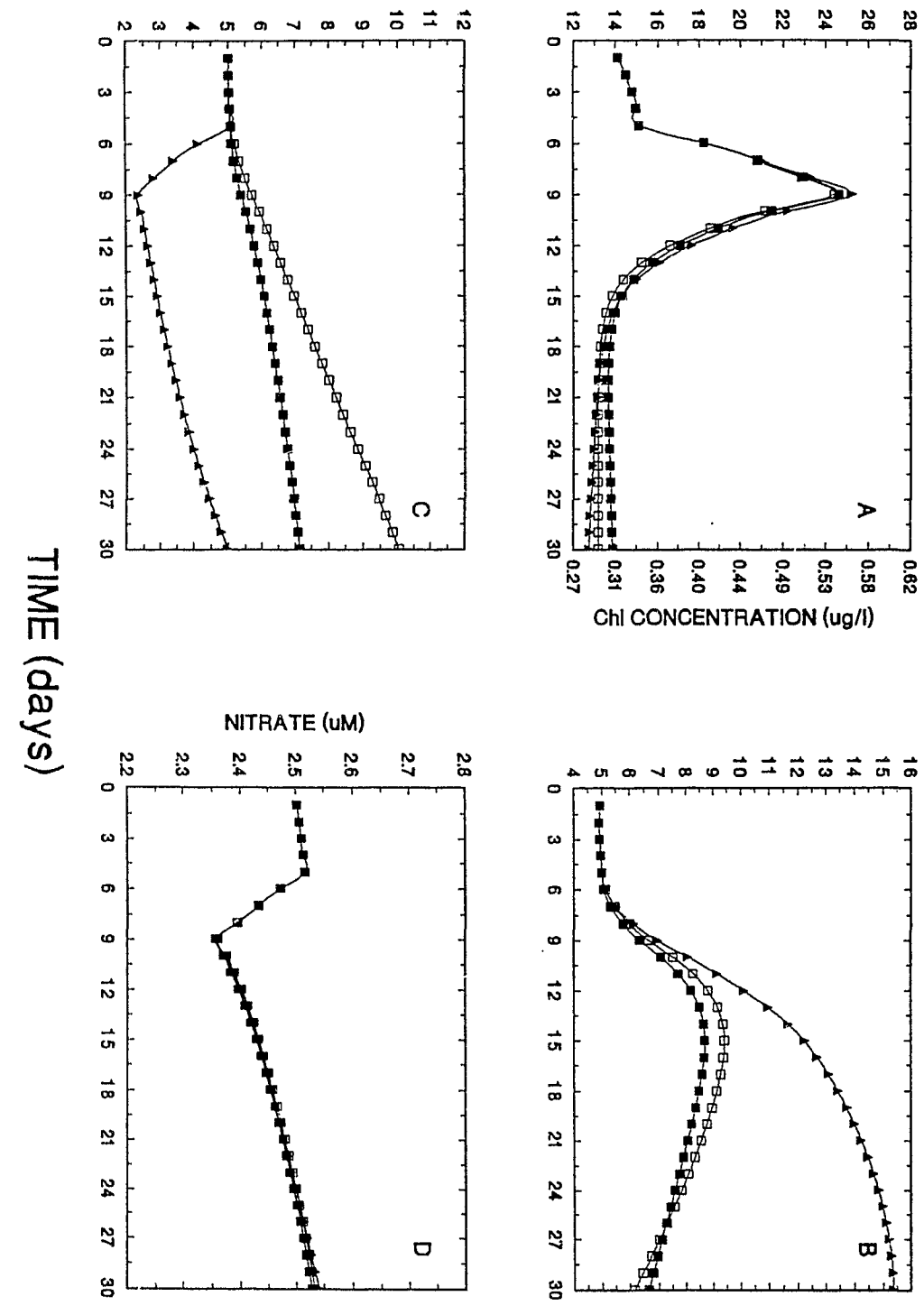
CONCENTRATION (ugC/l)
A
Chl CONCENTRATION (ug/l)
B
C
NITRATE (uM)
D
TIME (days)

largely unaffected by either predation scenario (Fig.30a,d). Compared to the no-predation trial, only a very slight increase in maximum Chl concentration occurs with fish predation on both micro- and mesozooplankton (0.56 versus 0.55 μg/l). Maximum Chl concentration decreases only slightly when predation is confined to the mesozooplankton. On day 30, final Chl concentration is lowest in the trial with fish predation on both micro- and mesozooplankton.

The stock of protozoans shows little response to fish predation on the mesozooplankton alone, the maximum protozoan concentration of 9.4 μgC/l being only ~7% higher than in the no-predation case (Fig.30b). When predation is extended to the microzooplankton as well, however, protozoan stocks undergo rapid growth (up to 0.15 day^{-1}, or 0.22 doublings day^{-1}) throughout the trial to a final concentration of 15.4 μgC/l.

Microzooplankton do respond to fish predation on the mesozooplankton (Fig.30c). When mesozooplankton stocks are reduced by 50%, the final microzooplankton stock of 10.1 μgC/l is 29% higher than in the no-predation trial. When subjected to a 20% daily mortality over the seamount, microzooplankton stocks decline rapidly to only 2.3 μgC/l, about 50% of the starting concentration. Beginning on day 10, when fish predation ends, microzooplankton stocks begin to increase again, and by the end of the trial have recovered to their initial concentration of 5 μgC/l.

4.5.5 Experiment 5: Mixing Rates and Nutrient Supply

Mixed layer nutrient concentration depends on both recycling, via zooplankton excretion, and on the entrainment of new nutrients from below the surface mixed layer. Near Cobb, nitrate concentration just below the mixed layer is ~5 μM. Here, I test the effect of varying the supply of nutrients by changing m, the mixing parameter.

For the 30-day trials considered in the model, phytoplankton stocks differ only slightly for values of m ranging from 0.01-0.05 day^{-1} (Fig.31a). Over this range, maximum Chl concentration increases with m. With no mixing, m = 0, the final Chl concentration falls below the starting value of 0.30 μg/l. Higher mixing rates also result in higher concentrations of protozoans and microzooplankton (Fig.31b,c). Except for a small decline during the four days the water parcel transits the seamount, the basic trial value of m = 0.02, keeps mixed layer nitrate virtually constant at 2.5 μM (Fig.31d). With m decreased to 0.01, mixed layer nitrate also remains high until the last day of the trial (~2 μM). Mixed layer nitrate actually begins to accumulate, to a final value of 3.7 μM, when m is increased to 0.05. When m is set to zero, the nitrate concentration declines throughout the trial and approaches the assumed phytoplankton half-saturation constant for nitrate, 1 μM, by day 30.

Figure 31: Predicted stocks of (a) phytoplankton, (b) protozoans, (c) microzooplankton and (d) nutrients with mixing, m, set to zero (solid squares), 0.01 day^{-1} (open squares), 0.02 day^{-1} (solid triangles) and 0.05 day^{-1} (open triangles). T_{tr} = 4 days and isopycnal doming is 15m in each case.

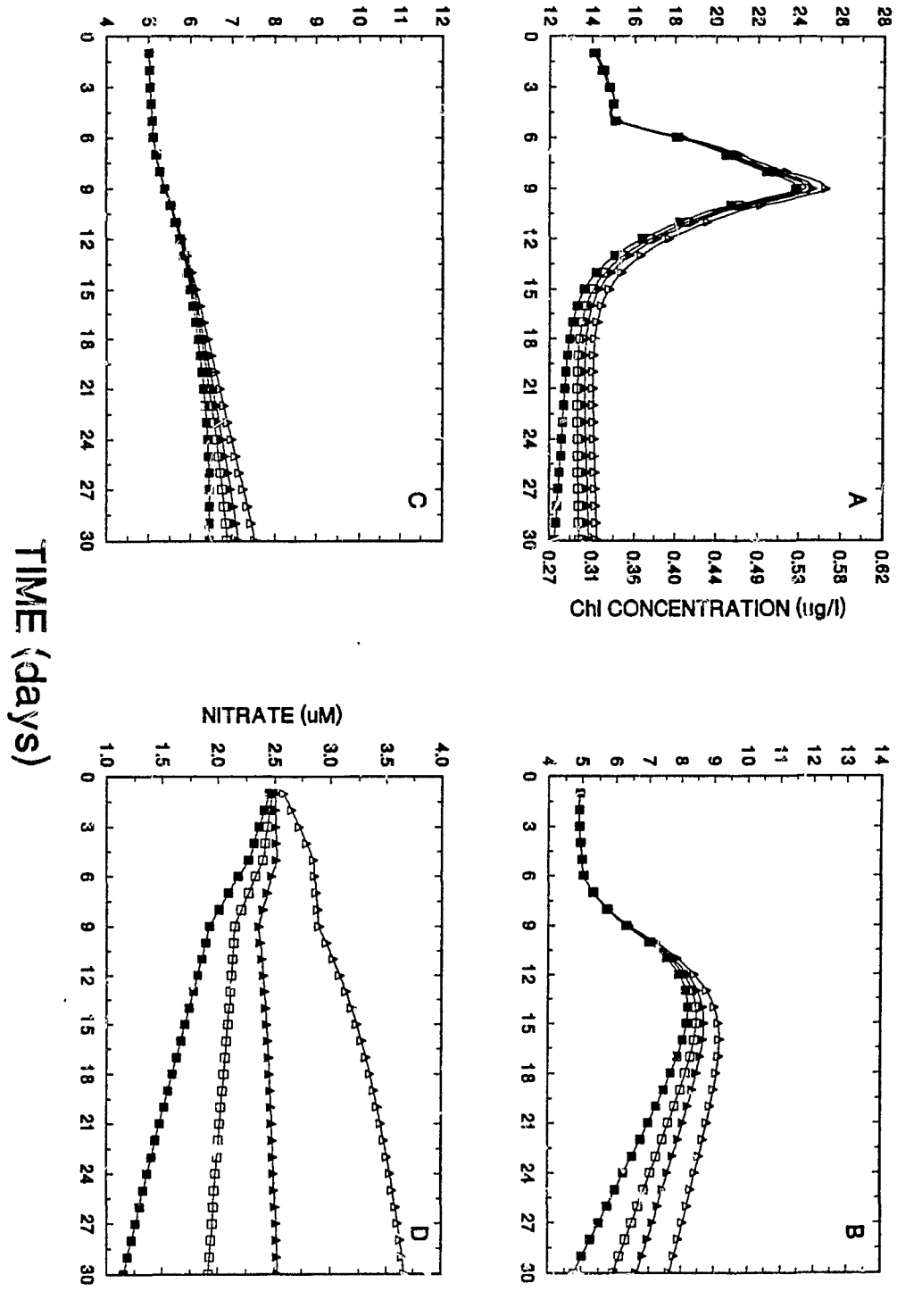
CONCENTRATION (ugC/l)
A
B
C
D
Chl CONCENTRATION (ug/l)
NITRATE (uM)
TIME (days)

4.5.6 Experiment 6: Phytoplankton Photosynthetic Efficiency

Here, I examine the effect of changing the photosynthetic efficiency of the phytoplankton, α, from the basic model value of 0.75 $\mu gC \cdot (\mu gChl)^{-1} \cdot ly^{-1}$ to 0.5 and 1.0 $\mu gC \cdot (\mu gChl)^{-1} \cdot ly^{-1}$. These values bracket those presented by Takahashi *et al.* (1972) for the Transition Zone and the subarctic Pacific in the summer.

If α is reduced to 0.5, phytoplankton stocks immediately begin to decline (Fig.32a), as phytoplankton growth is less than the daily grazing losses to protozoans and microzooplankton. In all the experiments, this is the only trial where such an initial decrease in phytoplankton stock is observed. Over the seamount the maximum Chl concentration increases to 0.40 $\mu g/l$, a 43% increase over the pre-seamount value. The reduced phytoplankton growth results in an increase in mixed layer nitrate, to a final value of ~2.75 μM (Fig.32d).

Raising α to 1.0 produces a rapid increase in the phytoplankton: over the seamount, the phytoplankton growth rate reaches 0.21 day^{-1} (0.31 doublings day^{-1}). The maximum Chl concentration of 0.65 $\mu g/l$ on day 9 is 20% higher than in the basic trial where α = 0.75. Increasing α results in a greater utilization of nitrate (Fig.32d), although by day 30 the concentration is still >2 μM.

With α = 0.5, phytoplankton production is clearly insufficient to support growth in either the protozoan or

Figure 32: Predicted stocks of (a) phytoplankton, (b) protozoans, (c) microzooplankton and (d) nutrients when phytoplankton photosynthetic efficiency, α, is 0.5 $\mu gC \cdot (\mu gChl)^{-1} \cdot ly^{-1}$ (solid squares), 0.75 (open squares) and 1.0 (solid triangles). T_{tr} = 4 days and isopycnal doming is 15m in each case.

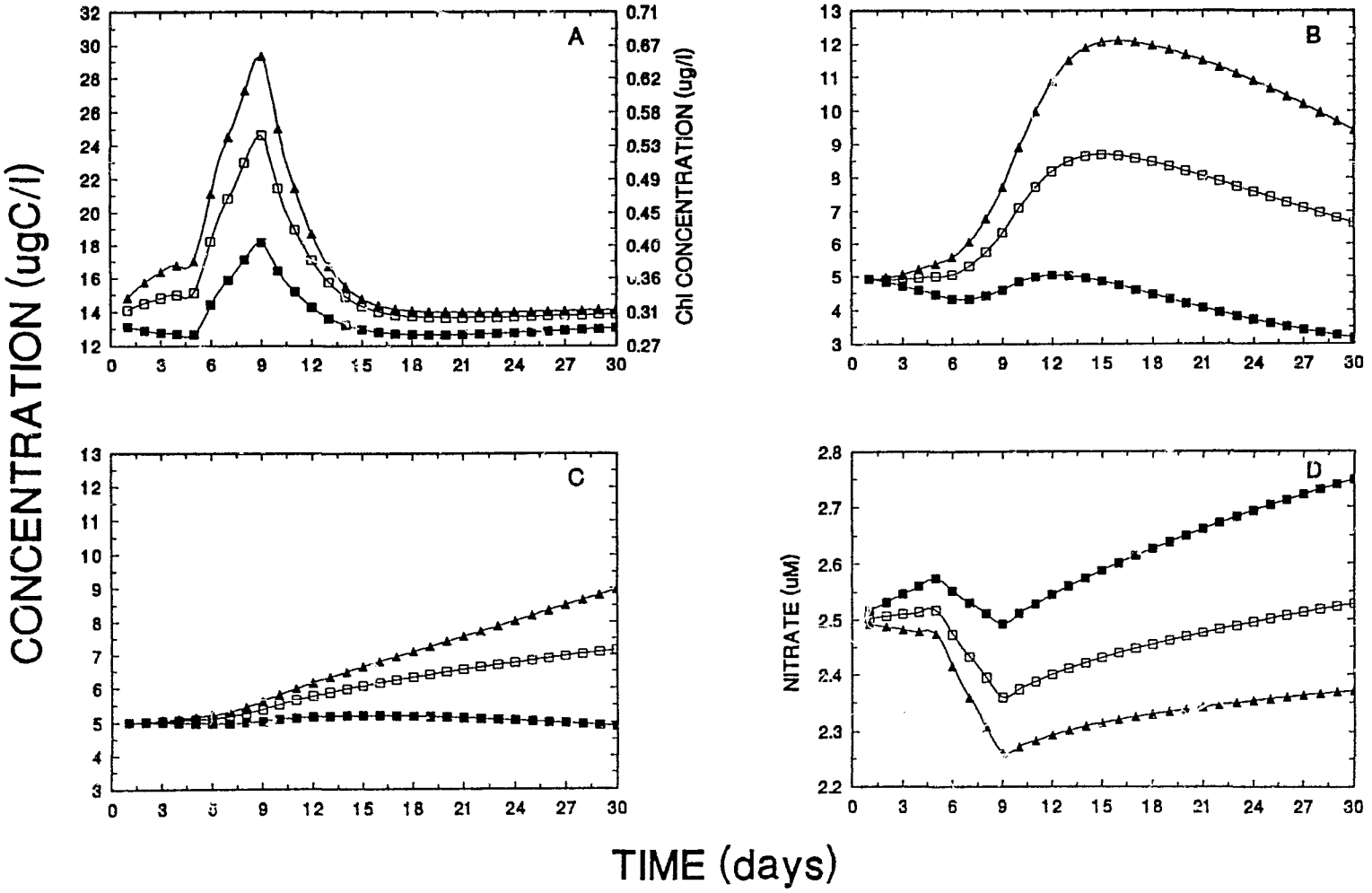
CONCENTRATION (ugC/l)
Chl CONCENTRATION (ug/l)
NITRATE (uM)
TIME (days)
A
B
C
D

the microzooplankton stocks (Figs.32b-c). Unlike other trials from any of the previous experiments, protozoan and microzooplankton stocks begin to decline even before the water parcel encounters the seamount. Both stocks do show brief increases, in response to the brief phytoplankton bloom over the seamount, but by the end of the trial both stocks fall below the starting concentration of 5 μgC/l.

4.6 Discussion

Two major goals of ecosystem modelling are (i) to provide an understanding of trophic linkages within ecosystems, and (ii) to allow quantitative predictions about the response of ecosystems to changes in environmental conditions. One of the most difficult tasks in this sort of modelling is determining what level of model complexity is necessary to answer the particular questions at hand. Too simplistic a model may fail to provide any new insights into the problems being addressed. Conversely, attempting to make a basic model more realistic by adding increasingly complex and detailed information can result in *decreased* predictive success, as the inclusion of additional parameters can make the model overly sensitive to the choice of starting conditions (Ulanowicz and Radach, 1981). In any case, the complexity of any model will still depend, to some extent, on the quantity and quality of the available data.

In this study, the main question to be answered is relatively simple: can persistent high chlorophyll conditions be maintained over shallow seamounts even in the absence of a recirculating flow? The available data are drawn primarily from 3 cruises, all to a single shallow seamount in summer. Consequently, the current model is quite simple. Nevertheless, the numerical experiments do provide some insights on the interactions between open ocean planktonic food webs and shallow topographies.

4.6.1 Implications of the Model Results

The main results can be seen in the basic seamount and no-seamount trials. The no-seamount trial shows that over periods of at least 30 days, grazing by protozoans and microzooplankton is sufficient to control summer phytoplankton stocks near the seamount. Thus, the 4 compartment food web recently proposed for Station P (Frost, 1991; Miller *et al.*, 1991) appears applicable to the southern subarctic as well. The basic seamount trial, however, points to an even more fundamental control on the phytoplankton stock: the availability of light. A 15m doming of the seasonal pycnocline as a water parcel transits the seamount produces a 67% increase in the standing stock of phytoplankton over the seamount. Experiment 3 (Fig.29) shows that a doming amplitude increased to 20m results in a doubling of the standing stock in just four days. Isopycnal

doming over Cobb Seamount is occasionally as high as 30m; for such a case (not shown) the model predicts a phytoplankton stock about 3.5 times higher than background levels.

Phytoplankton stocks are also influenced by the choice of α, the photosynthetic efficiency, and m, the mixing parameter. With 15m of doming, varying α within 33% (to 1.0 and 0.5 $\mu gC \cdot (\mu gChl)^{-1} \cdot ly^{-1}$) increases and decreases the seamount phytoplankton stock by +20% and -26%, relative to trials with α = 0.75. It is unlikely that the actual value of α is as low as 0.5, for at this level primary production becomes insufficient to meet the demands of grazing, and stocks of protozoans and microzooplankton decline. No such decline was observed during the CSEX cruises.

Experiment 5 shows that, for 30-day trials, phytoplankton stocks are only weakly dependent on m. A mixing rate of 0.01-0.02 day^{-1} keeps the mixed layer nutrient concentration relatively constant. These rates provide the best fit with observations from Cobb Seamount, where nutrient concentrations neither systematically increased nor decreased during the CSEX cruises. A higher m therefore seems unlikely, as the model predicts an accumulation of mixed layer nutrients if m is increased to 0.05 day^{-1}. The case where m = 0 is equally unlikely; in a trial where the model was allowed to run past the normal 30-day cutoff and m was set to zero (not shown), the entire

system ran down in about 100 days.

Thus, for the situation modelled here (but not necessarily for the actual Cobb system; see below), over timescales >30 days phytoplankton production *can* be considered nutrient limited in the sense that some small input of nutrients via vertical mixing is required to keep the model system from running down. Recall, however, that while the model assumes a vertically homogeneous chlorophyll distribution, profiles from Cobb Seamount show a marked subsurface chlorophyll maximum (Dower *et al.*, 1992). Despite the fact that near-surface nitrate concentrations near Cobb are usually ≥ 1μM the existence of such an SCM is usually taken to be indicative of some degree of nutrient limitation (Longhurst and Harrison, 1989).

Phytoplankton stocks shows no immediate response to fish predation on micro- or mesozooplankton. Since the phytoplankton are grazed primarily by protozoans, a brief exposure of the top two trophic compartments to fish predation over the seamount is unlikely to be felt at the base of the food web. However, when fish prey on both the micro- and mesozooplankton, the Chl concentration at the *end* of the trial is lower than the starting value (Fig.30a). This probably results from an increased grazing by the protozoans, which themselves experience reduced predation pressure over the seamount and in the days afterward while the microzooplankton stock is rebuilding. It appears then,

that subjecting micro- and mesozooplankton to a prolonged period of fish predation, as might occur if a water parcel were trapped over a seamount by a recirculating flow, could result in phytoplankton stocks being grazed to very low levels by the protozoans.

Despite the simplifying assumptions made regarding the vertical distribution of chlorophyll in the model, the predicted response of phytoplankton stocks to the shallow seamount shows good agreement with data from the CSEX cruises. Over the range of conditions used to simulate the waters around Cobb, the model predicts seamount phytoplankton stocks that are 67-350% higher than background levels. During the CSEX program, chlorophyll concentrations near Cobb were typically about twice the off-seamount values of 0.2-0.3 μg/l. Occasionally, however, integrated Chl values from Cobb were almost 4 times higher than background concentrations (Dower *et al.*, 1992).

Hence, the model shows that at shallow seamounts like Cobb even modest amounts of isopycnal doming are sufficient to produce localized phytoplankton blooms. Note, however, that while the model implies that the availability of light is the primary controlling factor, the SCM at Cobb (Dower *et al.*, 1992) suggests that the concomitant increase in nutrients accompanying doming may also be important to seamount phytoplankton stocks. To properly evaluate the relative importance of these two factors (*i.e.* light and

nutrients) at Cobb will require more information on the phytoplankton half-saturation constant for nitrate. The model assumes a value of 1μM; if the actual value is lower than this, then nutrient limitation diminishes in importance. Conversely, if it is found that half-saturation constants are > 1μM then phytoplankton at Cobb may be strongly nutrient-limited. This issue awaits further investigation.

The model shows that bloom intensity also depends on the background flow velocity. For a given doming amplitude, phytoplankton stocks are inversely proportional to the velocity of the background current (Fig.28a), since increased velocity results in a decreased transit time. Consequently, at higher velocities phytoplankton spend less time in the more favourable light conditions experienced during doming over the seamount. This effect is most pronounced when the original flow velocity is low. With 15m doming, increasing the background flow from 5 cm/s to 10 cm/s, which reduces T_{tr} from 8 to 4 days, produces a 28% decrease in maximum Chl concentration over the seamount. However, increasing velocity from 10 cm/s to 15 cm/s, thereby reducing T_{tr} from 4 to 2 days, only results in a further 12% decrease.

In actual fact, the relationship between background velocity and bloom intensity is likely more complex than the model suggests. While high velocities do result in

decreased transit times, evidence suggests that the velocity of the background current may also affect the amplitude of isopycnal doming near shallow topography (Roden, 1987). ADCP surveys near a small oceanic island show that isopycnal doming in the lee of the island increases with background velocity (Heywood *et al.*, 1990). It may be that, over a shallow seamount, the short transit resulting from a high velocity flow is offset by higher isopycnal doming. In fact, experiments 2 and 3 demonstrate that increased isopycnal doming can produce even stronger phytoplankton blooms than those resulting from increasing transit time.

The model also sheds light on the structure and function of the planktonic food web in the southern subarctic Pacific. Experiments 1-4 demonstrate a strong coupling between phytoplankton and grazers in the system. In the no-seamount case, grazing is sufficient to hold the phytoplankton stock fairly constant throughout the trial, removing about 85-102% of daily production. In the basic seamount trial (Fig.27), although grazing removes only 33-63% of daily production during the 4-day bloom, by day 12 (three days after the bloom has peaked) grazing is removing ~300% of daily production. In the case where doming is increased to 20m (Fig.29a), the model predicts that grazing can remove as much as 600% of daily phytoplankton production in the days following the bloom.

This coupling is due mainly to the grazing capacity of

the protozoans, which alone account for 50-80% of daily grazing in most trials. Marine protozoans have previously been shown to be capable of very high ingestion rates (Heinbokel, 1978) and, in some cases, can undergo 2-5 doublings in a single day (Lynn and Montagnes, 1991; Verity, 1991). The ingestion rate used here, 1 $\mu gC \cdot \mu gC^{-1} \cdot d^{-1}$, is near the lower end of reported values for protozoans. This high growth capacity enables the protozoans to respond to phytoplankton blooms almost instantly. Sime-Ngando *et al.* (1992) report increased small-scale (≤10km) patchiness in the ciliate community around Cobb and propose that ciliate growth in response to local patches of high primary production may play a role in generating this pattern.

As suggested by Frost (1991), the addition of another trophic level between the main grazers and the top predators does seem to insulate the grazers from destabilizing predation. In all but one of the seamount trials, the combined predation pressure from the micro- and mesozooplankton is sufficient to bring protozoans stocks back to near their initial concentration following the phytoplankton bloom. This finding is supported by observations of high rates of predation on protozoans by metazoan zooplankton (Stoecker and McDowell ,1990; Gifford and Dagg, 1991). The only case in which the protozoan stock actually "gets away" from its predators is that in which seamount fish prey on both micro- and mesozooplankton

(Fig.30). In this case, the stock of protozoans continues to grow to the end of the trial.

4.6.2 Persistence of High Chlorophyll Conditions

The model shows that due to the strong coupling in the subarctic Pacific food web, the phytoplankton bloom produced as the water parcel transits the seamount is quite ephemeral. Chlorophyll concentrations are typically reduced to pre-seamount concentrations (or lower) within 5-6 days after the peak of the bloom. To reconcile this conclusion with observations of persistent high chlorophyll conditions at shallow seamounts we must extend these results to the three dimensional situation.

Because of its one-dimensional nature, the present model only considers a single thin "column" of water transiting the seamount. Let us consider the more realistic three-dimensional case in which a steady current of 10cm/s is flowing over a shallow seamount such as Cobb with isopycnal doming comparable to that measured at Cobb. We will assume that (i) any recirculating current arising from this flow does not penetrate the surface and (ii) that the background chlorophyll concentration is reasonably invariable, as in the subarctic Pacific. With these assumptions, the net result of this flow is a region of persistently high phytoplankton standing stock situated over the seamount.

What appears to a stationary observer as a single persistent patch, however, is more a "conveyor belt" to which phytoplankton are added at one end and removed before reaching the other end. At the upstream end, phytoplankton and grazers are briefly decoupled as the phytoplankton bloom in response to the better light regime encountered as the current domes above the seamount. High phytoplankton growth rates continue while the phytoplankton transit the seamount but, shortly thereafter, grazing brings the stock back down to its normal level. This mechanism fits well with observations of a high chlorophyll region that persisted over Cobb Seamount for at least one month at a time when ADCP records showed no shallow recirculating current (Dower *et al.*, 1992; Freeland, *in press*).

There remains at least one problem with this mechanism. As presented here, the conveyor belt scenario should result in a "wake" of decreasing chlorophyll concentration downstream of the seamount, as protozoan and microzooplankton grazers consume the phytoplankton produced during the bloom. Examination of the chlorophyll data from the CSEX cruises (Figs.14, 18) shows only weak evidence of such a wake, the high chlorophyll regions generally being focused near Cobb. There are several possible explantions for the absence of a coherent chlorophyll wake downstream from Cobb.

First, it is possible that as the patches of high

chlorophyll water move away from the seamount they are rapidly degraded by other planktonic grazers that are attracted by the high phytoplankton concentrations. Second, the downstream wake may be physically disrupted: flow regimes downstream of seamounts can involve downwelling, lee waves, regions of return flows toward the seamount and further eddying motions (Davies et al., 1990; Boyer and Zhang, 1990; Chapman and Haidvogel, 1992; Smith, 1992). If this is the case near Cobb, then the lack of a consistent wake may result from the rapid decay of high chlorophyll patches in the flow field downstream of the seamount. Finally, failure to observe a coherent chlorophyll wake during the CSEX program may merely reflect the limitations imposed by the choice of hydrographic sampling design. Only during CSEX92 did sampling extend more than 1 seamount diameter downstream of Cobb. Unfortunately, during that year the background flow was strongly northwest-southeastward while the sampling grid ran west-east, making it extremely unlikely that a wake *could* be detected.

4.6.3 Implications for Nektonic Stocks at Cobb Seamount

The enhanced standing stock of seamount phytoplankton produced by this "conveyor belt" represents a potential source of energy for transfer to higher trophic levels. The pelagic juvenile stages of the *Sebastes spp.* found at Cobb Seamount are planktivorous (Brodeur and Pearcy, 1984; Reilly

et al., 1992). Thus, for the fish to benefit from this energy source first requires that the pulse of phytoplankton be converted into higher standing stocks of micro- and mesozooplankton.

The model predicts small increases in microzooplankton stocks by the end of most trials. Denman *et al.* (1989) calculate a timescale of ~25 days for a pulse of phytoplankton biomass to be converted into a pulse of new copepod biomass. In the absence of a trapping mechanism, and with an average velocity of 10cm/s, a water parcel will have moved ~200 km downstream of Cobb in 25 days. Therefore, if the fish are to gain any energy at all from the pulse of phytoplankton biomass, it seems that their zooplankton prey would somehow have to be maintained over the seamount for at least ~25 days.

The interaction of diel vertical migratory behaviour with a bottom-trapped recirculating current could retain zooplankton over a seamount. As long as the surface currents are not strong enough to advect the zooplankton off the seamount at night while feeding in surface waters, the deeper recirculating current could act to keep them over the seamount by day. It would be unlikely, however, that zooplankton retained in such a fashion could avoid predation by seamount fish for very long. Rather, it seems that the interaction of vertical migrators with shallow topography leads to both an increased patchiness and the generation of

"zooplankton gaps" over the topography (Genin *et al.*, 1988). These phenomena may be linked both to fish predation on mesozooplankton and active avoidance of the seamount topography by vertical migrators (Genin *et al.*, 1988; Genin *et al.*, *in press*; Haury *et al.*, *submitted*).

The mesozooplankton fauna at Cobb Seamount is dominated by species that do not perform extensive diel migrations and which are therefore confined mainly to the upper 100m of the water column. Hence, observations during CSEX91 that mesozooplankton biomass over Cobb was lower than in the surrounding waters (Dower, *unpublished data*) suggest either that (i) fish at Cobb ascend quite high into the water column to take advantage of this advected food source or (ii) zooplankton somehow actively avoid the seamount.

Except for a very small (<1 km^2) pinnacle that reaches to within 20m of the surface, most of the summit of Cobb lies 100-200m below the surface. However, other seamount-dwelling fish are known to make large vertical excursions into the water column (Boehlert and Genin, 1987; Wilson and Boehlert, 1993). Recently, Haury *et al.* (*submitted*) found evidence that fish over Fieberling Guyot may ascend as much as 400m to feed on near-surface zooplankton. It seems likely, then, that fish at Cobb behave in a similar fashion, consuming zooplankton that are advected over the seamount by the near-surface currents.

There is also some evidence to support the idea of a

behavioural response to the seamount by the zooplankton. Genin *et al.* (1989) find that vertically migrating euphausiids tend to avoid shallow topography. While most of the mesozooplankton at Cobb do not migrate vertically, it *is* possible that they do respond to the presence of the seamount over that area in which Cobb is shallower than ~100m. Another possibility recently suggested by Mackas *et al.* (1993) is that the vertical distributions of zooplankton may be determined by species specific preferences for different turbulent regimes. In such a case the increased internal wave energy and turbulent mixing over Cobb may cause zooplankton to vertically migrate or attempt to avoid the topography altogether.

The model results and the field evidence presented above suggest that while high chlorophyll conditions can persist at shallow seamounts even in the absence of a trapping mechanism, it is unlikely that this energy is transferred to the nektonic community. This conclusion finds support in the work of Tseitlen (1985) and Pudyakov and Tseitlen (1986) who suggest that the energetic requirements of a seamount fish population imply some allocthonous food supply.

The picture that emerges is one in which the various components of the pelagic food web are all affected by the presence of the seamount, but in which these same compartments are at least temporarily decoupled from one

another. This decoupling arises from the fact that different compartments "feel" the influence of the seamount in different ways. Phytoplankton respond to an improved light regime encountered over the seamount. Seamount fish receive a continuous, although patchily distributed, allochthonous food supply. Micro- and mesozooplankton may be exposed to increased mortality from fish or may actively attempt to avoid the seamount topography. Protozoans may experience a temporary release from predation pressure. In each case the response is transitory, and the "seamount effects" dissipate as the strongly coupled subarctic Pacific food web is re-established downstream of the seamount.

SUMMARY AND SYNTHESIS

This thesis set out to explore the role that current-topography interactions play in planktonic communities near shallow seamounts. It has long been suggested that such seamount flow phenomena contribute to the production and maintenance of the rich nektonic stocks often found over seamounts (Uda and Ishino, 1958; Hubbs, 1958). The previous four chapters show that although current-topography interactions do affect the composition and abundance of seamount biotas, the nature of the interaction is more complex than had previously been suspected. Simply put, the data from the Cobb Seamount Experiment do not support the classical explanation of seamount productivity. The results show that while a seamount effect *is* discernible in both pelagic and benthic communities, the "effect" is not based on an energy transfer along the food chain but rather, involves a suite of physical-biological interactions that are only loosely coupled.

A variety of seamount-flow phenomena have been documented from the CSEX data, chief among them the repeated observations of Taylor cones and associated regions of isopycnal doming. Prior to the Cobb Seamount Experiment, Taylor cones had only rarely been observed near shallow seamounts, and even then only fleetingly. While CSEX

totalled only 8 weeks of observations over a period of three years, it nevertheless provides the first strong evidence that Taylor cones may be *permanent* features, particularly over seamounts which, like Cobb, are situated in steady current systems. Additionally, observations from CSEX90 include the first record of isopycnal doming penetrating all the way to the surface. Although we only observed this effect once, it is interesting to speculate on whether outcropping might in fact be quite frequent at Cobb during other times of the year.

In the subarctic Pacific, winter mixing produces a water column that is isohaline and isothermal to the depth of the permanent halocline at about 100m (Favorite *et al.*, 1976). As there is little seasonal change in the strength of the background current near Cobb, it may be that the reduced stratification in the near-surface layer permits isopycnal doming to reach the surface throughout much of the winter. Likewise, while observations of the Taylor cone during CSEX showed the recirculation to be confined to depths >80m (Freeland, *submitted*) it is possible that during the winter the closed flow extends all the way to the surface. Such a flow at the surface flow should be visible via remote sensing of sea-surface temperature. However, the high degree of cloud cover makes it difficult to get good coverage in the subarctic Pacific, particularly in winter (Abbott, *pers. comm*). A winter cruise to Cobb would also do

much to clarify the issue of whether current-topography interactions of the sort discussed in this thesis are permanent features of shallow seamounts. To date, however, such an expedition has not been undertaken, largely because of the fact that winter conditions in the subarctic Pacific are not particularly conducive to oceanographic field work.

The clearest biological indication of a seamount effect is the repeated observation of a region of high chlorophyll water east of the Cobb summit. As with the Taylor cone observations, the CSEX data provide the first evidence that enhanced phytoplankton stocks may be quasi-permanent features around shallow seamounts. The degree of spatial correspondence between high chlorophyll concentrations and areas of isopycnal doming (Chapter 2) supports the notion that enhanced phytoplankton stocks near shallow seamounts are driven by current-topography interactions. However, whereas the classical hypothesis for seamount productivity suggests that primary production is fostered by retention in a region rich in upwelled nutrients, the CSEX data suggest a different scenario.

The model presented in Chapter 4 suggests a more fundamental control on photosynthesis: the availability of light. Average light levels in the subarctic Pacific are quite low, even during the summer, as a result of high cloud cover (Dodimead *et al.*, 1963). Consequently, while Frost

(1987, 1991) and Miller *et al.* (1991) demonstrate that grazing pressure, primarily from protozoans, removes almost 100% of daily production, the current model suggests that the level of the production is set largely by the amount of light available.

Observations from Cobb support the model predictions that, with as little as 15m of isopycnal doming, seamount phytoplankton stocks double in a few days (Figs.27, 29). The model also shows that under light limiting conditions, high phytoplankton stocks can be maintained without invoking any retention mechanism. The passage of phytoplankton over the seamount creates a dynamic situation in which phytoplankton bloom as they are uplifted over the seamount and are then consumed further downstream as the protozoan growth catches up with phytoplankton growth. The net result is a region of persistent high chlorophyll concentration that is constantly being renewed at the upstream edge of the seamount. Current-topography interactions further influence phytoplankton growth in the sense that doming amplitude and the amount of time that phytoplankton spend in the improved light conditions (*i.e.* transit time) are both related to the strength of the upstream flow.

One major issue that has yet to be resolved is the degree of nutrient limitation experienced by the phytoplankton near Cobb. The model suggests nutrients may not be strongly limiting, but it also makes the assumption

that phytoplankton stocks are distributed evenly throughout the mixed layer. In actual fact, there is a strong SCM evident in chlorophyll profiles from Cobb, suggesting some degree of nutrient limitation. Relative to Station P, where summer nitrate concentrations are usually > 6μM (Miller *et al.*, 1991) concentrations at Cobb (usually >1μM) are rather low. Relative to the highly oligotrophic subtropical North Pacific, however, nitrate concentrations around Cobb remain relatively high even in summer. The intensity of nutrient limitation is dependent on the phytoplankton half-saturation concentration for nitrate, and has yet to be studied for the waters near Cobb.

It has been also been proposed that phytoplankton production in the subarctic Pacific may be limited by the availability of iron, a micronutrient (Martin and Fitzwater, 1988). Since our analyses did not specifically measure iron concentration, it could be argued that the high phytoplankton stocks observed near Cobb result from the injection of additional iron into the surface waters by isopycnal doming. Two points argue against this possibility.

First, iron incubation experiments in the subarctic Pacific produce blooms of usually rare large diatoms after a few days (Miller *et al.*, 1991). A bloom of large diatoms *was* observed at the beginning of the CSEX cruise in early June of 1992. However, this bloom extended throughout the

region and was evident as much as 200km upstream of Cobb, making it highly unlikely that the bloom was mediated by any seamount phenomena. Second, as the major source of iron is aeolian rather than via upwelling, a persistent phytoplankton bloom driven by a localized increase in the aeolian flux of iron over Cobb Seamount seems highly unlikely.

There have been conflicting reports on the effects that seamounts have on zooplankton and ichthyoplankton communities. Observations of enhanced biomass, reduced biomass and of no change in biomass have all been reported (Boehlert and Genin, 1987; Boehlert, 1988). This does not fit well with the classical hypothesis of energy transmission from phytoplankton to zooplankton to nektonic stocks over seamounts (Uda and Ishino, 1958). The CSEX results show that high chlorophyll conditions probably *do* persist long enough to result in higher zooplankton stocks. The problem lies in the fact that there has yet to be demonstrated an effective means by which zooplankton can remain near the seamount long enough for biomass to accumulate there.

Chapter 3 shows a decrease in between-sample similarity in the mesozooplankton community composition near Cobb. It remains to be seen whether this pattern is caused by predation pressure on the mesozooplankton by seamount fish

or by some behavioural response of the mesozooplankton to the presence of the seamount. However, observations of similar patterns in community composition from other seamounts and shallow banks (Genin *et al.*, 1988; Haury *et al.*, *submitted*) indicate that these processes may be general phenomena at seamounts. In addition, the fact that fish stocks are often abundant on deep seamounts (Hughes, 1981; Raymore, 1982), over which increased phytoplankton stocks are not observed, provides further evidence that seamount fish rely on advected energy. This uncoupling of nektonic stocks from primary production raises some interesting questions regarding the importance of current-topography interactions to higher trophic levels.

If seamount fish rely on zooplankton advected over the seamount, then stock size will depend on a different set of current-topography interactions. The food available to fish resident on a seamount becomes a function of (i) the concentration of zooplankton in the upstream flow, (ii) the velocity of the flow, which will determine the flux of available food, and (iii) the areal extent of the seamount. Clearly, where (i) and (ii) are constant, larger seamounts should be capable of supporting larger fish stocks. Tseitlen (1985) and Pudyakov and Tseitlen (1986) use a numerical model to investigate seamount fish populations. They show that not only does stock size vary as a function of (i)-(iii) above, but that in most cases, the seamount

stocks could not be maintained without significant allochthonous energy inputs.

Going beyond the question of why seamounts are biologically productive, this work also points to the importance of physical-biological coupling (and indeed, uncoupling) as it relates to questions of top-down and bottom-up controls in marine communities. There has been much debate over whether planktonic communities are primarily regulated by nutrient supply (*i.e.* bottom-up) or predation (*i.e* top-down). The two prevailing views of the control on phytoplankton stocks in High-Nutrient-Low-Chlorophyll regions typify this argument. For the subarctic Pacific, Miller *et al.* (1991) have recently pointed out that while predation pressure is sufficient to control phytoplankton stocks, the composition of the phytoplankton stock may be influenced by iron availability.

A combination of top-down and bottom-up controls is also evident in the CSEX data. Away from the seamount, grazing can control phytoplankton stock. Over the seamount, the improved light conditions act as a pulse of bottom-up control, resulting in a brief uncoupling between phytoplankton and grazers, allowing rapid phytoplankton growth. The finding that planktonic communities are governed by combinations of top-down and bottom-up controls should come as no surprise, however. Organisms interact not

only with each other, but also with their environment. As this study shows, different organisms interact with the environment over very different temporal and spatial scales. To achieve a full understanding of any biological system then, first requires a detailed knowledge of the physical system. Our understanding of seamount biology has been hampered by the fact that biologists have tended to think of seamounts as isolated and closed systems. This is reflected in the classical explanation of seamount productivity, which centres on a mechanism in which energy is both created and retained within the system. As this work shows, when combined with an accurate representation of current-topography interactions, we find that rather than a tightly coupled, almost closed system, the picture that emerges is one of a highly dynamic system in which the various biological entities respond to the presence of the seamount in very different ways and are often only weakly coupled.

LITERATURE CITED

Agapitov, Y.N. and Gritsenko, A.M. (1988) Hydrophysical conditions in the vicinity of Pulkovskaya Seamount. Oceanology 28, 581-583.

Anderson, G.C. (1969) Subsurface chlorophyll maximum in the northeast Pacific Ocean. Limnol. Oceanogr. 14, 386-391.

Birkeland, C. (1971) Biological observations on Cobb Seamount. Northwest Science 45, 193-199.

Boehlert, G.W. (1988) Current-topography interactions at mid-ocean seamounts and the impact on pelagic ecosystems. GeoJournal 16, 45-52.

Boehlert, G.W. and Genin, A. (1987) A review of the effects of seamounts on biological processes. (in) Seamounts, Islands and Atolls, Keating,B.H., Fryer, P., Batiza, R. and Boehlert, G.W. (eds.) Geophysical Monograph 43, 319-334.

Boehlert, G.W., Mizuno, K. and Wilson, C.D. (1990) The origin and maintenance of Maurolicus muelleri populations on central north Pacific seamounts. Eos 71, 155.

Boehlert, G.W. and Seki, M.P. (1984) Enhanced micronekton abundance over mid-Pacific seamounts. EOS 65, 928.

Booth, B.C. (1988) Size classes and major taxonomic groups of phytoplankton at two locations in the subarctic Pacific Ocean in May and August, 1984. Mar. Biol. 97, 275-286.

Boyer, D.L. and Zhang, X. (1990) Motion of oscillatory currents past isolated topography. J. Phys.Oceanogr.20, 1425-1448.

Brink, K.H. (1989) The effect of stratification on seamount-trapped waves. Deep-Sea Res. 36, 825-844.

Brink, K.H. (1990) On the generation of seamount-trapped waves. Deep-Sea Research 37, 1569-1582.

Brodeur, R.D. and Pearcy, W.G. (1984) Food habits and dietary overlap of some shelf rockfishes (Genus Sebastes) from the northeastern Pacific Ocean. Fish. Bull. 82, 269-293.

Budinger, T.F. (1967) Cobb Seamount. Deep-Sea Res. 14, 191-201.

Budinger, T.F. and Enbysk, B.J. (1960) Cobb Seamount, a deep-sea feature off the Washington coast. Technical Report No.60, Department of Oceanography, University of Washington. 88pp.

Burkill, P.H., Edwards, E.S., John, A.W. and Sleigh, M.A. (1993) Microzooplankton and their herbivorous activity in the northeastern Atlantic Ocean. Deep-Sea Res. 40, 479-493.

Chapman, D.C. and Haidvogel, D.B. (1992) Formation of Taylor caps over a tall isolated seamount in a stratified ocean. Geophys. Astrophys. Fluid Dynamics 64, 31-65.

Cleveland, W.S. (1979) Robust locally weighted regression and smoothing scatterplots. J. Amer. Statist. Soc. 74, 829-836.

Cleveland, W.S. (1985) The elements of graphing data. Wadsworth Advanced Books, Monterey. 323pp.

Comeau, L.A., Vezina, A.F., Bourgeois, M. and Juniper, S.K. (submitted) Relationship between phytoplankton production and the physical structure of the water column near Cobb Seamount, northeast Pacific. Deep-Sea Res.

Cullen, J.J. (1991) Hypotheses to explain high-nutrient conditions in the open sea. Limnol. Oceanogr. 36, 1578-1599.

Dagg, M.J. and Walser, W.E. (1987) Ingestion, gut passage, and egestion by the copepod Neocalanus plumchrus in the laboratory and in the subarctic Pacific Ocean. Limnol. Oceanogr. 32, 178-188.

Dagg, M.J. and Wyman, K.D. (1983) Natural ingestion rates of the copepods Neocalanus plumchrus and N. cristatus calculated from gut contents. Mar. Ecol. Prog. Ser. 13, 37-46.

Davies, P.A., Davis, R.G. and Foster, M.R. (1990) Flow past a circular cylinder in a rotating stratified fluid. Phil. Trans. Royal Soc. Lond. a331, 245-286.

Davis, E.E. and Karsten, J.L. (1986) On the case of the asymmetric distribution of seamounts about the Juan de Fuca ridge: ridge-crest migration over a heterogeneous athenosphere. Earth Planet. Sci. Letters 79, 385-396.

Denman, K.L., Freeland, H.J. and Mackas, D.L. (1989) Comparisons of time scales for biomass transfer up the marine food web and coastal transport processes. (in) Beamish, R.J. and G.A. McFarlane Effects of Ocean Variability on Recruitment and an Evaluation of Parameters Used in Stock Assessment Models. Can. Special Publication of Fish and Aquat. Sci. 108, 255-264.

Dodimead, A.J., Favorite, F. and Hirano, T. (1963) Review of oceanography of the subarctic Pacific region. International North Pacific Fisheries Commission, Bulletin No 13., 195pp.

Dower, J., Freeland, H. and Juniper, K. (1992) A strong biological response to oceanic flow past Cobb Seamount. Deep-Sea Res. 39, 1139-1145.

Dymond, J.R., Watkins, N.D. and Nayudu, Y.R. (1968) Age of the Cobb Seamount. J. Geophys. Res. 73, 3977-3979.

Eriksen, C.C. (1982) Observations of internal wave reflection off sloping bottoms. J. Geophys. Res. 87, 525-538.

Eriksen, C.C. (1985) Implications of ocean bottom reflection for internal wave spectra and mixing. J. Phys. Oceanogr. 15, 1145-1156.

Farrow, G.E. and Durant, G.P. (1985) Carbonate-basaltic sediments from Cobb Seamount, northeast Pacific: zonation, bioerosion and petrology. Mar. Geol. 65, 73-102.

Favorite, F., Dodimead, A.J. and Nasu, K. (1976) Oceanography of the subarctic Pacific region, 1960-1971. International North Pacific Fisheries Commission, Bulletin No. 33, 187pp.

Fedosova, R.A. (1974) Distribution of some copepod species in the vicinity of the underwater Hawaiian Ridge. Oceanology 14, 724-727.

Flint, M.V. and Yakushev, Y.V. (1988) Spatial structure of mesoplankton and distribution of dissolved ammonia in the vicinity of Pulkovskaya Seamount. Oceanology 28, 655-660.

Freeland, H.J.(submitted) Ocean circulation at and near a shallow seamount in the N.E. Pacific Ocean. Deep-Sea Res.

Freeland, H.J., Crawford, W.R. and Thomson, R.E. (1984) Currents along the Pacific coast of Canada. Atmosphere-Ocean 22, 151-172.

Freeland, H.J. and Gould, W.J. (1976) Objective analysis of meso-scale ocean circulation features. Deep-Sea Res. 23, 915-924.

Frost, B.W. (1987) Grazing control of phytoplankton stock in the open subarctic Pacific Ocean: a model assessing the role of mesozooplankton, particularly the large calanoid copepods Neocalanus spp. Mar. Ecol. Prog. Ser. 39, 49-68.

Frost, B.W. (1991) The role of grazing in nutrient-rich areas of the open sea. Limnol. Oceanogr. 36, 1616-1630.

Frost, B.W., Landry, M.R. and Hassett, R.P. (1983) Feeding behavior of large calanoid copepods Neocalanus cristatus and N. plumchrus from the subarctic Pacific Ocean. Deep-Sea Res. 30, 1-13.

Fukasawa, M. and Nagata, Y. (1978) Detailed oceanic structure in the vicinity of the Shoal Kokusho-sone. J. Oceanogr. Soc. Japan 34, 41-49.

Gardner, G.A. and Szabo, I. (1982) British Columbia Pelagic Marine Copepoda. Canadian Special Publication of Fisheries and Aquatic Science No 62., 536pp.

Gargett, A.E. (1991) Physical processes and the maintenance of nutrient-rich euphotic zones. Limnol. Oceanogr. 36, 1527-1545.

Genin, A. (1990) The rarity of upwelling events over seamounts. Eos 71, 154-155.

Genin, A. and Boehlert, G.W. (1985) Dynamics of temperature and chlorophyll structures above a seamount: An oceanic experiment. J. Mar. Res. 43, 907-924.

Genin, A., Dayton, P.K., Lonsdale, P.F. and Speiss, F.N. (1986) Corals on seamount peaks provide evidence of current acceleration over deep-sea topography. Nature 322, 59-61.

Genin, A., Greene, C., Haury, L., Wiebe P. and Gal, G. (in press) Zooplankton patch dynamics: Daily gap formation over abrupt topography. Deep-Sea Res.

Genin, A., Haury, L. and Greenblatt, P. (1988) Interactions of migrating zooplankton with shallow topography:predation by rockfishes and intensification of patchiness. Deep-Sea Res. 35, 151-175.

Genin, A., Noble, M. and Lonsdale, P.F. (1989) Tidal currents and anticyclonic motions on two North Pacific seamounts. Deep-Sea Res. 36, 1803-1815.

Gifford, D.J. and Dagg, M.J. (1991) The microzooplankton-mesozooplankton link: consumption of planktonic protozoa by the calanoid copepods Acartia tonsa Dana and Neocalanus plumchrus Murukawa. Mar. Microb. Food Webs 5, 161-177.

Gilbert, D. and Garrett, C. (1989) Implications for ocean mixing of internal wave scattering off irregular topography. J. Phys. Oceanogr. 19, 1716-1729.

Gould, W.J., Hendry, R. and Huppert, H.E. (1981) An abyssal topographic experiment. Deep-Sea Res. 28, 409-440.

Haury, L., Fey, C., Gal, G. and Genin, A. (submitted) Copepod carcasses in the ocean. 1. Predation on zooplankton over seamounts. Mar. Ecol. Prog. Ser.

Haury, L.R. (1976) A comparison of zooplankton patterns in the California Current and North Pacific Central Gyre. Mar. Biol. 37, 159-167.

Heinbokel, J.F. (1978) Studies on the functional role of tintinnids in the Southern California Bight. 1. Grazing and growth rates in laboratory cultures. Mar. Biol. 47, 177-189.

Herlinveaux, R.H. (1971) Oceanographic features of and biological observations at Bowie Seamount 14-15, August,1969. Fisheries Research Board of Canada Technical Report No.27335pp..

Heywood, K.J., Barton, E.D. and Simpson, J.H. (1990) The effects of flow disturbance by an oceanic island. J. Mar. Res. 48, 55-73.

Hobson, L.A. (1980) Primary productivity of the North Pacific - A Review. (in) Salmonid ecosystems of the North Pacific. McNeil, W.J. and Himsworth, D.C.(eds.) Oregon State University Press, Corvallis.231-246.

Hobson, L.A. and Ketcham, D.E. (1974) Observations on subsurface distributions of chlorophyll *a* and phytoplankton carbon in the northeast Pacific Ocean. J. Fish. Res. Bd. Can. 31, 1919-1925.

Hogg, N.G. (1973) On the stratified Taylor column. J. Fluid Mech. 58, 517-537.

Hubbs, C.L. (1958) Initial discoveries of fish faunas on seamounts and offshore banks in the eastern Pacific. Pac. Science 13, 311-316.

Hughes, S.E. (1981) Initial U.S. exploration of nine Gulf of Alaska seamounts and their associated fish and shellfish resources. Marine Fisheries Review 43, 26-33.

Huppert, H.E. (1975) Some remarks on the initiation of inertial Taylor columns. J. Fluid Mech. 67, 397-412.

Huthnance, J.M. (1981) Waves and currents near the continental shelf edge. Prog. Oceanogr. 10, 193-226.

Isaacs, J.D. and Schwartzlose, R.A. (1965) Migrant sound scatterers: Interaction with the seafloor. Science 150, 1810-1813.

Jackson, G.A and Eldridge, P.M. (1992) Food web analysis of a planktonic system off Southern California. Prog. Oceanogr. 30, 223-251.

Johnson, E.R. (1982) Quasigeostrophic flow over isolated elongated topography. Deep-Sea Res. 29, 1085-1097.

Landry, M.R. and Lehner-Fournier, J.M. (1992) Control of phytoplankyon blooms in the subarctic Pacific Ocean-Experimental studies in Microcosms (in) Wong, C.S. and P.J. Harrison (eds.) Marine Ecosystem Enclosed Experiments. International Development Research Centre, Ottawa, pp.106-121.

Larsen, L.H. and Irish, J.D. (1975) Tides at Cobb Seamount. J. Geophys. Res. 80, 1691-1695.

LeBrasseur, R.J. (1965) Seasonal and annual variations of net zooplankton at Ocean Station P, 1956-1964. Fish. Res. Bb. Canada, Manuscript Report Series, No.202.

Legendre, P. and Fortin, M.J. (1989) Spatial pattern and ecological analysis. Vegetatio 80, 107-138.

Levitus, S., Conkright, M.E., Reid, J.L., Najjar, R.G. and Mantyla, A.(1993) Distribution of nitrate, phosphate and silicate in the world oceans. Prog. Oceanogr. 31, 245-273.

Longhurst, A.R. and Harrison, W.G. (1989) The biological pump: Profiles of plankton production and consumption in the upper ocean. Prog. Oceanogr. 22, 47-123.

Lynn, D.H. and Montagnes, J.S. (1991) Global production of heterotrophic marine planktonic ciliates. (in) P.C. Reid et al. (eds.) Protozoa and Their Role in Marine Processes. NATO ASI Series, Vol. G25, Springer-Verlag, Berlin, pp281-307.

Mackas, D.L. (1984) Spatial autocorrelation of plankton community composition in a continental shelf ecosystem. Limnol. Oceanogr. 29, 451-471.

Mackas, D.L., Denman, K.L. and Abbott, M.R. (1985) Plankton patchiness: Biology in the physical vernacular. Bull. Mar. Sci. 37, 652-674.

Mackas, D.L. and Sefton, H.A. (1982) Plankton assemblages off southern Vancouver Island: Geographic pattern and temporal variability. J. Mar. Res. 40, 1173-1200.

Mackas, D.L., Sefton, H., Miller, C.B. and Raich, A. (1993) Vertical habitat partitioning by large calanoid copepods in the oceanic subarctic Pacific during spring. Prog. Oceanogr. 32, 259-294.

Mackas, D.L., Washburn, L. and Smith, S.L. (1991) Zooplankton community pattern associated with a California Current cold filament. J. Geophys. Res. 96, 14781-14798.

Martin, J.H. and Fitzwater, S.E. (1988) Iron deficiency limits phytoplankton growth in the north-east Pacific subarctic. Nature 331, 341-343.

Martin, J.H., Gordon, R.M. and Fitzwater, S.E. (1991) The case for iron. Limnol. Oceanogr. 36, 1793-1802.

McCartney, M.S. (1975) Inertial Taylor columns on a beta plane. J. Fluid Mech. 68, 71-95.

McGowan, J.A. and Walker, P.W. (1979) Structure in the copepod community of the North Pacific Central Gyre. Ecol. Monogr. 49, 195-226.

McNally, G.J., Patzert, W.C., Kirwan, A.D. and Vastano, A.C. (1983) The near-surface circulation of the north Pacific using satellite tracked drifting buoys. J. Goeophys. Res. 88, 7507-7518.

Meincke, J. (1971) Observation of an anticyclonic vortex trapped above a seamount. J. Geophys. Res. 76, 7432-7440.

Merrill, R.T. and Burns, R.E. (1972) A detailed magnetic study of Cobb Seamount. Earth Planet. Sci. Letters 14, 413-418.

Miller, C.B., Frost, B.W., Wheeler, P.A., Landry M.R. and Welchmeyer, N., Powell, T.M. (1991) Ecological dynamics in the subarctic Pacific, a possibly iron-limited ecosystem. Limnol. Oceanogr. 36, 1600-1615.

Moiseyev, Y.V. (1986) Distribution of Protozoans near seamounts in the western Indian Ocean. Oceanology 26, 86-90.

Morris, B. (1970) Calanoid copepods from midwater trawls in the north Pacific along 160E. J. Fish. Res. Bd. Canada 27, 2297-2321.

Mullin, M.M. (1993) Webs and Scales: Physical and ecological processes in marine fish recruitment. Washington Sea Grant Program, Seattle, 135pp.

Nabatov, V.N. and Ozmidov, R.V. (1988) Study of turbulence above seamounts in the Atlantic Ocean. Oceanology 28, 161-166.

Noble, M., Cacchione, D.A. and Schwab, W.C. (1988) Observations of strong mid-Pacific internal tides over Horizon Guyot. J. Phys. Oceanogr. 18, 1300-1306.

Noble, M. and Mullineaux, L.S. (1989) Internal tidal currents over the summit of Cross Seamount. Deep-Sea Res. 36, 1791-1802.

Odland, J. (1988) Spatial autocorrelation. Sage Pub., London. 85pp.

Owens, W.B. and Hogg, N.G. (1980) Oceanic observations of stratified Taylor columns near a bump. Deep-Sea Res. 27, 1029-1045.

Parin, N.V. and Prutko, V.G. (1985) The thalassial mesobenthopelagic ichthyocoene above the Equator Seamount in the western tropical Indian Ocean. Oceanology 25, 781-783.

Park, T.S. (1968) Calanoid copepods from the central north Pacific Ocean. Fish. Bulletin 66, 527-572.

Parker, T. and Tunnicliffe, V.J. () (submitted) Dispersal strategies of the biota on an oceanic seamount. Biol. Bull.

Parsons, T.R., Takahashi, M. and Hargrave, B. (1984) Biological Oceanographic Processes. Pergamon Press, Oxford, 330pp.

Powell, D.E., Alverson, P.L. and Livingston, R. (1952) North Pacific albacore tuna exploration 1950. U.S. Fish and Wildlife Service, Fishery Leaflet 402, pp46-56.

Poyarkov, S.G. and Gusarova, A.N. (1988) Effect of Pulkovskaya Seamount on the hydrochemical structure. Oceanology 28, 595-599.

Pudyakov, Y.A. and Tseitlen, V.B (1986) Simulation model of separate fish populations inhabiting submarine rises. J. Ichthyology 26, 145-150.

Pudyakov, Y.A. and Tseitlin, V.B. (1986) Simulation Model of Separate Fish Populations Inhabiting Submarine Rises. Jour. Ichthyology 26, 145-150.

Raymore, P.A. (1982) Photographic investigations on three seamounts in the Gulf of Alaska. Pac. Sci. 36, 14-34.

Reilly, C.A., Wyllie Echeverria, T. and Ralston, S. (1992) Interannual variation and overlap in the diets of palagic juvenile rockfish (Genus: Sebastes) off central California. Fish. Bull. 90, 505-515.

Roden, G.I. (1970) Aspects of the mid-Pacific Transition Zone. J. Geophys. Res. 75, 1097-1109.

Roden, G.I. (1971) Aspects of the Transition Zone in the northeastern Pacific. J. Geophys. Res. 76, 3643-3675.

Roden, G.I. (1972) Temperature and salinity fronts at the boundaries of the subarctic-subtropical Transition Zone in the western Pacific. J. Geophys. Res. 77, 7175-7187.

Roden, G.I. (1984) Mesoscale sound speed fronts in the central and western North Pacific and in the Emperor Seamounts region. J. Physic. Oceanogr. 14, 1659-1669.

Roden, G.I. (1987) Effect of seamounts and seamount chains on ocean circulation and thermohaline structure. (in) Seamounts, Islands and Atolls, Keating B.H., Fryer, P., Batiza, R. and oehlert, G.W. (eds) Geophysical Monograph 43, 335-354.

Roden, G.I. (1991) Mesoscale flow and thermohaline structure around Fieberling Seamount. J. Geophys. Res. 96, 16653-16672.

Roden, G.I. and Taft, B.A. (1985) Effect of the Emperor Seamounts on the mesoscale thermohaline structure during the summer of 1982. J. Geophys. Res. 90, 839-855.

Sime-Ngando, T., Juniper, K. and Vezina, A. (1992) Ciliated protozoan communities over Cobb Seamount: increase in biomass and spatial patchiness. Mar. Ecol. Prog. Ser. 89, 37-51.

Smith, L.T. (1992) Numerical simulations of stratified rotating flow over finite amplitude topography. J. Phys. Oceanogr. 22, 686-696.

Smith, W.O. and Jordan, T.H. (1988) Seamount statistics in the Pacific Ocean. J. Geophys. Res. 93, 2899-2919.

Sneath, P.H and Sokal, R.R. (1973) Numerical Taxonomy. Freeman, San Franciso, 573pp.

Sorokin, Y.R. and Sorokina, O.V. (1985) Bacterioplankton in the vicinity of underwater rises in the eastern Indian Ocean. Oceanology 25, 772-777.

Starr, J.L. and Mullin, M.M. (1981) Zooplanktonic assemblages in three areas of the North Pacific as revealed by continuous horizontal transects. Deep-Sea Res. 28, 1303-1322.

Stoecker, D.K. and McDowell Capuzzo, J. (1990) Predation on protozoa: its importance to zooplankton. J. Plank. Res. 12, 891-908.

Tabata, S. (1965) Variability of oceanographic conditions at Ocean Station "P" in the northeast Pacific Ocean. Trans. Royal Soc. of Canada 3, 367-418.

Takahashi, M., Satake, K. and Nakamoto, N. (1972) Chlorophyll distribution and photosynthetic activity in the north and equatorial Pacific Ocean along 155 W. Journal of the Oceanographial Society of Japan 28, 27-34.

Talley, L.D., Joyce, T.M. and DeSzoeke, R.A. (1991) Transpacific sections at 47N and 152W: distribution of properties. Deep-Sea Res. 38(Suppl.1), s63-s82.

Trexler, J.C. and Travis, J. (1993) Nontraditional regression analysis. Ecology 74, 1629-1637.

Tseitlin, V.B. (1985) Energetics of fish populations inhabiting seamounts. Oceanology 25, 237-239.

Uchida, R.N. and Tagami, D.T. (1986) Groundfish fisheries and research in the vicinity of seamounts in the north Pacific Ocean. Mar. Fish. Rev. 46, 1-17.

Uda, M. (1963) Oceanography of the subarctic Pacific Ocean. J. Fish. Res. Br. Canada 20, 119-179.

Uda, M. and Ishino, M. (1958) Enrichment patterns resulting from eddy systems in relation to fishing grounds. J. Tokyo Univ. Fish. 44, 105-119.

Ulanowicz, R.E. and Radach, G. (1981) Coupled process models (in) Platt, T., Mann, K.H. and R.E. Ulanowicz (eds.) Mathematical Models in Biological Oceanography. Unesco, Paris, pp26-34.

Vastano, A.C. and Warren, B.A. (1976) Perturbations to the Gulf Stream by Atlantis II Seamount. Deep-Sea Res. 23, 681-694.

Verity, P.G. (1991) Measurement and simulation of prey uptake by marine planktonic ciliates fed plastidic and aplastidic nanoplankton. Limnol. Oceanogr. 36, 729-750.

Verity, P.G., Stoecker, D.K., Sieracki. M.E. and J.R. Nelson (1993) Grazing, growth and mortality of microzooplankton during the 1989 North Atlantic spring bloom at 47°N, 18°W. Deep-Sea Res. 40, 1793-1814.

Verron, J. and LeProvost, C. (1985) A numerical study of quasi-geostrophic flow over isolated topography. J. Fluid Mech. 154, 231-252.

Vezina, A.F. and Platt, T. (1988) Food web dynamics in the ocean. 1. Best-estimates of flow networks using inverse methods. Mar. Ecol. Prog. Ser. 42, 269-287.

Voronina, N.M. and Timonin, A.G. (1986) Zooplankton of the region of seamounts in the western Indian Ocean. Oceanology 26, 745-748.

Whittaker, R.H. (1975) Communities and ecosystems. 2nd ed. MacMillan.

Wilkinson, L. (1990) SYSTAT: the system for statistics. Systat Inc., Evanston Illinois.

Wilson, R.R. and Kaufmann, R.S. (1987) Seamount biota and biogeography. In: Seamounts, Islands and Atolls, B. Keating, P. Fryer and R. Batiza (eds.) American Geophysical Union, Washington, D.C., pp. 319-334.

Wishner, K., Levin, L., Gowing, M. and Mullineaux, L. (1990) Involvement of the oxygen minimum in benthic zonation on a deep seamount. Nature 346, 57-59.

APPENDIX

CTD DATA: The following records list all the hydrographic stations sampled during the three Cobb Seamount Experiment cruises. Data are archived at the Institute of Ocean Sciences, Sidney B.C. and can be accessed by both cruise number and CTD cast number. CSEX90 casts were generally to 1000m and include records of conductivity, temperature, pressure and percent light transmission. CSEX91 and CSEX92 casts were generally to 500m and 250m respectively, and include measurements of conductivity, temperature, pressure, percent light transmission and fluorescence.

Cobb Seamount Experiment, August 1990

Cruise ID: Institute of Ocean Sciences Cruise 9050
Chief Scientist: Howard Freeland, IOS
Vessel: CSS Parizeau

Filename	Cast#	ID	Latitude	Longitude	Date
90500001.CTD	001		48 44.21 N	123 17.84 W	90/07/31
90500002.CTD	002		46 43.56 N	130 48.67 W	90/08/02
90500003.CTD	003	S101	46 40.80 N	130 45.60 W	90/08/02
90500004.CTD	004	S102	46 41.60 N	130 46.30 W	90/08/02
90500005.CTD	005	S103	46 42.50 N	130 46.04 W	90/08/02
90500006.CTD	006	S104	46 43.40 N	130 47.70 W	90/08/02
90500007.CTD	007	S105	46 44.20 N	130 48.50 W	90/08/02
90500008.CTD	008	S106	46 45.11 N	130 49 02 W	90/08/02
90500009.CTD	009	S107	46 46.07 N	130 49.86 W	90/08/02
90500010.CTD	010	S108	46 46.70 N	130 50.74 W	90/08/02
90500011.CTD	011	S109	46 47.65 N	130 51.43 W	90/08/02
90500012.CTD	012	S110	46 48.58 N	130 52.27 W	90/08/02
90500013.CTD	013	S111	46 49.36 N	130 52.89 W	90/08/02
90500014.CTD	014	S201	46 49.24 N	130 45.49 W	90/08/02

90500015.CTD	015	S202	46	48.45	N	130	46.30	W	90/08/02
90500018.CTD	018	S204	46	46.80	N	130	47.75	W	90/08/02
90500019.CTD	019	S204	46	46.81	N	130	47.69	W	90/08/02
90500020.CTD	020	S205	46	46.00	N	130	48.50	W	90/08/02
90500021.CTD	021	S206	46	45.20	N	130	49.11	W	90/08/02
90500022.CTD	022	S207	46	44.28	N	130	49.69	W	90/08/02
90500023.CTD	023	S208	46	43.44	N	130	50.64	W	90/08/02
90500024.CTD	024	S209	46	42.55	N	130	51.27	W	90/08/02
90500025.CTD	025	S210	46	41.59	N	130	52.01	W	90/08/02
90500026.CTD	026	S211	46	40.80	N	130	52.60	W	90/08/02
90500027.CTD	027	S301	46	45.16	N	130	56.32	W	90/08/03
90500028.CTD	028	S302	46	45.16	N	130	54.83	W	90/08/03
90500029.CTD	029	S303	46	45.11	N	130	53.60	W	90/08/03
90500030.CTD	030	S304	46	45.24	N	130	51.83	W	90/08/03
90500031.CTD	031	S305	46	45.19	N	130	50.69	W	90/08/03
90500032.CTD	032	S306	46	45.28	N	130	48.97	W	90/08/03
90500033.CTD	033	S307	46	45.14	N	130	47.55	W	90/08/03
90500034.CTD	034	S308	46	45.18	N	130	46.16	W	90/08/03
90500035.CTD	035	S309	46	45.10	N	130	44.70	W	90/08/03
90500036.CTD	036	S310	46	45.14	N	130	43.19	W	90/08/03
90500037.CTD	037	S311	46	45.10	N	130	41.83	W	90/08/03
90500038.CTD	038	S101	46	40.61	N	130	45.61	W	90/08/03
90500039.CTD	039	S102	46	41.55	N	130	46.34	W	90/08/03
90500040.CTD	040	MV01	48	16.81	N	128	42.54	W	90/08/04
90500047.CTD	047	LS01	47	0.06	N	130	56.65	W	90/08/11
90500048.CTD	048	LS02	47	0.16	N	130	49.12	W	90/08/11
90500050.CTD	050	LS03	47	0.27	N	130	41.94	W	90/08/11
90500051.CTD	051	LS04	46	55.05	N	130	34.65	W	90/08/12
90500052.CTD	052	LS04	46	55.05	N	130	34.65	W	90/08/12
90500053.CTD	053	LS05	46	55.09	N	130	41.80	W	90/08/12
90500054.CTD	054	LS06	46	55.08	N	130	49.33	W	90/08/12
90500055.CTD	055	LS07	46	55.09	N	130	56.73	W	90/08/12
90500056.CTD	056	LS08	46	55.06	N	131	3.91	W	90/08/12
90500057.CTD	057	LS08	46	55.06	N	131	3.91	W	90/08/12
90500058.CTD	058	LS09	46	50.04	N	131	11.05	W	90/08/12

90500059.CTD	059	LS10	46	50.05	N	131	3.60	W	90/08/12
90500060.CTD	060	LS11	46	50.06	N	130	56.38	W	90/08/12
90500061.CTD	061	LS12	46	50.14	N	130	49.22	W	90/08/12
90500062.CTD	062	LS13	46	50.16	N	130	41.75	W	90/08/12
90500063.CTD	063	LS14	46	50.03	N	130	34.69	W	90/08/12
90500064.CTD	064	LS15	46	50.07	N	130	27.14	W	90/08/12
90500065.CTD	065	LS15	46	50.07	N	130	27.14	W	90/08/12
90500066.CTD	066	LS16	46	45.03	N	130	27.33	W	90/08/12
90500067.CTD	067	LS16	46	45.03	N	130	27.33	W	90/08/12
90500068.CTD	068	LS17	46	45.14	N	130	34.69	W	90/08/12
90500069.CTD	069	LS18	46	45.11	N	130	41.88	W	90/08/12
90500070.CTD	070	LS19	46	45.18	N	130	48.39	W	90/08/12
90500071.CTD	071	LS20	46	45.11	N	130	56.64	W	90/08/13
90500072.CTD	072	LS21	46	45.24	N	131	3.77	W	90/08/13
90500073.CTD	073	LS22	46	45.04	N	131	11.15	W	90/08/13
90500074.CTD	074	LS22	46	45.04	N	131	11.15	W	90/08/13
90500075.CTD	075	LS22	46	44.70	N	131	10.78	W	90/08/13
90500076.CTD	076	LS23	46	40.19	N	131	10.93	W	90/08/13
90500077.CTD	077	LS24	46	39.92	N	131	3.57	W	90/08/13
90500078.CTD	078	LS25	46	40.19	N	130	56.50	W	90/08/13
90500079.CTD	079	LS26	46	39.93	N	130	49.10	W	90/08/13
90500080.CTD	080	LS27	46	40.15	N	130	41.82	W	90/08/13
90500081.CTD	081	LS28	46	40.04	N	130	34.42	W	90/08/13
90500082.CTD	082	LS29	46	40.21	N	130	27.30	W	90/08/13
90500083.CTD	083	LS30	46	35.07	N	130	34.56	W	90/08/13
90500084.CTD	084	LS30	46	34.63	N	130	34.19	W	90/08/13
90500085.CTD	085	LS31	46	35.10	N	130	41.90	W	90/08/13
90500086.CTD	086	LS32	46	35.10	N	130	49.30	W	90/08/13
90500087.CTD	087	LS33	46	35.17	N	130	56.51	W	90/08/13
90500088.CTD	088	LS34	46	35.07	N	131	3.74	W	90/08/13
90500090.CTD	090	LS35	46	30.03	N	130	56.13	W	90/08/13
90500091.CTD	091	LS36	46	30.10	N	130	49.20	W	90/08/14
90500092.CTD	092	LS37	46	30.26	N	130	41.69	W	90/08/14
90500093.CTD	093	LS29	46	40.01	N	130	27.15	W	90/08/15
90500094.CTD	094	LS30	46	35.10	N	130	34.60	W	90/08/15

90500095.CTD	095	LS32	46 35.03 N	130 49.16 W	90/08/15
90500096.CTD	096	LS32	46 34.79 N	130 48.79 W	90/08/15
90500097.CTD	097	LS23	46 40.06 N	131 11.20 W	90/08/15

Cobb Seamount Experiment, August 1991

Cruise ID: Institute of Ocean Sciences Cruise 9113

Chief Scientist: Verena Tunnicliffe, UVic Biology

Vessel: CSS Parizeau

Filename	Cast#	ID	Latitude	Longitude	Date
91130002.CTD	002	NEWS	50 0.10 N	138 38.05 W	1991/07/29
91130004.CTD	004	1-7	46 58.06 N	130 58.88 W	1991/07/31
91130005.CTD	005	1-6	46 53.82 N	130 55.35 W	1991/07/31
91130006.CTD	006	1-6	46 53.90 N	130 55.35 W	1991/07/31
91130007.CTD	007	1-5	46 49.45 N	130 51.76 W	1991/07/31
91130008.CTD	008	1-4	46 48.62 N	130 51.15 W	1991/07/31
91130009.CTD	009	1-4	46 48.75 N	130 51.60 W	1991/07/31
91130010.CTD	010	1-3	46 47.73 N	130 50.37 W	1991/07/31
91130011.CTD	011	1-2	46 46.61 N	130 49.63 W	1991/07/31
91130013.CTD	013	1-2	46 46.84 N	130 50.01 W	1991/07/31
91130014.CTD	014	1-1	46 46.14 N	130 48.92 W	1991/07/31
91130015.CTD	015	3-7	46 45.23 N	130 26.90 W	1991/08/01
91130016.CTD	016	3-6	46 45.22 N	130 34.00 W	1991/08/01
91130017.CTD	017	3-6	46 45.22 N	130 34.00 W	1991/08/01
91130018.CTD	018	3-5	46 45.22 N	130 41.36 W	1991/08/01
91130019.CTD	019	3-4	46 45.06 N	130 42.74 W	1991/08/01
91130020.CTD	020	3-4	46 45.24 N	130 42.90 W	1991/08/01
91130021.CTD	021	3-3	46 45.21 N	130 44.10 W	1991/08/01
91130022.CTD	022	3-2	46 45.16 N	130 45.68 W	1991/08/01
91130023.CTD	023	3-1	46 45.22 N	130 45.53 W	1991/08/01
91130024.CTD	024	3-1	46 45.18 N	130 47.03 W	1991/08/01
91130025.CTD	025	5-7	46 32.19 N	130 58.62 W	1991/08/02
91130026.CTD	026	5-6	46 36.57 N	130 55.42 W	1991/08/02
91130027.CTD	027	5-6	46 36.65 N	130 55.50 W	1991/08/02

91130028.CTD	028	5-5	46	40.67	N	130	51.57	W	1991/08/02
91130029.CTD	029	5-4	46	41.78	N	130	51.00	W	1991/08/02
91130030.CTD	030	5-3	46	42.58	N	130	50.28	W	1991/08/02
91130031.CTD	031	5-2	46	43.52	N	130	49.66	W	1991/08/02
91130032.CTD	032	5-2	46	43.63	N	130	49.32	W	1991/08/02
91130033.CTD	033	5-1	46	44.32	N	130	49.25	W	1991/08/02
91130034.CTD	034	1-0	46	45.35	N	130	48.44	W	1991/08/02
91130035.CTD	035	YY1	46	44.02	N	130	45.27	W	1991/08/02
91130036.CTD	036	YY1	46	44.02	N	130	45.27	W	1991/08/02
91130037.CTD	037	YY1	46	44.02	N	130	45.27	W	1991/08/02
91130038.CTD	038	YY1	46	44.05	N	130	45.17	W	1991/08/02
91130039.CTD	039	YY1	46	44.05	N	130	45.17	W	1991/08/02
91130040.CTD	040	YY1	46	43.98	N	130	45.23	W	1991/08/02
91130041.CTD	041	YY1	46	44.02	N	130	45.27	W	1991/08/02
91130042.CTD	042	YY1	46	44.04	N	130	45.23	W	1991/08/02
91130043.CTD	043	YY1	46	44.04	N	130	45.27	W	1991/08/03
91130044.CTD	044	YY1	46	44.00	N	130	45.32	W	1991/08/03
91130045.CTD	045	YY1	46	44.00	N	130	45.29	W	1991/08/03
91130046.CTD	046	YY1	46	44.00	N	130	45.23	W	1991/08/03
91130047.CTD	047	YY1	46	44.02	N	130	45.20	W	1991/08/03
91130048.CTD	048	YY1	46	44.03	N	130	45.29	W	1991/08/03
91130049.CTD	049	YY1	46	44.03	N	130	45.30	W	1991/08/03
91130050.CTD	050	YY1	46	44.03	N	130	45.36	W	1991/08/03
91130051.CTD	051	YY1	46	44.01	N	130	45.42	W	1991/08/03
91130052.CTD	052	YY1	46	43.96	N	130	45.37	W	1991/08/03
91130053.CTD	053	YY1	46	44.03	N	130	45.40	W	1991/08/03
91130054.CTD	054	YY1	46	44.01	N	130	45.32	W	1991/08/03
91130055.CTD	055	YY1	46	44.01	N	130	45.29	W	1991/08/03
91130056.CTD	056	YY1	46	44.01	N	130	45.31	W	1991/08/03
91130057.CTD	057	YY1	46	44.00	N	130	45.36	W	1991/08/03
91130058.CTD	058	YY1	46	44.00	N	130	45.32	W	1991/08/03
91130059.CTD	059	YY1	46	44.02	N	130	45.27	W	1991/08/03
91130061.CTD	061	YY1	46	43.97	N	130	45.36	W	1991/08/03
91130063.CTD	063	YY2	46	45.25	N	130	26.93	W	1991/08/03
91130064.CTD	064	YY2	46	45.23	N	130	27.04	W	1991/08/03

91130065.CTD	065	YY2	46	45.25	N	130	27.13	W	1991/08/03
91130066.CTD	066	YY2	46	45.32	N	130	27.40	W	1991/08/03
91130067.CTD	067	YY2	46	45.43	N	130	27.54	W	1991/08/03
91130068.CTD	068	YY2	46	45.45	N	130	27.64	W	1991/08/03
91130069.CTD	069	YY2	46	45.44	N	130	27.64	W	1991/08/03
91130070.CTD	070	YY2	46	45.40	N	130	27.67	W	1991/08/03
91130071.CT	071	YY2	46	45.41	N	130	27.67	W	1991/08/03
91130072.CTD	072	YY2	46	45.40	N	130	27.62	W	1991/08/03
91130073.CTD	073	YY2	46	45.34	N	130	27.49	W	1991/08/03
91130074.CTD	074	YY2	46	45.21	N	130	27.44	W	1991/08/03
91130075.CTD	075	YY2	46	45.25	N	130	27.40	W	1991/08/03
91130076.CTD	076	YY2	46	45.27	N	130	27.40	W	1991/08/03
91130077.CTD	077	YY2	46	45.28	N	130	27.35	W	1991/08/03
91130078.CTD	078	YY2	46	45.27	N	130	27.32	W	1991/08/03
91130079.CTD	079	2-7	46	58.08	N	130	37.52	W	1991/08/03
91130080.CTD	080	2-6	46	53.70	N	130	41.17	W	1991/08/03
91130081.CTD	081	2-6	46	53.81	N	130	41.28	W	1991/08/03
91130082.CTD	082	2-5	46	49.43	N	130	44.69	W	1991/08/03
91130083.CTD	083	2-4	46	48.41	N	130	45.42	W	1991/08/03
91130084.CTD	084	2-4	46	48.29	N	130	45.82	W	1991/08/03
91130085.CTD	085	2-3	46	47.68	N	130	46.20	W	1991/08/03
91130086.CTD	086	2-2	46	46.84	N	130	46.81	W	1991/08/03
91130087.CTD	087	2-2	46	46.84	N	130	46.81	W	1991/08/03
91130088.CTD	088	2-1	46	46.10	N	130	47.57	W	1991/08/03
91130089.CTD	089	1-0	46	45.33	N	130	48.25	W	1991/08/03
91130090.CTD	090	1-2	46	46.99	N	130	49.80	W	1991/08/03
91130091.CTD	091	1-4	46	48.62	N	130	51.09	W	1991/08/03
91130092.CTD	092	1-8	46	50.55	N	130	52.86	W	1991/08/03
91130093.CTD	093	1-9	46	53.07	N	130	55.08	W	1991/08/04
91130094.CTD	094	1-10	46	55.58	N	130	57.29	W	1991/08/04
91130095.CTD	095	1-7	46	58.24	N	130	59.40	W	1991/08/04
91130096.CTD	096	3-2	46	45.19	N	130	45.31	W	1991/08/04
91130097.CTD	097	3-4	46	45.18	N	130	42.56	W	1991/08/04
91130098.CTD	098	3-8	46	45.11	N	130	39.71	W	1991/08/04
91130099.CTD	099	3-9	46	45.22	N	130	35.31	W	1991/08/04

91130101.CTD	101	3-10	46	45.29	N	130	30.80	W	1991/08/04
91130102.CTD	102	3-7	46	45.26	N	130	26.43	W	1991/08/04
91130103.CTD	103	4-7	46	32.17	N	130	37.49	W	1991/08/04
91130104.CTD	104	4-6	46	36.65	N	130	41.00	W	1991/08/04
91130105.CTD	105	4-6	46	36.65	N	130	41.00	W	1991/08/04
91130106.CTD	106	4-5	46	40.84	N	130	44.70	W	1991/08/04
91130107.CTD	107	4-4	46	41.67	N	130	45.56	W	1991/08/04
91130108.CTD	108	4-3	46	42.57	N	130	46.30	W	1991/08/04
91130109.CTD	109	4-2	46	43.43	N	130	46.91	W	1991/08/04
91130110.CTD	110	4-2	46	43.43	N	130	47.02	W	1991/08/04
91130111.CTD	111	4-1	46	44.30	N	130	47.64	W	1991/08/04
91130112.CTD	112	2-2	46	46.98	N	130	47.04	W	1991/08/04
91130113.CTD	113	2-4	46	48.60	N	130	45.54	W	1991/08/04
91130114.CTD	114	2-8	46	50.36	N	130	44.12	W	1991/08/04
91130115.CTD	115	2-9	46	52.94	N	130	41.95	W	1991/08/04
91130116.CTD	116	2-10	46	55.62	N	130	39.75	W	1991/08/04
91130117.CTD	117	2-7	46	58.27	N	130	37.44	W	1991/08/04
91130118.CTD	118	5-2	46	43.42	N	130	49.62	W	1991/08/05
91130119.CTD	119	5-4	46	41.63	N	130	51.09	W	1991/08/05
91130120.CTD	120	5-8	46	40.00	N	130	52.87	W	1991/08/05
91130121.CTD	121	5-9	46	37.46	N	130	55.08	W	1991/08/05
91130122.CTD	122	5-10	46	34.86	N	130	57.25	W	1991/08/05
91130123.CTD	123	5-7	46	32.16	N	130	59.38	W	1991/08/05
91130124.CTD	124	CORN	46	33.23	N	131	12.93	W	1991/08/05
91130125.CTD	125	CORN	46	37.60	N	131	16.59	W	1991/08/05
91130126.CTD	126	CORN	46	39.30	N	131	18.12	W	1991/08/05
91130127.CTD	127	CORN	46	41.89	N	131	20.32	W	1991/08/05
91130128.CTD	128	6-7	46	45.20	N	131	10.40	W	1991/08/05
91130130.CTD	130	6-6	46	45.26	N	131	3.06	W	1991/08/05
91130131.CTD	131	6-6	46	45.26	N	131	3.06	W	1991/08/05
91130133.CTD	133	6-5	46	45.24	N	130	55.44	W	1991/08/05
91130134.CTD	134	6-4	46	45.11	N	130	54.37	W	1991/08/05
91130136.CTD	136	6-3	46	45.23	N	130	52.74	W	1991/08/05
91130137.CTD	137	6-2	46	45.21	N	130	51.37	W	1991/08/05
91130138.CTD	138	6-1	46	45.13	N	130	51.59	W	1991/08/05

91130139.CTD	139	6-1	46	45.21	N	130	49.94	W	1991/08/05
91130140.CTD	140	6-0	46	45.23	N	130	48.52	W	1991/08/05
91130141.CTD	141	OFFS	47	10.04	N	130	48.09	W	1991/08/05
91130142.CTD	142	OFFS	47	10.13	N	130	48.26	W	1991/08/06
91130143.CTD	143	OFFS	47	10.02	N	130	48.20	W	1991/08/06
91130144.CTD	144	OFFS	47	10.11	N	130	48.19	W	1991/08/06
91130145.CTD	145	OFFS	47	10.15	N	130	48.05	W	1991/08/06
91130146.CTD	146	OFFS	47	10.00	N	130	48.32	W	1991/08/06
91130147.CTD	147	OFFS	47	10.11	N	130	48.15	W	1991/08/06
91130148.CTD	148	OFFS	47	10.09	N	130	48.09	W	1991/08/06
91130149.CTD	149	OFFS	47	10.18	N	130	48.09	W	1991/08/06
91130150.CTD	150	OFFS	47	10.15	N	130	48.14	W	1991/08/06
91130151.CTD	151	OFFS	47	10.10	N	130	48.07	W	1991/08/06
91130152.CTD	152	OFFS	47	10.06	N	130	47.86	W	1991/08/06
91130153.CTD	153	OFFS	47	10.06	N	130	47.86	W	1991/08/06
91130154.CTD	154	6-7	46	45.17	N	131	10.40	W	1991/08/06
91130155.CTD	155	6-10	46	45.16	N	131	5.96	W	1991/08/06
91130156.CTD	156	6-9	46	45.20	N	131	1.70	W	1991/08/06
91130157.CTD	157	6-8	46	45.19	N	130	57.36	W	1991/08/06
91130158.CTD	158	6-4	46	45.19	N	130	54.22	W	1991/08/06
91130159.CTD	159	6-2	46	45.21	N	130	51.50	W	1991/08/06
91130161.CTD	161	6-2	46	45.32	N	130	47.33	W	1991/08/06
91130162.CTD	162	4-2	46	43.39	N	130	46.69	W	1991/08/07
91130163.CTD	163	4-4	46	41.70	N	130	45.40	W	1991/08/07
91130164.CTD	164	4-8	46	40.05	N	130	43.64	W	1991/08/07
91130165.CTD	165	4-9	46	37.48	N	130	41.84	W	1991/08/07
91130166.CTD	166	4-10	46	34.89	N	130	39.65	W	1991/08/07
91130167.CTD	167	4-7	46	32.19	N	130	37.41	W	1991/08/07
91130168.CTD	168	M2	46	44.07	N	130	45.38	W	1991/08/07
91130169.CTD	169	M2	46	44.10	N	130	45.35	W	1991/08/07
91130170.CTD	170	M2	46	44.18	N	130	45.45	W	1991/08/07
91130171.CTD	171	M2	46	44.26	N	130	45.49	W	1991/08/07
91130174.CTD	174	M2	46	44.09	N	130	45.16	W	1991/08/07
91130175.CTD	175	M2	46	44.20	N	130	45.18	W	1991/08/07
91130176.CTD	176	M2	46	44.10	N	130	45.35	W	1991/08/07

91130177.CTD	177	M2	46 44.09 N	130 45.21 W	1991/08/07

Cobb Seamount Experiment, June 1992

Cruise ID: Institute of Ocean Sciences Cruise 9211
Chief Scientist: Howard Freeland, IOS
Vessel: John P. Tully

Filename	Cast#	ID	Latitude	Longitude	Date
92110001.CTD	001	NEWS	46 45.46 N	130 46.98 W	1992/06/24
92110002.CTD	002	LS01	46 35.70 N	132 18.00 W	1992/06/24
92110003.CTD	003	LS02	46 36.57 N	132 10.85 W	1992/06/24
92110004.CTD	004	LS03	46 37.29 N	132 3.59 W	1992/06/24
92110005.CTD	005	LS04	46 38.05 N	131 56.38 W	1992/06/24
92110006.CTD	006	LS05	46 38.84 N	131 49.17 W	1992/06/24
92110007.CTD	007	LS06	46 39.55 N	131 41.96 W	1992/06/24
92110008.CTD	008	LS07	46 40.39 N	131 34.75 W	1992/06/24
92110009.CTD	009	LS08	46 41.16 N	131 27.54 W	1992/06/24
92110010.CTD	010	LS09	46 41.63 N	131 23.21 W	1992/06/25
92110011.CTD	011	LS10	46 41.94 N	131 20.33 W	1992/06/25
92110012.CTD	012	LS11	46 42.25 N	131 17.44 W	1992/06/25
92110013.CTD	013	LS12	46 42.64 N	131 13.12 W	1992/06/25
92110014.CTD	014	LS13	46 43.07 N	131 8.84 W	1992/06/25
92110015.CTD	015	LS14	46 44.14 N	130 59.86 W	1992/06/25
92110016.CTD	016	LS15	46 44.14 N	130 55.59 W	1992/06/25
92110017.CTD	017	LS16	46 44.94 N	130 52.71 W	1992/06/25
92110018.CTD	018	LS17	46 45.07 N	130 51.26 W	1992/06/25
9211001[illegible].CTD	019	LS18	46 45.22 N	130 49.77 W	1992/06/25
92110020.CTD	020	LS20	46 45.53 N	130 46.98 W	1992/06/25
92110021.CTD	021	LS21	46 45.59 N	130 45.49 W	1992/06/25
92110022.CTD	022	LS22	46 45.65 N	130 44.05 W	1992/06/25
92110023.CTD	023	LS23	46 46.10 N	130 41.17 W	1992/06/25
92110024.CTD	024	LS24	46 46.82 N	130 33.96 W	1992/06/25
92110025.CTD	025	LS25	46 47.71 N	130 26.75 W	1992/06/25
92110026.CTD	026	LS26	46 48.41 N	130 19.43 W	1992/06/25
92110027.CTD	027	LS27	46 49.15 N	130 12.33 W	1992/06/25

92110028.CTD	028	LS28	46	49.96	N	130	5.12	W	1992/06/25
92110029.CTD	029	LS28	46	50.03	N	130	5.12	W	1992/06/25
92110030.CTD	030	LS29	46	50.61	N	129	57.91	W	1992/06/25
92110031.CTD	031	LS30	46	51.50	N	129	50.88	W	1992/06/25
92110032.CTD	032	LS31	46	30.56	N	130	44.98	W	1992/06/26
92110033.CTD	033	LS32	46	35.50	N	130	46.11	W	1992/06/26
92110034.CTD	034	LS33	46	40.43	N	130	47.25	W	1992/06/26
92110035.CTD	035	LS34	46	42.40	N	130	47.80	W	1992/06/26
92110036.CTD	036	LS35	46	43.47	N	130	47.93	W	1992/06/26
92110037.CTD	037	LS36	46	44.54	N	130	48.24	W	1992/06/26
92110038.CTD	038	LS38	46	46.37	N	130	48.60	W	1992/06/26
92110039.CTD	039	LS39	46	47.39	N	130	48.73	W	1992/06/26
92110040.CTD	040	LS40	46	48.34	N	130	49.06	W	1992/06/26
92110041.CTD	041	LS41	46	50.33	N	130	49.47	W	1992/06/26
92110042.CTD	042	LS42	46	55.15	N	130	50.64	W	1992/06/26
92110043.CTD	043	LS43	47	0.16	N	130	51.78	W	1992/06/26
92110044.CTD	044	LS44	46	58.48	N	131	7.75	W	1992/06/26
92110045.CTD	045	LS44	46	58.48	N	131	7.86	W	1992/06/26
92110046.CTD	046	LS45	46	53.50	N	131	6.39	W	1992/06/26
92110047.CTD	047	LS46	46	48.53	N	131	5.49	W	1992/06/26
92110048.CTD	048	LS47	46	43.28	N	131	4.19	W	1992/06/26
92110049.CTD	049	LS48	46	38.50	N	131	3.10	W	1992/06/26
92110050.CTD	050	LS49	46	33.76	N	131	1.98	W	1992/06/26
92110051.CTD	051	LS50	46	28.81	N	131	1.06	W	1992/06/27
92110052.CTD	052	LS51	46	27.07	N	131	16.90	W	1992/06/27
92110053.CTD	053	LS52	46	32.16	N	131	18.06	W	1992/06/27
92110054.CTD	054	LS53	46	37.06	N	131	18.06	W	1992/06/27
92110055.CTD	055	LS54	46	40.05	N	131	19.88	W	1992/06/27
92110056.CTD	056	LS55	46	42.01	N	131	20.27	W	1992/06/27
92110057.CTD	057	LS56	46	42.01	N	131	20.78	W	1992/06/27
92110058.CTD	058	LS57	46	46.88	N	131	21.46	W	1992/06/27
92110059.CTD	059	LS58	46	51.82	N	131	22.73	W	1992/06/27
92110060.CTD	060	LS59	46	56.76	N	131	23.80	W	1992/06/27
92110061.CTD	061	LS36	46	44.34	N	130	48.15	W	1992/06/27
92110062.CTD	062	LS38	46	47.81	N	130	49.94	W	1992/06/28

92110063.CTD	063	LS21	46	45.11	N	130	44.93	W	1992/06/28
92110064.CTD	064	LS33	46	40.44	N	130	47.25	W	1992/06/29
92110065.CTD	065	LS35	46	43.34	N	130	47.93	W	1992/06/29
92110067.CTD	067	LS35	46	49.96	N	130	48.29	W	1992/06/29
92110068.CTD	068	LS35	46	43.31	N	130	47.70	W	1992/06/29
92110069.CTD	069	LS35	46	43.20	N	130	47.93	W	1992/06/29
92110070.CTD	070	LS35	46	43.47	N	130	47.74	W	1992/06/29
92110071.CTD	071	LS35	46	43.27	N	130	47.93	W	1992/06/29
92110072.CTD	072	LS35	46	43.36	N	130	48.52	W	1992/06/29
92110073.CTD	073	LS35	46	43.30	N	130	48.28	W	1992/06/29
92110074.CTD	074	LS35	46	43.40	N	130	47.70	W	1992/06/29
92110075.CTD	075	LS35	46	43.40	N	130	47.55	W	1992/06/29
92110076.CTD	076	LS35	46	43.25	N	130	47.79	W	1992/06/29
92110077.CTD	077	LS35	46	43.28	N	130	48.10	W	1992/06/29
92110078.CTD	078	LS35	46	43.40	N	130	47.93	W	1992/06/29
92110079.CTD	079	LS35	46	43.40	N	130	47.93	W	1992/06/29
92110080.CTD	080	LS35	46	43.40	N	130	48.37	W	1992/06/29
92110081.CTD	081	LS35	46	43.16	N	130	48.84	W	1992/06/29
92110082.CTD	082	LS35	46	43.02	N	130	48.27	W	1992/06/29
92110083.CTD	083	LS35	46	43.43	N	130	47.93	W	1992/06/29
92110084.CTD	084	LS35	46	42.89	N	130	47.81	W	1992/06/29
92110085.CTD	085	LS35	46	43.32	N	130	48.22	W	1992/06/29
92110086.CTD	086	LS35	46	42.72	N	130	48.23	W	1992/06/29
92110087.CTD	087	LS35	46	43.72	N	130	47.71	W	1992/06/29
92110088.CTD	088	LS35	46	42.91	N	130	48.27	W	1992/06/29
92110089.CTD	089	LS35	46	43.28	N	130	47.77	W	1992/06/29
92110090.CTD	090	LS35	46	42.95	N	130	47.70	W	1992/06/29
92110091.CTD	091	LS15	46	44.59	N	130	55.62	W	1992/06/29
92110092.CTD	092	LS23	46	45.83	N	130	41.09	W	1992/06/30

ZOOPLANKTON DATA: The following are those stations for which zooplankton samples were collected as part of the Cobb Seamount Experiment. "Stations" correspond to the ID numbers used in the previous lists: latitude, longitude also correspond to those given in the lists. Samples were collected using bongo nets with a 236μm mesh. Tows were typically from 250m to the surface. Samples were stored in 5% formalin and are held by Verena Tunnicliffe at the University of Victoria.

CSEX90 Cruise: IOS CRUISE 9050, August 1990
Stations: LS04, LS08, LS09, LS12
LS15, LS16, LS19, LS22
LS23, LS29, LS26, LS29, LS32

CSEX91 Cruise: IOS CRUISE 9113, August 1991
Stations: 1-0, 1-1, 1-2, 1-4, 1-6
2-1, 2-2, 2-4, 2-6
3-1, 3-2, 3-4, 3-6
4-2, 4-6
5-1, 5-2, 5-4, 5-6
6-1, 6-2, 6-4, 6-6

CSEX92 Cruise: IOS CRUISE 9211, June 1992
Stations: LS03, LS05, LS07, LS09, LS11, LS13, LS14, LS16, LS17,
LS22, LS24, LS26, LS28, LS30, LS32, LS34, LS35, LS38,
LS40, LS42, LS44, LS46, LS48, LS50, LS52, LS54, LS56,
LS58

VITA

Name: John Francis Dower

Place of Birth: St. John's, Newfoundland

Date of Birth: 24/11/66

Educational Institutions Attended:

Memorial University of Newfoundland	1984-89
University of Victoria	1989-94

Degrees Awarded:

B.Sc. (Honours) Memorial University of Newfoundland, 1989

Academic Awards:

1992-93	NSERC Postgraduate Scholarship
1992-92	President's Research Scholarship (UVic.)
1991-92	NSERC Postgraduate Scholarship
1991-92	President's Research Scholarship (Uvic.)
1990	Maureen de Burgh Memorial Scholarship in Marine Biology (Uvic.)
1989	Newfoundland Gov't Career Development Award (MUN)
1988	NSERC Undergraduate Summer Research Award (MUN)
1987	NSERC Undergraduate Summer Research Award (MUN)

Publications:

Dower, J., Freeland, H. and Juniper, K. (1992) A strong biological response to oceanic flow past Cobb Seamount. Deep-Sea Research 39:1139-1145.

Dower, J. (1989) The ecology of *Terebratulina septentrionalis*, an articulate brachiopod, from Bonne Bay, Newfoundland. (Unpublished B.Sc. Honours thesis) 112pp.

OVERLAY 1

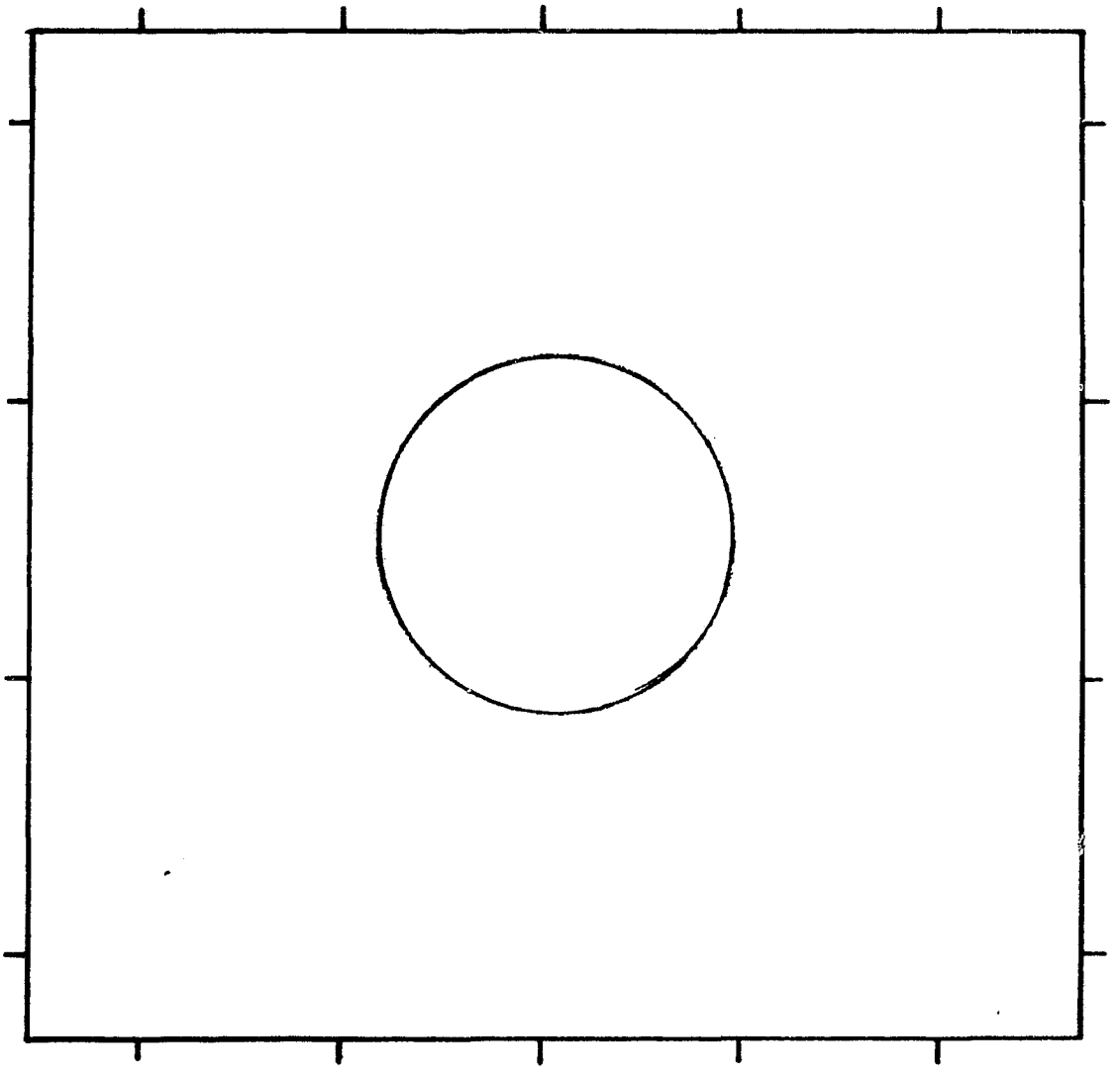

OVERLAY 2

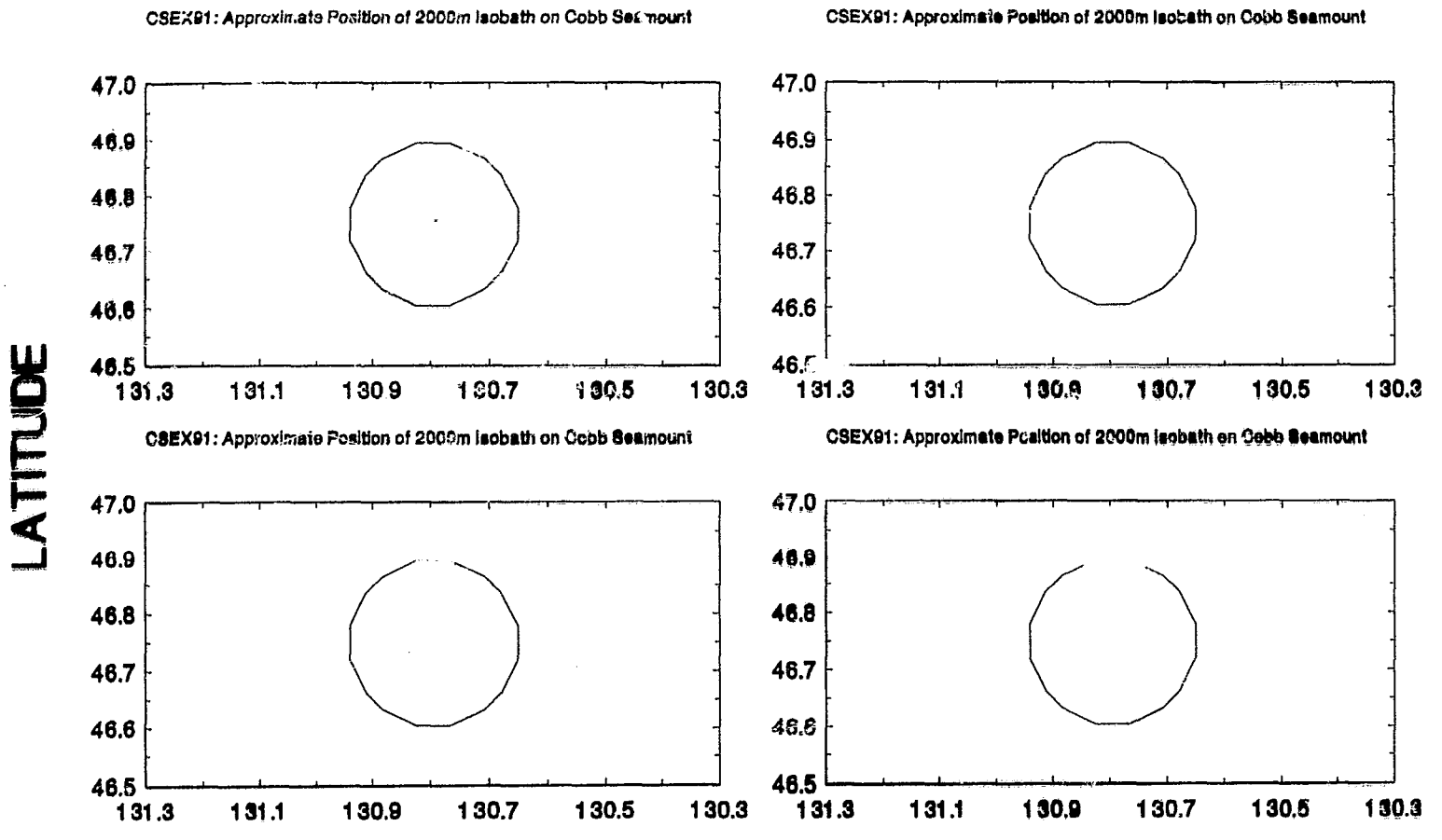
CSEX91: Approximate Position of 2000m Isobath on Cobb Seamount
CSEX91: Approximate Position of 2000m Isobath on Cobb Seamount
CSEX91: Approximate Position of 2000m Isobath on Cobb Seamount
CSEX91: Approximate Position of 2000m Isobath on Cobb Seamount
47.0
46.9
46.8
46.7
46.6
46.5
131.3
131.1
130.9
130.7
130.5
130.3
LATITUDE
LONGITUDE

OVERLAY 3

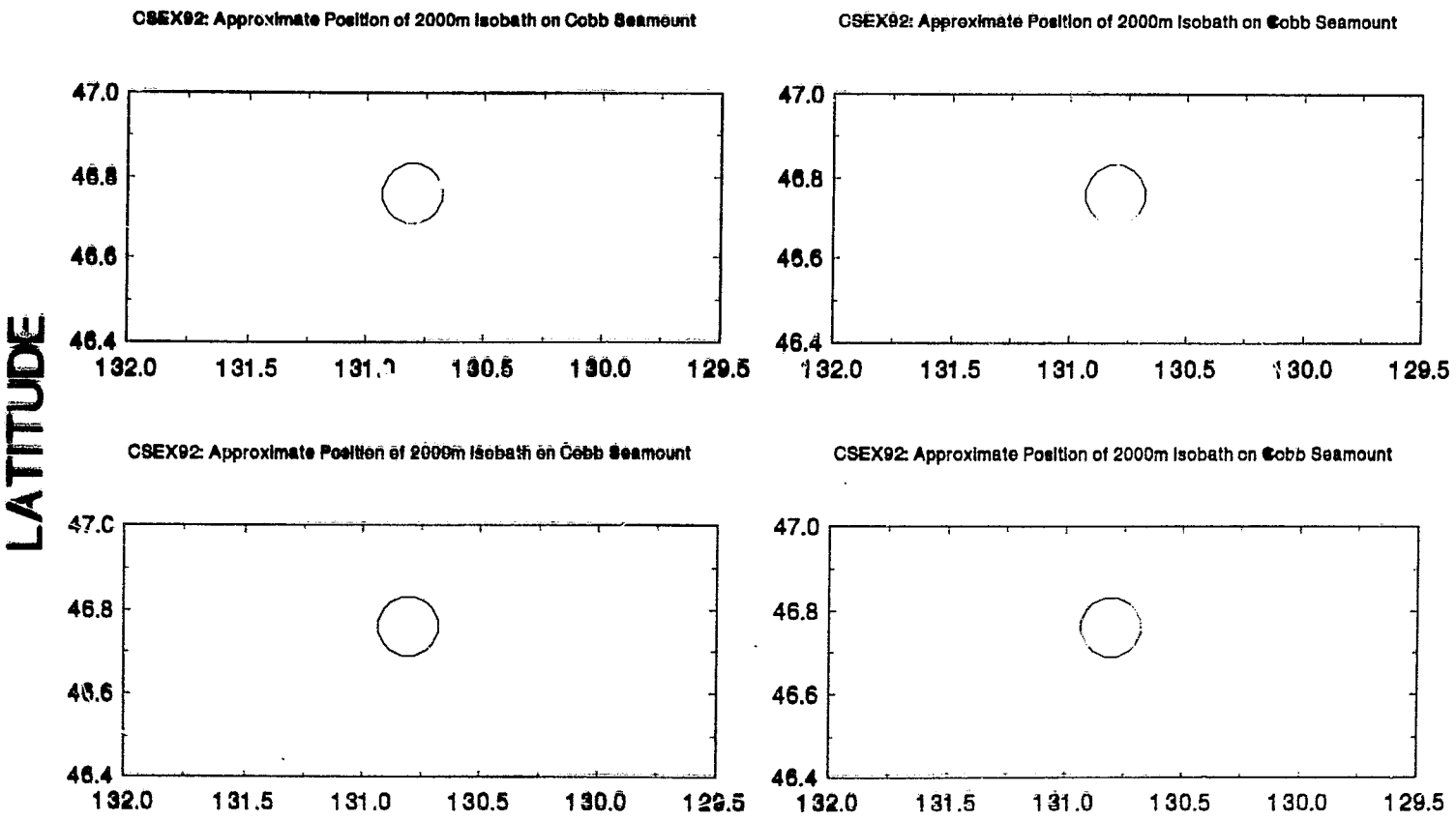
CSEX92: Approximate Position of 2000m Isobath on Cobb Seamount
CSEX92: Approximate Position of 2000m Isobath on Cobb Seamount
CSEX92: Approximate Position of 2000m Isobath on Cobb Seamount
CSEX92: Approximate Position of 2000m Isobath on Cobb Seamount
47.0
46.8
46.6
46.4
132.0
131.5
131.0
130.5
130.0
129.5
LATITUDE
LONGITUDE

OVERLAY 4

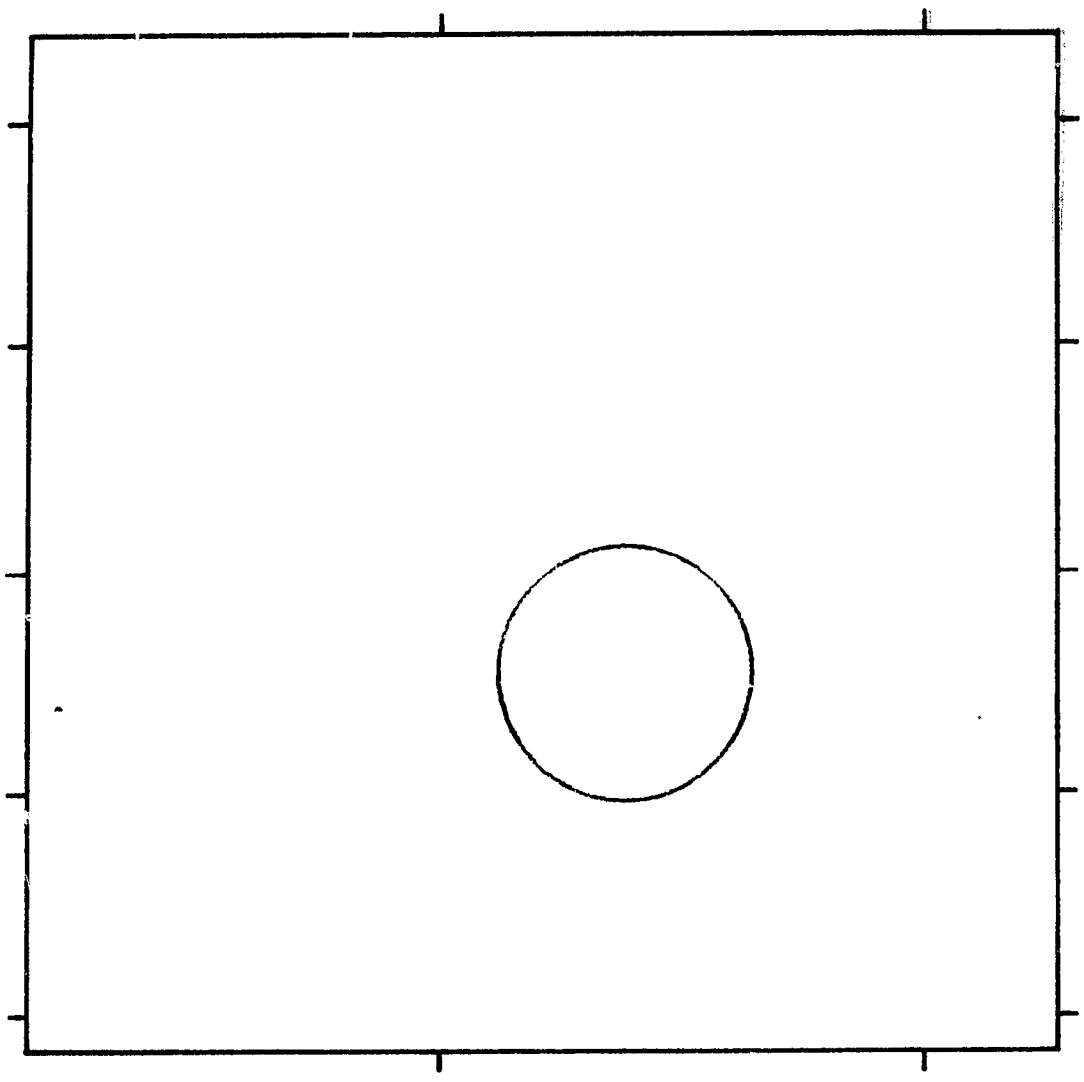

OVERLAY 5